Higgs Bundles for
4d $\mathcal{N} = 1$ Gauge Theories

Max Hübner

The Queen's College

University of Oxford

A thesis submitted for the degree of

Doctor of Philosophy

Trinity 2021

Higgs Bundles for 4d $\mathcal{N} = 1$ Gauge Theories

Max Hübner

The Queen's College

University of Oxford

Advisor: Prof. Sakura Schäfer-Nameki, Mathematical Institute, University of Oxford.

Internal examiner: Prof. Christopher Beem, Mathematical Institute, University of Oxford.

External examiner: Prof. Bobby Acharya, Department of Physics, King's College London & Abdus Salam International Centre for Theoretical Physics, Trieste, Italy.

Abstract: We consider two constructions of 4d $\mathcal{N} = 1$ gauge theories in M-theory. The first is purely geometric and involves compactifying M-theory on singular manifolds of G_2-holonomy. The geometries studied are ALE-fibered over a compact base M_3. This fibration admits a description in terms of a Higgs bundle with three-dimensional base M_3 which arises as the BPS equations of M-theory reduced adiabatically along the ALE fibers. The gauge theory sector of these compactifications originates from M2-branes wrapped on vanishing cycles of the ALE fibration with interactions set by Euclidean M2-branes wrapped on associative submanifolds traced out by the vanishing cycles. The first part of this thesis develops the physics of these models and introduces a colored supersymmetric quantum mechanics organizing and quantifying non-perturbative effects due to M2-brane instantons. In this framework we study the local models of twisted connected sum G_2-manifolds and describe their possible chiral deformations.

The second construction considered in this thesis utilizes M5-branes wrapped on Riemann surfaces embedded in local Calabi-Yau threefolds. We focus on the subset of such

configurations derived from 4d $\mathcal{N} = 2$ theories of class S breaking to $\mathcal{N} = 1$. Their BPS equations construct Higgs bundles differing from the standard class S Higgs bundle by an additional Higgs field. The associated $\mathcal{N} = 1$ curve collects the spectral data of both Higgs fields and different curves describe distinct vacua of the same gauge theory. The second part of this thesis studies the construction of such Higgs bundles and derives the confinement properties of each vacuum from the associated $\mathcal{N} = 1$ curve. This allows for the study of confinement in non-Lagrangian $\mathcal{N} = 1$ theories which is illustrated by constructing an infinite class of non-Lagrangian $\mathcal{N} = 1$ theories that contain confining vacua.

Statement of Originality

This thesis is based on the results of the following papers, all to which the author contributed substantially:

[1]   A. P. Braun, S. Cizel, M. Hübner, S. Schäfer-Nameki. *Higgs Bundles for M-theory on G_2-Manifolds.* JHEP **03** (2018), [1812.06072].

[2]   Max Hübner. *Local G_2-manifolds, Higgs bundles and a colored quantum mechanics.* JHEP **05** (2021), [2009.07136].

[3]   L. Bhardwaj, M. Hübner, S. Schäfer-Nameki. *1-form Symmetries of 4d $\mathcal{N} = 2$ Class S Theories.* (2021), [2102.01693].

[4]   L. Bhardwaj, M. Hübner, S. Schäfer-Nameki. *Liberating Confinement from Lagrangians: 1-form Symmetries and Lines in 4d $\mathcal{N} = 1$ from 6d $\mathcal{N} = (2,0)$.* (2021), [2106.10265].

The first and second part of this thesis present the contents of [1], [2] and [3], [4] respectively. Versions of the results contained in [1] have appeared in the DPhil thesis submitted to the University of Oxford by the coauthor Sebastjan Cizel.

Acknowledgements

Oxford, 9 July 2021

I dedicate this thesis to my brothers and parents,

Marcus, Lucas, Athina and Stefan.

Contents

Part I
Introduction

Quantum field theories have been at the heart of theoretical and experimental particle physics for close to a decade. Their predictive power is unprecedented and their contributions to mathematics and physics numerous. Yet they resist rigours mathematical formulation and exploring their properties remains an active field of research. Wide ranging progress has been made for topological, conformal and supersymmetric quantum field theories and others. In these cases non-trivializing structures are imposed on the dynamics of the field theory and as a consequence methods of analysis beyond perturbation theory become available. In this thesis we focus on supersymmetric field theories which in many cases allow for embeddings into string and M-theory establishing common higher dimensional origins, classifications and non-trivial equivalences. In this fashion string and M-theory have proven to be an invaluable tool in deepening the understanding of supersymmetric quantum field theories, which display many semi-realistic features relevant for more generic quantum field theories.

In this thesis we consider two constructions of 4d $\mathcal{N} = 1$ gauge theories in M-theory. String theory realizations of such gauge theories allow for geometric interpretations of their moduli spaces and dynamical properties. Often, the former is a favorable perspective for exploring regimes of strong coupling, following theories through phase transitions and describing non-Lagrangian theories. Complementary, the latter regularly elucidates non-perturbative aspects of the gauge theory and geometrifies its spectrum and symmetries. Whenever string theory backgrounds are purely geometric, perhaps supporting various branes, these methods are referred to collectively as the tool set of geometric engineering with many ideas tracing back to the seminal papers [5–8].

Since its inception geometric engineering has been at the heart of many applications

of string theory, starting with model building for particle physics [9–18], the study of superconformal field theories [19–26], or sharpening the boundaries of the string theory landscape [27–30]. For many of these applications F-theory has been the framework of choice in recent years. In F-theory however, the defining data of 4d $\mathcal{N} = 1$ theories is not purely geometric, but includes a choice of G_4-flux, which pushes this construction beyond a purely geometric framework and yet is crucial for the resulting 4d $\mathcal{N} = 1$ theory to be chiral.

An alternative construction that yields minimal supersymmetry in 4d is obtained from M-theory on G_2-holonomy manifolds[1] and will be the focus of part II of this thesis. The main challenge in this set-up is the construction of compact G_2-manifolds with singularities, which yield both gauge (codimension 4) and chiral matter (codimension 7) degrees of freedom in 4d [9, 10, 31–34]. To this moment this is an open question. These singularities are necessary ingredients in an attempt to replicate semi-realistic physics, without them the 4d theory contains at most an abelian gauge symmetry and no light charged matter.

Until recently, even the number of known smooth, compact G_2-manifolds was rather limited: the only concrete examples were the Joyce orbifolds given by resolutions of T^7/Γ [35], constructions based on orbifolds of a Calabi-Yau three-fold times S^1 and the construction of Joyce and Karigiannis [36] giving G_2-manifolds constructed from compact G_2-orbifolds by gluing in Eguchi-Hanson spaces along the orbifold locus. Recently, a comparatively large class of examples (order millions) of compact G_2-manifolds was described in [37–39] as twisted connected sums (TCS).

The physics of M-theory and string theory on TCS G_2-manifolds has been investigated in [40–48]. One key property common to all TCS manifolds, which is a direct consequence of this particular construction, is that singularities will occur (if at all) in codimension 4 and 6, but not 7. From the standard geometric engineering dictionary for G_2-manifolds it then follows that the resulting models in 4d do not have chiral matter. An obvious question is then which type of deformations are required to remedy this limitation.

---

[1]We shall often simply refer to these as G_2-manifolds.

Part II of this thesis provides a setting which gives some answers to this question and explores how such transitions would be characterized in TCS geometries, by providing a local model description in terms of a Higgs bundle. We set out to develop this Higgs bundle description for the class of ALE-fibered G_2-manifolds in great generality before applying it to the local limits of TCS G_2-manifolds. This local model framework was advocated for in [49] with the heterotic dual picture initially presented in [34].

We begin by reviewing of the Higgs bundle descriptions of ALE-fibered G_2-manifolds and the associated gauge theory sector engineered in M-theory. Chiral matter is localized at distinct codimension 7 singularities of the geometry and therefore interactions are generated purely by Euclidean M2-brane instantons. A critical contribution of the presented research lies in the analysis of these non-perturbative interactions by studying these at low energies where they permit a description in terms of Euclidean instantons of a quantum mechanical system. The latter allows for their computation using localization techniques and therefore these geometries constitute a class of examples with exceptional control over such membrane instanton effects. Further, we study certain non-generic Higgs bundles, called to be of type Morse-Bott, describing ALE-fibered G_2-manifolds with codimension 6 singularities. Armed with these local models we study chiral deformations of local TCS G_2-manifolds.

We now pivot to introduce the contents of part III in this thesis. Gauge theories with minimal supersymmetry in four dimensions can exhibit confinement. A celebrated result in G_2-physics is the description of confinement in 4d $\mathcal{N} = 1$ super Yang-Mills (SYM) theory [31, 32, 50]. Here the geometric transition of (a quotient of) the Bryant-Salamon cone [51] is found to describe the transition from the gauge theory phase to the confining phase. Confining strings are realized in M-theory as wrapped M2-branes and other objects such as domain walls and glueballs are also understood string theoretically. Here, another example is MQCD [52], the diagnostics for confinement are the confining strings and their charges under unbroken 1-form symmetries. These are rare occasions in which characterizing confinement does not rely on a field theoretic, Lagrangian perspective.

Many celebrated results on supersymmetric field theories, with roots in string theory, involve the construction and classification of non-Lagrangian theories [19–21, 24–26, 53–56]. These are engineered by geometries or on the world volumes of brane systems and therefore defined without an explicit reference to a perturbative Lagrangian formulation. This presses the question on how to determine the higher form global symmetries [57] for this class of theories and understand their description at long distances.

Very recently a plethora of results concerning the string theory origin of 1-form symmetries and more generally higher form global symmetries have been derived. Highlights include the study of geometrically engineered (superconformal) field theories in 5d [58–62], in 4d [63–66] and related holographic considerations [67–70]. In many cases these advances have freed the analysis of higher form symmetries from an underlying Lagrangian formulation and added additional tools for the study of the IR physics of non-Lagrangian theories.

Part III of this thesis pushes forward along these ideas. We consider 4d $\mathcal{N} = 1$ gauge theories realized on the world volume of M5-branes wrapped on Riemann surfaces embedded in Calabi-Yau three-folds. This construction accesses a larger class of theories than those engineered from G_2-manifolds and in particular we focus on theories arising as deformations (rotations) of theories in class S. Here we start with 6d $\mathcal{N} = (2,0)$ theories and construct the spectrum of line operators in 4d by wrapping surface operators on one-cycles of the Riemann surface, extending the results presented in [3].

The most prominent example of this class of theories is MQCD [52] which lies in the same universality class as 4d $\mathcal{N} = 1$ SYM. It is the simplest and first class of examples we consider in part III of this thesis. We further study 4d $\mathcal{N} = 1$ SYM with an adjoint chiral superfield subject to various polynomials superpotentials [71–74] and finally give a new class of non-Lagrangian $\mathcal{N} = 1$ theories exhibiting confinement constructed from theories in class S using multiple irregular punctures. We derive the preserved 1-form symmetry in each vacuum from its $\mathcal{N} = 1$ curve. Notably the input data for this procedure is solely the topology of the $\mathcal{N} = 1$ curve and requires no Lagrangian to be specified. The $\mathcal{N} = 1$ curve

is a solution to a Higgs bundle over the Riemann surface wrapped by the M5-branes. This Higgs bundle is an extension of the standard class S Higgs bundle [75–77] by an additional Higgs field [78, 79]. Crucially this BPS system requires both Higgs fields to commute and therefore, as we explain, the diagonal curve of the spectral curves for both Higgs fields can be constructed. This combination of spectral curves is the $\mathcal{N} = 1$ curve and its derivation and properties are subject of part III.

The structure for this thesis is as follows. In part II, III we give the content of $[1, 2]$ and $[3, 4]$ respectively. Part II merges the two papers contained into a unified presentation and part III presents the key results of [4] preceded by the content of [3] on which these build upon. For both parts additional details can be found in the appendices of the original papers which we reference where appropriate. Finally in part IV we conclude and offer an outlook on interesting future research directions.

Part II
Higgs Bundles for M-theory on G_2-manifolds

We briefly discuss the geometries considered in this part of the thesis and the methods we developed to analyse them. Consider a G_2-manifold realizing in M-theory an ADE gauge group in 4d and take its local model to have a description in terms of an ALE-fibration over a compact supersymmetric cycle M_3

$$\mathbb{C}^2/\Gamma_{ADE} \to M_3 \,. \tag{1}$$

The supersymmetric three-cycle M_3 is an associative cycle in the G_2-manifold. We collect some background on G_2-manifolds, their associative submanifolds and ALE spaces in sections 1.1 and 1.2.

As M-theory compactified on an ALE space gives a 7d super Yang-Mills (SYM) theory with ADE gauge group [10,18,80], the effective 4d $\mathcal{N} = 1$ theory of an ALE-fibration can be found by studying a topologically twisted 7d SYM theory on the three-manifold M_3. The BPS equations then determine the field configurations along M_3 that ensure that $\mathcal{N} = 1$ supersymmetry is preserved in 4d. They are given in terms of a Higgs bundle specified by an adjoint valued one-form Higgs field ϕ and a gauge connection A along M_3. We will focus mainly on diagonalizable Higgs fields, which implies that the connection A furthermore has to be flat. The diagonalizability implies that we can equivalently describe the Higgs bundle via its eigenvalues or spectral data.

The BPS equations are $D_A\phi = D_A^\dagger\phi = 0$ and $F_A = i[\phi,\phi]$ which requires the complex connection $\mathcal{D} = d + \varphi$ with $\varphi = \phi + iA$ to be flat. The spectrum is characterized by the zero modes of the operator $\mathcal{D}$ and in general the zero mode counting problem for a given BPS configuration is difficult to solve. However, progress can be made by instead studying

approximate zero modes localized at the zeros of ϕ. These modes result from M2-branes wrapped on vanishing cycles in an ALE fiber. Their masses are generated non-perturbatively by M2-brane instantons wrapped on associative cycles spanned by the vanishing cycles in the ALE-fibration. Consequently, the massless spectrum follows by finding those linear combinations of approximate zero mode for which these mass terms cancel.

This point of view motivates the study of a colored supersymmetric quantum mechanics (SQM). The approximate ground states and flow-line instantons in this quantum mechanics are in correspondence with the approximate zero modes and non-perturbative effects due to M2-brane instantons. The field space of the 7d SYM theory is the Hilbert space of the colored SQM on which the operator $\mathcal{D}$ acts as the supercharge. Compactification integrals are interpreted as amplitudes of the colored SQM. It is natural to conjecture that the quantum mechanics is an effective description of a probe M2-brane wrapped on the vanishing cycles of the ALE-fibration. Rather than deriving this statement from M-theory, we argue bottom up starting from the 7d SYM that all non-perturbative effects here are correctly accounted for by this colored SQM. We then leverage the colored SQM as computational and organizational tool for the M-theory compactification. The relationship between the SYM and SQM is discussed in more detail in section 6.4.

While this approach elucidates the light modes of the compactification and interactions between these, the final answer to the zero mode counting problem remain difficult to determine. However, in certain simple cases we can give an explicit answer [1,49]. We consider the simplified setting with BPS equations $d\phi = d^\dagger \phi = 0$ and so $\phi = df$, where f is a harmonic function. We allow source terms, i.e., $\Delta f = \rho$. In this set-up the problem of finding the zero mode spectrum and interactions maps to generalizations of Morse-Bott cohomology on $\mathcal{M}_3$, which is a manifold with boundary constructed from M_3 by excising the support of the sources ρ. More general configurations relate to generalizations of Novikov cohomology. As a preview of the results to follow, we summarize some relations between the G_2-manifold, partially twisted 7d SYM, effective 4d theory and the colored SQM in table 1.

Another virtue of this simplified set-up is that it suffices for the modelling of the local geometry of M-theory compactifications on TCS G_2-manifolds, which have an ALE-fibration over S^3 (e.g., as in [45]) with fully factored spectral covers. Moreover it allows us – in the framework of the local Higgs bundle description of the geometry – to make a concrete proposal for the types of deformations and transitions that the geometry needs to undergo. Although we necessarily lose the concrete description of the geometry offered in terms of a twisted connected sum[2] we may nevertheless track what happens to our model in the language of the local geometry, which may be useful in modifying/improving the TCS construction.

Part II of the thesis is structured as follows. Chapter 1.1 reviews background material on G_2-manifolds, ALE spaces and other geometric constructions prevalent throughout this thesis part. Chapter 2 studies the partially twisted 7d SYM theory describing M-theory on ALE-fibered G_2-manifolds at low energies. We derive the Lagrangian, its supersymmetry variations, the resulting BPS equations, field content and characterize the zero mode spectrum. In chapter 3 we consider solutions to the BPS equations with flat connections. These permit a spectral cover description which allows for a clear interpretation of source terms in the BPS equations as defects. For fixed backgrounds with fully reducible spectral covers we analyze in chapter 4 the localized matter sector. In these cases the zero modes are counted by relative de Rham cohomology groups. This result hinges on an isomorphism which can not be constructed in more general cases and in chapter 5 we interpret the results of chapter 4 from a more physical perspective using Morse-Bott cohomology. This approach allows for the generalizations to all solutions of the BPS equations (with or without flat connection) which are presented in chapter 6. Here the Morse-Bott picture is expanded to a particle probing the Higgs bundle, this is the colored SQM. Chapter 7 then pushes beyond considerations of the spectrum and focuses on the Yukawa couplings and higher point interactions. These are computed via supersymmetric localization in the colored SQM. Chapter 9 then

---

[2]Studying such transitions in a compact setting seems to go beyond the current tools available in geometry, as it can no longer be a TCS. However, see also [81].

ALE-fibered G_2-manifold	7d $\mathcal{N}=1$ Twisted SYM	4d $\mathcal{N}=1$ Effective Theory	$\mathcal{N}=2=(1,1)$ Colored SQM
Codim. 4 singularity along M_3	Non-abelian gauge symmetry	Non-abelian gauge symmetry	Bulk sector
Singularity enhancement	Approx. localized zero mode on M_3	Matter	Perturbative ground state
Decompactification of vanishing cycle	Defect, 'Transverse Brane'	–	Higgs field pole
Associative S^3	Flow lines of ϕ	Mass terms	Instanton and differential ∂_{MW}
Associative S^3	Y-Flow tree of ϕ	Yukawa coupling	Generalized instanton and cup-product $\cup$
Associative S^3	Flow-tree of ϕ	Higher-point coupling	Generalized instanton, Massey product m_n
Globally defined ALE 2-cycles	Split spectral cover	Maximal # of $U(1)$ symmetries	dim $\mathfrak{g}_{\text{ADE}}$ embedded Witten SQMs
Monodromy mixed ALE 2-cycles	Non-split spectral cover, Higgs field with branch cuts	Submaximal # of $U(1)$ symmetries	Combination of Witten SQMs

Table 1: Dictionary between ALE-fibration/G_2 geometric data of the fibration over M_3, the partially twisted 7d SYM, effective 4d theory and the colored SQM and the 4d $\mathcal{N}=1$ low energy effective theory.

generalizes the results for solutions of the BPS equations with fully reducible spectral covers presented in chapters 4 and 5 to solutions with irreducible spectral covers where sheets are mixed by monodromies. Finally, in chapter 8 we apply our local model analysis to the local models of TCS G_2-manifolds and study which deformations would be necessary to generate a chiral spectrum.

Chapter 1
G_2-manifolds, Associatives and ALE spaces

1.1 Lie Group G_2 and G_2-Manifolds

We review facts about the group G_2 and G_2-manifolds as presented in [82] relevant for chapter II of this thesis. The group G_2 is a compact, connected, simply-connected, semisimple 14d Lie group defined as the subgroup of $GL(7, \mathbb{R})$ preserving the 3-form

$$\Phi' = dx^{123} + dx^{145} + dx^{167} + dx^{246} - dx^{257} - dx^{347} - dx^{356}. \tag{1.1}$$

Here the abbreviation $dx^{ijk} = dx^i \wedge dx^j \wedge dx^k$ was used. It further preserves the flat metric, an orientation of $\mathbb{R}^7$ and as a consequence the Hodge dual $*\Phi'$. Its Lie algebra has the Dykin diagram

$$\bullet\!\!=\!\!\Longleftarrow\!\!\bullet\,,$$

and its lowest dimensional irreducible representation are of dimension $1, 7, 14$ and 27 respectively with a unique representation for each dimension.

A G_2-manifold is a triple (X_7, Φ, g) consisting of a (compact) manifold X_7 and torsion-free G_2-structure (Φ, g). A torsion-free G_2-structure (Φ, g) is a G_2-structure (Φ, g) where the 3-form $\Phi \in \Omega^3(X_7)$ is covariantly constant $\nabla \Phi = 0$ with respect to the Levi-Civita connection ∇ of the metric g. A G_2-structure (Φ, g) is a positive 3-form Φ together with its associated metric g. A positive 3-form Φ is a 3-form Φ for which at each point $p \in X_7$ there exists an oriented isomorphism $\sigma_p : T_p X_7 \to \mathbb{R}^7$ mapping Φ_p to Φ'. The metric g associated to a positive 3-form Φ is the unique metric g such that σ_p maps g_p to the flat metric on $\mathbb{R}^7$.

In this case the frame bundle F of X_7 permits a principle sub-bundle whose fiber at a point $p \in X_7$ is given by all isomorphisms $T_p X_7 \to \mathbb{R}^7$ mapping Φ_p to Φ'. Any such fiber is due to the definition of Φ' isomorphic to the group G_2. By this reduction of the structure

group the holonomy group of the manifold is contained within G_2. For compact X_7 the condition of covariant constance $\nabla\Phi = 0$ is equivalent to the requirement of closure and coclosure

$$d\Phi = 0\,, \qquad d^\dagger\Phi = d *_\Phi \Phi = 0\,. \tag{1.2}$$

As the Hodge star depends on the metric which itself depends on the 3-form Φ the property of for the G_2-structure to be torsion-free is a non-linear PDE for Φ.

Of interest in G_2-manifolds are calibrated 3-cycles. These are 3d submanifolds $N \subset X_7$ which are calibrated with respect to the 3-form Φ. Given a 3d submanifold $N \subset M$ the metric on X_7 induces a metric on N via restriction and upon a choice of orientation on N this gives rise to a natural volume form vol_N on N. The 3-form Φ is a calibration on X_7 by which we mean that $\Phi|_N \leq \mathrm{vol}_N$ for any 3d submanifold N. A submanifold which is such that $\Phi|_N = \mathrm{vol}_N$ is called calibrated with respect to Φ.

Submanifolds N calibrated with respect to Φ minimize the volume within their homology class. Let $N' \in [N]$ be a 3-cycle homologous to $N \subset X_7$, then

$$\mathrm{Vol}\left(N'\right) = \int_{N'} \mathrm{vol}_{N'} \geq \int_{N'} \Phi = \int_N \Phi = \int_N \mathrm{vol}_N = \mathrm{Vol}\left(N\right)\,. \tag{1.3}$$

G_2-manifolds may exhibit holonomy groups properly contained within G_2. We call a G_2-manifold whose holonomy group is exactly G_2 a manifold of G_2-holonomy.

1.2 ADE Singularities and ALE Spaces

ADE singularities are quotient singularities arising from fixed points in $\mathbb{C}^2/\Gamma$ where Γ is taken to be a finite subgroup of $SU(2)$. Physically the group Γ is required to be a subgroup of $SU(2)$ as upon equipping $\mathbb{C}^2/\Gamma$ with the flat metric δ the holonomy group simply becomes

$$\mathrm{Hol}(\mathbb{C}^2/\Gamma, \delta) = \Gamma \subset SU(2)\,, \tag{1.4}$$

making $\mathbb{C}^2/\Gamma$ an orbifold of special holonomy whereby half of the supersymmetry is preserved in compactifications involving $\mathbb{C}^2/\Gamma$. Mathematically this is motivated by the goal

to preserve the canonical class of a surface when introducing or resolving ADE singularities embedded in them. These quotients are also realisable as singular varities in $(x, y, z) \in \mathbb{C}^3$ and have been classified [83–85]. Their equations read

$$
\begin{aligned}
A_n : \quad & 0 = x^2 + y^2 + z^{n+1} \,, \\
D_n : \quad & 0 = x^2 + y^2 z + z^{n-1} \,, \\
E_6 : \quad & 0 = x^2 + y^3 + z^4 \,, \\
E_7 : \quad & 0 = x^2 + y^3 + yz^3 \,, \\
E_8 : \quad & 0 = x^2 + y^3 + z^5 \,,
\end{aligned}
\tag{1.5}
$$

where the index of the A_n and D_n series starts at $n = 1$ and $n = 4$ respectively. They are related to the Dykin diagrams via minimal resolutions[1] obtained by blowing up the singularities at the origin m times, where m references the index featured in (1.5). This introduces m exceptional divisors C_i of self intersection -2 with mutual intersection numbers $C_i \cdot C_j = 0$ or 1. The collection of curves C_i are always connected and their intersection matrix reproduces the Dynkin diagram of the simply laced semi-simple Lie algebras of type ADE. Further these resolutions are smooth manifolds and can be equipped with metrics of $SU(2)$ holonomy which asymptote the flat metric away from the resolved singularity. These are the ALE spaces constructed in [86]. These spaces are further hyperkahler, i.e. each can be equipped with a triplet (I, J, K) of complex structures satisfying

$$
I^2 = J^2 = K^2 = -1 \,, \qquad IJ = -JI = K \,, \qquad \nabla I = \nabla J = \nabla K = 0 \,.
\tag{1.6}
$$

We give an example taken from [87]. Let the group $G = U(1)^n$ act on the $4n$ dimensional complex vector space $X = \mathbb{H}^{n+1}$ by assigning alternating charges to neighbouring factors of the quaternions $\mathbb{H}$, i.e. the first two factors in X are charged $+1, -1$ respectively under the first factor of $U(1)$, the second and third factor are charged $+1, -1$ respectively under the second factor of $U(1)$ an so on. Each factor of $\mathbb{H}$ can be equipped with a hyperkahler structure with respect to the flat metric. These give rise to a hyperkahler structure (I, J, K, δ)

---

[1]A resolution of a singular variety X is a proper birational map $f : Y \to X$ where Y is a non-singular variety. A resolution is called minimal if all other resolutions factor through it. For surfaces these always exist.

on X with respect to the flat metric δ on X together with the associated Kahler forms $(\omega_I, \omega_J, \omega_K)$. Each factor of $U(1)$ now acts freely on X preserving the metric δ and Kahler forms $(\omega_I, \omega_J, \omega_K)$ and gives rise n vector fields V_i generating this action. Focussing on the complex structure I we see that from

$$0 = \mathcal{L}_{V_i} \omega_I = d\left(V_i \lrcorner \omega_I\right), \tag{1.7}$$

we obtain the existence of a function $(\mu_I)_i$ satisfying

$$d(\mu_I)_i = V_i \lrcorner \omega_I. \tag{1.8}$$

Denoting the Lie algebra of $U(1)$ by $\mathfrak{u}(1)$ and setting $\mathfrak{g} = \mathfrak{u}(1)^n$ we can package the n maps $(\mu_I)_i$ into a single map

$$\mu_I : X \to \mathfrak{g}^*, \qquad \langle \mu_I(m), \xi_i \rangle = (\mu_I)_i(m), \tag{1.9}$$

where ξ_i is an element of the $i-$th factor of $\mathfrak{u}(1)$. The Lie group G acts naturally on both X and $\mathfrak{g}^*$ and if μ_I is equivariant with respect to these we call it a moment map. We can proceed similarly for the other two complex structures J, K to receive maps μ_J, μ_K. For $G = U(1)^n$ these three maps are indeed moment maps and as the action of G fixes the origin in $\mathfrak{g}^*$ it descends to an action on the space

$$N = \mu_I^{-1}(0) \cap \mu_J^{-1}(0) \cap \mu_K^{-1}(0). \tag{1.10}$$

We can now form the quotient $Z = N/G$ and it can be shown that the the hyperkahler structure of X induces a hyperkahler structure on the quotient Z which is of dimension $\dim Z = \dim X - 4 \dim G = 4$ dropping a summand $\dim G$ for each intersection in (1.10) and an additonal one for the final quotient by G. The space Z is referred to as the hyperkahler quotient of X by G, denoted by $X//G$ and was first introduced in [88]. It can be shown that it is isomorphic to $\mathbb{C}^2/\mathbb{Z}_{n+1}$.

In [86] it is shown that the desingularisations can be described in this setup by slightly altering the above construction. Changing (1.10) to

$$N = \mu_I^{-1}(\alpha) \cap \mu_J^{-1}(\beta) \cap \mu_K^{-1}(\gamma), \qquad \alpha, \beta, \gamma \in \mathfrak{g}, \tag{1.11}$$

we generically obtain a non singular space to which the action of G on X descends as a fixed point free action. Taking the quotient by this action we obtain a generically smooth asymptotically locally euclidean (ALE) space Z of $SU(2)$ holonomy. In addition Z is a hyperkahler manifold itself as the hyperkahler structures of X descend to Z.

To study the topology of these solutions we start by considering the unresolved case of $n = 2$ with $\alpha = \beta = \gamma = 0$ which is isomorphic to $\mathbb{C}^2/\mathbb{Z}_2$ given by (1.5) as the the singular variety

$$x^2 + y^2 + z^2 = 0, \qquad (x, y, z) \in \mathbb{C}^3. \tag{1.12}$$

Grouping real and imaginary parts of x, y, z into vectors u and v respectively (1.12) becomes

$$u^2 = v^2, \qquad uv = 0, \tag{1.13}$$

which describes a circle bundle over $\mathbb{R}^3$ with the base parametrised by say u as the equations assert that we are dealing with a sphere bundle where each fiber has been intersected with a plane through the origin. One notices in addition that restricting to a sphere of constant radius $B|_r$ in the base the plane determined by the second equation in (1.13) completes one rotation when traversing any great circle. This circle bundle $\pi : Z_r \to B_r$ is characterised by $\pi^* : H_2(B_r, \mathbb{Z}) \cong \mathbb{Z} \to H_2(Z_r, \mathbb{Z})$ where restriction to points of a fixed radius r within the base have been denoted by the corresponding subscript. In the above setup $H_2(Z_r, \mathbb{Z}) \cong \mathbb{Z}$ and so the π^* is characterised by a number α called the winding number, here $\alpha = 1$. The more general case of $\mathbb{C}^2/\mathbb{Z}_2$ described by

$$x^2 + y^2 + z^{n+1} = 0, \qquad (x, y, z) \in \mathbb{C}^3, \tag{1.14}$$

is treated similarly its topology is also that of a circle fibration but now $\alpha = n$. A topological defect sits at the origin.

Resolving the singularity and executing the hyperkahler quotient construction as in [87] we find the metric on Z to be the multi centred Taub-NUT metric [89]

$$ds^2 = U d\vec{X} d\vec{X} + \frac{1}{U}(d\theta + \vec{\eta} d\vec{X})^2, \qquad U = \sum_{k=1}^{n} \frac{\mu}{|\vec{X} - \vec{x}_k|} + \frac{1}{\lambda^2} \tag{1.15}$$

in the limit $\lambda \to \infty$ with $\vec{x}_i = \vec{x}_j$. Here $\vec{X}$ are coordinates on $\mathbb{R}^3$ and θ is an angular coordinate, the structure of a circle fibration has persisted. The vector $\vec{\eta}$ is such that the $U(1)$ connection $\Omega = \vec{\eta} d\vec{X}$ on $\mathbb{R}^3$ satisfies $dU = *d\Omega$. The position vectors $\vec{x}_k(\alpha, \beta, \gamma)$ collect the $3n$ moduli of the metric marking the points at which the circle fibres degenerate. The resolution Z develops singularities of type $\mathbb{C}^2/\mathbb{Z}_m$ whenever m of the $\vec{x}_k$ collide. This corresponds to a remnant singularity or equivalently only a partial resolution of the singularity. Other ADE singularities can be resolved similarly by ALE spaces of $SU(2)$ holonomy.

Chapter 2
The Gauge Theory Sector of M-theory on G_2-manifolds

M-theory compactified on a G_2-manifold gives rise to a 4d $\mathcal{N} = 1$ supersymmetric gauge theory with matter fields, coupled to supergravity. In this thesis we will be interested in the gauge theories obtained from such compactifications and therefore will decouple gravity. Gauge degrees of freedom in an M-theory compactification on a holonomy G_2-manifold are localized on codimension 4 subspaces, which are associative (i.e., calibrated) three-cycles M_3. Locally the geometry takes the form of an ALE-fibration over M_3 as in (1). A useful way to characterize the gauge sector is to think in terms of the 7d SYM theory obtained from M-theory on the ALE-fiber: the gauge bosons in the Cartan subalgebra of the gauge group arise from dimensional reduction of the M-theory three-form C_3 on the two-forms in the ALE-fiber, and the remaining non-abelian gauge bosons arise from wrapped M2-branes. In an adiabatic approximation, where the ALE-fibration varies slowly over M_3, the 4d effective action can be obtained by dimensionally reducing this 7d SYM theory on the three-cycle M_3, with a partial topological twist. In this section we carry out this reduction and determine the spectrum of gauge and matter fields, which are determined by solutions of BPS equations along M_3 (see (2.18)). The solutions are given in terms of a Higgs bundle over M_3, that is specified by a one-form Higgs field ϕ and an internal gauge field A.

2.1 Partial Topological Twist and BPS Equations

We start with 7d SYM with ADE gauge group $\widetilde{G}$. This theory can be obtained by dimensional reduction of the maximally supersymmetric 10d SYM on $\mathbb{R}^{1,6} \times T^3$. Our conventions are such that the 10d gauge multiplet consists of a (hermitian) gauge field A and a Majorana-Weyl spinor λ both valued in the adjoint representation of an ADE group $\widetilde{G}$. The Lorentz group, and thereby the vector multiplet, reduce as follows

$$
\begin{aligned}
SO(1,9)_L &\quad \rightarrow \quad SO(1,6)_L \times SO(3)_R \\
A: \quad \mathbf{10} &\quad \rightarrow \quad (\mathbf{7},\mathbf{1}) \oplus (\mathbf{1},\mathbf{3}) \equiv (A_M, \phi_i) \\
\lambda: \quad \mathbf{16} &\quad \rightarrow \quad (\mathbf{8},\mathbf{2}) \equiv (\lambda_{\alpha\hat{\alpha}}) \,,
\end{aligned}
\tag{2.1}
$$

where the 10d vector indices are split into $M = 0,\dots,6$ and $i = 1,2,3$ and the spinor indices decompose as $\alpha = 1,\dots,8$ and $\hat{\alpha} = 1,2$, where we denote the R-symmetry indices with a hat. The 10d Majorana condition descends to a 7d symplectic Majorana-condition[1]. Denoting the gauge coupling in 7d by g_7 the action becomes

$$
\begin{aligned}
S_{\text{7d}} = \frac{1}{g_7^2} \int d^7x &\left[-\frac{1}{4}\text{Tr}\left(F_{MN}F^{MN}\right) - \frac{1}{2}\text{Tr}\left(D_M\phi_i D^M\phi^i\right) + \frac{1}{4}\text{Tr}\left([\phi_i,\phi_j][\phi^i,\phi^j]\right) \right] \\
&+ \frac{1}{g_7^2} \int d^7x \left[+\frac{i}{2}\text{Tr}\left(\bar{\lambda}^{\alpha\hat{\alpha}}(\hat{\gamma}^M)_\alpha{}^\beta D_M\lambda_{\beta\hat{\alpha}}\right) - \frac{i}{2}\text{Tr}\left(\bar{\lambda}^{\alpha\hat{\alpha}}(\sigma^i)_{\hat{\alpha}}{}^{\hat{\beta}}[\phi_i,\lambda_{\alpha\hat{\beta}}]\right) \right] \,,
\end{aligned}
\tag{2.2}
$$

where $D_M = \partial_M - i[A_M,\cdot\,]$ and F is the field strength associated to A. The supersymmetry variations are

$$
\begin{aligned}
\delta A_M &= +\frac{i}{2}\bar{\epsilon}^{\alpha\hat{\alpha}}(\hat{\gamma}_M)_\alpha{}^\beta \lambda_{\beta\hat{\alpha}} \\
\delta\phi_i &= +\frac{1}{2}\bar{\epsilon}^{\alpha\hat{\alpha}}(\sigma_i)_{\hat{\alpha}}{}^{\hat{\beta}}\lambda_{\alpha\hat{\beta}} \\
\delta\lambda_{\alpha\hat{\alpha}} &= -\frac{1}{4}F_{MN}(\hat{\gamma}^{MN})_\alpha{}^\beta\epsilon_{\beta\hat{\alpha}} + \frac{i}{2}D_M\phi_i(\hat{\gamma}^M)_\alpha{}^\beta(\sigma^i)_{\hat{\alpha}}{}^{\hat{\beta}}\epsilon_{\beta\hat{\beta}} - \frac{1}{4}[\phi_i,\phi_j]\epsilon^{ij}{}_k(\sigma^k)_{\hat{\alpha}}{}^{\hat{\beta}}\epsilon_{\alpha\hat{\beta}} \,,
\end{aligned}
\tag{2.3}
$$

where $\hat{\gamma}$ denotes the 7d gamma matrices.

This 7d SYM theory is the starting point for the analysis of gauge degrees of freedom in a local G_2-holonomy compactification of M-theory. For a given ALE-fiber, the singularity determines the 7d gauge group $\widetilde{G}$. We now reduce this theory further on an associative three-cycle M_3. Since this will be generically curved with holonomy group $SO(3)$, the 4d

---

[1]We refer to appendix A of [1] for our conventions with regards to spinors and supersymmetry.

theory will in turn only retain supersymmetry if we partially topologically twist the local Lorentz group $SO(3)_M$ with the R-symmetry $SU(2)_R$. Upon compactification on M_3 the local Lorentz symmetry is broken to

$$
\begin{aligned}
SO(1,6)_L \times SU(2)_R \quad &\rightarrow \quad SO(1,3)_L \times SO(3)_M \times SU(2)_R \\
A: \quad (\mathbf{7},\mathbf{1}) \quad &\rightarrow \quad (\mathbf{2},\mathbf{2};\mathbf{1},\mathbf{1}) \oplus (\mathbf{1},\mathbf{1};\mathbf{3},\mathbf{1}) \equiv (W_\mu, A_{\underline{i}}) \\
\phi: \quad (\mathbf{1},\mathbf{3}) \quad &\rightarrow \quad (\mathbf{1},\mathbf{1};\mathbf{1},\mathbf{3}) \equiv (\phi_{\hat{i}}) \\
\epsilon,\ \lambda: \quad (\mathbf{8},\mathbf{2}) \quad &\rightarrow \quad (\mathbf{2},\mathbf{1};\mathbf{2},\mathbf{2}) \oplus (\mathbf{1},\mathbf{2};\mathbf{2},\mathbf{2}) \equiv (\lambda_{\alpha\underline{\alpha}\hat{\alpha}}, \bar{\lambda}_{\dot{\alpha}\underline{\alpha}\hat{\alpha}}),
\end{aligned}
\tag{2.4}
$$

where the vector indices split as $\mu = 0,\ldots,3$ and $\underline{i}, \hat{i} = 1,2,3$ and the spinor indices are $\alpha, \dot{\alpha}, \underline{\alpha}, \hat{\alpha} = 1,2$. The fermions $\lambda_{\alpha\underline{\alpha}\hat{\alpha}}$ satisfy a Majorana-condition.

The supersymmetry parameter ϵ transforms non-trivially under $SO(3)_M$, so that to preserve supersymmetry in 4d, we redefine the local Lorentz group $SO(3)_M$ by an R-symmetry transformation[2] [10, 18, 80]

$$
SU(2)_{\text{twist}} = \text{diag}(SO(3)_M, SU(2)_R),
\tag{2.5}
$$

with generators $(\Sigma_M)_i + (\Sigma_R)_i$, where Σ denotes the generators of the respective algebras. The field content and supersymmetry parameters transform under the partially twisted Lorentz group as follows

$$
\begin{aligned}
SO(1,3)_L \times SU(2)_M \times SU(2)_R \quad &\rightarrow \quad SO(1,3)_L \times SU(2)_{\text{twist}} \\
W: \quad (\mathbf{2},\mathbf{2};\mathbf{1};\mathbf{1}) \quad &\rightarrow \quad (\mathbf{2},\mathbf{2};\mathbf{1}) \equiv (W_\mu) \\
A: \quad (\mathbf{1},\mathbf{1};\mathbf{3},\mathbf{1}) \quad &\rightarrow \quad (\mathbf{1},\mathbf{1};\mathbf{3}) \equiv (A_i) \\
\phi: \quad (\mathbf{1},\mathbf{1};\mathbf{1},\mathbf{3}) \quad &\rightarrow \quad (\mathbf{1},\mathbf{1};\mathbf{3}) \equiv (\phi_i) \\
\epsilon,\ \lambda: \quad (\mathbf{2},\mathbf{1};\mathbf{2},\mathbf{2}) \quad &\rightarrow \quad (\mathbf{2},\mathbf{1};\mathbf{1}) \oplus (\mathbf{2},\mathbf{1};\mathbf{3}) \equiv (\chi_\alpha, \psi_{i\alpha}) \\
\bar{\epsilon},\ \bar{\lambda}: \quad (\mathbf{1},\mathbf{2};\mathbf{2},\mathbf{2}) \quad &\rightarrow \quad (\mathbf{1},\mathbf{2};\mathbf{1}) \oplus (\mathbf{1},\mathbf{2};\mathbf{3}) \equiv (\bar{\chi}^{\dot{\alpha}}, \bar{\psi}_i{}^{\dot{\alpha}}).
\end{aligned}
\tag{2.6}
$$

It follows that there are four real supercharges, as required for 4d $\mathcal{N} = 1$ supersymmetry,

$$
\epsilon_\alpha = (\mathbf{2},\mathbf{1};\mathbf{1}), \qquad \bar{\epsilon}_{\dot{\alpha}} = (\mathbf{1},\mathbf{2};\mathbf{1}).
\tag{2.7}
$$

---

[2] We will be slightly casual here and in the following, in that the twist involves the Lie algebras, rather than the groups.

After the twist the fermions χ and ψ transform as singlets and triplets of the twisted Lorentz group and are identified with 0- and 1-forms on M_3 valued in $\mathrm{ad}(P)$, i.e.,

$$\chi \in \Omega^0(M_3, \mathrm{ad}(P)) \otimes \mathbb{C}$$
$$\psi \in \Omega^1(M_3, \mathrm{ad}(P)) \otimes \mathbb{C}, \tag{2.8}$$

where P is a $\widetilde{G}$-principal bundle. We denote the field strengths associated to the gauge fields W_μ and the internal connection A_i by $F_{\mu\nu}$ and $(F_A)_{ij}$, respectively, and their associated covariant derivatives as D_μ and D_i. The latter can be combined with the scalars ϕ_i, which both transform as a **3** of $SU(2)_{\mathrm{twist}}$, into a complex 1-form

$$\varphi_i = \phi_i + iA_i, \qquad \bar\varphi_i = \phi_i - iA_i, \qquad \mathcal{D}_i = \partial_i + [\varphi_i, \cdot], \qquad \bar{\mathcal{D}}_i = \partial_i - [\bar\varphi_i, \cdot]. \tag{2.9}$$

Note that $\varphi, \bar\varphi$ and $\mathcal{D}, \bar{\mathcal{D}}$ are related by conjugation in the gauge algebra. We further introduce

$$(\mathcal{F}_\varphi)_{ij} = [\mathcal{D}_i, \mathcal{D}_j], \qquad (\mathcal{F}_\varphi)_{\mu i} = [D_\mu, \mathcal{D}_i], \qquad (\mathcal{F}_{\bar\varphi})_{\mu i} = [D_\mu, \bar{\mathcal{D}}_i], \tag{2.10}$$

and its conjugate $\mathcal{F}_{\bar\varphi} = \mathcal{F}_\varphi^\dagger$. We assume that the 4d gauge fields A_μ are independent of the internal coordinates along M_3, so that the latter two expressions become standard space-time derivatives of the complex scalars $\varphi, \bar\varphi$

$$(\mathcal{F}_\varphi)_{\mu i} = D_\mu \varphi_i, \qquad (\mathcal{F}_{\bar\varphi})_{\mu i} = D_\mu \bar\varphi_i. \tag{2.11}$$

Define the interaction term

$$I_{\varphi,\bar\varphi} \equiv 2D_i\phi^i = \partial_i\varphi^i + \partial_i\bar\varphi^i + [\varphi_i, \bar\varphi^i]. \tag{2.12}$$

The partially twisted 7d SYM action is then

$$S_{F,\,\mathrm{twist}} = \frac{1}{g_7^2} \int d^7x \left\{ \mathrm{Tr}\left[-i\bar\chi\bar\sigma^\mu D_\mu\chi - i\bar\psi^i\bar\sigma^\mu D_\mu\psi_i + \sqrt{2}i\bar\chi\mathcal{D}^i\bar\psi_i - \sqrt{2}i\chi\bar{\mathcal{D}}^i\psi_i \right. \right.$$
$$\left. + \frac{i}{\sqrt{2}}\epsilon^{ijk}\bar\psi_i\bar{\mathcal{D}}_j\bar\psi_k - \frac{i}{\sqrt{2}}\epsilon^{ijk}\psi_i\mathcal{D}_j\psi_k \right] \Bigg\}$$
$$S_{B,\,\mathrm{twist}} = \frac{1}{g_7^2} \int d^7x \left\{ -\frac{1}{4}\mathrm{Tr}\left[F_{\mu\nu}F^{\mu\nu}\right] - \mathrm{Tr}\left[(\mathcal{F}_\varphi)_{\mu i}(\mathcal{F}_{\bar\varphi})^{\mu i}\right] - \mathrm{Tr}\left[(\mathcal{F}_\varphi)_{ij}(\mathcal{F}_{\bar\varphi})^{ij}\right] \right.$$
$$\left. -\frac{1}{2}\mathrm{Tr}\left[I_{\varphi,\bar\varphi}^2\right] \right\}. \tag{2.13}$$

The supersymmetry variations for the bosonic fields are

$$\delta W_\mu = i\epsilon\sigma_\mu\bar\chi\,, \qquad \bar\delta W_\mu = -i\bar\epsilon\bar\sigma_\mu\chi$$

$$\delta A_i = -\frac{i}{\sqrt{2}}\epsilon\psi_i\,, \qquad \bar\delta A_i = \frac{i}{\sqrt{2}}\bar\epsilon\bar\psi_i$$

$$\delta\phi_i = \frac{1}{\sqrt{2}}\epsilon\psi_i\,, \qquad \bar\delta\phi_i = \frac{1}{\sqrt{2}}\bar\epsilon\bar\psi_i \qquad (2.14)$$

$$\delta\varphi_i = \sqrt{2}\epsilon\psi_i\,, \qquad \bar\delta\varphi_i = 0$$

$$\delta\bar\varphi_i = 0\,, \qquad \bar\delta\bar\varphi_i = \sqrt{2}\bar\epsilon\bar\psi_i\,,$$

and for the fermionic ones we find

$$\delta\chi = F_{\mu\nu}\sigma^{\mu\nu}\epsilon + iI_{\varphi,\bar\varphi}\epsilon\,, \qquad \bar\delta\chi = 0$$

$$\delta\bar\chi = 0\,, \qquad \bar\delta\bar\chi = F_{\mu\nu}\bar\epsilon\bar\sigma^{\mu\nu} - iI_{\varphi,\bar\varphi}\bar\epsilon$$

$$\delta\psi^k = i(\mathcal{F}_{\bar\varphi})_{ij}\epsilon^{ijk}\epsilon\,, \qquad \bar\delta\psi^k = \sqrt{2}i(\mathcal{F}_\varphi)_\mu{}^k\sigma^\mu\bar\epsilon \qquad (2.15)$$

$$\delta\bar\psi^k = \sqrt{2}i(\mathcal{F}_{\bar\varphi})_\mu{}^k\bar\sigma^\mu\epsilon\,, \qquad \bar\delta\bar\psi^k = -i(\mathcal{F}_\varphi)_{ij}\epsilon^{ijk}\bar\epsilon\,.$$

To obtain a 4d supersymmetric theory upon twisted dimensional reduction, the field configuration along M_3 needs to preserve supersymmetry. We further require the background to enjoy 4d Poincaré-invariance and therefore require it to be independent of the coordinates along $\mathbb{R}^{1,3}$

$$(\mathcal{F}_\varphi)_{\mu i} = 0\,, \qquad (\mathcal{F}_{\bar\varphi})_{\mu i} = 0\,. \qquad (2.16)$$

The BPS equations are then obtained by setting $\langle\delta\lambda\rangle = 0$ and are

$$I_{\varphi,\bar\varphi} = \partial_i\varphi^i + \partial_i\bar\varphi^i + [\varphi_i,\bar\varphi^i] = 0\,, \qquad (\mathcal{F}_\varphi)_{ij} = 0\,, \qquad (\mathcal{F}_{\bar\varphi})_{ij} = 0\,, \qquad (2.17)$$

where the first equation is obtained by setting the real and imaginary parts of $\delta\chi$ to zero separately. 4d Poincaré invariance requires $\langle F_{\mu\nu}\rangle = 0$. Rewriting (2.17) with respect to the notation in (2.6) the BPS equations become the F- and D-term equations

$$\boxed{\begin{aligned} 0 &= F_A - i[\phi,\phi] \\[4pt] 0 &= D_A\phi \\[4pt] 0 &= D_A^\dagger\phi\,. \end{aligned}} \qquad (2.18)$$

Background values for the Higgs field ϕ and gauge field W along M_3 that solve these equations will determine the effective field theory in 4d[3] and describe the classical supersymmetric vacua for the compactified theory. In components the BPS equations are

$$0 = \partial_i A_j - \partial_j A_i + i[A_i, A_j] - i[\phi_i, \phi_j]$$

$$0 = \partial_i \phi_j + i[A_i, \phi_j] - \partial_j \phi_i - i[A_j, \phi_i] \qquad (2.19)$$

$$0 = g^{ij} \left(\partial_i \phi_j + i[A_i, \phi_j] \right) .$$

Depending on the topology of M_3 there are various solutions to these equations. The simplest set of solutions are obtained for commuting Higgs fields

$$[\phi, \phi] = 0 , \qquad F_A = 0 . \qquad (2.20)$$

We will generally assume this to be the case. The Higgs field backgrounds derived from an ALE-fibered G_2-manifold necessarily commute and so this class of solutions is sufficient for the study of local geometries. Solutions with non-vanishing field strength are referred to as T-branes [90] but are not straight forwardly related to geometries with G_2 holonomy but offer an alternative approach in the construction of chiral 4d theories. The remaining equations are $D_A \phi = *D_A^\dagger \phi = 0$. If M_3 is a compact three-manifold without boundaries and ϕ is regular, there are two cases to consider:

$$\pi_1(M_3) = 0 \quad \Rightarrow \quad A = 0 , \quad d\phi = *d*\phi = 0 \quad \Rightarrow \quad \phi = 0$$

$$\pi_1(M_3) \neq 0 \quad \Rightarrow \quad D_A \phi = D_A^\dagger \phi = 0 . \qquad (2.21)$$

In the first case ϕ has to be a harmonic 1-form and thus must be trivial, in the second case it can be non-trivial.

We will be interested in simply-connected three-manifolds in the following. To nevertheless have non-trivial solutions we relax the assumption that ϕ is regular, which can be achieved by including sources into the D-term equations. Writing $\phi = df$, the function f is then required to satisfy Poisson's equation

$$\phi = df , \qquad \Delta f = \rho , \qquad (2.22)$$

---

[3]Note that we have chosen Hermitian representatives for the gauge algebra. Transitioning to anti-Hermitian representatives we recover the results of [49].
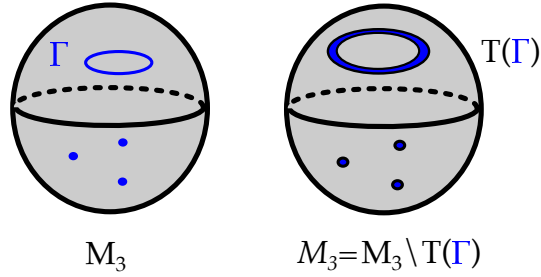
Figure 2.1: On the left hand side the three-cycle M_3 is shown, with the charge distribution ρ that is located along Γ. On the right hand side, a tubular neighborhood $T(\Gamma)$ is excised and the resulting manifold is $\mathcal{M}_3$.

where ρ models the sources supported on a closed subset Γ. This maps the solution of the BPS equations to an electrostatics problem with the identification

$$f = \text{electrostatic potential}$$
$$\rho = \text{charge density, supported on } \Gamma \subset M_3 \,.$$

(2.23)

Alternatively this system can be described by excising a tubular neighborhood $T(\Gamma)$ of the charge support Γ, and studying the problem of finding solutions on $\mathcal{M}_3 = M_3 \setminus T(\Gamma)$ – see figure 2.1. In this case ϕ needs to be regular, with suitable boundary conditions along $\partial \mathcal{M}_3$. In summary one of the setups will we consider is

$$\boxed{\phi \text{ regular} , \quad \phi = df , \quad \Delta f = 0 , \quad \partial \mathcal{M}_3 = T(\Gamma) \neq \emptyset}$$

(2.24)

which will be used in chapter 4 to determine physically interesting solutions to the BPS equations including localized matter. Localized matter is characterized by the vanishing of ϕ. When f is Morse (i.e., it has no degenerate critical points) these are isolated points and we will discuss this setup in chapter 4. By relaxing the constraint of f only having isolated critical points this can be generalized to situations where f is a Morse-Bott function and higher-dimensional matter loci can be included as well. We will discuss this in chapter 5.4 and apply it to TCS G_2-manifolds in chapter 8.

The Higgs field of the solutions to (2.24) is well-defined away from the support of the source terms, where it diverges. In particular there are no monodromies of the Higgs field eigenvalues when encircling the graph Γ. The graph Γ is codimension 2 in M_3 and the

solution to the Poisson's equation with such sources is branch cut free, this changes when considering sources of codimension 1. In this case the function f is not differentiable across surface sources and the corresponding electric field jumps, signalling a possible branch cut. We refer to Higgs fields whose eigenvalues can be globally distinguished as *split* and to all other cases as *non-split*. The eigenvalues of a non-split Higgs field glue to a connected covering and separating this covering into sheets amounts to specifying the surface sources realizing the discontinuities in the Higgs field eigenvalues. Dissecting a covering in this fashion both electric and magnetic sources in codimension one can appear. Therefore non-split Higgs bundles are described by generalizing (2.22) to

$$d\phi = *j\,, \qquad *d*\phi = \rho\,. \qquad (2.25)$$

The Higgs field eigenvalues now display finite discontinuities across surfaces supporting j, ρ which must be such that the set of eigenvalues glue consistently across the codimension one source loci. We consider these cases in chapter 3. The interpretation for particular source terms is taken from the corresponding IIA string theory set-up for gauge algebras $\mathfrak{g}_{\text{ADE}} = \mathfrak{su}(n)$ which is given by space-time filling D6-branes on $\mathbb{R}^{1,3} \times T^*M_3$ wrapping a special Lagrangian submanifold in T^*M_3 [49,91]. Sources of codimension 2 and 3 lead to singularities in the Higgs field and D6-branes associated with the corresponding eigenvalues are non-compact as they extend to infinity in the fiber direction. Embedding the local model into a compact geometry these would simply describe D6-branes extending beyond the approximated region. Magnetic and electric sources j and ρ of codimension 2 along a knot $K \subset S^3 \subset T^*M_3$, represent the world volume perspective of D6-branes intersecting along the knot K which have recombined due to a condensation of the bifundamental chiral superfields localized at their intersection [92,93]. In the remainder of this section, we assume that ϕ is non-trivial and regular, but make no further assumptions on the details of the loci $\phi = 0$.

2.2 Higgs Bundles

Before studying the low energy effective theory, let us briefly recall the relation between the Higgs bundle and the local ALE-fibration. The BPS equations (in the absence of sources) (2.18) are in fact precisely the odd dimensional analogue of the Hitchin equations for the Higgs field ϕ giving rise to the data of a Higgs bundle. In the case $[\phi, \phi] = 0$ there is an elegant geometric description of the Higgs field ϕ in terms of an ALE-fibration over M_3, which we now summarize [49]. This construction is analogous to the one in F-theory, where the Higgs field specifies the unfolding (a complex structure deformation) of the ALE singularity and is closely connected to the compact Calabi-Yau underlying the F-theory compactification [11, 15, 94]. Recently this was developed also for Spin(7) manifolds [95]. In our case the Higgs field describes the deformations of the full hyper-Kähler structure of an ALE fiber.

Recall that ϕ is an adjoint valued 1-form $\Omega^1(\mathcal{M}_3)$ or a section of $T^*(\mathcal{M}_3)$, and we take it to be non-trivial along the commutant $G_\perp$ of the 4d gauge group G in

$$\widetilde{G} \to G_\perp \times G. \tag{2.26}$$

The Higgs field is

$$\phi \in \Gamma(T^*(\mathcal{M}_3) \otimes \mathrm{Ad}(G_\perp)), \tag{2.27}$$

i.e., ϕ lives in a local geometry in the vicinity of $\mathcal{M}_3$ which is the total space of the cotangent bundle $T^*(\mathcal{M}_3)$. This is a local Calabi-Yau threefold. Since $[\phi, \phi] = 0$, we can diagonalize the Higgs field to obtain n 1-forms ϕ_j, where n is the rank of the Lie algebra $\mathfrak{g}_\perp$ of $G_\perp$. To locally recover the ALE-fibration over $\mathcal{M}_3$ associated to this Higgs field, we use the Kronheimer construction [34, 96]. Every hyper-Kähler ALE-orbifold is of the form $\mathbb{C}^2/\Gamma_{\mathrm{ADE}}$, where Γ_{ADE} is a finite subgroup of $SU(2)$, which are classified by the corresponding ADE Dynkin diagrams. The second homology of the resolution of singularities of $\mathbb{C}^2/\Gamma_{\mathrm{ADE}}$ is isomorphic to the Cartan subalgebra of $\mathfrak{g}$ and we can think of the components ϕ_j as measuring the periods of the hyper-Kähler structure forms. More explicitly, over a local patch of M_3 we

can write the fibration as $\mathbb{R}^3 \times \mathbb{C}^2/\Gamma_{\text{ADE}}$. We chose a basis σ_j of $H_2(\mathbb{C}^2/\Gamma_{\text{ADE}}, \mathbb{Z})$ and fix a hyper-Kähler triple $(\omega_I, \omega_J, \omega_K)$. The 1-form ϕ_j can be written as

$$\phi_j = \phi_{j,I} dx^1 + \phi_{j,J} dx^2 + \phi_{j,K} dx^3 \,, \tag{2.28}$$

where we identify

$$\phi_{j,I} = \int_{\sigma_j} \omega_I, \qquad \phi_{j,J} = \int_{\sigma_j} \omega_J, \qquad \phi_{j,K} = \int_{\sigma_j} \omega_K \,. \tag{2.29}$$

This uniquely defines the hyper-Kähler structure on each fiber. Observe that the Higgs field has an $SO(3)$ symmetry arising from the $SO(3)$ acting on ω_I, ω_J and ω_K.

In geometric terms we can describe our situation as follows. For simplicity, assume that we have a $G_\perp = U(1)$-valued Higgs field ϕ. We are considering a local model for a G_2-manifold with ADE-singularities located along an associative submanifold $\mathcal{M}_3$, which physically means that gauge degrees of freedom are localized along $\mathcal{M}_3$ and the gauge group is given by the ADE type of the singularity. Consider the gauge group $\widetilde{G}$, which by turning on a non-trivial background vev for ϕ generically higgses to $\widetilde{G} \rightarrow G \times U(1)$. This means that the ALE fiber over a generic point of $\mathcal{M}_3$ will have the singularity corresponding to G via the ADE correspondence and there will be a two-cycle in the $U(1)$ direction with non-zero volume, given by ϕ. Over the points where $\phi = 0$, the two-cycle collapses and the ALE singularity worsens; equivalently the gauge group enhances from G to $\widetilde{G}$. We will elaborate this point in chapter 7.

We can in fact make the local geometry of the gauge enhancement fairly explicit. For the moment let us restrict our attention to the case where $\widetilde{G} = SU(2)$ which corresponds to a $\mathbb{C}^2/\mathbb{Z}_2$ singularity over $\mathcal{M}_3$. Giving a non-trivial background vev for ϕ corresponds to deforming the generic fiber to a smooth Eguchi-Hanson space. More precisely, consider the generator σ of $H_2(\widetilde{\mathbb{C}^2/\mathbb{Z}_2}, \mathbb{Z})$ of the resolved geometry. Recall that σ is topologically a two-sphere. From (2.28) and (2.29) we see that at a generic point $x \in \mathcal{M}_3$ (which for this purpose is approxated locally by $\mathbb{R}^3$) we have

$$\text{Vol}(\sigma) = |\phi(x)| \,, \tag{2.30}$$

by which we mean the volume of σ in the Eguchi-Hanson space above x. Consider now a neighborhood of a non-degenerate zero of ϕ, which we can assume to be at $0 \in \mathbb{R}^3$. We can locally write $\phi = df$, where

$$f(x_1, x_2, x_3) = f(0) + \frac{1}{2} \sum_{i=1}^{3} \pm x_i^2. \tag{2.31}$$

The signs depend on the eigenvalue of the Hessian at 0. The Higgs field ϕ now has an isolated zero at the origin. The explicit local description of the ALE-fibration is given by

$$X = \left\{ (z_1, z_2, z_3),\, (x_1, x_2, x_3) \,\middle|\, z_1^2 + z_2^2 + z_3^2 = \sum_{i=1}^{3} x_i^2 \right\} \subset \mathbb{C}^3 \times \mathbb{R}^3. \tag{2.32}$$

Viewing X as a fibration over $\mathbb{R}^3$ all of the fibers are smooth apart from the fiber over $(0,0,0)$ i.e., the zero of ϕ. Moreover, X is a cone in $\mathbb{C}^3 \times \mathbb{R}^3$ with the apex at the origin. The link of the cone can be found by intersecting X with the unit sphere in $\mathbb{C}^3 \times \mathbb{R}^3$ and is in fact $\mathbb{P}^3$ realized as the twistor bundle over S^4. The approximate G_2-metric on X is given by

$$\Phi = dx_1 \wedge dx_2 \wedge dx_3 + dx_1 \wedge \omega_I + dx_2 \wedge \omega_J + dx_3 \wedge \omega_K + \phi \wedge \eta, \tag{2.33}$$

where η is the 2-form dual to the two-cycle σ.

This can be generalized to arbitrary ALE-fibrations. The local geometry is of the form $\mathbb{C}^2/\Gamma_G \times \mathbb{R}^3$, with a $\mathbb{C}^2/\Gamma_{\widetilde{G}}$ fiber over the origin. We again work with $\widetilde{G} = SU(n+1)$. For the deformations of other ADE singularities see [97]. The topology in a neighborhood of an isolated zero is

$$X = \left\{ (z_1, z_2, z_3),\, (x_1, x_2, x_3) \,\middle|\, z_1^2 + z_2^2 + z_3^n \left(z_3 - \sum_{i=1}^{3} x_i^2 \right) = 0 \right\} \subset \mathbb{C}^3 \times \mathbb{R}^3. \tag{2.34}$$

This describes a family of $SU(n)$ singularities, with enhancement to $SU(n+1)$ at the origin (note that we again write $\phi = df$ as above). There are also explicit deformations for other ADE groups. Topologically X is now a cone over the weighted projective space $\mathbb{P}^3_{n,n,1,1}$ with coordinates (y_1, y_2, y_3, y_4) [34]. In the link, there is a family of $SU(n)$ singularities along an S^2 given by $y_3 = y_4 = 0$. In the ambient space, the location of the singularities is a cone

$\mathbb{R}^+ \times S^2 = \mathbb{R}^3$, which is identified in our context with a local patch of the base $\mathbb{R}^3$ of X. As before, the apex of the cone is where the cycle σ collapses to zero volume.

This therefore establishes a key piece of the dictionary between properties of ϕ and the ambient G_2-geometry. The isolated zeroes of ϕ give rise to conical singularities of the ALE-fibered G_2-manifold. As we show in chapter 5, this fits together nicely with the physics side as zeroes of ϕ which occur at codimension 7 are precisely the loci where chiral fermions are localized.

2.3   Massless Spectrum

Given a solution to the BPS equations (2.18) with regular Higgs field we can ask what the spectrum of the 4d gauge theory is. The equations of motion of the fermions follow from (2.13) to be

$$0 = \bar{\sigma}^\mu D_\mu \chi - \sqrt{2} \mathcal{D}_i \bar{\psi}^i$$
$$0 = \bar{\sigma}^\mu D_\mu \psi^i + \sqrt{2} \mathcal{D}^i \bar{\chi} - \sqrt{2} \epsilon^{ijk} \bar{\mathcal{D}}_j \bar{\psi}_k \,, \tag{2.35}$$

which imply the decoupled equations

$$0 = D_\mu D^\mu \chi + 2 \mathcal{D}_i \bar{\mathcal{D}}^i \chi$$
$$0 = D_\mu D^\mu \psi_i + 2[\mathcal{D}_i, \bar{\mathcal{D}}_j]\psi^j + 2 \bar{\mathcal{D}}_j \mathcal{D}^j \psi_i \,. \tag{2.36}$$

So far we have not imposed $[\phi, \phi] = 0$. Define the twisted exterior derivative and Laplace operator

$$\mathcal{D} = d + [\varphi \wedge \cdot] \,, \qquad \bar{\mathcal{D}} = d - [\bar{\varphi} \wedge \cdot] \,, \qquad \Delta = \mathcal{D}^\dagger \mathcal{D} + \mathcal{D} \mathcal{D}^\dagger \,, \qquad \bar{\Delta} = \bar{\mathcal{D}}^\dagger \bar{\mathcal{D}} + \bar{\mathcal{D}} \bar{\mathcal{D}}^\dagger \,, \tag{2.37}$$

where the adjoint is taken with respect to the Hermitian inner product

$$\langle \, \cdot \, , \cdot \, \rangle : \Omega^p(M_3, \mathrm{ad}(P)) \times \Omega^p(M_3, \mathrm{ad}(P)) \;\to\; \mathbb{C}$$
$$(\alpha, \beta) \;\to\; \langle \alpha, \beta \rangle = \int_{M_3} \mathrm{Tr}\,(\bar{\alpha} \wedge *\beta) \,. \tag{2.38}$$

Acting on functions $g \in \Omega^0(M_3, \mathrm{ad}\, P)$ and written in coordinates, e.g., the operator $\bar{\Delta}$ becomes

$$\bar{\Delta} g = \bar{\mathcal{D}}^\dagger \bar{\mathcal{D}} g = \bar{\mathcal{D}}^\dagger (\bar{\mathcal{D}}_m g \, dx^m) = \mathcal{D}^m \bar{\mathcal{D}}_m g \,, \tag{2.39}$$

where we pick up a conjugation due to the inner product. We find that (2.36) may be rewritten as

$$0 = D_\mu D^\mu \chi + 2\bar{\Delta}\chi$$
$$0 = D_\mu D^\mu \psi + 2\Delta\psi\,,$$

$$(2.40)$$

where by (2.8), χ and ψ are 0- and 1-forms, respectively. Massless modes are therefore described by the kernels of the Laplacians $\Delta, \bar{\Delta}$ or equivalently by closed and co-closed forms with respect to the operators in (2.37)

$$\bar{\mathcal{D}}\chi = 0\,, \qquad \bar{\mathcal{D}}^\dagger \chi = 0$$
$$\mathcal{D}\psi = 0\,, \qquad \mathcal{D}^\dagger \psi = 0\,.$$

$$(2.41)$$

By the BPS equations the co-boundary operators $\mathcal{D}, \bar{\mathcal{D}}$ and their adjoints close $\mathcal{D}^2 = \bar{\mathcal{D}}^2 = 0$ and $(\mathcal{D}^\dagger)^2 = (\bar{\mathcal{D}}^\dagger)^2 = 0$, and via the Hodge correspondence for elliptic complexes we can describe the zero modes equivalently as cohomology groups. The non-vanishing background value of ϕ or W oriented along a subgroup $G_\perp$ of $\widetilde{G}$ breaks the gauge group to its commutant $G \subset \widetilde{G}$. The adjoint fermions ψ, χ will decompose accordingly to give matter valued in irreducible representations. In this higgsed theory the fermions are sections of the associated gauge bundles, E. The action of $\mathcal{D}$ restricts to each of these subbundles allowing us to make the identification

$$\chi_\alpha \in H^0_{\mathcal{D}}(M_3, E)\,, \qquad \bar{\chi}_{\dot{\alpha}} \in H^0_{\mathcal{D}}(M_3, E)$$
$$\psi_\alpha \in H^1_{\mathcal{D}}(M_3, E)\,, \qquad \bar{\psi}_{\dot{\alpha}} \in H^1_{\mathcal{D}}(M_3, E)\,.$$

$$(2.42)$$

We next rewrite these cohomology groups with respect to the same co-boundary operator by dualising $H^0_{\mathcal{D}}, H^1_{\mathcal{D}}$ with the Hodge star. Note that by (2.38) we have $\mathcal{D}^\dagger = *\bar{\mathcal{D}}*$ and $\bar{\mathcal{D}}^\dagger = *\mathcal{D}*$ so that taking $\chi_\alpha \in H^0_{\mathcal{D}}(M_3, E)$ for example we find that $*\chi_\alpha$ is annihilated by the operators $\mathcal{D}, \mathcal{D}^\dagger$

$$\mathcal{D}^\dagger(*\chi_\alpha) = *\bar{\mathcal{D}}\chi_\alpha = 0\,, \qquad \mathcal{D} * \chi_\alpha = *\bar{\mathcal{D}}^\dagger \chi = 0\,. \qquad (2.43)$$

This precisely states that $*\chi_\alpha \in H^3_{\mathcal{D}}(M_3, E)$, i.e., we have mapped from $\bar{\mathcal{D}}$-cohomology to $\mathcal{D}$-cohomology using the Hodge star. The same observations hold true for $\bar{\psi}_\alpha$. The Hodge star relates

$$H^0_{\mathcal{D}}(M_3, E) \cong H^3_{\mathcal{D}}(M_3, E)\,, \qquad H^1_{\mathcal{D}}(M_3, E) \cong H^2_{\mathcal{D}}(M_3, E)\,. \qquad (2.44)$$

This allows us to make the following identifications

$$
\boxed{
\begin{array}{ll}
\chi_\alpha \in H^3_{\mathcal{D}}(M_3, E)\,, & \bar{\chi}_{\dot{\alpha}} \in H^0_{\mathcal{D}}(M_3, E)\,, \\[2mm]
\psi_\alpha \in H^1_{\mathcal{D}}(M_3, E)\,, & \bar{\psi}_{\dot{\alpha}} \in H^2_{\mathcal{D}}(M_3, E)\,,
\end{array}
}
\tag{2.45}
$$

where now all cohomologies are with respect to $\mathcal{D}$ and forms of all degrees are employed. Note that the $\mathbb{Z}_2$-grading of the exterior algebra aligns with the 4d chirality of the fermionic zero modes. The Hodge star depends on the metric of M_3 which itself is induced from the metric of G_2-holonomy of the ambient 7d manifold.

Since M_3 is associative and so calibrated with respect to Φ_{ijk} we equivalently could have used the G_2 3-form Φ_{ijk} to dualize since it restricts to a volume form of M_3. Contracting elements of $H^0_{\mathcal{D}}$ and $H^1_{\mathcal{D}}$ with the 3-form Φ_{ijk} is then exactly the same as taking their Hodge dual.

2.4   Bulk Matter

The first type of matter we will discuss arises from a background Higgs bundle, where $\langle\phi\rangle = 0$, which solves the BPS equations, but $W \neq 0$ with $F_W = 0$. This will be referred to as bulk matter, as the modes will not be localized. We will see that for $\pi_1(\mathcal{M}_3) = 0$ there is no chiral index for this matter type. It may be interesting to extend this to non-trivial π_1 setups, which we relegate to future work, and also has been discussed in earlier works from a different point of view (see e.g., [98]).

Turning on a flat gauge field along a subgroup $G_\perp \subset \widetilde{G}$ the gauge group $\widetilde{G}$ is Higgsed to the commutant G of $G_\perp$ in $\widetilde{G}$ and the adjoint representation of $\widetilde{G}$ decomposes as

$$
\begin{aligned}
\widetilde{G} &\;\to\; G \times G_\perp \\
\mathrm{Ad}(\widetilde{G}) &\;\to\; (\mathrm{Ad}(G) \otimes \mathbf{1}) \oplus (\mathbf{1} \otimes \mathrm{Ad}(G_\perp)) \oplus \bigoplus_n \mathbf{R}_n \otimes \mathbf{S}_n\,.
\end{aligned}
\tag{2.46}
$$

For the fields of the theory this decomposition is lifted to the bundle level, where $\mathrm{Ad}(P)$ decomposes into the vector bundles $\mathcal{R}_n \otimes \mathcal{S}_n$ in the representations $\mathbf{R}_n$ and $\mathbf{S}_n$ of G and $G_\perp$, respectively. The chiral and conjugate-chiral zero modes transforming in $\mathbf{R}_n$ are then

counted by the cohomology groups

$$
\text{Chiral :} \qquad
\begin{aligned}
(\chi_{\mathbf{R}_n})_\alpha &\in H^0_{\bar{\mathcal{D}}}(M_3, \mathcal{S}_n) \\
(\psi_{\mathbf{R}_n})_\alpha &\in H^1_{\bar{\mathcal{D}}}(M_3, \mathcal{S}_n)
\end{aligned}
\qquad
\text{Conjugate-chiral :} \qquad
\begin{aligned}
(\bar{\chi}_{\mathbf{R}_n})_{\dot{\alpha}} &\in H^0_{\mathcal{D}}(M_3, \mathcal{S}_n) \\
(\bar{\psi}_{\mathbf{R}_n})_{\dot{\alpha}} &\in H^1_{\mathcal{D}}(M_3, \mathcal{S}_n) \,.
\end{aligned}
\tag{2.47}
$$

Their CPT-conjugate zero modes in $\overline{\mathbf{R}}_n$ are obtained by Hermitian conjugation in the gauge algebra or equivalently from (2.42) with $E = \bar{\mathcal{S}}$. In order to rewrite these cohomology groups with respect to the same boundary operator $\mathcal{D}$ we again dualise $H^0_{\bar{\mathcal{D}}}, H^1_{\bar{\mathcal{D}}}$ using the Hodge star and obtain

$$
\text{Chiral :} \qquad
\begin{aligned}
(\chi_{\mathbf{R}_n})_\alpha &\in H^3_{\mathcal{D}}(M_3, \mathcal{S}_n) \\
(\psi_{\mathbf{R}_n})_\alpha &\in H^1_{\mathcal{D}}(M_3, \mathcal{S}_n)
\end{aligned}
\qquad
\text{Conjugate-chiral :} \qquad
\begin{aligned}
(\bar{\chi}_{\mathbf{R}_n})_{\dot{\alpha}} &\in H^0_{\mathcal{D}}(M_3, \mathcal{S}_n) \\
(\bar{\psi}_{\mathbf{R}_n})_{\dot{\alpha}} &\in H^2_{\mathcal{D}}(M_3, \mathcal{S}_n) \,.
\end{aligned}
\tag{2.48}
$$

These cohomology groups completely determine the chiral and conjugate-chiral spectrum in 4d transforming in $\mathbf{R}_n$ of the remnant gauge symmetry G

$$
\begin{aligned}
\text{Chiral fermion zero modes :} \qquad & H^3_{\mathcal{D}}(M_3, \mathcal{S}_n) \oplus H^1_{\mathcal{D}}(M_3, \mathcal{S}_n) \,, \\
\text{Conjugate-chiral fermion zero modes :} \qquad & H^0_{\mathcal{D}}(M_3, \mathcal{S}_n) \oplus H^2_{\mathcal{D}}(M_3, \mathcal{S}_n) \,.
\end{aligned}
\tag{2.49}
$$

The chiral index of the representation $\mathbf{R}_n$ is

$$
\chi(M_3, \mathbf{R}_n, \mathcal{D}) = \sum_{i=0}^3 (-1)^i \dim_{\mathbb{C}} H^i_{\mathcal{D}}(M_3, \mathcal{S}_n) \,,
\tag{2.50}
$$

which is nothing other than the Euler characteristic of the $\mathcal{D}$-complex. In the case of trivial fundamental group $\pi_1(M_3)$, there is no flat bundle to break the gauge group, and $\dim H^i_{\mathcal{D}}(M_3, \mathcal{S}_n) = b^i(M_3, \mathcal{D})$ reduce to the Betti numbers of the de Rham complex on M_3. The chiral index is then given by the usual Euler characteristic, which vanishes for odd dimensional closed manifolds

$$
\pi_1(M_3) = 0 : \qquad \chi(M_3, \mathbf{R}_n, \mathcal{D}) = 0 \,.
\tag{2.51}
$$

This concludes our discussion of 'bulk' matter. In the following we will focus our attention on localized matter modes, which arise from non-trivial ϕ background values. Since these

are best characterized in terms of spectral covers we next develop this framework.

Chapter 3
Spectral Covers

3.1 Spectral Cover for the Higgs Field

For the case when a higher rank Higgs bundle is turned on but the Higgs field commutes, it is useful to describe the solution to the BPS equations in terms of the spectral data of the Higgs field. This framework is of course very familiar from F-theory spectral covers, see e.g., [15, 94, 99, 100], and for the Lagrangians in Calabi-Yau threefolds and the associated G_2-manifolds with pointlike singularities was touched upon in [49]. Here we will prepare the setup to also account for more general Higgs field configurations, with the goal to apply it to the TCS-manifolds.

Recall that ϕ is a section of $\Omega^1(\mathcal{M}_3) \otimes \mathrm{Ad}(G_\perp)$. For concreteness let $G_\perp = SU(n)$. For a commuting Higgs field we can choose to diagonalize it and study the resulting spectral cover

$$\mathcal{C}: \qquad 0 = \det(\phi - s) = \sum_{i=0}^{n} b_{n-i} s^i = b_0 \prod_{k=1}^{n} (s - \lambda_k) = \{(s, \lambda_k(s)) \,|\, s \in M_3\}\,, \qquad (3.1)$$

where b_i are symmetric polynomials in the eigenvalues of ϕ and for $SU(n)$, $b_1 = 0$. The eigenvalues λ_k labeled $k = 1, \ldots, n$ are one-forms which give rise to an n-sheeted cover of M_3 and

$$b_i \in S^i(T^* \mathcal{M}_3)\,, \qquad (3.2)$$

where b_0 is the zero-section. Here $\mathcal{M}_3$ is M_3 with the singularities of the eigenvalues λ_k excised. A cartoon of the set-ups considered is given in figure 3.1. Using the spectral cover the associated ALE-fibration is simply

$$y^2 = x^2 + \mathcal{C}(s)\,. \qquad (3.3)$$
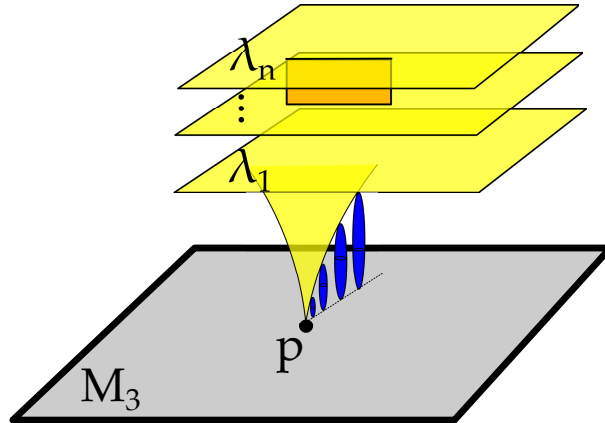
Figure 3.1:   Higgs bundle spectral cover over $\mathcal{M}_3$. Each sheet is labeled by an eigenvalue λ_k of $G_\perp$. Each λ_k is a one-form and their vanishing thus implies that they intersect the 'zero section', i.e., the locus of the ADE singularity of type G present in every ALE fiber, over points p_i on M_3. Those points p_i are precisely the loci where matter is localized. In the generic case of non-factored spectral covers, the sheets are furthermore connected by branch-cuts (orange). As we will see later on: In case the point p is connected by a flow line in M_3 to another critical point, there is a corresponding associative three-cycle which is built by fibering the collapsing S^2 (blue) over the flow line. The resulting contribution to the superpotential gives a mass term for the localized states.

Each λ_k parametrizes the volumes of a corresponding two-sphere in the $G_\perp$-ALE-fiber. The gauge symmetry $\widetilde{G}$ is generically higgsed to G, except at the loci

$$b_n = b_0 \prod_{k=1}^{n} \lambda_k = 0 \,, \tag{3.4}$$

when the gauge symmetry enhances. Since λ_k is a one-form, this condition implies that this happens generically over points in $\mathcal{M}_3$, though we will encounter other situations as well. The relation between the eigenvalues λ_k and coefficients in the ALE-fibration b_i is not linear, and generically the sheets of the spectral cover will be connected by branch-cuts. This effect implies in particular that the $U(1)$-symmetries associated to the Higgs bundle are not actually present in the low energy effective theory.

The classic example for spectral cover models starts with an $E_8 \to SU(5) \times SU(5)_\perp$. The spectral cover is five-sheeted and $\lambda_k = 0$ characterizes the location of **10** matter representations (we refer the reader to the F-theory literature where these models have been

studied in depth [15, 94, 99, 100]).

3.2 $U(1)$ Symmetries

Generically the sheets of the cover are connected by branch-cuts and therefore, although locally it may appear otherwise, the independent gauge group is G, the commutant of $G_\perp = SU(n)$ in $\widetilde{G}$. If however the coefficients of the spectral cover are tuned such that it globally factors over $\mathcal{M}_3$

$$\mathcal{C}(s) = \prod_{K=1}^{N+1} \mathcal{C}^{(K)}(s), \qquad (3.5)$$

then this corresponds to N independent $U(1)$ factors in the 4d effective theory [100]. The possibilities of factorization depend on the monodromy group that acts on the spectral cover, which for $SU(n)$ covers is S_n. If the group acts transitively on the n sheets then there is no additional $U(1)$ symmetry. If it has $N+1$ orbits then there are N globally defined two-forms, which define $U(1)$ symmetries. To see this, we consider the difference between the factored cover components $\mathcal{C}^{(K)} - \mathcal{C}^{(L)}$. Fibered over $\mathcal{M}_3$, the associated two-cycles define a non-trivial five-cycle in both the local model and in the compact G_2 manifold J. The Poincaré dual two-form to this five-cycle then gives a $U(1)$ gauge boson in the Kaluza-Klein reduction of the three-form C_3 in compactification of M-theory. This can be also be seen concretely in the context of TCS G_2, see chapter 8.

When the spectral cover fully factors we refer to it as split. In the above example with $G_\perp = SU(n)$ this situation occurs when $N = n$ in (3.5). When $N < n$ the spectral cover is non-split. When $N = 0$ it is irreducible. The general twisted cohomology computes the zero mode spectrum in both cases. For split spectral covers with exact Higgs fields we find these groups to reduce to Morse homology groups which can be computed via relative de Rham cohomology groups of the associative submanifold. When the Higgs field is closed but not exact these generalize to Novikov homology groups which generically do not relate to singular homology and are more difficult to determine. For non-split covers one finds

Novikov homology groups for covering spaces of the associative submanifold. We discuss these cases in chapter 9.

3.3   Non-split Spectral Covers

An irreducible, non-split spectral cover $\mathcal{C}$ is traced out by a diagonal Higgs field $\phi = \mathrm{diag}(\lambda_k)$. It constitutes an n-fold covering of M_3 away from singularities of the Higgs field. In this section we specialize to $M_3 = S^3$. The n eigenvalues $\lambda_k \in \Omega^1(S^3)$ of the Higgs field are not globally defined, but exhibit a one-dimensional branch locus. These branch loci lie along closed submanifolds of the base S^3 and therefore realize a collection of interlinked circles K_{ik} which are embedded into S^3 as knots. We collect all linked knots K_{ik}, labelled by i, k, into a total of l links L_i. The branch locus becomes

$$\text{Branch Locus:} \qquad L_i = \bigcup_k K_{ik}, \qquad K_{ik} \cong S^1 \subset S^3, \qquad i = 1, \ldots, l. \qquad (3.6)$$

The eigenvalues λ_k of the Higgs field $\phi = \mathrm{diag}(\lambda_k)$ are only well-defined on a simply connected neighbourhood of the link complement $S^3 \setminus \cup_i L_i$ and are acted on by a monodromy action when encircling any component of the branch locus. Equivalently, when encircling the branch locus the Higgs field ϕ returns to its original value up to a gauge transformation implementing the action the Weyl group[1]

$$\text{Monodromy action:} \qquad \phi \quad \rightarrow \quad g_i \phi g_i^{-1}, \qquad g_i \in G_{\mathrm{ADE}}. \qquad (3.7)$$

We denote by $s_i \in \mathrm{Weyl}(\mathfrak{g}_{\mathrm{ADE}})$ the monodromy element associated to components of the links L_i. For $\mathfrak{g}_{\mathrm{ADE}} = \mathfrak{su}(n)$ we have for example $\mathrm{Weyl}(\mathfrak{g}_{\mathrm{ADE}}) = S_n$ where S_n is the symmetric group on n letters.

To every link L_i there exists an orientable two-dimensional surface F_i, called the Seifert surface of the link L_i [101], bounded by the link

$$\partial F_i = L_i. \qquad (3.8)$$

---

[1]These are inner automorphisms of the Lie algebra. As familiar from constructions in class S we could also consider outer automorphisms and introduce twist lines running between singularities of the Higgs field, this case we will not consider here.

We refer to the two sides of the Seifert surface F_i as its positive F_i^+ and negative F_i^- side. Any circle linking the collection of knots L_i intersect its associated Seifert surface F_i. The eigenvalues λ_k of the Higgs field are therefore well-defined on $S^3 \setminus \cup_i F_i$ above which the sheets of the spectral cover can be distinguished.

The Higgs field ϕ is constrained by the BPS equations and consequently its eigenvalues $\lambda_k \in \Omega^1(S^3)$ are closed and coclosed on $S^3 \setminus \cup_i F_i$. The graphs of these 1-forms in the cotangent space T^*S^3 join above the Seifert surfaces F_i to form the spectral cover $\mathcal{C} \subset T^*S^3$. We refer to the graphs of λ_k as the k-th sheet of this cover with respect to a choice of Seifert surfaces $\cup_i F_i$. The BPS-equations descend to each sheet up to surface sources given by a one-form current j_k and a zero-form density ρ_k support on the Seifert surfaces $\cup_i F_i$

$$d\lambda_k = *j_k\,, \qquad *d*\lambda_k = \rho_k\,, \qquad \operatorname{supp} j_k = \operatorname{supp}\rho_k = \bigcup_i F_i \subset S^3\,. \qquad (3.9)$$

These are subject to two sets of consistency conditions, the first set of which are between sheets of the cover and read

$$\sum_{k=1}^n \rho_k = \sum_{k=1}^n j_k = 0\,, \qquad \lambda_k\big|_{F_i^+} = \lambda_l\big|_{F_i^-}\,. \qquad (3.10)$$

These require all sources to cancel between sheets and further constrain these to have profiles compatible with gluing the k-th sheet to l-th sheet along the two sides $F_i^\pm$ of the Seifert surface. In the gluing condition k, l run over pairs such that both indices exhaust all sheets. The second set of conditions are between sources for the same sheet and follow from the compactness of S^3. The equations (3.9) can only be solved when the integrated sources ρ_k vanish on each sheet

$$\int_{S^3} *\rho_k = \sum_i \int_{S^3} *\rho_k\big|_{F_i} = 0\,. \qquad (3.11)$$

In this way the sources (3.9), which are subject to (3.10) and (3.11), determine the boundary conditions for the eigenvalues λ_k when decomposing the cover $\mathcal{C}$ into sheets. The cancellation of sources between sheets ensures that the Higgs field ϕ is harmonic across the Seifert surfaces F_i and traceless. The gluing condition encodes the monodromy action
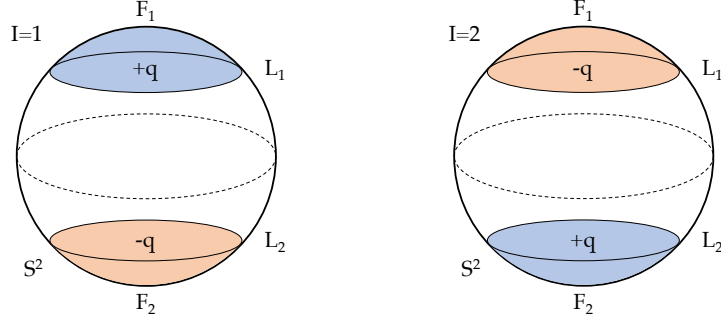
Figure 3.2: The picture shows a pair of unknots L_i and their Seifert surfaces $F_i \subset S^2 \subset S^3$ along with the sources ρ_k, j_k these support with respect to each sheet $k = 1, 2$. They are supported on the 2-sphere $S^2_{\pi/2}$ which projects onto $\theta = \pi/2$ in (3.12). The sourced Higgs field (3.9) realizes a branched double cover of S^3.

around the Links L_i as each sheet is glued along the two sides $F_i^{\pm}$ to two other sheets. Equation (3.11) is a tadpole cancellation constraint.

3.4   Example: Non-split Double Covers

We give a simple example of sources ρ_k, j_k satisfying the conditions (3.10) and (3.11) with $K = 1, 2$ realizing non-compact, branched, double covers of the 3-sphere with a collection of circles removed. Consider the 3-sphere S^3 as a fibration of 2-spheres over an interval which we parametrize by $\theta \in [0, \pi]$

$$S^2 \hookrightarrow S^3 \to [0, \pi] \,. \tag{3.12}$$

At $\theta = 0, \pi$ the fibral 2-sphere collapses. The 3-sphere S^3 is equipped with the round metric such that the geometry is symmetric under a reflection $\theta \to \pi - \theta$ fixing the central 2-sphere fiber $S^2_{\pi/2}$ projecting to $\theta = \pi/2$. On this 2-sphere we consider a total of l separated unknots S^1_i each bounding a disk D_i

$$L_i = S^1_i \subset S^2_{\pi/2} \,, \qquad F_i = D_i \subset S^2_{\pi/2} \,, \qquad i = 1, \ldots, l \,, \tag{3.13}$$

which function as the links and Seifert surfaces of (3.6) and (3.8) respectively.

We now consider source profiles ρ_k, j_k with $k = 1, 2$ supported on the surfaces D_i realizing non-compact double covers of S^3 away from the unknots S^1_i. These are constructed

electrostatically by setting $j_k = 0$ and declaring the disks D_i to be perfect conductors for the electric source ρ_k. The eigenvalues λ_k of the Higgs field $\phi = \text{diag}(\lambda_1, \lambda_2)$ are then identified with the electric field of the configurations in each sheet. In the first sheet $k = 1$ the disk D_i is assigned the electric charge q_i, while in the second sheet $k = 2$ it is assigned the opposing charge $-q_i$. The distributed charge must further sum to vanish on each sheet $\sum_i q_i = 0$. This manifestly satisfies two of the conditions in (3.10) and (3.11). The gluing condition across the surfaces D_i is then satisfied as the source distribution in both sheets is symmetric under reflection about $\theta = \pi/2$. This realizes an irreducible double cover

$$\mathcal{C} \ \to \ S^3 \setminus \cup_i L_i \,. \tag{3.14}$$

We have depicted the set-up in the case of $l = 2$ unknots and disks in figure 3.2.

The charge distributions ρ_k diverges to the boundary and consequently so do the eigenvalues λ_k. In a local normal coordinate system $(z, x) \in \mathbb{C} \times \mathbb{R}$ where one of the unknots is centered at $z = 0$ and its associated disk D_i stretches along $\mathbb{R}_- \times \mathbb{R}$, where $\mathbb{R}_- \subset \mathbb{C}$ is the negative real axis, we have

$$\lambda_k = c_k \left(\frac{dz}{\sqrt{z}} + \frac{d\bar{z}}{\sqrt{\bar{z}}} \right) + \dots \,, \tag{3.15}$$

approaching the unknot with some real constant c_k. The omitted terms are regular in the $z \to 0$ limit and the branch cut of the square root stretches along $\mathbb{R}_-$. These asymptotics follow from the closure and co-closure of the Higgs field away from the branch locus and the discontinuity across the charged Seifert surface. The former requires the eigenvalue to be harmonic away from the unknot, while the latter forces a branch cut along the disk D_i. The growth of the eigenvalue is necessarily slower than the case for which sources concentrate along the unknot, predicting (3.15) which is confirmed by explicit computation.

We now determine the topology of this cover and characterize the vanishing of the Higgs field, both will be of interest later. The homology groups of the constructed double cover $\mathcal{C}$ are computed using the Mayer-Vietoris sequence and read

$$H_0(\mathcal{C}, \mathbb{Z}) = \mathbb{Z} \,, \qquad H_1(\mathcal{C}, \mathbb{Z}) = \mathbb{Z}^{2l-1} \,, \qquad H_2(\mathcal{C}, \mathbb{Z}) = \mathbb{Z}^{l-1} \,, \qquad H_3(\mathcal{C}, \mathbb{Z}) = 0 \,. \tag{3.16}$$

The supersymmetric deformations of the cover are given by altering the charges q_i assigned to each disk D_i with respect to one of the sheets. The constraints (3.10) determine the associated opposite deformations on the second sheet. The condition (3.11) removes one degree of freedom yielding an $l - 1$ dimensional deformation space.

The zeros of the Higgs field eigenvalues λ_1, λ_2 lie on $S^2_{\pi/2}$. They come in pairs as $\lambda_1 + \lambda_2 = 0$ and there are a total of $2l - 4$ zeros. Each eigenvalue derives from an electrostatic potential f such that $df = \lambda_1 = -\lambda_2$. For generic charge set-ups the potential f is a Morse function. The zeros of the eigenvalues are critical points of this function and they can be distinguished according to their Morse-index. Let N_μ be the number of critical points of Morse-index μ, here we have

$$N_1 = N_2 = l - 2, \qquad N_0 = N_3 = 0, \tag{3.17}$$

The Morse index characterizes topological properties of the Higgs field zeros and determines the matter localized at these.

3.5 Cyclically Branched Covers

The data of the 4d theory engineered by a geometry with a split or non-split spectral cover can be extracted from a particle probing S^3 with a potential set by the Higgs field, as we explain in the next chapter. Of interest here is in part the topology of the spectral cover, which we discuss here for a simple class of non-split spectral covers. For concreteness we consider spectral covers associated with the Lie algebra $\mathfrak{g}_{\mathrm{ADE}} = \mathfrak{su}(n)$. The spectral covers of the local models of many TCS G_2-manifolds exhibit non-split covers. The covers discussed in this section are toy models for these situations.

We focus on irreducible spectral covers with a single component, more general covers are given by unions of these irreducible covers. Further we restrict to set-ups for which the monodromy elements $s_i = s \in S_n$ are identical for all components of the branch locus and of order n for n-sheeted coverings. In this setting the topology in the vicinity of branch link L_i is that of the branched multi-covering studied in knot theory [101], from which we excise
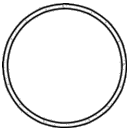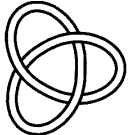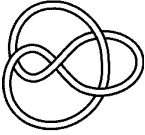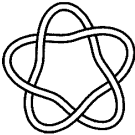
Knot Name	Sketch	2-fold $\mathcal{C}$	3-fold $\mathcal{C}$	4-fold $\mathcal{C}$	5-fold $\mathcal{C}$
0_1		1	1	1	1
3_1		$\mathbb{Z}_3$	$\mathbb{Z}_2 \times \mathbb{Z}_2$	$\mathbb{Z}_3$	1
4_1		$\mathbb{Z}_5$	$\mathbb{Z}_4 \times \mathbb{Z}_4$	$\mathbb{Z}_3 \times \mathbb{Z}_{15}$	$\mathbb{Z}_{11} \times \mathbb{Z}_{11}$
5_1		$\mathbb{Z}_5$	1	$\mathbb{Z}_5$	$\mathbb{Z}_2 \times \mathbb{Z}_2 \times \mathbb{Z}_2 \times \mathbb{Z}_2$

Table 3.1: We table examples of knots. Each column list the torsion component of the first homology of the n-fold covering space $\mathcal{C} \to S^3$ of the knot [101]. The torsion numbers are tabled in [102]. The pictures are taken from [103].

the links L_i along which the Higgs field diverges. We refer to these covers as irreducible, cyclically branched n-sheeted coverings. The example of section 3.4 realizes such a cover for $n = 2$ and $\mathfrak{g}_{\text{ADE}} = \mathfrak{su}(2)$ with $L_i = S^1$ and $s = -1 \in S_2$.

We start with a solution to (3.9) for eigenvalue 1-forms λ_k where $K = 1, \ldots, n$. The eigenvalues λ_k sweep out a $n : 1$ cover $\mathcal{C} \to S^3 \setminus \cup_i L_i$ away from the branch locus and picking Seifert surfaces for each link (L_i, F_i) the spectral cover $\mathcal{C}$ can be written as

$$\mathcal{C} = \tilde{\mathcal{C}} \setminus \cup_i L_i \,, \tag{3.18}$$

where the covering $\tilde{\mathcal{C}}$ is glued from n copies of the base with the Seifert surfaces removed

$$\tilde{\mathcal{C}} = \left(S^3 \setminus \cup_i F_i \right)_1 \# \ldots \# \left(S^3 \setminus \cup_i F_i \right)_n \,. \tag{3.19}$$

The cut out $S^3 \setminus \cup_i F_i$ contains two copies of the Seifert surfaces $F_i^{\pm}$ corresponding to its positive and negative sides which intersect along the links L_i. The gluing in (3.19) is performed by identifying F_i^+ in the i-th gluing factor with F_i^- in the $(i + 1)$-th factor and finally gluing F_i^+ in the n-th gluing factor to F_i^- in the first. Each gluing factor is in correspondence with a sheet of the spectral cover. For further details we refer to [101, 104].

The homology groups of the cover (3.19) are computed by an application of the Mayer-Vietoris sequence to a decomposition of the cover $\tilde{\mathcal{C}}$ into patches whose projection to the base contain at most a single Seifert surface F_i. The homology groups of the spectral cover (3.18) are then computed by another application of the Mayer-Vietoris sequence to the covering $\tilde{\mathcal{C}} = \mathcal{C} \cup T$ where T is tubular neighbourhood of the links $\cup_i L_i \subset T$. We restrict to the case in which the links $L_i = K_i$ are simply knots and T thus becomes a collection of l solid tori. For an n-sheeted cover with l knots K_i the result reads

$$H_1(\mathcal{C}, \mathbb{Z}) = \mathbb{Z}^{(n-1)(l-1)+l} \oplus \bigoplus_{i=1}^{l} H_1^{(n)}(K_i) \,, \qquad H_2(\mathcal{C}, \mathbb{Z}) = \mathbb{Z}^{(n-1)(l-1)} \,, \tag{3.20}$$

together with $H_0(\mathcal{C}, \mathbb{Z}) = \mathbb{Z}$ and $H_3(\mathcal{C}, \mathbb{Z}) = 0$. Each knot contributes a torsion factor to the first homology group while the number of links and sheets determines the free factor in (3.20). In table 3.1 we list the group $H_1^{(n)}(K_i)$ for some low component coverings, a

substantially more extensive list of examples is given in [102]. These torsion groups give rise to light but massive modes beneath the KK scale upon compactification to 4d, see section 7 in [2].

The cover (3.18) inherits a natural metric from its gluing factors. The eigenvalues λ_k of the Higgs field then combine to a harmonic 1-form on the spectral cover

$$\lambda \in \Omega^1(\mathcal{C}) , \qquad \lambda\big|_{[S^3\setminus\cup_i F_i]_K} = \lambda_k , \qquad K = 1, \ldots, n , \tag{3.21}$$

which by constructions restricts on each gluing factor to one of the local 1-form eigenvalues λ_k of the Higgs field. Supersymmetric deformations of the cover $\mathcal{C}$ are now described by harmonic perturbations $\lambda \to \lambda + \delta\lambda$ or equivalently n harmonic perturbations $\lambda_k \to \lambda_k + \delta\lambda_k$ which glue consistently across the branch sheets $\cup_i F_i$.

Finally note that we have an auxiliary Calabi-Yau structure on the cotangent bundle T^*S^3 whose symplectic 2-form ω and holomorphic 3-form Ω are given by

$$\omega = \frac{i}{2} \sum_{i=1}^{3} dz^i \wedge d\bar{z}^i , \qquad \Omega = dz_1 \wedge dz_2 \wedge dz_3 , \tag{3.22}$$

where $dz^i = dx^i + idy^i$ with x^i, y^i being local coordinates on $S^3, T_x^*S^3$ respectively. With respect to this auxiliary Calabi-Yau geometry the spectral cover $\mathcal{C}$ is an immersed, non-compact Lagrangian submanifold, which follows from $\omega|_{\mathcal{C}} = d\phi = 0$.

Chapter 4
Localised Matter

We will now study the more interesting and richer class of matter fields, localized on points or one-dimensional loci of $\mathcal{M}_3$. So far in chapter 2.4 we considered only flat gauge fields on along $\mathcal{M}_3$, which corresponds to bulk matter. Turning on vevs for the Higgs fields ϕ will enlarge the possible matter structure and will allow us to engineer spectra with non-trivial chiral index. The simplest case is an abelian Higgs field configuration

$$\widetilde{G} \;\to\; G \times U(1)_\perp$$
$$\mathrm{Ad}(\widetilde{G}) \;\to\; \mathrm{Ad}(G) \oplus \mathrm{Ad}(U(1)) \oplus \mathbf{R}_{+q} \oplus \overline{\mathbf{R}}_{-q} , \tag{4.1}$$

where G is the 4d gauge group and $U(1)_\perp$ the commutant, along which the Higgs fields is turned on. The expectation is that since ϕ is in the **3** of $SO(3)_{\text{twist}}$, the condition for local gauge enhancement to G occurs at codimension 3 in the base M_3, i.e., codimension 7 in the G_2-manifold J. This is also suggested by the earlier spectral cover discussion. We will discuss this case of codimension 7 localized matter first. In less generic situations, such as the twisted connected sums, however, enhancement occurs at codimension 6 loci.

We begin with split Higgs bundles (2.24) with sources ρ supported on a graph Γ. For this class of set-ups the twisted cohomology groups characterizing the spectrum can be simplified to relative de Rham homology groups. The solution to the BPS equations on M_3 will be constructed by excising a tubular neighborhood $T(\Gamma)$ of a graph Γ, with boundary conditions, which we will discuss in detail. The central question is how the zero modes in $\mathbf{R}_{+q}$ and $\overline{\mathbf{R}}_{-q}$ are counted. In this section we provide the cohomological answer to this question, which applies to both codimension 6 and 7 gauge enhancements. In the next section we will provide specific solutions to the BPS-equations, to which the general analysis in this section can be applied, thereby computing the zero mode spectrum.

4.1 Zero Modes from Relative Cohomology

We now turn on a background value for the Higgs field ϕ, which to begin with is $U(1)$-valued and solving (2.24). As explained in chapter 2, we now set out to solve the D-term equation (2.18) for $\phi = df$ with sources, i.e., the Poisson equation

$$\Delta f = \rho \,, \tag{4.2}$$

where the charge density ρ satisfies charge conservation

$$\int_{M_3} \rho = 0 \,. \tag{4.3}$$

We take ρ to be localized on links Γ_i in M_3 of definite signs of the charges, $\Gamma_\pm$,

$$\Gamma = \Gamma_+ \cup \Gamma_- \,. \tag{4.4}$$

Both the Higgs field ϕ and f diverge along Γ. We again excise a tubular neighborhood as in chapter 2. The boundary $\partial\mathcal{M}_3$ splits into connected components Σ_i, which correspond to the connected components of the underlying links Γ_i and correspondingly the boundary splits as

$$\partial\mathcal{M}_3 = \bigcup_i \Sigma_i = \Sigma_+ \cup \Sigma_- \,. \tag{4.5}$$

The normal derivatives of f, which are computed with respect to the outward pointing unit normal vector fields, have to be positive (resp. negative) restricted to Σ_+ (resp. Σ_-).

The zero modes of the fields in the representation $\mathbf{R}_q$ and $\overline{\mathbf{R}}_{-q}$ in the presence of a background Higgs vev $\phi = df$ are obtained from the twisted Laplacian

$$\Delta_f = \mathcal{D}\mathcal{D}^\dagger + \mathcal{D}^\dagger\mathcal{D} = \left(d^\dagger d + dd^\dagger\right) + q^2|df|^2 + q\sum_{i,j=1}^{3}(H_f)_{ij}\left[(a^i)^\dagger, a^j\right] \,, \tag{4.6}$$

where

$$\mathcal{D} = d + qdf\wedge\,, \qquad \mathcal{D}^\dagger = d^\dagger + q\,\iota_{\mathrm{grad}f}\,, \tag{4.7}$$

and H_f is the Hessian of f. Furthermore we defined the raising/lowering operators

$$(a^i)^\dagger = dx^i\wedge\,, \qquad a^i = \iota_{\partial_i}\,. \tag{4.8}$$

Note that $\mathcal{D}^\dagger$ is not necessarily adjoint to $\mathcal{D}$ on manifolds with boundary Σ as

$$\langle\mathcal{D}\alpha, \beta\rangle - \langle\alpha, \mathcal{D}^\dagger\beta\rangle = \int_\Sigma \bar{\alpha}\wedge *\beta\,. \tag{4.9}$$

Requiring appropriate boundary conditions fixes this problem. Consider a form α split into its tangential and normal component to the boundary

$$\alpha = \alpha_t + \alpha_n\,. \tag{4.10}$$

The tangential part α_t is defined as the pullback of α to the boundary and the normal part as $\alpha_n = \alpha - \alpha_t$. The boundary contribution is sensitive only to the tangential components i.e.,

$$\int_\Sigma \bar{\alpha}\wedge *\beta = \int_\Sigma \bar{\alpha}_t\wedge *\beta_n = \sum_i\int_{\Sigma_i}\bar{\alpha}_t\wedge *\beta_n\,, \tag{4.11}$$

where we have used the fact that $(*\alpha)_t = *\alpha_n$. The two types of boundary conditions are

$$\text{Dirichlet}: \qquad \alpha_t|_{\Sigma_i} = 0$$

$$\text{Neumann}: \qquad *\alpha_n|_{\Sigma_i} = 0\,,$$

(4.12)

which can be imposed on every boundary component Σ_i independently. Choosing one of the above boundary conditions for every Σ_i amounts to restricting the domains of the operators $\mathcal{D}$ and $\mathcal{D}^\dagger$ to an appropriate subspace of forms. Within the restricted domains, the operators then become adjoints to each other. Moreover, by restricting the domain of Δ_f to make it self-adjoint, we can identify the zero modes of Δ_f with the elements of cohomology groups $H_\mathcal{D}^*(\mathcal{M}_3)$ using Hodge theory.

A natural choice is to split the boundary conditions according to whether the normal derivative $\partial_n f$ is inward or outward pointing at a particular component of the boundary. This is the unique choice of boundary conditions that preclude localization of zero modes on the boundary Σ. The relevance of this choice will become clear in section 5.4. Extending the set-up in [105] we first restrict the domains of d and $d^\dagger$ to

$$D(d) := \left\{\alpha \in \Omega^p(\mathcal{M}_3) \,\middle|\, \alpha_t|_{\Sigma_-} = 0 \text{ (Dirichlet)} \right\}$$

$$D(d^\dagger) := \left\{\alpha \in \Omega^p(\mathcal{M}_3) \,\middle|\, *\alpha_n|_{\Sigma_+} = 0 \text{ (Neumann)} \right\}\,,$$

(4.13)

i.e., we are imposing Neumann conditions on the positive boundary and Dirichlet conditions on the negative. Moreover, we define the domains of $\mathcal{D}$ and $\mathcal{D}^\dagger$ to be $D(\mathcal{D}) = D(d)$ and $D(\mathcal{D}^\dagger) = D(d^\dagger)$. The corresponding boundary conditions on the metric Laplace operator are given as

$$D^{\text{matter}}(\Delta) = \left\{\alpha \in \Omega^p(\mathcal{M}_3) \,\middle|\, \alpha_t|_{\Sigma_-} = (d^\dagger\alpha)_t|_{\Sigma_-} = 0 \quad \text{and} \quad *\alpha_n|_{\Sigma_+} = *(d\alpha)_n|_{\Sigma_+} = 0 \right\}\,,$$

(4.14)

where we set again $D^{\text{matter}}(\Delta_f) = D^{\text{matter}}(\Delta)$. Note that the d-complex and $\mathcal{D}$-complex are isomorphic, so they have isomorphic cohomology groups. In this case, the d-complex is restricted to forms which vanish on Σ_-. This computes the relative cohomology of the pair $(\mathcal{M}_3, \Sigma_-)$ [106] so we get

$$H_\mathcal{D}^p(\mathcal{M}_3) = H^p(\mathcal{M}_3, \Sigma_-)\,.$$

(4.15)

The sign of the $U(1)$-charge q is important. Changing it amounts to changing the sign of f, which inverts the signs of normal derivatives and consequently exchanges the boundary conditions imposed on the positive and negative boundaries, and we obtain the cohomology groups with respect to the positive boundary. In terms of the operators defined in section 2.3 changing the sign of q corresponds to computing the cohomology with respect to the operator $\bar{\mathcal{D}}$, which is isomorphic to the $\mathcal{D}$-cohomology but this time with respect to the conjugate representation $\overline{\mathbf{R}}$.

Returning to the analysis of the spectrum above, we have seen that it is computed by the relative cohomology with respect to the negatively charged boundary components. Clearly, $H^0(\mathcal{M}_3, \Sigma_-)$ vanishes since any constant function which vanishes on the boundary is identically zero. Moreover, by Lefschetz duality[1] $H^3(\mathcal{M}_3, \Sigma_-)$ also vanishes. Therefore, the discussion from section 2.3 shows that the chiral fermions are counted by $H^1(\mathcal{M}_3, \Sigma_-)$, while the conjugate-chiral fermions are counted by $H^2(\mathcal{M}_3, \Sigma_-)$

$$\begin{aligned} \text{chiral}: \quad & H^1(\mathcal{M}_3, \Sigma_-) \\ \text{conjugate-chiral}: \quad & H^2(\mathcal{M}_3, \Sigma_-)\,. \end{aligned} \tag{4.16}$$

The net amount of chiral matter transforming in the representation $\mathbf{R}$ is therefore given by the relative Euler characteristic

$$\chi(\mathcal{M}_3, \Sigma_-) = b^2(\mathcal{M}_3, \Sigma_-) - b^1(\mathcal{M}_3, \Sigma_-), \tag{4.17}$$

where $b^1(\mathcal{M}_3, \Sigma_-)$ and $b^2(\mathcal{M}_3, \Sigma_-)$ are the dimensions of the respective cohomology groups. The Hodge star induces the isomorphism $H^*(\mathcal{M}_3, \Sigma_-) = H^{3-*}(\mathcal{M}_3, \Sigma_+)$, so that

$$\chi(\mathcal{M}_3, \Sigma_-) = -\chi(\mathcal{M}_3, \Sigma_+)\,. \tag{4.18}$$

We have seen that for an M_3 without boundary there is a 4d vector multiplet in the spectrum. Once we introduce sources along Γ and excise a tubular neighborhood around

---

[1]The standard statement of Lefschetz duality is: Let M be an orientable compact manifold of dimension n, with boundary N, then $H^k(M, N) \cong H_{n-k}(M)$ and $H_k(M, N) \cong H^{n-k}(M)$ with integer coefficients. When the boundary has at least two disconnected components $N = N_+ \cup N_-$ a generalization of this theorem gives $H^k(M, N_+) \cong H_{n-k}(M, N_-)$ and $H_k(M, N_+) \cong H^{n-k}(M, N_-)$.

them, we need to check that the vector multiplets remain in the spectrum. Since these adjoint fields are uncharged under the $U(1)$, the associated forms cannot have any tangential boundary conditions, and we impose purely normal boundary conditions. In this case the domain of the relevant Laplace operator becomes

$$D^{\text{gauge}}(\Delta) := \left\{ \alpha \in \Omega^p(\mathcal{M}_3) \mid *\alpha_n|_\Sigma = *(d\alpha)_n|_\Sigma = 0 \right\}. \tag{4.19}$$

The kernel is then isomorphic to the de Rham cohomology groups [105] and we obtain the required zero modes for the vector multiplets in 4d.

4.2 Higher Rank Higgs bundles

Next we generalize to higher rank Higgs bundles in $G_\perp$. We still assume that $[\phi, \phi] = 0$. If the Higgs field eigenvalues and by extension linear combinations thereof are not globally defined (i.e., in the spectral cover language the spectral cover is non-split and does not fully factor) then we still have a local description in terms of the Higgs field along the Cartan subalgebra:

$$\text{locally on } M_3: \qquad \phi = H^i df_i, \tag{4.20}$$

away from the sources $\rho = H^i \rho_i$ and $j = H^i j_i$ in (2.25). Here $n = \text{rk}\, G_\perp$ and H^i the generators of the CSA. Locally this background breaks the gauge symmetry into

$$\begin{aligned} \widetilde{G} &\rightarrow G \times U(1)^n, \\ \text{Ad}\,\widetilde{G} &\rightarrow \text{Ad}\,G \oplus \text{Ad}(U(1)^n) \oplus \bigoplus_{Q=(q_1,\dots,q_n)} \mathbf{R}_Q, \end{aligned} \tag{4.21}$$

where $Q = (q_1, \dots, q_n)$ denotes a vector of $U(1)$-charges. If the spectral cover has $N+1$ irreducible components (as in (3.5)), N of these n $U(1)$ factors descend to the gauge group of the 4d effective theory. The operator $\mathcal{D}$ defined in (2.37) acts on $\mathbf{R}_Q$

$$\begin{aligned} \mathcal{D}|_{\mathbf{R}_Q} &= \mathcal{D}_Q = d + (q_1 df_1 + \cdots + q_n df_n) \wedge, \\ \mathcal{D}^\dagger|_{\mathbf{R}_Q} &= \mathcal{D}_Q^\dagger = d^\dagger + \iota_{\text{grad}(q_1 f_1 + \cdots + q_n f_n)}. \end{aligned} \tag{4.22}$$

Let us introduce

$$f_Q = q_1 f_1 + \cdots + q_n f_n. \tag{4.23}$$

	$\operatorname{Ad} G$	$\operatorname{Ad} U(1)^n$	$\mathbf{R}_Q$	$\overline{\mathbf{R}}_{-Q}$
Vector multiplets	1	1	0	0
Chiral multiplets	$b^1(\mathcal{M}_3)$	$b^1(\mathcal{M}_3)$	$b^1(\mathcal{M}_3, \Sigma_Q^-)$	$b^2(\mathcal{M}_3, \Sigma_Q^-)$

Table 4.1: The 4d $\mathcal{N} = 1$ matter content for a background given by a $U(1)^n$ valued Higgs bundle whose spectral cover is fully factored. Here Σ_Q^- denotes the negative boundary of $\mathcal{M}_3$ with respect to the function f_Q. Note $b^1(\mathcal{M}_3) = b^2(\mathcal{M}_3)$ and $b^1(\mathcal{M}_3, \Sigma_Q^\mp) = b^2(\mathcal{M}_3, \Sigma_Q^\pm)$.

The zero modes are counted by (2.45) where $E = \operatorname{Ad} G_\perp$. If the spectral cover does not factor, i.e., the sheets mix under monodromy, the cohomologies of the operator $\mathcal{D}$ cannot be rewritten in terms of, e.g., de Rham cohomologies. For the case of rank 1 Higgs bundles the isomorphism given between the corresponding complexes was given by conjugation with e^{qf^2}. This required a globally defined function f whose role for fully reducible Higgs bundles is played by f_Q as we will explain in the next section. This isomorphism cannot be adapted in a straightforward manner to general Higgs bundles.

Restricting $\mathcal{D}$ to $\operatorname{Ad} G$ or $\operatorname{Ad}(U(1)^n)$, it is reduced to the exterior derivative

$$\mathcal{D}|_{\operatorname{Ad} G} = \mathcal{D}|_{U(1)} = d, \qquad \mathcal{D}^\dagger|_{\operatorname{Ad} G} = \mathcal{D}^\dagger|_{U(1)} = d^\dagger. \qquad (4.24)$$

Vector and chiral multiplets transforming in these representations are thus simply counted by the zeroth and first Betti numbers of $\mathcal{M}_3$, respectively.

However, if the Higgs bundle diagonalizes globally, i.e., if we have rank $G_\perp$ many $U(1)$ symmetries, then a simple generalization of the rank one case applies. The zero modes are counted with respect to

$$\mathcal{D} = d + df_Q \wedge, \qquad (4.25)$$

where f_Q is globally well-defined and a function. As a consequence the results of chapter 4.1 carry over upon making the replacement $qf \to f_Q$. $\mathcal{M}_3$ is obtained by excising the singularities of all the f_i and the boundary decomposes again into positive and negative

---

[2]For further explanation we refer to appendix C of [1])
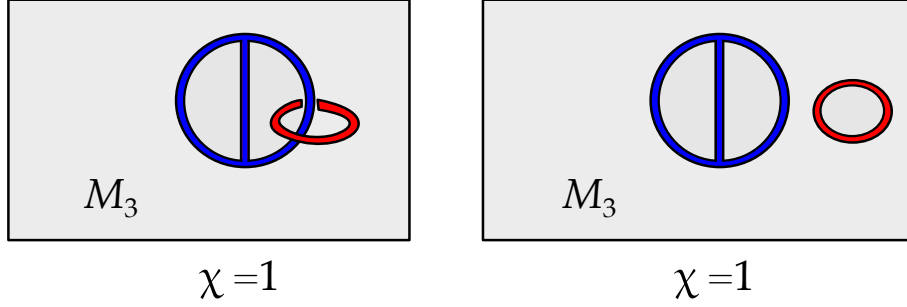
Figure 4.1: Examples of charged graphs in $\mathcal{M}_3$. Positive, negative charges are coloured red, blue respectively. Both charge distribution give rise to the same chiral index but a different number of zero modes.

parts

$$\Sigma = \Sigma_Q^+ \cup \Sigma_Q^-\,, \tag{4.26}$$

depending on whether $f_Q \rightarrow \pm\infty$ when approaching the excised charge. By (4.23) the charge vector can flip the sign of a boundary as seen by the individual functions f_i used to define f_Q, i.e., for differently charged representation $\mathbf{R}_Q$ each zero mode counting requires an alternate decomposition of the boundary. We therefore find the fermionic zero mode spectrum in the representation $\mathbf{R}_Q$ to be enumerated by the relative Betti numbers

$$
\begin{aligned}
b^1(\mathcal{M}_3, \Sigma_Q^-) &= \text{ number of chiral zero modes in } \mathbf{R}_Q\,, \\
b^2(\mathcal{M}_3, \Sigma_Q^-) &= \text{ number of conjugate-chiral zero modes in } \mathbf{R}_Q\,.
\end{aligned}
\tag{4.27}
$$

This parallels the identification of cohomologies as in (4.15). Each of these fermionic zero modes contributes to a chiral multiplet upon reduction to 4d by supersymmetry. The CPT conjugate of the fermionic zero modes enumerated by $b^2(\mathcal{M}_3, \Sigma_Q^-)$ will be of positive chirality in 4d and contribute to a chiral multiplet valued in $\overline{\mathbf{R}}_{-Q}$.

For the representations uncharged under any of the factors of $U(1)$ we have $\mathcal{D} = d$ and their boundary conditions on $\mathcal{M}_3$ are chosen purely normal as in (4.19), and they are counted by de Rham cohomology. The complete 4d spectrum is summarized in table 4.1.

4.3   Example: Wires in S^3

We now turn to describing concrete charge configurations – these configurations were studied in [49] and we revisit them here. Let $M_3 = S^3$ and embed charges in S^3 which are localized on a graph Γ. The positively and negatively charged components of the graph are disjoint $\Gamma = \Gamma_+ \cup \Gamma_-$. We denote by n_+, n_- the number of components and by ℓ_+, ℓ_- the number of loops of Γ_+, Γ_- respectively. The total charge on $\Gamma_\pm$ is again constrained to vanish. Excising tubular neighbourhoods of $\Gamma_\pm$ we obtain $\mathcal{M}_3$ with associated boundaries $\Sigma_\pm$. By (4.15) the number of non perturbative chiral and conjugate-chiral zero modes are then given by the Betti numbers $b^i(\mathcal{M}_3, \Sigma_-)$ for $i = 1, 2$ respectively. The top and bottom cohomologies vanish as discussed in chapter 4.1. The first and second cohomology are

$$b^1(\mathcal{M}_3, \Sigma_-) = \ell_+ + n_- - r - 1$$
$$b^2(\mathcal{M}_3, \Sigma_-) = \ell_- + n_+ - r - 1 \,, \tag{4.28}$$

where r counts the number of negative loops which are independent in homology when embedded in $M_3 \setminus \Gamma_+$. The chiral index is then computed to be

$$\chi(\mathcal{M}_3, \mathbf{R}_q) = (n_+ - \ell_+) - (n_- - \ell_-) \,. \tag{4.29}$$

It solely depends on the charge configuration Γ and is independent of the number r. A chiral spectrum is therefore easily generated. Multiple charged graphs will give rise to the same spectrum. Another point to note here is that a non-trivial chiral index will only arise if for some sign of the charge, the number of loops and components is different, i.e., the charge distribution is not localized solely on a disjoint union of circles. This will later on give hints as to how to deform the Higgs bundles for TCS G_2-manifolds whose local model exhibits a

split spectral cover.

Chapter 5
BPS-Configurations, SQM and Morse-Bott Theory

In the discussion above we were not interested in any particular features of the harmonic function f on $\mathcal{M}_3$ and the computation of the spectrum is in fact valid for any such f. In this section we first specialize to the case where the Higgs field $\phi = df$ has isolated, non-degenerate zeros, which is the same as requiring f to be a Morse function – this is the case already studied in [49]. We show that massless chiral matter is localized at the zeros of the Higgs field. We then generalize this to the case where f can have critical loci of dimension one, in which case it is Morse-Bott. The latter will be essential for the TCS geometries. The main tool here is reformulating the problem of finding the kernel of the Laplacian Δ_f in terms of a supersymmetric quantum mechanics and Morse theory. This approach is useful as it lends itself to the generalized Morse-Bott setup that we are interested in. In section 6 we extend this approach to arbitrary solutions of the BPS equations (2.18).

5.1   Matter, Morse and Witten's SQM

Let us consider again the abelian case where $\phi = df$ with f harmonic in the decomposition (4.1), which counts the fermionic zero modes transforming in the representation $\mathbf{R}_q$, that are in the kernel of

$$\Delta_f = \mathcal{D}\mathcal{D}^\dagger + \mathcal{D}^\dagger\mathcal{D} = \left(d^\dagger d + dd^\dagger\right) + q^2|df|^2 + q\{d, \iota_{\mathrm{grad}\, f}\} + q\{d^\dagger, df\wedge\}\,. \qquad (5.1)$$

The twisted Laplacian Δ_f can be interpreted as the Hamiltonian of a supersymmetric quantum mechanics (SQM) with the target space $\mathcal{M}_3$ where the supercharges are given by the operators $\mathcal{D}$ and $\bar{\mathcal{D}}$ [107]. In section 2.3 we have shown that (due to the partial topological twist) the state space is identified with the space of differential forms on $\mathcal{M}_3$. However, since $\mathcal{M}_3$ is now a manifold with boundary, we have to restrict the state space to forms

satisfying the boundary conditions given in (4.13), which we denote by $\mathcal{H} = \oplus_i \Omega_b^i(\mathcal{M}_3)$. The subscript b indicates that the forms satisfy the boundary conditions. The function f now plays the role of a superpotential and the kernel of Δ_f characterizing the true zero modes in the reduction to 4d is now enumerating the supersymmetric ground states of the SQM [107]. In summary:

4d Effective Theory	SQM
Matter fields	State Space
$\mathcal{D}, \mathcal{D}^\dagger$	Supercharges
Δ_f	Hamiltonian
Higgs field $\phi = df$	$f = $ Superpotential
Matter zero modes	Ground states

As in Witten's analysis, we can now use perturbation theory to compute the zero mode spectrum. To compute the perturbative kernel of Δ_f, rescale $f \mapsto tf$. In terms of the electrostatics problem (4.2), this amounts to rescaling the charges globally by a factor of t, which does not alter the overall ground state count. The term $q^2|df|^2$ in (5.1) scales quadratically in t. Hence, for large t, the solutions of the equation $\Delta_{tf}\psi = 0$ are localized at the points where $df = 0$ i.e., the zeros of the Higgs field ϕ.

In this discussion we focus on harmonic functions f which are Morse. The local physics will then be given by a supersymmetric harmonic oscillator. Before continuing with the computation we recall the definition of a Morse function. A smooth function $f : \mathcal{M}_3 \to \mathbb{R}$ is called Morse if its set of critical points

$$N = \{p \in \mathcal{M}_3 : df(p) = 0\} \tag{5.2}$$

is discrete and all points $p \in N$ are non-degenerate. A critical point $p \in N$ is called non-degenerate if its Hessian $H_f(p)$ is non-degenerate as a bilinear map. In this case $p \in N$ is assigned a number $\mu(p)$ called the Morse index given by the number of negative eigenvalues of $H(p)$

$$p \in N : \qquad \mu(p) = |\{c = \text{eigenvalue of } H_f(p); \ c < 0\}| \ . \tag{5.3}$$

In the case of manifolds with boundary, we further assume that there are no critical points of f on $\partial \mathcal{M}_3$. Note that this is true in our case, since the normal derivative of f at the boundary is non-zero (see chapter 4.1). For more details on Morse theory we refer the reader to [108, 109].

We can choose a normal coordinate system in which f and the metric g on $\mathcal{M}_3$ take the form

$$f(x) = f(0) + \frac{1}{2} \sum_{i=1}^{3} c_i(x^i)^2 + \mathcal{O}((x^i)^3),$$

$$g_{ij}(x) = \delta_{ij} + \mathcal{O}((x^i)^2),$$

(5.4)

where we assumed that $p = 0$ and c_i are the eigenvalues of the Hessian, which due to the harmonicity of f sum to zero. This means that only points with Morse index 1 and 2 can occur. Expanded in these coordinates Δ_{tf} reduces to the Hamiltonian of a supersymmetric harmonic oscillator with

$$\Delta_{tf} = \sum_{i=1}^{3} \left(-\frac{\partial^2}{\partial (x^i)^2} + q^2 t^2 c_i^2 (x^i)^2 + qt c_i [dx^i, \iota_{\partial/\partial x^i}] \right) + \mathcal{O}((x^i)^3).$$

(5.5)

Solving for the ground states of the harmonic oscillator locally, near a critical point p of Morse index $\mu(p)$, we find a unique solution given by a differential form of degree $\mu(p)$. The zero modes of ψ, which are identified with 1-forms in (2.45), localize at critical points of Morse index 1. For c_i with signature $(-, +, +)$, the solution to leading order is

$$\mu(p) = 1: \quad \psi = \psi_{(p,q)} \exp\left(-qt \sum_{i=1}^{3} |c_i|(x^i)^2 \right) dx^1.$$

(5.6)

In other words the form part is oriented along the negative eigenspaces of the Hessian of the function f. Here we have decomposed the 7d spinor ψ into a Weyl-spinor $\psi_{(p,q)}$ carrying the anti-commuting, gauge and 4d spinor structure and its internal profile along $\mathcal{M}_3$. The index (p, q) indicates the point p, where the corresponding perturbative ground state localizes and q keeps track of the charge of $\mathbf{R}_q$. The boundary conditions we described in chapter 4.1 are exactly such that the solutions of (5.6) collected from all critical points of f of Morse index 1 span the complete perturbative kernel of Δ_f at degree 1 [105].

If p has Morse index 2, the ground state localized near p is of degree 2 and letting c_i have signature $(-, -, +)$, the solution is

$$\mu(p) = 2: \quad \bar{\psi} = \bar{\psi}_{(p,q)} \exp\left(-qt \sum_{i=1}^{3} |c_i|(x^i)^2\right) dx^1 \wedge dx^2 \,. \tag{5.7}$$

Likewise the fermions in $\overline{\mathbf{R}}_{-q}$ are obviously counted by replacing f with $-f$.

5.2 Exact Spectrum from SQM

The perturbative calculation in the previous section does not necessarily give the exact spectrum of the full theory. On the SQM side this is due to the fact that quantum mechanical instanton corrections can cause perturbative ground states to acquire a mass and be lifted in the full theory [107, 108]. We now complete the dictionary between the 4d effective theory of 7d SYM and SQM by showing that masses of perturbative zero modes in the 4d theory arise precisely from instanton corrections on the SQM side.

We start our analysis with the action in (2.13) and split the complex 1-form $\varphi = \varphi_0 + \delta\varphi$ into its background $\varphi_0 = tdf$ and fluctuations $\delta\varphi$. The 7d fields are expanded in terms of a basis of perturbative ground states of the twisted Laplacian as

$$\begin{aligned}
\psi(x, y) &= \psi_{(a,q)}(x)\psi^{(a,q)}(y)\,, \\
\varphi(x, y) &= tdf(y) + \delta\varphi(x, y) = tdf(y) + \delta\varphi_{(a,q)}(x)\delta\varphi^{(a,q)}(y)\,,
\end{aligned} \tag{5.8}$$

where $(x, y) \in \mathbb{R}^{1,3} \times \mathcal{M}_3$. Here the sum runs over the charged representations, $\mathbf{R}_q$ and $\overline{\mathbf{R}}_{-q}$, and all critical points p_a of Morse index 1 with respect to the relevant Morse function, f and $-f$ respectively. The fermionic field $\psi_{(a,q)}(x)$ carries the anti-commuting, gauge and 4d spinor structure while $\psi^{(a,q)}(y)$ is a 1-form on $\mathcal{M}_3$ annihilated by the twisted Laplacian in perturbation theory. In leading order in t these are (5.6) or the CPT conjugate of (5.7). The decompositions for $\delta\varphi$ are of analogous structure.

A mass term in 4d descends from the 7d interaction

$$\mathrm{Tr}\,[\psi \wedge \mathcal{D}\psi] = \mathrm{Tr}\,[\psi \wedge (d\psi + [\varphi\wedge, \psi])]\,, \tag{5.9}$$

which for an abelian Higgs background yields the mass matrix

$$M^{ab} = \int_{\mathcal{M}_3} \psi^{(a,-q)} \wedge (d + tqdf\wedge)\psi^{(b,q)} = \int_{\mathcal{M}_3} \bar{\psi}^{(a,q)} \wedge *(d + tqdf\wedge)\psi^{(b,q)} \,. \qquad (5.10)$$

This precisely computes the instanton corrections between the perturbative ground states in SQM theory and is simply the matrix element

$$M^{ab} = \langle \psi^{(a,q)}|\mathcal{D}\psi^{(b,q)}\rangle \,. \qquad (5.11)$$

Let us briefly summarize the classic results on these instanton corrections, see [107, 108] for a detailed treatment. The (Euclidean) action of the SQM with target space $\mathcal{M}_3$ is given by a standard sigma-model action

$$S_{\text{SQM}} = \int_{\mathbb{R}} ds \left(\frac{1}{2}g_{ij}\frac{d\gamma^i}{ds}\frac{d\gamma^j}{ds} + \frac{q^2 t^2}{2}g^{ij}\partial_i f\partial_j f \right.$$
$$\left. + g_{ij}\bar{\eta}^i D_s\eta^j + qtD_i\partial_j f\bar{\eta}^i\bar{\eta}^j + \frac{1}{2}R_{ijkl}\eta^i\bar{\eta}^j\eta^k\bar{\eta}^l \right) \,, \qquad (5.12)$$

where g_{ij} is the metric on $\mathcal{M}_3$, D the covariant derivative and R_{ijkl} the curvature tensor. Canonically quantizing this action, one gets the SQM we have described in the previous section [107]. The matrix element (5.11) now has the following path integral expression

$$\langle \psi^{(a,q)}|\mathcal{D}\psi^{(b,q)}\rangle = \frac{1}{qf(p_a) - qf(p_b) + O(1/t)} \lim_{T\to\infty} \langle \psi^{(a,q)}|e^{T\Delta_{tf}}[\mathcal{D}, f]e^{-T\Delta_{tf}}\psi^{(b,q)}\rangle$$
$$= \frac{1}{qf(p_a) - qf(p_b) + O(1/t)} \int_{\substack{\gamma(+\infty)=p_a \\ \gamma(-\infty)=p_b}} D\gamma D\eta D\bar{\eta}\, [\mathcal{D}, f]e^{-S_{\text{SQM}}} \,, \qquad (5.13)$$

which is valid to leading order in $1/t$. The path integral is taken over the space of all trajectories γ connecting the critical point p_b to p_a, where $\mu(p_b) = 1$ and $\mu(p_a) = 2$. The integrand $[\mathcal{D}, f]$ is $\mathcal{D}$-exact and hence the path integral receives contributions only from fixed points of the fermionic variations generated by the corresponding supercharge $\mathcal{D}$. Such fixed points are given by trajectories γ

$$\frac{d\gamma^i}{ds} = tqg^{ij}\partial_j f \,, \qquad (5.14)$$

which is the gradient flow equation. With this the mass matrix is evaluated in [108] to leading order in $1/t$ as

$$M^{ab} = \sum_\gamma n_\gamma e^{-tq(f(p_a)-f(p_b))} \,. \qquad (5.15)$$
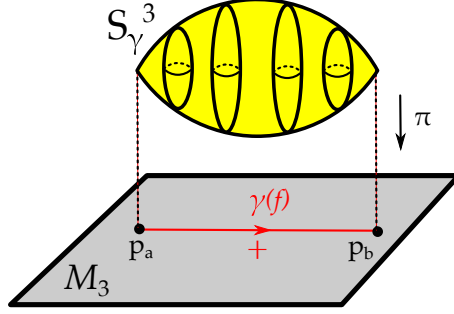
Figure 5.1: The supersymmetric three-cycle responsible for mass terms. The two critical points p_a and p_b of the function Morse f in the base of the ALE-fibration $\mathcal{M}_3$ are connected by a gradient flow line $\gamma(f)$. Above each point along this path there is a two-spheres in the ALE fiber. Traversing along a gradient flow line of f a 3-sphere S^3_γ is traced out.

Here the sum runs over all ascending gradient flow lines γ starting at p_b and ending at p_a. The contribution from a flow line γ is weighted by a sign $n_\gamma = \pm 1$, which arises from a choice of orientation on the moduli space of gradient trajectories. The precise derivation from the SQM context is intricate and is given in [110, Appendix F]. The main takeaway is that perturbative ground states form a complex, where the coboundary operator is given by

$$\mathcal{D}\psi^{(b,q)} = \sum_a M^{ab}\bar{\psi}^{(a,q)} \,. \tag{5.16}$$

This is exactly the Morse-Witten complex for the Morse function f. Massless states are counted by the cohomology of this complex and can be found by diagonalising M^{ab}. Recall from chapter 4.1 that f is a solution of an electrostatics problem and satisfies $\partial_n f < 0$ (resp. $\partial_n f > 0$) on Σ_- (resp. Σ_-). The Morse-Witten complex therefore recovers the relative cohomology of a pair $(\mathcal{M}_3, \Sigma_-)$ [111]. In 4d these give rise to $b^1(\mathcal{M}_3, \Sigma_-)$ chiral multiplets valued in $\mathbf{R}_q$ and $b^2(\mathcal{M}_3, \Sigma_-)$ chiral multiplets valued in $\overline{\mathbf{R}}_{-q}$.

It is possible that the boundary operator of the Morse-Witten complex is trivial. This is equivalent to a vanishing of the mass matrix $M^{ab} = 0$, i.e., all perturbative ground states are true ground states. In this case the Morse function f is called perfect. This is precisely the case when f has $b^i(\mathcal{M}_3, \Sigma_-)$ critical points of Morse index i, for $i = 1, 2$.

We can consider these mass terms also in the M-theory picture. In section 2.2 we have

interpreted the Higgs field $\phi = df$ as measuring the periods of the vanishing cycle in an ALE-fibration, with respect to a reference hyper-Kähler structure. For an abelian Higgs field there is exactly one such vanishing cycle which is of finite volume through-out $\mathcal{M}_3$ and collapses precisely at the critical points of f. As this vanishing cycle is a two-sphere, paths connecting two critical points lifts to a 3-sphere in the ALE geometry. This 3-sphere is of minimal volume whenever it projects to a gradient flow line in $\mathcal{M}_3$. This is depicted in figure 5.1.

We can consider an M2-brane probing the ALE fibered G_2-manifold. The stationary points of the M2-brane action are expected to correspond to associative three-cycles and are fibered by vanishing cycle of the ALE-fiber over the gradient trajectories $\gamma(f)$ determined by the Morse function f. This gives the interpretation that the particle of the SQM is the W-boson constructed by wrapping an M2-brane on vanishing cycles of the resolution. We expand on this point of view in the next section. The associatives wrapped by the M2-branes then give a non-perturbative correction to the superpotential [112, 113] which is of the form

$$\Delta W \sim n_\gamma \exp\left(i \int_{S_\gamma^3} (C + i\Phi)\right). \tag{5.17}$$

In particular, the coefficients originating from a one-loop determinant in the M2-brane action are the same as the those computed in the supersymmetric quantum mechanics and hence give the same coefficients $n_\gamma = \pm 1$ as those appearing in the Morse theory analysis. In the case of several flow lines connecting the same critical loci p_a, p_b, the corresponding associatives are homologous and there can hence be cancellations among the different contributions depending on the relative orientation.

5.3   Example: $n_+ + n_-$ Point Charges in S^3

We apply the analysis of section 5.1 and 5.2 to point charges on the three-sphere. Example configurations are shown in figure 5.2. Let $M_3 = S^3$ and $\widetilde{G} = SU(n+1)$. Consider $n_\pm$ positive/negative point charges with the total charge vanishing. The function $f : M_3 \to \mathbb{R}$ is
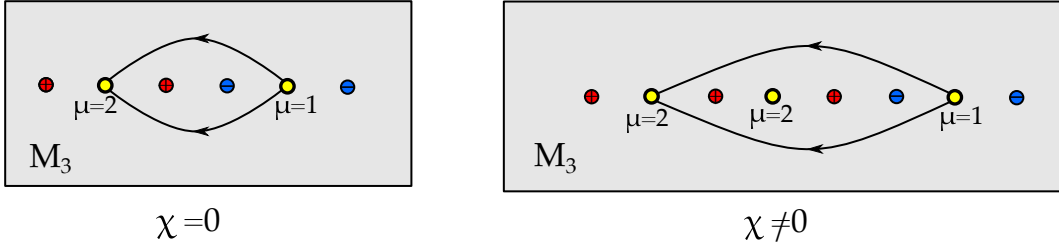
Figure 5.2: Examples of point like charge configurations in $\mathcal{M}_3$. Depicted are positive (red) and negative (blue) charges, critical points (yellow) and flow lines starting and ending at critical points. The critical points have Morse index μ. The contributions of the flow lines cancels and for generic set-ups each critical point will give rise to a ground state of positive, negative chirality if $\mu = 1, 2$ respectively. The LHS thus has an equal number of chiral and conjugate-chiral ground states, the chiral index vanishes. For the same reasons the chiral index does not vanish on the RHS.

the electrostatic potential generated by these charges. This function gives rise to a singular abelian Higgs field background on S^3 via $\phi = df$ which breaks

$$\mathrm{Ad}\, SU(n+1) \to \mathrm{Ad}\, SU(n) \oplus \mathrm{Ad}\, U(1) \oplus \mathbf{n}_q \oplus \overline{\mathbf{n}}_{-q}\,, \tag{5.18}$$

Perturbative ground states localize at the critical points of the harmonic function f. Let n_μ be the number of points with Morse index μ, then there are n_1 chiral fermions ψ and n_2 conjugate-chiral fermions $\bar{\psi}$ transforming in $\mathbf{n}_q$. The harmonicity of f forbids points of Morse index 0 or 3 as these are minima or maxima respectively. The chiral index as defined (2.50) is given by the difference

$$\chi\left(S^3, \mathbf{n}_q\right) = n_2 - n_1\,, \tag{5.19}$$

as perturbative ground states are lifted by M2-brane corrections in pairs leaving the difference of ground states of positive and negative chirality unchanged.

Next smear out the charges to small balls so that the singularities of f are removed without altering f away from the support of the charge distribution. In this case grad f becomes a smooth vector field on M_3 and the Poincaré-Hopf theorem can be applied. We denote the critical points of f by x_i, then the topological index $I(x_i, f)$ of grad f at x_i is

determined by the topological index of the map

$$\frac{\text{grad } f}{|\text{grad } f|} : \quad S^2_{x_i} \to S^2 , \tag{5.20}$$

where $S^2_{x_i}$ is a small ball containing the critical point x_i. The Poincaré-Hopf theorem asserts

that the sum of all indices is the Euler characteristic of $M_3 = S^3$

$$\sum_i I(x_i, f) = \chi\left(S^3\right) = 0 . \tag{5.21}$$

Note that $I(x_i, f) = (-1)^{\mu(x_i)}$ for all critical points x_i and that each charge contributes one

maximum or minimum upon smearing it out, whereby (5.21) simplifies to

$$0 = n_- - n_1 + n_2 - n_+ . \tag{5.22}$$

Combining this result with (5.19) we find the chiral index to be determined solely by the

composition of the initial charge configuration

$$\chi\left(S^3, \mathbf{n}_q\right) = n_+ - n_- . \tag{5.23}$$

We thus find a rather simple criterion to determine whether the true ground state spectrum

of the theory is chiral or not:

$$n_+ \neq n_- \quad \leftrightarrow \quad \text{chiral spectrum} . \tag{5.24}$$

Two examples are shown in figure 5.2. This result is of course recovered from the more

general charge distributions discussed in section 4.3 upon setting the number of loops l_+

and l_- to zero. In particular for generic placements of the $n_+ + n_-$ charges one has

$$n_1 = n_- - 1 , \qquad n_2 = n_+ - 1 . \tag{5.25}$$

Each critical point thus constitutes a true ground state and we recover (4.28). This is made

explicit in figure 5.2. If flow lines between critical points exist, they always do so in pairs

with $n_\gamma = \pm 1$. Hence the corresponding ground states are not lifted.
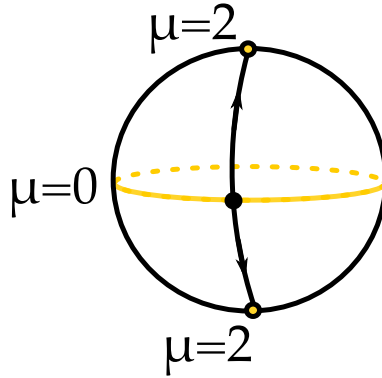
Figure 5.3: S^2 with the Morse-Bott function given by $f(x, y, z) = z^2$. The critical locus is colored in yellow and consists of two critical points of index 2 (north ant south pole) and a critical circle of index 0 (the equatorial circle). The gradient curves are depicted in black. Note that $\mathcal{M}(N_0, N_2) = \mathbb{S}^1 \coprod \mathbb{S}^1$. These two circles parametrize the gradient trajectories in the upper and lower hemisphere.

5.4 Generalized Critical Loci and Morse-Bott Theory

The setup studied in [49] and in the last section assumes that the critical loci of the function f are isolated points. Although this is the generic situation, it will be important to relax this assumption and consider the generalized setup in which the critical locus of f can be one-dimensional, which happens for the recent TCS constructions of G_2-manifolds. Functions f with critical loci of dimension greater than zero whose Hessian at its critical closed submanifold is non-degenerate in the normal direction are called Morse-Bott functions. An example is given in figure 5.3. For further background on this see [108, 114].

The starting point is once more an abelian Higgs field $\phi = df$ as in section 5.1 where now f is taken to be a harmonic Morse-Bott function. We are again interested in the fermionic zero modes transforming in the representation $\mathbf{R}_q$ which are in the kernel of the twisted Laplacian (5.1). As before, rescaling $f \to tf$ these localize on the critical loci of f and we can solve for the zero mode solutions locally. However, f now has higher dimensional critical loci and our previous analysis needs to be adapted. We begin by analyzing the critical loci of f.

The local analysis of the perturbative ground states is now the same as in section 5.1,

although some extra care is required to keep track of the critical loci of different dimensions. The critical locus of f splits into connected components all of which are compact closed submanifolds of $\mathcal{M}_3$. Let N denote a single connected component. The normal bundle νN splits into the positive and negative eigenspace of the Hessian H_f of f

$$\nu N = \nu_+ N \oplus \nu_- N \tag{5.26}$$

and the Morse index of N is defined as the rank of $\nu_- N$. In our context the Morse-Bott function f is also harmonic. This precludes critical submanifolds of dimension 2 since harmonicity of f implies that $\operatorname{tr} H_f = 0$, which would mean that H_f is degenerate in the normal direction, which is not possible since f is Morse-Bott by assumption. For harmonic Morse-Bott functions on a three-manifold, N can thus only be a point or a circle. Moreover, if $N = \mathbb{S}^1$, it can only have index 1. This is again due to the requirement that $\operatorname{Tr} H_f$ vanishes everywhere. The case where N is a point has been analyzed in section 5.1.

If $N = \mathbb{S}^1$ we can proceed analogously. As N has index 1, f is locally of the form

$$f(x) = f(0) - \frac{c}{2}\left((x^1)^2 - (x^2)^2\right) + O((x^i)^3), \tag{5.27}$$

in a suitable normal coordinate chart centered at a point $p \in N$. In this coordinate system x^3 is the coordinate tangential to N and the Hessian H_f is diagonalized with the eigenvalues c and $-c$. In these coordinates the twisted Laplacian (5.1) now takes the form

$$\Delta_{tf} = (\Delta_{tf})_\perp + (\Delta_{tf})_\parallel + \mathcal{O}((x^i)^3),$$

$$(\Delta_{tf})_\perp = \sum_{i=1}^{2}\left(-\frac{\partial^2}{\partial(x^i)^2} + q^2 t^2 c^2 (x^i)^2\right) - qtc[dx^1, \iota_{\partial/\partial x^1}] + qtc[dx^2, \iota_{\partial/\partial x^2}], \tag{5.28}$$

$$(\Delta_{tf})_\parallel = -\frac{\partial^2}{\partial(x^3)^2}.$$

The analysis of perturbative ground states thus splits into normal and tangential parts relative to N. In the normal direction we get a single 1-form solution $\psi_\perp$ given by

$$\psi_\perp = \psi_{(n,q)} \exp\left(-qtc\left((x^1)^2 + (x^2)^2\right)\right) dx^1. \tag{5.29}$$

Here we have split $\psi_\perp$ into a 4d Weyl spinor $\psi_{(n,q)}$ carrying the anti-commuting, gauge and spinor structure and its internal profile normal to N. In principle $\psi_\perp$ is defined only locally

on N. However, observe that $\psi_\perp$ is a volume form on the fiber of $\nu_- N$. Hence, assuming that the negative eigenbundle $\nu_- N$ is orientable, the local solutions can be patched together to a global form on N. Since f is constant on N the tangential equation reduces to a Laplace equation on $\mathbb{S}^1$. Let the coordinate on the circle be θ. Then we obtain two solutions

$$\psi_1 = \psi_\perp\,, \qquad \psi_2 = d\theta \wedge \psi_\perp\,. \tag{5.30}$$

For every circle N contributing to the perturbative spectrum we therefore obtain a pair of states consisting of a 1- and 2-form. From (2.45) we know that the degree of the ground state correlates with the 4d chirality of fermions, i.e., the state described by a 1,2-form has positive, negative chirality upon a reduction to 4d. These fermionic states again contribute to chiral multiplets in 4d.

As in the case of Morse functions, perturbative zero modes for $\chi, \bar\chi$ transforming in $\mathbf{R}_q$ are absent as f is harmonic. To conclude we again remark that the analysis above extends to fermionic ground states transforming in $\overline{\mathbf{R}}_{-q}$ by replacing f with $-f$. The function $-f$ now exhibits the same critical loci. A critical point of Morse index μ with respect to f has a Morse index of $\mu-3$ with respect to $-f$, however critical circles exhibit an unchanged Morse index of 1 with respect to both f and $-f$. The modes localising on the critical circles of $-f$ transforming in $\overline{\mathbf{R}}_{-q}$ are CPT conjugate to the solutions found in (5.30). As a consequence we find the localized perturbative ground states on every critical circle contributing to the perturbative spectrum to assemble to two chiral multiplets transforming in $\mathbf{R}_q$ and $\overline{\mathbf{R}}_{-q}$.

5.5 Generalized Critical Loci and SQM

We now turn to the computation of the exact spectrum from the perturbative solutions in the Morse-Bott case, where the critical loci of f consist of points and circles. While it is possible to compute the SQM instanton correction in much greater generality [108, 114], the applications for TCS local models allow us to consider only the set-up with this restriction. The instanton calculation in this case effectively reduces to the one considered in section 5.2.

To find the exact spectrum, we again want to compute the matrix element (5.15) between perturbative zero modes localized at critical submanifolds we use the analogous SQM computation. Let N_m denote the disjoint union of critical submanifolds of Morse-Bott index m (recall that this is the dimension of the negative eigenspace of the Hessian matrix). In our case, m can take the values 1 or 2. For $m = 2$, all of the components of N_2 must be points, whereas N_1 can contain points as well as circles.

Recall that among the ground states localized at critical circles there are chiral multiplets transforming in the representation $\mathbf{R}_q$ and $\overline{\mathbf{R}}_{-q}$. As already discussed in section 5.4, this is because perturbative ground states are of the form

$$\psi = \alpha \wedge \psi_\perp, \tag{5.31}$$

with $\deg(\psi_\perp) = 1$ and α a harmonic form on N_1. When N_1 is a circle, α can be a function or a one-form. Consider again the matrix element

$$M^{ab} = \int_{\mathcal{M}_3} \bar{\psi}^{(a,q)} \wedge *(d + tqdf\wedge)\psi^{(b,q)}\,. \tag{5.32}$$

Here we again use the indices a and b to enumerate all the perturbative ground states of total degree 2 and 1 respectively. However, note that for Morse-Bott functions the index is no longer in one-to-one correspondence with critical loci since there are two perturbative ground states localized at each critical $\mathbb{S}^1 \subset N_1$. For the following we will require the assumption that there are no ascending gradient flow lines between connected components in N_1.[1]

To compute M^{ab} we need to consider three cases. First, both $\bar{\psi}^{(a,q)}$ and $\psi^{(b,q)}$ may be localized at points in which case the discussion of section 5.2 applies verbatim. We now turn to the second possibility, where the ground states are both localized at the same circle critical circle $\mathbb{S}^1 \subset N_1$. The matrix element is then given by the integral

$$\int_{\mathcal{M}_3} d\theta \wedge \psi_\perp \wedge *(d + tqdf\wedge)\psi_\perp\,, \tag{5.33}$$

---

[1]In this case f is said to be weakly self-indexing. This assumption can be avoided at a cost of making the exposition much more technical [114].

where we have used the explicit expression of for such ground states given in (5.30). Using the expression for $\psi_\perp$ in (5.29) one can see that $d\theta \wedge *(df \wedge \psi_\perp) = 0$ and also $d\theta \wedge \psi_\perp \wedge *d\psi_\perp = 0$. This implies that the matrix element M^{ab} is zero, if $\bar\psi^{(a,q)}$ and $\psi^{(b,q)}$ are both localized at the same circle.

The third possibility is that $\bar\psi^{(a,q)}$ is localized at a point p_a in N_2 and $\psi^{(b,q)}$ is localized at a circle $\mathbb{S}_b^1 \in N_1$. To keep track of all of the gradient curves between critical loci of f, we introduce the moduli space of gradient trajectories between N_m and N_n

$$
\mathcal{M}(N_m, N_n) = \frac{\left\{ \gamma : \mathbb{R} \to M \mid \lim_{t \to -\infty} \gamma(t) \in N_m, \quad \lim_{t \to \infty} \gamma(t) \in N_n, \quad \frac{d\gamma^i}{ds} = tqg^{ij}\partial_j f \right\}}{\mathbb{R}}
$$

(5.34)

where the quotient is taken with respect to the remaining reparametrization invariance of the gradient flow: $\gamma(t) \mapsto \gamma'(t) = \gamma(t + \delta t)$. The moduli space $\mathcal{M}(N_m, N_n)$ is a smooth manifold, and it follows from simple dimensional analysis that its dimension is $m - n - 1$. An illustrative example is given by S^2 with the Morse-Bott function $f(x, y, z) = z^2$, see figure 5.3.

For our purposes, the only relevant case is $m = 1$ and $n = 2$ in which case the moduli space is a finite set of points. This means that there are finitely many gradient trajectories connecting N_1 and N_2 and there are finitely many ascending gradient flow lines connecting $\mathbb{S}_b^1$ and p_a. We can now continue with the computation. In terms of the SQM path integral we have the expression

$$
M^{ab} = \langle \psi^{(a,q)} | \mathcal{D}\psi^{(b,q)} \rangle = \frac{1}{qf(p_a) - qf(p_b) + O(1/t)} \int_{\substack{\gamma(+\infty)=p_a \\ \gamma(-\infty)\in\mathbb{S}_b^1}} D\gamma D\eta D\bar\eta \, [\mathcal{D}, f] e^{-S_{\text{SQM}}},
$$

(5.35)

where p_b is an arbitrary point in $\mathbb{S}_b^1$ (note that f is constant along $\mathbb{S}_b^1$). This is nearly the same expression as in (5.13), with the only difference being that we integrate over all curves with $\gamma(-\infty) \in \mathbb{S}_b^1$. However, the same localization argument as before applies. As we have seen above, the number of gradient trajectories is still finite and the result of the path

integral computation has exactly the same form as for points, i.e., (5.15). The expression for the operator $\mathcal{D}$ also remains unchanged

$$\mathcal{D}\psi^{(b,q)} = \sum_a M^{ab}\bar{\psi}^{(a,q)} \,. \tag{5.36}$$

The exact spectrum is given as the cohomology of $\mathcal{D}$, which acts on the following complex

$$C^1 = \Omega^0(N_1)\,, \qquad C^2 = \Omega^1(N_1) \oplus \Omega^0(N_2)\,. \tag{5.37}$$

This complex is a convenient way to arrange all the perturbative ground states of degree p in C^p. It is a specific instance of a Morse-Bott complex for f, which can be defined for f with critical loci of arbitrary dimension [114]. If f is a solution to the electrostatics problem in section 4.1, the Morse-Bott cohomology again recovers the relative cohomology of a pair $(\mathcal{M}_3, \Sigma_-)$.

5.6   Chiral Index from Spectral Covers

We close this section by introducing yet another picture for counting the perturbative zero modes, namely using the spectral cover introduced in section 3. For certain configurations it is possible to read off the exact spectrum using the spectral cover, this was already observed for the $U(1)$ case in [49].

For simplicity let us begin by recalling the statement for the rank 1 Higgsing in (5.18) where $\widetilde{G} = SU(n+1)$. There we turned on a single abelian Higgs background parametrised by the Morse function f via $\phi = df$. The spectral cover $\mathcal{C}$ in this case is simply the graph of ϕ. The intersection number of $\mathcal{C}$ with the zero section $b_0 = 0$ (i.e., $\mathcal{M}_3$) at a critical point p is denoted by n_p. This can be identified with the degree of the vector field grad f at the critical point p. In a coordinate system where the Hessian H_f is diagonal it follows immediately that the degree is determined by the Morse index $\mu(p)$ of f at p as $n_p = (-1)^{\mu(p)}$. We can therefore recast the counting of perturbative ground states as

$$|(\mathcal{C} \cap \mathcal{M}_3)_-| = \text{chiral perturbative zero modes in } \mathbf{R}_q$$

$$|(\mathcal{C} \cap \mathcal{M}_3)_+| = \text{conjugate-chiral perturbative zero modes in } \mathbf{R}_q \,, \tag{5.38}$$

where $(\mathcal{C} \cap \mathcal{M}_3)_\pm$ counts the number of critical points p with $n_p = \pm 1$. The chiral index is thus simply given by the signed count of all points of intersection

$$\chi(\mathcal{M}_3, \mathbf{R}_q) = \mathcal{C} \cap \mathcal{M}_3 = \sum_{p \in \mathcal{M}_3 \,:\, df(p)=0} n_p = (\mathcal{C} \cap \mathcal{M}_3)_+ - (\mathcal{C} \cap \mathcal{M}_3)_- . \tag{5.39}$$

The above carries over straightforwardly to higher rank Higgs bundles if their corresponding spectral cover factors completely. We start from the set-up in which we have broken the gauge symmetry to $G \times U(1)^n$ by turning on sources for the Higgs field along the CSA of $\widetilde{G}$ as in section 4.2. The representation $\mathrm{Ad}\,\widetilde{G}$ decomposes into irreducible representation $\mathbf{R}_Q$ of $G \times U(1)^n$ where Q denotes a vector of $U(1)$ charges. Generically the representation $\mathrm{Ad}\,\widetilde{G}$ decomposes into irreducible representation of $G \times G_\perp$ with the weights λ_i of the representation of $G_\perp$ determining the different spectral covers. Due to the special choice of background the representations of $G_\perp$ have decomposed into representations of $U(1)^n$ and to construct the spectral cover we must group the representations $\mathbf{R}_Q$ according to this decomposition. This grouping depends on $\widetilde{G}$ but the weights will always be determined by the corresponding effective Morse functions as $\lambda_i = df_{Q_i}$ where $i = 1, \ldots, N$. The effective Morse function f_{Q_i} was defined in (4.23) and N denotes the rank of the spectral cover. A spectral cover is thus the union of graphs of multiple df_{Q_i} and an N-fold covering of $\mathcal{M}_3$. The matter loci are as before the critical points of f_{Q_i}, i.e., the intersection of the spectral cover with the zero section. This is just $b_0 = 0$ in the language of section 3.

To compute the perturbative spectrum we thus just need to count the intersections of the different sheets with their signs as in the rank 1 case above. Let $\mathcal{C}_i \subset \mathcal{C}$ denote the sheet of a spectral cover $\mathcal{C}$ with $\mathrm{Graph}(df_{Q_i}) = \mathcal{C}_i$ then

$$|(\mathcal{C}_i \cap \mathcal{M}_3)_-| = \text{chiral perturbative zero modes in } \mathbf{R}_{Q_i}$$
$$|(\mathcal{C}_i \cap \mathcal{M}_3)_+| = \text{conjugate-chiral perturbative zero modes in } \mathbf{R}_{Q_i}, \tag{5.40}$$

where the notation is as in (5.38). Similarly we compute the chiral index to

$$\chi(\mathcal{M}_3, \mathbf{R}_{Q_i}) = \mathcal{C}_i \cap \mathcal{M}_3 = (\mathcal{C}_i \cap \mathcal{M}_3)_+ + (\mathcal{C}_i \cap \mathcal{M}_3)_- . \tag{5.41}$$

Perturbative zero modes transforming a representation $\mathbf{R}_{Q_i}$ which is not associated by $\lambda_i = df_{Q_i}$ to a sheet of this spectral cover are enumerated by the intersection of the different sheets

$$|(\mathcal{C}_i \cap \mathcal{C}_j)_-| = \text{chiral perturbative zero modes in } \mathbf{R}_{Q_i - Q_j}$$

$$|(\mathcal{C}_i \cap \mathcal{C}_j)_+| = \text{conjugate-chiral perturbative zero modes in } \mathbf{R}_{Q_i - Q_j}.$$

(5.42)

The chiral index again given by the difference

$$\chi(\mathcal{M}_3, \mathbf{R}_{Q_i - Q_j}) = \mathcal{C}_i \cap \mathcal{C}_j = (\mathcal{C}_i \cap \mathcal{C}_j)_+ + (\mathcal{C}_i \cap \mathcal{C}_j)_-. \tag{5.43}$$

This is pictorially most clear in the case of A_n singularities. In this case the ALE-fiber is given by a circle fibration over $\mathbb{R}^3$ and the eigenvalues λ_i, which are characterised by the sheets of the spectral cover, correspond to the points at which the circle collapses. A vanishing sphere is stretched between any pair of these points and collapses whenever they come together, i.e., when the sheets intersect. This enhances the spectrum and constitutes an additional ground state.

Chapter 6
M2-brane Instantons and Colored SQMs

We now generalize the SQM description of the previous section to all solutions of the BPS-equations. These cases covered also include T-brane like configurations with non-flat connections, although we will not study them here. Recall that, given a vacuum of the 7d SYM in terms of a solution to the BPS equations (2.18), the 4d physics follows from a compactification of the Lagrangian (2.13) on M_3. The bosonic and fermionic fields (2.45) are Lie algebra valued forms valued in $\Lambda(M_3, \mathrm{ad}\, P_{\mathrm{ADE}})$ and the Laplacian Δ determining the zero mode expansion is given in (2.37). The Laplacian Δ is associated to the differential $\mathcal{D}$. We rename $\mathcal{Q} = \mathcal{D}$ and $H = \Delta$ in this section. In chapter 4 we argued that in favorable situations we can twist the differential $\mathcal{D}$ and use Hodge theory to determine the spectrum.

Alternatively one can characterize the zero mode spectrum in terms of approximate zero modes and their non-perturbative corrections. Approximate zero modes are Lie algebra

valued 1-forms on M_3

$$\text{Approximate Zero Mode}: \qquad \chi \in \Omega^*(M_3, \mathcal{S}_n) \qquad (6.1)$$

which are annihilated by the Laplacian $H = \frac{1}{2}\left\{\mathcal{Q}, \mathcal{Q}^\dagger\right\}$ to all orders in perturbation theory. In the set-up of the last section these could be approximated to (5.6) and (5.7). The 7d SYM gives following mass matrix for these modes

$$\text{Mass Matrix}: \qquad M_{AB} = \int_{M_3} \langle \chi_A, \mathcal{Q}\chi_B \rangle \,, \qquad (6.2)$$

where the bracket is anti-linear in the first argument and contracts the Riemannian and Lie algebra indices using the metric on M_3 and Killing form of the Lie algebra $\mathfrak{g}_{\text{ADE}}$ respectively. Generators for the cohomologies (2.45) are then determined by the kernel of the matrix (6.2).

With this approach the Yukawa couplings also become accessible. The SYM gives the 4d Yukawa couplings as the overlap integral

$$\text{Yukawa Couplings}: \qquad Y_{ABC} = \int_{M_3} \langle \chi_C, [\chi_A \wedge, \chi_B] \rangle \,, \qquad (6.3)$$

between three approximate zero modes labelled by A, B, C. Zero modes are determined by (6.2) to linear combinations of approximate zero modes whereby (6.3) also sets the Yukawa couplings between these.

In this section we interpreted the overlap integrals (6.2) and (6.3) as amplitudes of a colored $\mathcal{N} = 2$ supersymmetric quantum mechanics. The relevant structures of the SQM for this identification are its physical Hilbert space $\mathcal{H}_{\text{phys.}}$ and supercharge $\mathcal{Q}$ which are

$$\mathcal{H}_{\text{phys.}} = \Lambda\left(M_3, \text{ad}\, P_{\text{ADE}}\right) \,, \qquad \mathcal{Q} = d + [(\phi + iA) \wedge, \cdot]. \qquad (6.4)$$

Here we present this new $\mathcal{N} = 2$ supersymmetric quantum mechanics. In [115, 116] similar quantum mechanical systems with less supersymmetry have been considered. We refer to the SQM as 'colored' due to the presence of additional fermions over the SQM considered in (5.12) (originally [107]) which extend the Hilbert space by color degrees of freedom associated with the Lie algebra $\mathfrak{g}_{\text{ADE}}$. The colored SQM is constructed bottom-up from (6.4). We

expect there to be a top-down derivation of the colored SQM as a dimensional reduction of an M2-branes probing the G_2-manifold. The colored SQM probing the Higgs bundle encodes the memberane instanton effects of M-theory on the ALE-fibered G_2-manifold. The Higgs bundle was derived from the periods of the G_2 3-form Φ over the vanishing cycles in the ALE fibers. Similarly we can wrap an M2-brane on these vanishing cycles of the ALE fibers and reduce the brane to a particle moving on the base associative M_3. This is now the natural candidate for the particle described by the colored SQM.

6.1 Set-up and Conventions

We consider the manifold M_3 with metric g and a principal bundle $P_{\mathrm{ADE}} \to M_3$ with gauge group G_{ADE} over it. The corresponding Lie algebra is denoted $\mathfrak{g}_{\mathrm{ADE}}$. This gives rise to the associated adjoint vector bundle $\mathrm{ad}\, P_{\mathrm{ADE}} \to M_3$. Both are naturally complexified. Greek indices run as $\alpha, \beta, \gamma = 1, \ldots, \dim G_{\mathrm{ADE}}$ and are associated to the fiber while latin indices run as $i, j, k = 1, 2, 3$ and are associated to the base. The Killing form $\kappa_{\alpha\beta}$ gives rise to a non-degenerate pairing on the fibers of $\mathrm{ad}\, P_{\mathrm{ADE}} \to M_3$ which is used to raise and lower greek indices. Latin indices are raised and lowered with the metric g_{ij}. The generators of the Lie algebra $\mathfrak{g}_{\mathrm{ADE}}$ are denoted by T_α and are taken to satisfy

$$[T_\alpha, T_\beta] = ic_{\alpha\beta\gamma}T^\gamma \,. \tag{6.5}$$

We probe the geometry $\mathrm{ad}\, P_{\mathrm{ADE}} \to M_3$ with a non-linear supersymmetric sigma model. We denote the flat worldline by $\mathbb{R}_\tau$ and take τ to denote the time coordinate on it. The bosonic and fermionic fields are given by the maps $x : \mathbb{R}_\tau \to M_3$ and sections $\psi : \mathbb{R}_\tau \to x^*(TM_3)$ respectively. Further we add a color field given by sections $\lambda : \mathbb{R}_\tau \to x^*(\mathrm{ad}\, P_{\mathrm{ADE}})$. The dynamics of the model are governed by a non-dynamical background connection $A \in \Omega^1(M_3, \mathrm{ad}\, P_{\mathrm{ADE}})$ and Higgs field $\phi \in \Omega^1(M_3, \mathrm{ad}\, P_{\mathrm{ADE}})$ on the target manifold M_3. These are real Lie algebra valued 1-forms on the target manifold M_3. The connection $A_{i\alpha}$ and Higgs field $\phi_{i\alpha}$ are required to satisfy the BPS equations (2.18). Note that these conventions differ from (5.12).

The sigma model can thus be summarized as

$$x^*(TM_3 \oplus \mathrm{ad}\, P_{\mathrm{ADE}}) \otimes \mathbb{C} \xleftarrow{\ x^*\ } (TM_3 \oplus \mathrm{ad}\, P_{\mathrm{ADE}}) \otimes \mathbb{C} \tag{6.6}$$

where π, π_τ denote the canonical projections. Expanded in components the fields ψ, λ read

$$\psi(\tau) = \psi^i(\tau) \frac{\partial}{\partial x^i}\bigg|_{x(\tau)}, \qquad \lambda(\tau) = \lambda^\alpha(\tau) e_\alpha\big|_{x(\tau)}, \tag{6.7}$$

where e_α are fiber coordinates induced by a local trivialisation of $\mathrm{ad}\, P_{\mathrm{ADE}}$. Both $\psi, \bar{\psi}$ and $\lambda, \bar{\lambda}$ are taken to be anti-commuting fermionic fields. The latter we package into bilinears

$$\tilde{T} = -\left[\bar{\lambda}, \lambda\right] = \tilde{T}^\alpha e_\alpha = -i c^\alpha{}_{\beta\gamma} \bar{\lambda}^\beta \lambda^\gamma e_\alpha, \qquad \tilde{T}_\alpha^\dagger = \tilde{T}_\alpha, \tag{6.8}$$

which we pair with the connection $A_{i\alpha}$ and Higgs field $\phi_{i\alpha}$ to form the color contracted 1-forms

$$A_\lambda = (A_\lambda)_i \, dx^i = A_i^\alpha \tilde{T}_\alpha dx^i = \kappa \left(\bar{\lambda}, [A_i, \lambda]\right) dx^i,$$
$$\phi_\lambda = (\phi_\lambda)_i \, dx^i = \phi_i^\alpha \tilde{T}_\alpha dx^i = \kappa \left(\bar{\lambda}, [\phi_i, \lambda]\right) dx^i. \tag{6.9}$$

The bilinears $\tilde{T}$ quantize to the Lie algebra generators T. To remind of this contraction we introduce a subscript λ as in (6.9).

We combine the connection $A_{i\alpha}$ and Higgs field $\phi_{i\alpha}$ into a complex Lie algebra valued 1-form φ with components

$$\varphi_{i\alpha} = \phi_{i\alpha} + i A_{i\alpha}. \tag{6.10}$$

There are now three connections on M_3 given by the natural connection D on $\mathrm{ad}\, P_{\mathrm{ADE}}$ and its complexification $\mathcal{Q}$ which read

$$D = d + i[A \wedge, \cdot], \qquad \mathcal{Q} = d + [\varphi \wedge, \cdot], \tag{6.11}$$

together with the Levi-Civita connection ∇ of the metric g_{ij}. Each of these pulls back to the world line $\mathbb{R}_\tau$ in (6.6) and acts on the fermions $\psi, \bar{\psi}, \lambda, \bar{\lambda}$ of (6.7) as

$$\nabla_\tau \psi^i = \partial_\tau \psi^i + \Gamma^i_{jk} \dot{x}^j \psi^k,$$
$$D_\tau \lambda_\alpha = \partial_\tau \lambda_\alpha + c_{\alpha\beta\gamma} \dot{x}^i A_i^\beta \lambda^\gamma, \tag{6.12}$$
$$\mathcal{Q}_\tau \lambda_\alpha = \partial_\tau \lambda_\alpha - i c_{\alpha\beta\gamma} \dot{x}^i \varphi_i^\beta \lambda^\gamma.$$

The pullback is referenced by adding the world line parameter τ as an index to the respective connections.

6.2 Colored $\mathcal{N} = (1,1)$ Supersymmetric QM

The dynamics of the sigma model described in section 6.1 is governed by the Lagrangian

$$\begin{aligned}
\mathcal{L} = \frac{1}{2}\dot{x}^i \dot{x}_i + i\bar{\psi}^i \nabla_\tau \psi_i + i\bar{\lambda}^\alpha D_\tau \lambda_\alpha + \frac{i}{2}\left(F_{ij}\right)_\lambda \bar{\psi}^i \psi^j - \frac{1}{2}R_{ijkl}\psi^i\bar{\psi}^j\psi^k\bar{\psi}^l \\
- \left(D_{(i}\phi_{j)}\right)_\lambda \bar{\psi}^i\psi^j - \frac{1}{2}\phi_\lambda^i \phi_{\lambda,i} - \frac{1}{2}[\phi_i,\phi_j]_\lambda \bar{\psi}^i\psi^j + \zeta\left(\bar{\lambda}^\alpha \lambda_\alpha - n\right) .
\end{aligned} \tag{6.13}$$

Here R_{ijkl} denotes the Riemann curvature tensor, the bracket notation $D_{(i}\phi_{j)}$ denotes a symmetrisation of indices, the integer n is set to $n = 1$ and ζ is a Lagrange multiplier. The action (6.13) is invariant under

$$\delta x^i = \epsilon\bar{\psi}^i - \bar{\epsilon}\psi^i ,$$

$$\delta\psi^i = i\epsilon\dot{x}^i + \epsilon\phi_\lambda^i - \epsilon\Gamma^i_{jk}\bar{\psi}^j\psi^k ,$$

$$\delta\bar{\psi}^i = -i\bar{\epsilon}\dot{x}^i + \bar{\epsilon}\phi_\lambda^i - \bar{\epsilon}\Gamma^i_{jk}\bar{\psi}^j\psi^k , \tag{6.14}$$

$$\delta\lambda^\alpha = -i\epsilon c^\alpha{}_{\beta\gamma}\bar{\psi}^i\varphi_i^\beta\lambda^\gamma - i\bar{\epsilon}c^\alpha{}_{\beta\gamma}\psi^i\bar{\varphi}_i^\beta\lambda^\gamma ,$$

$$\delta\bar{\lambda}^\alpha = -i\epsilon c^\alpha{}_{\beta\gamma}\bar{\psi}^i\varphi_i^\beta\bar{\lambda}^\gamma - i\bar{\epsilon}c^\alpha{}_{\beta\gamma}\psi^i\bar{\varphi}_i^\beta\bar{\lambda}^\gamma .$$

The supercharges associated to the variations (6.14) are given by

$$\mathcal{Q} = \bar{\psi}^i\left(i\dot{x}_i + \phi_\lambda^i\right) , \qquad \mathcal{Q}^\dagger = \psi^i\left(-i\dot{x}_i + \phi_\lambda^i\right) . \tag{6.15}$$

There is no R-symmetry rotating the supercharges.

The physics of the quantum mechanics (6.13) is that of a particle moving in the target space M_3. In addition to its position, its state is characterized by its fermion and color content which are given by vectors in the pullback of the exterior algebra ΛM_3 and adjoint bundle $\mathrm{ad}\, P_{\mathrm{ADE}}$ to the world line respectively. The latter are the fermions $\lambda, \bar{\lambda}$ and determine the color contracted Higgs field ϕ_λ setting the potential for the particle via (6.9).

Quantization of the SQM (6.13) leads to the physical Hilbert space

$$\mathcal{H}_{\mathrm{phys.}} = \Lambda\left(M_3, \mathrm{ad}\, P_{\mathrm{ADE}}\right) , \tag{6.16}$$

consisting of Lie algebra valued forms on M_3. The Lagrange multiplier in (6.13) gives rise to the constraint that only states with a single $\bar{\lambda}$ excitations are considered physical which precludes states in higher powers of the adjoint representation of $\mathfrak{g}_{\text{ADE}}$ from contributing to the spectrum. States of even, odd degrees are bosonic, fermionic respectively. The supercharge is realized on $\mathcal{H}_{\text{phys.}}$ as the operator

$$\mathcal{Q} = d + [(\phi + iA) \wedge, \cdot]. \tag{6.17}$$

6.3 Perturbative Ground States and Instantons

Perturbative ground states of the quantized SQM are given by Lie-algebra valued forms $\chi \in \Omega^p(M_3, \text{ad } P_{\text{ADE}})$ annihilated by the Hamiltonian $H = \frac{1}{2}\{\mathcal{Q}, \mathcal{Q}^\dagger\}$ or equivalently by the two supercharges $\mathcal{Q}, \mathcal{Q}^\dagger$ to all orders in perturbation theory

$$H\chi = 0 \quad \leftrightarrow \quad \mathcal{Q}\chi = 0, \quad \mathcal{Q}^\dagger \chi = 0. \tag{6.18}$$

In the path integral formulation of the SQM perturbative ground states correspond to constant maps fixed by the Euclidean fermionic supersymmetry variations $\delta^E \psi^i, \delta^E \bar{\psi}^i$ which emphasizes the second condition given in (6.18). A characterization of the perturbative ground states already follows from inspection of the unquantized supercharges (6.15), constant maps annihilated by the supercharges necessarily map to points at which the Higgs field ϕ_λ vanishes. We conclude that perturbative ground states are labelled by pairs

$$(x_A, \lambda_A) \in M_3 \times \mathfrak{g}_{\text{ADE}}, \tag{6.19}$$

which are such that the color contracted Higgs field at x_A with respect to λ_A vanishes

$$\phi_{\lambda_A}(x_A) = \kappa\left(\bar{\lambda}_A, [\phi_i(x_A), \lambda_A]\right) dx^i = 0. \tag{6.20}$$

Here we have introduced capital latin indices A, B, C which label pairs in $M_3 \times \mathfrak{g}_{\text{ADE}}$. Further we assume that ϕ_{λ_A} has simple isolated zeros or equivalently that it is a Morse 1-form.

To fully determine a perturbative ground state (6.19) we further need to specify its $\psi, \bar{\psi}$ fermion content. This however is already fixed by a given pair (x_A, λ_A) by considering how the 1-form $\phi_{\lambda_A} \in \Omega^1(M_3)$ vanishes at $x_A \in M_3$. Consider a small sphere $S_\epsilon^2 \subset M_3$ on which the color contracted Higgs field ϕ_{λ_A} does not vanish and which encloses the point $x_A \in M_3$. Then we have a map of spheres

$$\frac{\phi_{\lambda_A}}{||\phi_{\lambda_A}||} : S_\epsilon^2 \to S^2 \,. \tag{6.21}$$

The degree $\mu(x_A, \lambda_A)$ of this map topological characterizes the vanishing of the 1-form ϕ_{λ_A} at $x_A \in M_3$. The number of $\bar{\psi}$ excitations of the perturbative ground state, or equivalently its degree p as a differential form, is given by $p = \mu(x_A, \lambda_A)$. This generalizes the notion of Morse index as introduced in [107]. The pairs (6.19) thus fully label perturbative ground states[1]. In Dirac notation we denote these by

$$\chi_A = |x_A, \lambda_A, \mu_A\rangle \in \Omega^{\mu_A}(M_3, \operatorname{ad} P_{\mathrm{ADE}}) \,. \tag{6.22}$$

Given two perturbative ground states χ_A, χ_B we construct a third perturbative ground state $\chi_{AB} = [\chi_A \wedge, \chi_B]$ as, if χ_A, χ_B are annihilated to all orders in perturbation theory by $\mathcal{Q}$, then so is χ_{AB} by

$$\mathcal{Q}[\chi_A \wedge, \chi_B] = [\mathcal{Q}\chi_A \wedge, \chi_B] + (-1)^{\mu_A}[\chi_A \wedge, \mathcal{Q}\chi_B] \,. \tag{6.23}$$

It is also annihilated to all orders in perturbation theory by an analogous relation for $\mathcal{Q}^\dagger$ proving it a perturbative ground state itself. Perturbative ground states are thus seen to come in families, the above procedure can be repeated with either of the pairs $(\chi_{A,B}, \chi_{AB})$. However $\chi_{AB} \neq 0$ is not necessarily true, the terms in (6.23) may potentially cancel or more trivially the degree of χ_{AB} may exceed the dimension of the target space M_3.

---

[1]Here we have discussed generic localized perturbative ground states. To a given Higgs field background ϕ there also exist color vectors λ such that the color contracted Higgs field $\phi_\lambda \equiv 0$ vanishes identically. We say that these color vectors and associated ground states of $\mathcal{Q}, \mathcal{Q}^\dagger$ live in the bulk as the groundstates are now determined by the differential $\mathcal{Q} = d$ which is as in chapter 2.4. Whenever $\phi_\lambda \neq 0$ we refer to the color vectors and their associated perturbative ground states as localized. Generically the local 1-form ϕ_λ has isolated simple zeros, this is the case discussed here.

Half-BPS instantons are field configurations minimizing the Euclidean Lagrangian and are annihilated by half of the supercharges (6.15) in Euclidean time. They are distinguished by boundary conditions fixing the initial and final position of the particle. Field configuration may only converge to stationary points on M_3 allowing for $\dot{x} = 0$, i.e., instantons necessarily connect perturbative ground states. From the Euclidean Lagrangian we obtain the flow and parallel transport equations

$$\dot{x}^i \pm \phi_\lambda^i = \dot{x}^i \pm i c_{\alpha\beta\gamma} g^{ij} \bar{\lambda}^\alpha \phi_j^\beta \lambda^\gamma = 0 \,, \qquad D_\tau \lambda_\alpha = 0 \,, \tag{6.24}$$

supplemented with the constraint $\bar{\lambda}\lambda = 1$ enforced by the Lagrange multiplier. An instanton of the colored SQM solves (6.24) piecewise and connects multiple perturbative ground states. We refer to instantons of the SQM as generalized instantons whenever they connect more than two perturbative ground states, this more general class of instantons is absent in SQMs without $\lambda, \bar{\lambda}$ color degrees of freedom.

Instanton connecting two perturbative ground states, as familiar from Witten's SQM or Morse theory, start out at a point $(x_A, \lambda_A) \in \mathrm{ad}\, P_{\mathrm{ADE}}$ satisfying $\phi_{\lambda_A}(x_A) = 0$ where the color contracted Higgs field ϕ_{λ_A} is given in (6.20). From this initial configuration the instanton flows on M_3 along a path γ determined by the 1-form $\phi_{\lambda(\tau)}$ where $\lambda(\tau)$ is the parallel transport of λ_A along the path γ with respect to the background connection A on M_3. The flow can end at a point $(x_B, \lambda_B) \in \mathrm{ad}\, P_{\mathrm{ADE}}$ satisfying $\phi_{\lambda_B}(x_B) = 0$. Summarizing we have

$$(x_A, \lambda_A) \,, \ \phi_{\lambda_A}(x_A) = 0 \qquad \xrightarrow[\ D_\tau \lambda(\tau) = 0\ ]{\ \dot{x}(\tau) = \pm \phi_{\lambda(\tau)}\ } \qquad (x_B, \lambda_B) \,, \ \phi_{\lambda_B}(x_B) = 0 \,, \tag{6.25}$$

where τ runs from $-\infty$ to $+\infty$ from left to right. Completing the square in the Euclidean Lagrangian, instanton effects are found to be suppressed by

$$S_{\mathrm{inst}} = \mp \int_{-\infty}^{+\infty} d\tau \, \dot{x}^i \phi_{\lambda,i} > 0 \,, \tag{6.26}$$

where the sign depends on whether ascending or descending flows are considered in (6.24).
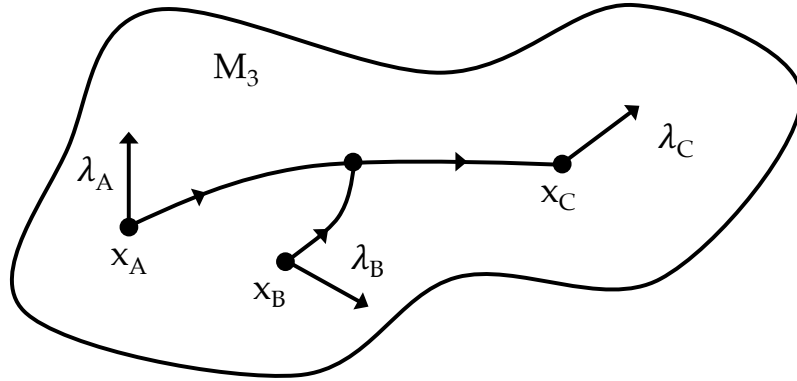
Figure 6.1: Sketch of an instanton connecting three perturbative ground states labeled by (x_A, λ_A), (x_B, λ_B) and (x_C, λ_C). The color degrees of freedom are valued in the pull back bundle $x^*(\mathrm{ad}\, P_{\mathrm{ADE}})$ and are depicted as internal vectors attached to the localization site of the perturbative ground states. The three legs of the instanton are piecewise determined by the flow equations (6.24).

Generalized instantons connecting three perturbative ground states are pieced together from flows parametrized by half-lines where τ runs from $-\infty$ to 0 or from 0 to $+\infty$ on each segment. We depict such a generalized instantons connecting three perturbative ground states labelled by $(x_A, \lambda_A), (x_B, \lambda_B)$ and (x_C, λ_C) in figure 6.1. Along each leg the instanton is determined by the flow equations (6.24) and boundary conditions imposed at the junction and perturbative ground states. We discuss these generalized instantons in greater detail in section 7.2.2.

6.4   SYM and SQM

The colored SQM is a powerful computational and organisational tool when applied to the compactification of the partially twisted 7d SYM on M_3, we briefly discuss the dictionary between the SQM and SYM which follows from (6.4).

The perturbative ground states of the SQM (6.22) are to be identified with the approximate zero modes (6.1) of the partially twisted 7d SYM. As a consequence the matrix elements of the supercharge $\mathcal{Q}$ with respect to the perturbative ground states is given by the mass matrix (6.2) of the 4d modes associated with the approximate zero modes. The ground

states of the SQM then determine the massless spectrum in 4d (2.45). The identification of perturbative ground states and approximate zero modes allows for an interpretation of the Yukawa overlap integral (6.3) as a tunneling amplitude. States occupying two perturbative ground states χ_A, χ_B can tunnel to a third χ_C and the overlap Y_{ABC} then gives the amplitude for this process. This extends the table following (5.1).

The treatment of the SYM in this thesis part is purely classical and the effects computed by the SQM are the leading order effects in a standard Kaluza-Klein reduction of the field theory. The overlap integrals result from standard expansions in zero modes, massive modes are simply truncated as they do not contribute in the large Higgs field limit $t \to \infty$. Away from this limit quantum effects enter and their analysis poses an open problem.

The non-perturbative effects of the SYM derived from an ALE-geometry are understood to originate from M2-brane instantons wrapping supersymmetric 3-cycles. In the SYM these effects are in correspondence with flow trees of the Higgs field which are given by the projection of the supersymmetric 3-cycle to the base M_3, see e.g., figures 5.1 and 7.1. These flow trees are precisely piece-wise solutions to the flow equations (6.24) and thereby in one to one correspondence with the generalized instantons of the SQM. Along these graphs the approximate zero modes and perturbative ground states have maximal overlap and consequently these give the dominant contributions to the two integrals (6.2) and (6.3).

6.5 Higgs Bundles with Split Spectral Covers

The simplest backgrounds to study the correspondence between non-perturbative effects in the 7d SYM, which originate from M2-brane instantons in M-theory, and generalized instantons of the colored SQM are abelian solutions to the BPS-equations with split spectral covers. These backgrounds have previously been studied in [49, 90, 95, 117] and serve as a precursor to studying abelian solutions to the BPS equations with non-split spectral covers. The SQM interpretation of chapter 5 emerges as a degenerate case of the colored SQM formulation.

Here we find that the single particle sector of the colored SQM decomposes into a direct sum of Witten SQMs [107], one for each generator of the Lie algebra $\mathfrak{g}_{\text{ADE}}$. These interact via multi-particle effects encoded in higher order operations on the Morse-Witten complex of the colored SQM. They originate from M2-branes associated with the Y-shaped instantons and higher-point instantons.

6.5.1 Colored SQM and Witten's SQM

We consider backgrounds with a trivial connection $d_A = d$ and a diagonal Higgs field $\phi = \phi_I H^I$. The Cartan components $\phi_I \in \Omega^1(M_3)$ are 1-forms on M_3 solving the sourced equations (3.9). The color contracted Higgs field ϕ_λ given in (6.9) now becomes

$$\phi_\lambda = \kappa\left(\bar{\lambda}, [\phi, \lambda]\right) = \sum_\alpha \alpha^I \phi_I \bar{\lambda}^\alpha \lambda_\alpha \,, \tag{6.27}$$

where the sum runs over all roots α of the Lie algebra $\mathfrak{g}_{\text{ADE}}$. The Lagrangian of the SQM probing the Higgs bundle simplifies from (6.13) to

$$\begin{aligned}
\mathcal{L} = {} & \frac{1}{2}\dot{x}^i \dot{x}_i + i\bar{\psi}^i \nabla_\tau \psi_i + i\bar{\lambda}^\beta \dot{\lambda}_\beta - \left(\nabla_{(i}\phi_{j)}\right)_\lambda \bar{\psi}^i \psi^j - \frac{1}{2}\phi_\lambda^i \phi_{\lambda,i} \\
& - \frac{1}{2}R_{ijkl}\psi^i \bar{\psi}^j \psi^k \bar{\psi}^l + \zeta\left(\bar{\lambda}^\beta \lambda_\beta - n\right) \,,
\end{aligned} \tag{6.28}$$

where $\beta = 1, \ldots, \dim \mathfrak{g}_{\text{ADE}}$ runs over all generators T^β of the Lie algebra $\mathfrak{g}_{\text{ADE}}$. The bundle geometry is $\text{ad}\, P_{\text{ADE}} = M_3 \times \mathfrak{g}_{\text{ADE}}$ and as a consequence the Hilbert space (6.16) which is now given by Lie algebra valued forms $\mathcal{H}_{\text{phys.}} = \Lambda\left(M_3, \mathfrak{g}_{\text{ADE}}\right)$ decomposes into the direct sum

$$\begin{aligned}
\mathcal{H}_{\text{phys.}} &= \bigoplus_\beta \mathcal{H}_{\text{phys.}}^{(\beta)} \,, \\
\mathcal{H}_{\text{phys.}}^{(\beta)} &= \Lambda\left(M_3\right) \otimes T^\beta \,,
\end{aligned} \tag{6.29}$$

paralleling the decomposition of $\text{ad}\, P_{\text{ADE}}$ into a sum of line bundles. States in $\mathcal{H}_{\text{phys.}}^{(\beta)}$ are p-forms oriented along the generator T^β in $\Omega^p(M_3, \mathfrak{g}_{\text{ADE}})$. Specializing to a Cartan-Weyl Basis $\left\{H^I, E^\alpha\right\}$ of the Lie algebra $\mathfrak{g}_{\text{ADE}}$ we can sharpen the decomposition (6.29) to

$$\mathcal{H}_{\text{phys.}} = \bigoplus_\alpha \mathcal{H}_{\text{phys.}}^{(\alpha)} \oplus \bigoplus_I \mathcal{H}_{\text{phys.}}^{(I)} \,, \tag{6.30}$$

and refer to the first summand $\oplus_\alpha \mathcal{H}_{\text{phys.}}^{(\alpha)}$ as the localized sector and to the second summand $\oplus_I \mathcal{H}_{\text{phys.}}^{(I)}$ as the bulk sector of this SQM. They are built from

$$\mathcal{H}_{\text{phys.}}^{(\alpha)} = \Lambda(M_3) \otimes E^\alpha \,, \qquad \mathcal{H}_{\text{phys.}}^{(I)} = \Lambda(M_3) \otimes H^I \,. \tag{6.31}$$

The supercharge $\mathcal{Q}$ respects this decomposition as all component functions ϕ_i of the Higgs field $\phi = \phi_i dx^i$ are valued in the Cartan subalgebra, i.e., it restricts to operators on the subspaces (6.31)

$$\begin{aligned}
\mathcal{Q}^{(\alpha)} : & \quad \mathcal{H}_{\text{phys.}}^{(\alpha)} \;\to\; \mathcal{H}_{\text{phys.}}^{(\alpha)} \,, & \chi \otimes E^\alpha \;\mapsto\; \left(d\chi + \alpha^I \phi_I \wedge \chi\right) \otimes E^\alpha \,, \\
\mathcal{Q}^{(I)} : & \quad \mathcal{H}_{\text{phys.}}^{(I)} \;\to\; \mathcal{H}_{\text{phys.}}^{(I)} \,, & \chi \otimes H^I \;\mapsto\; d\chi \otimes H^I \,,
\end{aligned} \tag{6.32}$$

where $\chi \in \Omega^p(M_3)$ is a p-form on M_3. The Hamiltonian $H = \frac{1}{2}\left\{\mathcal{Q}, \mathcal{Q}^\dagger\right\}$ decomposes similarly into restrictions as (6.32) which govern the time evolution of states of definite color

$$H^{(\alpha)} = \frac{1}{2}\left\{\mathcal{Q}^{(\alpha)}, \mathcal{Q}^{(\alpha)\dagger}\right\} \,, \qquad H^{(I)} = \frac{1}{2}\left\{\mathcal{Q}^{(I)}, \mathcal{Q}^{(I)\dagger}\right\} \,, \tag{6.33}$$

Stripping off the trivial Lie algebra generator in each sector we obtain Hamiltonians acting on the exterior algebra $\Lambda(M_3)$. We thus find a copy of Witten's SQM for every Lie algebra generator and more precisely obtain the correspondences

$$\begin{aligned}
E^\alpha \in \mathfrak{g}_{\text{ADE}} & \quad \leftrightarrow \quad & \text{Witten's SQM with supercharge } \mathcal{Q} = d + \alpha^I \phi_I \wedge \,, \\
H^I \in \mathfrak{g}_{\text{ADE}} & \quad \leftrightarrow \quad & \text{Witten's SQM with supercharge } \mathcal{Q} = d \,.
\end{aligned} \tag{6.34}$$

The study of colored SQMs with split Higgs fields thus equates to studying the interaction between the family of (uncolored) SQMs (6.34) embedded within it.

6.5.2 Partial Higgsing

When the group G_{ADE} is only partially Higgsed the correspondence (6.34) degenerates. Consider the rank n Higgsing

$$\begin{aligned}
G_{\text{ADE}} & \quad \to \quad & G_{\text{GUT}} \times U(1)^n \,, \\
\operatorname{Ad} G_{\text{ADE}} & \quad \to \quad & (\operatorname{Ad} G_{\text{GUT}} \otimes \mathbf{1}) \oplus (\mathbf{1} \otimes \operatorname{Ad} U(1)^n) \oplus \sum_Q \mathbf{R}_Q \,,
\end{aligned} \tag{6.35}$$

where $Q = (q_1, \ldots, q_n)$ is a vector of $U(1)$ charges. Then for every generator $E^\alpha \in \mathbf{R}_Q$ the supercharge of the associated SQM reads $\mathcal{Q} = d + Q^I \phi_I \wedge$. The correspondence (6.34) can be rephrased as

$$\mathbf{R}_Q \qquad \leftrightarrow \qquad \text{Witten's SQM with supercharge } \mathcal{Q} = d + Q^I \phi_I \wedge \,, \qquad (6.36)$$

making the degeneracy manifest. Representation not transforming under $U(1)^n$ correspond to a free SQM mapping into M_3 whose supercharge is the exterior derivative. This set-up is the one described initially in chapter 5.

Chapter 7
Yukawa Couplings and Higher-Point Interactions

In this section we discuss the interactions of localized matter[1]. We consider the case of a fully factored spectral cover first. In M-theory interactions between localized matter fields come from M2-instantons wrapped on calibrated 3-spheres of the local ALE-fibration. This is simply a generalisation of the results of section 5.2, where we interpreted non-perturbative mass terms as arising from M2-instantons wrapping three-cycles which connect two critical points over a gradient flow line. For higher point interactions these three-cycles project to gradient flow trees on $\mathcal{M}_3$ and studying the moduli space of these constrains the corresponding interactions in 4d. For example, Yukawa couplings must support a cup-product structure on the associated Morse-Witten complex.

Consider in this section again the background of section 4.2, globally on M_3 we have

$$\langle \phi \rangle = \mathrm{diag}(\lambda_1, \cdots, \lambda_n) = \sum_{i=1}^{n} H^i df_i \,, \quad \Delta f_i = \rho_i \,, \quad \int_{M_3} \rho_i = 0 \,. \qquad (7.1)$$

The matter content is summarized in table 4.1. We first consider interactions between fields resulting from the expansion of the approximate zero modes (5.6) and (5.7). The interaction between the true zero modes then follow by linearity. Leading order corrections

---

[1]For the interaction between bulk and localized matter we refer to section 6.1 of [1].
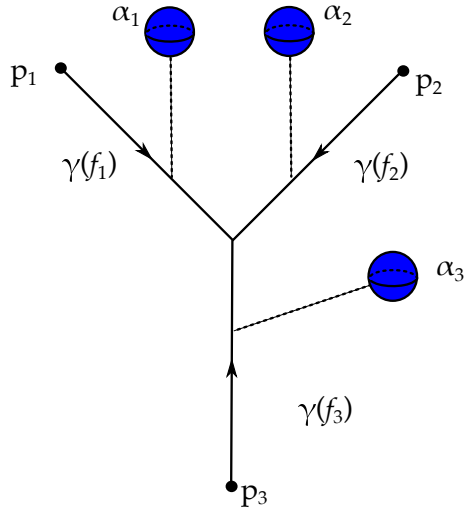
Figure 7.1: Gradient flow tree for Yukawa couplings. The picture shows three critical points p_i of the functions f_i of Morse index $\mu_{f_i}(p_i) = 1$. The gradient flow lines $\gamma(f_i)$ of the f_i are marked by arrows. Every f_i controls the size of a 2-cycle α_i which has the topology of a two-sphere and collapses over the points p_i. The three three-chains formed by fibering the two-spheres α_i over the segments $\gamma(f_i)$ can be joined at their meeting point as $\alpha_1 + \alpha_2 + \alpha_3 = 0$, and the resulting three-cycle is expected to be an associative.

to these couplings are obtained from integrating out states with masses purely induced by M2-instantons as discussed in section 5.2.

Yukawa couplings can be approached by either arguing M2-brane instanton contributions in M-theory as in [112] or studying non-perturbative effects in the 7d SYM. Higher-point interactions can only be analysed from the first perspective. Non-renormalizable interactions do not descend from the 7d SYM via a simple zero mode expansion and we argue their contributions from M-theory generalizing results for Yukawa couplings. The quantative analysis of Yukawa couplings requires the colored SQM interpretation of the relevant overlap integral which allows for their computation via supersymmetric localization.

7.1 Yukawa Couplings from the 7d SYM

For Yukawa couplings to occur we need a rank $n = 2$ Higgs bundle (or higher). There are two Morse functions f_1 and f_2 and the combination $f_Q = q_1 f_1 + q_2 f_2$. From the effective field theory we obtain this coupling by expanding the action (2.13) in approximate zero

modes

$$Y_{abc}^{pqr} = \int_{\mathcal{M}_3} \psi^{(a,p)} \wedge \varphi^{(b,q)} \wedge \psi^{(c,r)}, \qquad Q_p + Q_q + Q_r = 0, \qquad (7.2)$$

where (a,p) refers to the internal profile of the perturbative zero mode localized at the critical point $x_a \in M_3$ transforming in $\mathbf{R}_{Q_p}$, specifying the indices in (6.3). The profiles wedged in the integrand of (7.2) are all of the form (5.6). The Yukawa couplings arise from M2-instantons wrapping associative three-cycles. To characterize the three-cycles consider the Morse functions

$$Q_1 = (1,0), \qquad Q_2 = (0,-1), \qquad Q_3 = (-1,1)$$

$$f_{Q_1} = f_1, \qquad f_{Q_2} = -f_2, \qquad f_{Q_3} = -f_1 + f_2 = f_3, \qquad (7.3)$$

which describe an $SU(3)$ ALE-fibration over the base $\mathcal{M}_3$. Each of the functions f_i controls the volume of a corresponding two-sphere α_i in the ALE fiber, which satisfy

$$\alpha_1 + \alpha_2 + \alpha_3 = 0 \qquad (7.4)$$

in the homology of every fiber. Recall that α_i shrinks to zero volume precisely over the points p_i where $df_i = 0$. To every gradient trajectory $\gamma(f_i)$ starting at a point p_i we can associate a 3-chain, which is given by tracing out the corresponding α_i in the ALE-fibration. Given three sufficiently generic Morse functions f_i, there will be finitely many gradient flow trees connecting the three critical points p_i (see figure 7.1). Adding the associated three-chains produces a three-cycle, the boundary of which is given by $\sum_i \alpha_i$ in the ALE fiber. We may produce a closed three-cycle with the topology of a three-sphere by adding a three-cycle β such that $\partial \beta = \alpha_1 + \alpha_2 + \alpha_3$. Moreover, this S^3 is expected to be an associative, since it projects to the tree of gradient trajectories and hence minimizes the volume among all the three-cycles which project down to trees connecting p_1, p_2 and p_3. Wrapping an M2-brane on such a cycle gives rise to Yukawa couplings between modes localized at the critical points of f_1, f_2 and f_3. Consequently, the overlap integral (7.2) vanishes if there exists no trivalent gradient flow tree connecting the critical points[2].

---

[2]Massless chiral multiplets are found when expanding the 7d action in true zero modes. These are in general linear combinations of the localised perturbative profiles used in (7.2). The relevant linear combina-
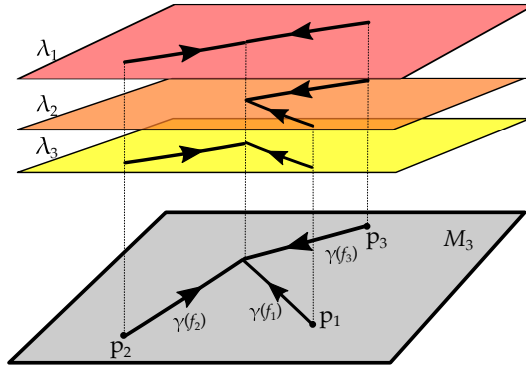
Figure 7.2: Construction of three-cycle that gives rise to the Yukawa couplings in the spectral Cover picture. The critical loci p_i correspond to the loci where two of the weights λ_i are equal, i.e., the corresponding sheets of the spectral cover meet. The uplift of the gradient flow lines $\gamma(f_i)$ sweeps out the associative three-cycle S^3 that can then be wrapped by an M2-instanton. This gives rise to the coupling between the three matter states localized at $\lambda_i = 0$. The combined flow lines give rise to the gradient flow tree $\gamma(f_1, f_2, f_3)$.

Similarly, in the spectral cover description, the Yukawa coupling is modeled in terms of a three-sheeted cover, which is determined by the graph of df_i. The segments of the gradient flow trees determined by the function f_i thus lift to paths on the corresponding sheets; see figure 7.2. The paths connect the points where two sheets pairwise intersect. One can think of the 2-cycles α_j in the ALE-fibration as being stretched between the sheets and the corresponding cycle collapses precisely at points where two sheets meet.

The strength of these interactions is governed by the choice of functions f_i. The three-sphere giving rise to the Yukawa coupling is a supersymmetric rigid homology sphere within the G_2-manifold and its contribution to the superpotential is again given by (5.17). The sign $n_\gamma = \pm 1$ arises in the same manner and is given by an orientation on the moduli space of gradient flow trees. As the Higgs field ϕ_i and the gauge field W_i are identified with the periods of the supergravity 3-form C and associative 3-form Φ the integral is evaluated as

$$\int_{S^3_\gamma} (C + i\Phi) = \sum_{j=1}^{3} \int_{\gamma(f_j)} \int_{\alpha_j} (C + i\Phi) = \sum_{j=1}^{3} \int_{\gamma(f_j)} (W_j + i\phi_j) = i \sum_{j=1}^{3} \int_{\gamma(f_j)} tdf_{Q_j}, \quad (7.5)$$

Here, we have used that we can gauge the background for the gauge field W_i to zero.

tions are determined by the Morse-Witten complex. The overlap integral determining the Yukawa couplings between the massless modes are thereby linear combinations of (7.2).

Evaluating the final integrals and using that the homological relation between the α implies $\sum_i^3 f_i = 0$ we find

$$\Delta W \sim n_\gamma \exp\left(-\sum_{i=1}^3 t f_{Q_i}(p_i)\right).$$
(7.6)

We now make this M-theory derivation rigorous by computing the Yukawa overlap integral directly via supersymmetric localization in the colored quantum mechanics.

7.2 Yukawa Couplings from the colored SQM

We now compute the Yukawa overlap integrals for the fully reducible (split) Higgs field background (7.1) and discuss their interpretation in the colored SQM. We further restrict to backgrounds for which the gauge group has been Higgsed to its maximal torus $U(1)^n$ where n is the rank of the gauge group $\tilde{G}$. Consquently the representations $\mathbf{R}_Q$ in (4.21) are one-dimensional and labelled by roots α of the Lie algebra $\tilde{\mathfrak{g}}$. Here the n-component roots play the role of the charge vector Q in (4.21) and the Higgs field $\phi = \phi^I H_I$ determine the charge weighted Higgs field, given in (4.22), to $\alpha^I \phi_I = \alpha^I df_I$, which is a 1-form on M_3 derived from the Morse function $\alpha^I f_I$. Backgrounds preserving a non-abelian gauge group G in 4d are discussed subsequently and occur as a degenerate case of this set-up with some Cartan components ϕ_I tuned to vanish.

We first discuss how the approximate zero modes appearing in the integrand of the Yukawa integral (6.3) are organized by the colored SQM into a Morse-Witten complex. This Morse-Witten complex is the direct sum of the complexes associated to the SQMs in (6.34). The Yukawa overlap integral (6.3) then gives a cup product mapping between these complexes.

7.2.1 Organizing Approximate Zero Modes

Each approximate zero mode is a Lie algebra valued 1-form and oriented along a Lie algebra generator E^α. Taking the trace in (6.3) results in the integral of forms (7.2). Linear combinations of these modes constitute zero modes along M_3 and are determined by the cohomology groups of the Morse-Witten complex associated to the function $\alpha^I f_I$ on M_3.

With this the Morse-Witten complex of the colored SQM is built from the free abelian groups $C^\mu(M_3, \phi)$ generated by the perturbative ground states (6.22) over the complex numbers

$$C^\mu(M_3, \phi) = \bigoplus_\alpha C^{\mu,\alpha}(M_3, \alpha^I \phi_I)\,,$$
$$C^{\mu,\alpha}(M_3, \alpha^I \phi_I) = \bigoplus_a \mathbb{C}\,|x_a, \lambda^\alpha, \mu_a\rangle \equiv C_\alpha^\mu(M_3, \phi)\,, \tag{7.7}$$

where μ fixes the degree of the perturbative ground state as a differential form. It is graded by the fermion number operators associated with the fermions $\psi, \bar{\psi}$ and $\lambda, \bar{\lambda}$. The supercharge gives rise to the boundary map on the complex (7.7) and as a consequence of the decomposition (6.32) the colored Morse-Witten complex is found to decompose into multiple standard Morse-Witten complexes whose chain groups are $C_\alpha^\mu(M_3, \phi)$ for fixed color α. We take capital latin indices to run over generic perturbative ground states of the colored SQM and decapitalized latin indices to run over all perturbative ground states of a fixed color, or equivalently over all perturbative ground states of a subcomplex of the SQMs in (6.34).

The color restricted supercharge $\mathcal{Q}^{(\alpha)}$ of (6.32) now gives rise to the standard boundary map [107, 108, 110] generated by oriented flow lines (6.24) of $\alpha^I \phi_I$ we have

$$C_\alpha^3(M_3, \phi) \xleftarrow{\mathcal{Q}^{(\alpha)}} C_\alpha^2(M_3, \phi) \xleftarrow{\mathcal{Q}^{(\alpha)}} C_\alpha^1(M_3, \phi) \xleftarrow{\mathcal{Q}^{(\alpha)}} C_\alpha^0(M_3, \phi)\,. \tag{7.8}$$

The adjoint of the supercharge $\mathcal{Q}^{(\alpha)}$ maps in the opposite direction. There is no such complex for colors in the bulk of the SQM. Each of the complexes (7.8) can be analyzed separately and its cohomologies are the Novikov/Lichnerowicz cohomologies [111, 118, 119] with respect to the closed 1-form $\alpha^I \phi_I$ on M_3. The cohomology groups of the supercharge $\mathcal{Q}$ of the colored SQM thus decomposes into a direct sum

$$H_\mathcal{Q}^*(M_3, \mathfrak{g}_{\text{ADE}}) \cong \left(\bigoplus_{I=1}^n H_{\text{dR}}^*(M_3)\right) \oplus \left(\bigoplus_{E^\alpha \in \mathfrak{g}_{\text{ADE}}} H_{\text{Nov.}}^*(M_3, \alpha^I \phi_I)\right)\,, \tag{7.9}$$

where each summand is in correspondence with an SQM of (6.34). Here the exact 1-forms $\alpha^I \phi_I = \alpha^I df_I$ are derived from Morse functions $\alpha^I f_I$ and the complex (7.8) is that of Morse theory on a manifold with boundary, as discussed in chapter 5. The boundary $\Sigma = \Sigma_+^\alpha \cup \Sigma_-^\alpha$ follows from excising the source terms and is again partitioned according to the direction

of the 1-form $\alpha^I \phi_I$ with respect to its normal vector. In the notation of chapter 5 we find (7.9) to simplify to

$$H^*_{\mathcal{Q}}(M_3, \mathfrak{g}_{\mathrm{ADE}}) \cong \left(\bigoplus_{I=1}^{n} H^*_{\mathrm{dR}}(M_3) \right) \oplus \left(\bigoplus_{E^\alpha \in \mathfrak{g}_{\mathrm{ADE}}} H^*(\mathcal{M}_3, \Sigma^\alpha_-) \right) . \qquad (7.10)$$

7.2.2   Yukawa Integrals as Cup Product

The complexes (7.8) of different color can interact via a cup product originating from (6.23) and mediated by Y-shaped instantons. These multi-particle effects are absent in ordinary SQMs. Consider three perturbative ground states

$$\chi_a = |x_a, \lambda^\alpha, \mu_a\rangle \in \Omega^{\mu_a}(M_3) \otimes E^\alpha \, ,$$

$$\chi_b = |x_b, \lambda^\beta, \mu_b\rangle \in \Omega^{\mu_b}(M_3) \otimes E^\beta \, , \qquad (7.11)$$

$$\chi_c = |x_c, \lambda^\gamma, \mu_c\rangle \in \Omega^{\mu_c}(M_3) \otimes E^\gamma \, ,$$

which we assume to be energy eigenstates with energies $E_{0,r}$ of the Hamiltonian $H = \frac{1}{2}\{\mathcal{Q}, \mathcal{Q}^\dagger\}$. In general energy eigenstates will be linear combinations of the perturbative ground states to which the arguments below extend naturally. We further restrict to cases which allow for the normalisation $\kappa(T_a, T_b) = \delta_{ab}$ of generators to simplify exposition.

The Y-shaped instantons determine the leading order contribution to the overlap integral (6.3). The integral vanishes unless three selection rules are satisfied

$$\mu_a + \mu_b = \mu_c \, , \qquad \alpha + \beta = \gamma \, , \qquad E_{0,a} + E_{0,b} = E_{0,c} \, . \qquad (7.12)$$

If these are satisfied the Yukawa integral can be simplified to

$$Y^{\alpha\beta\gamma}_{abc} = \int_{M_3} \langle \chi_c, [\chi_a \wedge, \chi_b] \rangle = \int_{M_3} *\overline{\chi}^{(\gamma)}_c \wedge \chi^{(\alpha)}_a \wedge \chi^{(\beta)}_b \, . \qquad (7.13)$$

where we took the trace over the Lie algebra generators in the second equality and made the complex conjugation in the first factor explicit. Here the raised indices (α, β, γ) refer to the differential form part of the perturbative ground state stripped of its Lie algebra generator[3].

---

[3]The connection to (7.2) is made by the isomorphism (2.44) together with some change in labels which reflect that the formula (7.2) holds in the degenerate, but physically interesting setting (6.35) of partial Higgsing.

We evaluate this integral in three steps. The first step consists of rewriting the perturbative ground states as projections of profiles which are highly localized at the point $x_r \in M_3$ associated to the perturbative ground state with $r = a, b, c$. We then rewrite the overlap integral as a path integral of the colored SQM in which the unprojected localized profiles go over into boundary conditions. This path integral then splits into three pieces each associated with a definite color which we evaluate via supersymmetric localization.

To begin note that the operator creating a perturbative ground state can be rewritten as

$$\chi_r = \lim_{T \to -\infty(1+i\delta)} \frac{e^{-iHT} \Psi_r \, e^{iHT}}{e^{-iE_{0,r}T} \langle \chi_r | \Psi_r \rangle} \equiv \Psi_r \big|_{-\infty}, \qquad (7.14)$$

where $0 < \delta \ll 1$ and $r = a, b, c$. The Hamiltonian H is the Legendre transform of the Lagrangian given in (6.28). Here $\Psi_r = \Psi_r^{(\alpha)} \bar{\lambda}^\alpha$ (no sum) creates a Lie algebra valued μ_r-form oriented along the generator E^α whose compact support only contains the point $x_r \in M_3$ and no other points at which perturbative ground states localize. The slightly imaginary limit projects Ψ_r onto the state of lowest energy with non-trivial overlap, this state is χ_r. Using the basis

$$\mathcal{B} = \left\{ \bar{\lambda}^\alpha |x^l\rangle, \ \bar{\lambda}^\alpha \bar{\psi}^i |x\rangle, \ \bar{\lambda}^\alpha \bar{\psi}^i \bar{\psi}^j |x\rangle, \ \bar{\lambda}^\alpha \bar{\psi}^i \bar{\psi}^j \bar{\psi}^k |x\rangle \right\} \qquad (7.15)$$

for the Hilbert space (6.16) we extract the component functions. Here $\alpha = 1, \ldots, d$ and $i, j, k = 1, 2, 3$ and $x \in M_3$. We separated these delta functions by their degree as differential

forms. With respect to this basis we have

$$
\begin{aligned}
\left(\Psi_r\big|_{-\infty}\right)^{(\alpha)}_{i_1\ldots i_{\mu_r}}(x) &= \langle x|\lambda^\alpha \psi_{i_1}\ldots\psi_{i_{\mu_r}}\,\Psi_r\big|_{-\infty}|0\rangle \\
&= \lim_{T\to-\infty(1+i\delta)} \langle x|\lambda^\alpha\psi_{i_1}\ldots\psi_{i_{\mu_r}}\left(e^{-iHT}\Psi_r\right)\left(e^{-iE_{0,r}T}\langle\chi_r|\Psi_r\rangle\right)^{-1}|0\rangle \\
&= \lim_{T\to-\infty(1+i\delta)} \left(e^{-iE_{0,r}T}\langle\chi_r|\Psi_r\rangle\right)^{-1}\langle x|\lambda^\alpha\psi_{i_1}\ldots\psi_{i_{\mu_r}}e^{-iHT}|\Psi_r\rangle \\
&= \lim_{T\to-\infty(1+i\delta)} \left(e^{-iE_{0,r}T}\langle\chi_r|\Psi_r\rangle\right)^{-1} \\
&\quad\times \langle x|\lambda^\alpha\psi_{i_1}\ldots\psi_{i_{\mu_r}}e^{-iHT}\left(\sum_s|\chi_s\rangle\langle\chi_s| + \sum_n|n\rangle\langle n|\right)|\Psi_r\rangle \\
&= \lim_{T\to-\infty(1+i\delta)} \left(e^{-iE_{0,r}T}\langle\chi_r|\Psi_r\rangle\right)^{-1}\langle x|\lambda^\alpha_{(r)}\psi_{i_1}\ldots\psi_{i_{\mu_r}}e^{-iHT}|\chi_r\rangle\,\langle\chi_r|\Psi_r\rangle \\
&= \langle x|\lambda^\alpha\psi_{i_1}\ldots\psi_{i_{\mu_r}}|\chi_r\rangle \\
&= \chi^{(\alpha)}_{r,i_1\ldots i_{\mu_r}}(x)\,,
\end{aligned}
\tag{7.16}
$$

which proves (7.14). Here the sum $\sum_s$ runs over all perturbative ground states while the sum $\sum_n$ runs over all higher energy eigenstates in the physical Hilbertspace $\mathcal{H}_{\text{phys.}}$ of (6.30). The support of the states Ψ_r is localized at x_r and excludes the sites of localization of all other perturbative ground states. Consequentially $\langle\chi_s|\Psi_r\rangle = \delta_{sr}\langle\chi_r|\Psi_r\rangle$ holds. Note further that we can anticommute the color fermions $\lambda,\bar\lambda$ past another in (7.16) which results in a simplification of the Hamiltonian evolving the states. We have

$$
\chi^{(\alpha)}_{r,i_1\ldots i_{\mu_r}}(x) = \lim_{T\to-\infty(1+i\delta)}\langle x|\psi_{i_1}\ldots\psi_{i_{\mu_r}}\left(e^{-iH^{(\alpha)}T}\Psi^{(\alpha)}_r\right)\left(e^{-iE_{0,r}T}\langle\chi_r|\Psi_r\rangle\right)^{-1}|0\rangle\,, \tag{7.17}
$$

where $H^{(\alpha)}$ is the Hamiltonian given in (6.33).

Next we rewrite the overlap integral (7.13) using the expression (7.17) for the profile of the perturbative ground states

$$
\begin{aligned}
Y^{\alpha\beta\gamma}_{abc} &= \lim_{T\to-\infty(1+i\delta)}\int_{M_3} d^3x \left(e^{-i\left(E_{0,a}+E_{0,b}-E_{0,c}\right)T}\langle\chi_a|\Psi_a\rangle\langle\chi_b|\Psi_b\rangle\overline{\langle\chi_c|\Psi_c\rangle}\right)^{-1} \\
&\quad\times \langle x|\psi_{i_1}\ldots\psi_{i_{\mu_a}}\left(e^{-iH^{(\alpha)}T}\Psi^{(\alpha)}_a\right)|0\rangle \\
&\quad\times \langle x|\psi_{j_1}\ldots\psi_{j_{\mu_b}}\left(e^{-iH^{(\beta)}T}\Psi^{(\beta)}_b\right)|0\rangle \\
&\quad\times \langle x|\psi_{k_1}\ldots\psi_{k_{3-\mu_c}}\left(e^{iH^{(\gamma)}T}*\overline{\Psi}^{(\gamma)}_c\right)|0\rangle \\
&\quad\times \epsilon^{i_1\ldots i_{\mu_a}j_1\ldots j_{\mu_b}k_1\ldots k_{3-\mu_c}}
\end{aligned}
\tag{7.18}
$$

We take Ψ_r to be δ-function like supported at x_r, rescale the Higgs field $\phi \to t\phi$ and from now on work to leading order in $1/t$. In the $t \to \infty$ limit the profile of the normalized perturbative ground states χ_r increasingly localizes at x_r. To leading order we thus have

$$\langle \chi_r | \Psi_r \rangle = 1 + \mathcal{O}(1/t).\tag{7.19}$$

The energies cancel by (7.12) and together with (7.19) we find (7.18) to simplify to

$$\begin{aligned}
Y^{\alpha\beta\gamma}_{abc} = &\lim_{T \to -\infty(1+i\delta)} \int_{M_3} d^3x \, \epsilon^{i_1...i_{\mu_a} j_1...j_{\mu_b} k_1...k_{3-\mu_c}} \\
&\times \langle x | \psi_{i_1} \ldots \psi_{i_{\mu_a}} \left(e^{-iH^{(\alpha)}T} \Psi^{(\alpha)}_a \right) |0\rangle \\
&\times \langle x | \psi_{i_1} \ldots \psi_{i_{\mu_b}} \left(e^{-iH^{(\beta)}T} \Psi^{(\beta)}_b \right) |0\rangle \\
&\times \langle x | \psi_{i_1} \ldots \psi_{i_{3-\mu_c}} \left(e^{iH^{(\gamma)}T} * \overline{\Psi}^{(\gamma)}_c \right) |0\rangle \\
&+ \mathcal{O}(1/t).
\end{aligned}\tag{7.20}$$

We now transition to the path integral representation by rewriting each matrix element above as a separate path integral. These are associated to paths with time intervals $(T, 0]_{a,b}$ and $[0, -T)_c$. The profiles Ψ_r are supported at x_r and give rise to boundary conditions for the path integral at infinite times. All in all we have

$$\begin{aligned}
Y_{abc} = \int_{M_3} d^3x_0 \int \prod_{\substack{-\infty < \tau < 0 \\ x_{a,-\infty} = x_a \\ x_{b,-\infty} = x_b}} dx_{a,\tau} \, d\psi_{a,\tau} \, d\bar{\psi}_{a,\tau} \, dx_{b,\tau} \, d\psi_{b,\tau} \, d\bar{\psi}_{b,\tau} \prod_{\substack{0 < \tau < \infty \\ x_{c,\infty} = x_c}} dx_{c,\tau} \, d\psi_{c,\tau} \, d\bar{\psi}_{c,\tau} \\
\exp \left[i \left(S^{(\alpha)}[x_a, \psi_a, \bar{\psi}_a] + S^{(\beta)}[x_b, \psi_b, \bar{\psi}_b] + S^{(\gamma)}[x_c, \psi_c, \bar{\psi}_c] \right) \right] \;+\; \mathcal{O}(1/t).
\end{aligned}\tag{7.21}$$

Here we have introduced the half line actions

$$S^{(\alpha)} = \int_{-\infty}^0 d\tau \, \mathcal{L}^{(\alpha)}, \qquad S^{(\beta)} = \int_{-\infty}^0 d\tau \, \mathcal{L}^{(\beta)}, \qquad S^{(\gamma)} = \int_0^\infty d\tau \, \mathcal{L}^{(\gamma)},\tag{7.22}$$

where the color restricted Lagrangians $\mathcal{L}^{(\alpha)}$ are the Legendre transformation of the color restricted Hamiltonians (6.33). These actions are associated with the time intervals $(T, 0]_{a,b}$ and $[0, -T)_c$ in the $T \to -\infty$ limit. The slightly imaginary limit makes the Feynman propagator the relevant propagator here. Further we have have written $x(\tau) = x_\tau$ and denoted the three paths generated by insertions of the identity operator by the labels a, b, c.

Note that these are only defined on half of the real line. These are constrained to start or end at the points $x_a, x_b, x_c \in M_3$ where the perturbative ground states localizes at infinite time and join at a common point $x_0 \in M_3$.

The expression (7.21) is technically not a path integral, the space of field configurations integrated over is that of all Y-shaped graphs whose end points are given by $x_{a,b,c}$. We depict such a configuration in figure 7.3. In the SQM Y_{abc} is to be identified with the tunneling amplitude of two particles of color λ_a, λ_b located at x_a, x_b respectively combining to a particle of color λ_c located at x_c.

As the final step we now evaluate the integral (7.21) via supersymmetric localization. We rotate to euclidean time $\tau \to -i\tau$ and denote the resulting actions with a subscript, we have

$$Y_{abc}^{\alpha\beta\gamma} = \int_{M_3} d^3x_0 \prod_{\substack{r=a,b,c \\ \alpha_r=\alpha,\beta,\gamma}} \int Dx_r D\psi_r D\bar{\psi}_r \, e^{-S_E^{(\alpha_r)}[x_r,\psi_r,\bar{\psi}_r]} + \mathcal{O}(1/t). \qquad (7.23)$$

The total action

$$S_E = S_E^{(\alpha)} + S_E^{(\beta)} + S_E^{(\gamma)}, \qquad (7.24)$$

is not invariant under the supersymmetries derived from (6.14). Half of the supersymmetry is broken by the boundaries of the actions (7.22), explicit computation[4] yields

$$\delta S_E = \bar{\epsilon} \left(\psi_a^i \dot{x}_{a,i} + \psi_b^i \dot{x}_{b,i} + \psi_c^i \dot{x}_{c,i} \right)_{\tau=0}, \qquad (7.25)$$

whereby only the symmetry generated by ϵ is unbroken. Considering the factors of (7.23) separately we see that the path integral thus localizes to ascending flow-lines of the 1-forms $\alpha^I \phi_I, \beta^I \phi_I$ on each leg emanating from $x_{a,b}$ and to ascending flow lines of $\gamma^I \phi_I$ on the leg ending at x_c of the Y-shaped configuration depicted in figure 7.3. These flow-lines are required to meet at a common point $x_0 \in M_3$ at time $\tau = 0$. We refer to such a BPS configuration as a flow tree Γ_{abc}. In a three dimensional set-up the only relevant triplet of perturbative ground state have degrees $\mu_a = \mu_b = 1$ and $\mu_c = 2$ as the D-term constraint

---

[4]See appendix C in [2] for details.

excludes perturbative ground states of degree 0 or 3. The moduli space of such flow trees is generically zero dimensional which follows by dimension count. Ascending, descending flow lines emanating from a point of Morse index $\mu = 1, 2$ sweep out a manifold of codimension 1 respectively. A common point of these flows is obtained upon intersecting these submanifolds whose expected codimension is 3. Due to the common center point x_0 there is no zero mode associated to time translations.

With this we localize on Y-shaped flow trees as depicted in figure 7.3. The standard localization computation then gives the result

$$Y_{abc}^{\alpha\beta\gamma} = \sum_{\Gamma_{abc}} (\pm)_{\Gamma_{abc}} \exp\left(-t\int_{\Gamma_\alpha} \alpha^I \phi_I - t\int_{\Gamma_\beta} \beta^I \phi_I + t\int_{\Gamma_\gamma} \gamma^I \phi_I\right) \qquad (7.26)$$
$$+ \mathcal{O}(1/t),$$

where Γ_σ with $\sigma = \alpha, \beta, \gamma$ are flow lines of the 1-form $\sigma^I \phi_I$ originating and ending at the respective perturbative ground states at $x_{a,b,c}$ and x_0. They glue to the flow tree Γ_{abc} over which the sum runs. The sign $(\pm)_{\Gamma_{abc}}$ denotes a fermion determinant. When $\sigma^I \phi_I = df^{(\sigma)}$ is exact this simplifies to

$$Y_{abc}^{\alpha\beta\gamma} = \sum_{\Gamma_{abc}} (\pm)_{\Gamma_{abc}} \exp\left(-tf^{(\alpha)}(x_a) - tf^{(\beta)}(x_b) + tf^{(\gamma)}(x_c)\right) + \mathcal{O}(1/t). \qquad (7.27)$$

For exact Higgs fields $df^{(\sigma)}$ the moduli space of Y-shaped flow trees has been described in [120], where it is shown to be an oriented 0d manifold, the relative signs $(\pm)_{\Gamma_{abc}}$ are then a choice of orientation on this discrete moduli space.

The overlap integral Y_{abc} therefore gives rise to a map between the chain groups of Morse-Witten subcomplexes

$$Y = [\cdot \wedge, \cdot] : \quad C_\alpha^{\mu_a}(M_3) \times C_\beta^{\mu_b}(M_3) \quad \rightarrow \quad C_{\alpha+\beta}^{\mu_a+\mu_b}(M_3), \qquad (7.28)$$

which maps pairs of perturbative ground states according to the Y-shaped flow trees

$$(\chi_a, \chi_b) \quad \mapsto \quad \sum_c Y_{abc}^{\alpha\beta\gamma} \chi_c, \qquad (7.29)$$
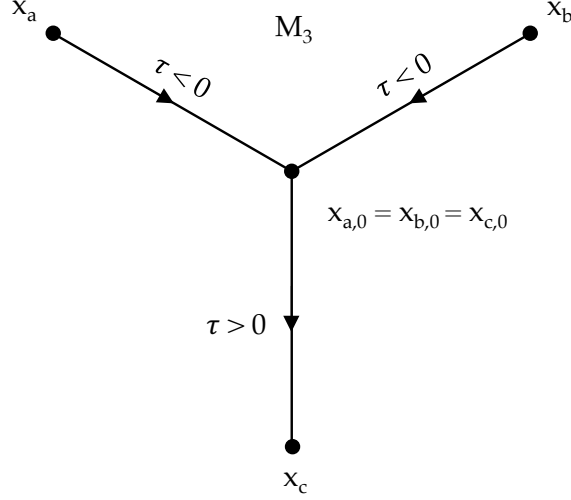
Figure 7.3: The figure shows an example of a Y-shaped graph whose end points are fixed at the points $x_{a,b,c}$. It is parametrized by two copies of $\mathbb{R}_-$ and one copy of $\mathbb{R}_+$. The set of Y-shaped graphs constrained in this manner constitute the configuration space the path integral in (7.20) localizes to. These Y-shaped flow trees are examples of generalized instantons which are a novel phenomenon of colored SQMs.

where χ_a, χ_b, χ_c are carry color $\alpha\beta\gamma$ and are given in (7.11). Ground states of the colored SQM are linear combination of perturbative ground states and thus the map Y descends to the cohomology of the colored SQM complex (7.7) where it describes a cup product.

We briefly describe the generalization to higher point interactions. However note, that the partially twisted 7d SYM does not derive these in terms of overlap integrals, rather we will argue for these geometrically in the next chapter.

The Massey products m_n of length n generalize the cup product Y. These are realized by gradient flow trees connecting $n+1$ perturbative ground states and are associated to a collection of Y-shaped gradient flow trees and gradient flow lines. We restrict our discussion to the Massey products of length 3 which are given by the map

$$m_3 : \quad C_\alpha^{\mu_a}(M_3) \times C_\beta^{\mu_b}(M_3) \times C_\gamma^{\mu_c}(M_3) \quad \rightarrow \quad C_{\alpha+\beta+\gamma}^{\mu_a+\mu_b+\mu_c-1}(M_3) \tag{7.30}$$

and is defined by

$$\left(|x_a, \lambda^\alpha, \mu_a\rangle, |x_b, \lambda^\beta, \mu_b\rangle, |x_c, \lambda^\gamma, \mu_c\rangle\right) \quad \mapsto \quad (-1)^{\mu_a+\mu_b-1} Y(S, |x_c, \lambda^\gamma, \mu_c\rangle)$$
$$+ (-1)^{\mu_b+\mu_c-1} Y(|x_a, \lambda^\alpha, \mu_a\rangle, T), \tag{7.31}$$
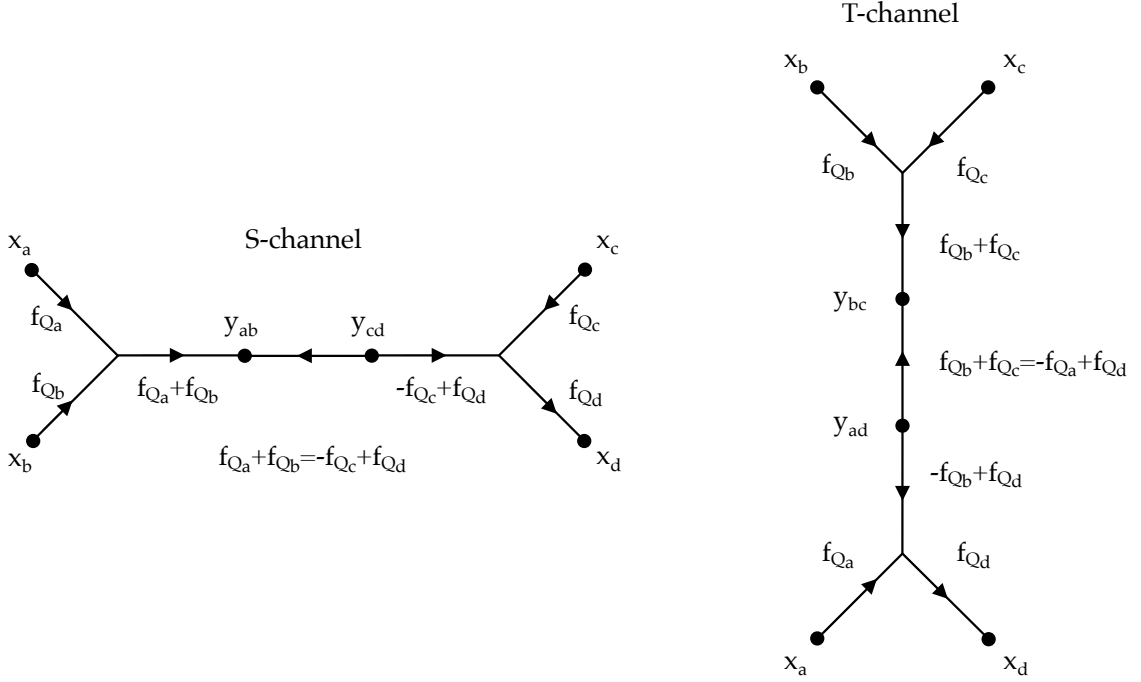
Figure 7.4: Picture of the flow trees contributing to the Massey product of length 3. Two summands marked with S, T respectively contribute to the Massey product m_3 in (7.31). Pictorially these are given by S-channel and T-channel like contributions. The Massey product m_3 maps perturbative ground states localized at the points x_a, x_b, x_c to one localized at x_d. Both channels are a given by two Y-shaped gradient flow trees connect by a gradient flow line. This structure descend from (7.31) which involves two cup products Y and a single boundary operator $\mathcal{Q}$. Here we assume globally exact Higgs fields $\phi_{Q_r} = df_{Q_r}$. In the picture we mark the functions governing the gradient flows. Two intermediate perturbative ground states are label by y_{rs} for each channel.

where S, T are perturbative ground states determined by the reverse flows

$$QS = (-1)^{\mu_a} Y\left(|x_a, \lambda^\alpha, \mu_a\rangle, |x_b, \lambda^\beta, \mu_b\rangle\right),$$
$$QT = (-1)^{\mu_b} Y\left(|x_b, \lambda^\beta, \mu_b\rangle, |x_c, \lambda^\gamma, \mu_c\rangle\right).$$
(7.32)

Up to signs these maps are easily understood as concatenations of gradient flow lines and Y-shaped flow trees. The quantities $Y(S, |x_c, \lambda_c, \mu_c\rangle)$ and $Y(|x_a, \lambda_a, \mu_a\rangle, T)$ corresponds to s,t-channel like graphs respectively. They are depicted in figure 7.4. General Massey products of length n are described similarly. By linear extension all Massey products m_n descend to the cohomolgies of the complexes of (7.8).

Summarizing we note that the set of perturbative ground states of the colored SQM can

be organized into separate Morse-Witten complexes whose boundary maps are given by the color restrictions $\mathcal{Q}^{(\alpha)}$ of the supercharge $\mathcal{Q}$. The supercharge $\mathcal{Q}$ giving rise to boundary maps. These complexes interact via the cup product Y and Massey products m_n with $n \geq 3$ which give rise to 3-point and $(n+1)$-point tunneling amplitutdes among the perturbative ground states. We summarize the corresponding geometrical and field theoretic structures in 1. Generalizing from (6.2) and (6.3) the massey products are in correspondence with irrelevant couplings in the 4d $\mathcal{N} = 1$ gauge theory.

7.3 Associatives and Gradient Flow Trees

The generation of Yukawa couplings and mass terms from associative three-cycles which project to flow trees on M_3 has a natural generalization [120], which in the effective theory realizes higher point couplings. We briefly touched on their cohomological properties from the perspective of the colored quantum mechanics, but did not give a global characterization of these structures. Further the partially twisted 7d SYM does not give an expression in terms of overlap integrals for the higher point couplings and so we must resort to geometric reasoning and dimensional analysis to argue for these non-renormalizable couplings and determine their strength. Here we close this gap taking a more geometrical point of view.

We consider a setup in which $G_\perp = S[U(1)^k]$, so that the Higgs background is described by k smooth Morse functions f_i. As the associated two-spheres α_i in the ALE fiber sum to zero in homology, the same must be true of the functions f_i. Choosing a critical point p_i of each f_i with Morse index $\mu(p_i)$, one can define the moduli space of gradient flow trees

$$\mathcal{M}(M; f_1, \ldots, f_k; p_1, \ldots, p_k), \tag{7.33}$$

as the set of gradient flow trees with external vertices $p_1, \ldots, p_k$ such that the lines emanating from p_i are ascending gradient flow lines of f_i. These form the external edges of the gradient flow tree. Of course we also allow for internal vertices and edges. The flow of these is governed by the associated integral linear combinations of the f_i, which are in turn

$$\alpha_1 + \alpha_2 + \alpha_3 + \alpha_4 + \alpha_5 = 0$$
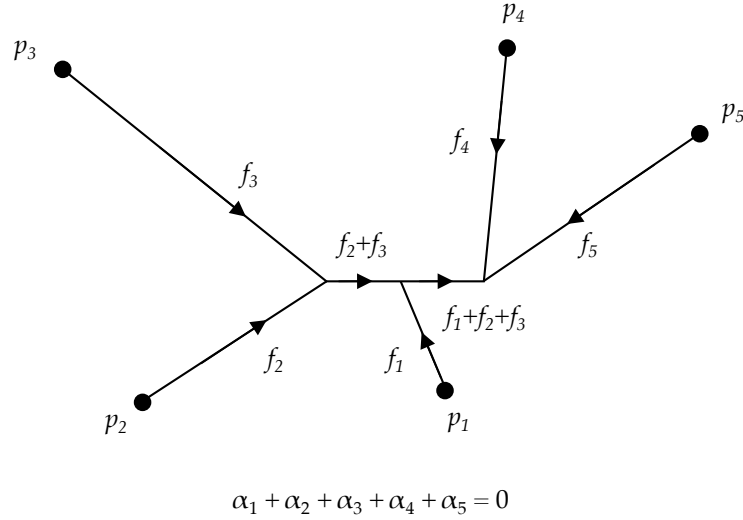
Figure 7.5: A gradient flow tree with 5 external vertices of Morse index 1.

determined by a charge conservation constraint. This moduli space $\mathcal{M}$ has dimension

$$\dim \mathcal{M}(M; f_1, \ldots, f_k; p_1, \ldots, p_k) = k - \sum_{i=1}^{k} \mu(p_i), \tag{7.34}$$

and there are thus finitely many gradient flow trees connecting k points of Morse index 1. An example of a gradient flow tree for the case of $k = 5$ is shown in figure 7.5.

As before, we can construct a three-cycle by fibering the two-sphere α associated with the Morse function f over each segment $\gamma(f)$. This both guarantees that we end up with an associative, and also that α collapses at the end-points of the flow tree. Furthermore, the fact that we have a tree in M_3 implies that the resulting associative three-cycle has the topology of a three-sphere, so that it contributes to the effective superpotential. Using the same manipulations as in (7.5), we can compute the volume of such a 3-sphere γ as

$$\text{Vol}\,\gamma(f_1, \ldots, f_k; p_1, \ldots, p_k) = \sum_{i=1}^{k} f_i(p_i). \tag{7.35}$$

so that the resulting contribution to the superpotential is

$$\Delta W \sim \frac{1}{M_\phi^{k-3}} \sum_{\gamma} n_\gamma e^{-\sum_{i=1}^{k} f_i(p_{a_i})}. \tag{7.36}$$

The scale M_ϕ is set by the vev of ϕ. Note that there can in general exist several flow trees connecting matter localized at the same loci p_i, which can cancel out.
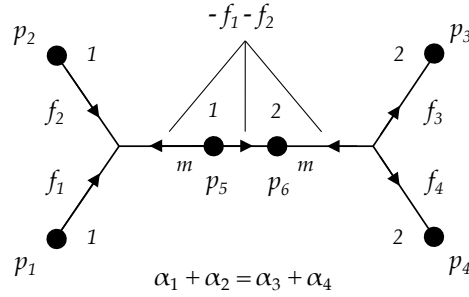
Figure 7.6: The figure shows how perturbative ground states participate in 4-point interaction between states localized at p_1, p_2, p_3, p_4. The gradient flow tree consists of two trivalent trees connected by a gradient flow line between p_5 and p_6. We have indicated the relevant Morse functions and Morse indices in the picture. The states localized at p_5 and p_6 are lifted by instanton corrections and develop a mass $m \sim M_{\mathrm{Inst}}$. In the 4d effective field theory this gives rise to a 4-point interaction.

The modes participating in the Yukawa (and higher) couplings are not just the massless states, but in fact all perturbative ground states of the SQM. Below the mass scale

$$M_{\mathrm{Inst}} \sim M_\phi e^{-tV} \tag{7.37}$$

induced by associates over flow lines between two points, we may integrate out the corresponding massive fields, thereby generating higher-dimensional operators in the effective field theory. As $M_{\mathrm{Inst}} \ll M_\phi$ these corrections are dominant compared to the couplings induced between the same fields by associatives. An example is shown in figure 7.6.

For non-generic choices of the charge distribution the moduli space of gradient flow lines may increase and (7.34) is no longer valid. In this case the moduli space of gradient flow lines is not discrete but of dimension 1 and isomorphic to a circle. In the ALE geometry this corresponds to a continuous family of associative submanifolds. In [113] it is shown that the contribution of such a family $\mathcal{C}$ of associatives is proportional to $\chi(\mathcal{C})$.

In the more generic set-up of unfactored spectral cover of rank n the Higgs background can only be diagonalised locally as in (4.20). The source terms ρ in the BPS equations are now oriented arbitrarily along $G_\perp$ breaking the gauge symmetry to its commutant G in $\widetilde{G}$. Assuming we can diagonalizing the Higgs field in a tubular neighbourhood T of the

singularity as

$$U(x)\phi(x)U^{-1}(x) = \mathrm{diag}(\lambda_1(x), \ldots, \lambda_n(x)) \quad x \in T \supset \mathrm{supp}\,(\rho)\,, \tag{7.38}$$

we can impose boundary conditions on our field content as in section 4.2 and proceed with a local analysis. Chiral multiplets still localize at the vanishing points of the Higgs field and the boundary conditions again preclude perturbative zero modes from localising at the boundary. Due to the mixing of the sheets of the spectral cover the background is no longer determined by a set of globally defined functions and we can not relate the cohomologies of $\mathcal{D}$ counting the zero modes to de Rham cohomologies. The local geometric picture however persists, all interactions are determined by three-cycles of the ALE geometry as in the previous sections with strengths determined by their volumes as in (7.6).

Finally, let us briefly comment on the case in which the critical loci are circles, i.e., we are allowing f_Q to be Morse-Bott. Perturbing the set-up slightly we return to the case of Morse theory. The ground states of (5.31) now decompose into multiple perturbative ground states

$$\alpha \wedge \psi_\perp \quad \rightarrow \quad \frac{1}{\sqrt{n}}\eta_i \quad i = 1, \ldots, n\,, \tag{7.39}$$

where we have assumed that the circle decomposes into $2n$ critical point of which n have Morse index 1 and n have a Morse index of 2. The forms η_i are $1, 2$-forms depending on whether α is a $0, 1$-form and localize at these critical points of Morse index $1, 2$ respectively. We further assume that the states $\alpha \wedge \psi_\perp$ and η_i are of unit norm. After this perturbation, the previous analysis applies. The true ground state corresponding to $\alpha \wedge \psi_\perp$ is

$$\frac{1}{\sqrt{n}}\sum_{i=1}^{n} \eta_i\,. \tag{7.40}$$

Chapter 8
Higgs Bundles and TCS G_2-manifolds

In this section we consider local models associated with twisted connected sum (TCS) G_2-manifolds, which form the largest known class of examples of compact G_2-manifolds [37,38]. The TCS construction has by now been covered extensively in the literature, so we will only briefly recapitulate the main points and refer the reader to [37, 38, 45] for further details. In a nutshell, the power of the TCS construction is that it shows how compact G_2-manifolds can be glued from simpler building blocks, which can in turn be constructed using algebraic geometry. Although this makes finding examples relatively straight-forward, TCS G_2-manifolds appear to be a rather special class within the set of all G_2-manifolds [45]. Our analysis of local models for G_2-manifolds allows us to move away (at least in local models) from the TCS description and explore how to connect TCS G_2-manifolds to G_2-manifolds giving rise to chiral spectra.

8.1   TCS G_2-Manifolds

The basic ingredient for the twisted connected sum construction is a pair of algebraic three-folds $Z_\pm$, which each admit a K3 fibration

$$S_\pm \longrightarrow Z_\pm$$
$$\downarrow \pi_\pm \tag{8.1}$$
$$\mathbb{P}^1_\pm$$

with generic K3 fiber $S_\pm$. The manifolds $Z_\pm$ have to satisfy

$$c_1(Z_\pm) = [S_\pm], \tag{8.2}$$

i.e., the first Chern class of $Z_\pm$ must be equal to the class of a generic K3-fiber. With some further assumptions on the topology (see [38, Definition 3.5]) $Z_\pm$ are then called the building
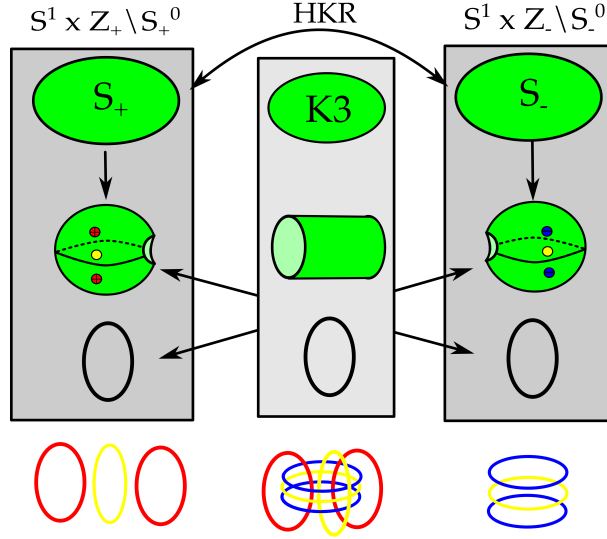
Figure 8.1: TCS construction of G_2-manifolds. Top: Building blocks that are aCyl Calabi-Yau and hyper-Kähler rotation (HKR) in asymptotic cyclindrical region. Bottom: Higgs bundle data. The critical loci of the Morse-Bott function f (in yellow) and the charge configuration ρ (in red and blue) corresponding to the local limit of a TCS G_2-manifold. The figure on the top shows the decomposition of S^3 into $\mathbb{C}_\pm \times \mathbb{S}^1_\pm$ and the figure on the bottom shows the location of the same critical loci and charges in a patch $\mathbb{R}^3$ of S^3. Every every circle in $X_+ \times \mathbb{S}^1_+$ has linking number one with any of the circles in $X_+ \times \mathbb{S}^1_+$. Note that charge conservation requires that not all loops carry identical charges in this example.

blocks. Excising a generic fiber $S^0_\pm$ from $Z_\pm$ one obtains a pair of non-compact threefolds $X_\pm = Z_\pm \setminus S^0_\pm$, fibered over a punctured Riemann sphere,

$$
\begin{array}{c}
S_\pm \longrightarrow X_\pm \\[1mm]
\downarrow \pi_\pm \\[1mm]
\mathbb{C}_\pm
\end{array} \quad , \tag{8.3}
$$

which are asymptotically cylindrical (aCyl) Calabi-Yau threefolds. Away from a compact submanifold, the $X_\pm$ have the topology of the cylinder $\mathbb{R}^+ \times \mathbb{S}^1_{b,\pm} \times S^0_\pm$ and the Ricci-flat metrics on $X_\pm$ asymptote to the Ricci-flat product metric on this cylinder. The situation is sketched in figure 8.1.

To form a compact G_2-manifold, the aCyl Calabi-Yaus $X_\pm$ are then multiplied by an extra circle $\mathbb{S}^1_{e,\pm}$ and glued together along a their cylindrical regions. The diffeomorphism

used for the gluing exchanges the 'internal' circles $\mathbb{S}^1_{b,\pm}$ with the 'external' circles $\mathbb{S}^1_{e,\mp}$ and identifies the K3 surfaces $S^0_\pm$ by a diffeomorphism which induces a hyper-Kähler rotation, or Donaldson matching,

$$\mathrm{Re}(\Omega^{2,0}_\pm) = \omega_\mp$$

$$\mathrm{Im}(\Omega^{2,0}_+) = -\mathrm{Im}(\Omega^{2,0}_+).$$

(8.4)

Here, $\Omega^{2,0}_\pm$ and $\omega_\pm$ are the holomorphic $(2,0)$ forms and Kähler forms on $S^0_\pm$ which are induced by the complex structures on $X_\pm$. The compact topological manifold J resulting from this gluing then admits a metric with holonomy G_2, which is close to the Ricci-flat metrics on $X_\pm \times \mathbb{S}^1_{e,\pm}$. More precisely, there exists a limit, which we will call 'Kovalev limit', in which the cylindrical region becomes arbitrarily long and in this limit the Ricci flat G_2-holonomy metric approaches the Calabi-Yau metrics on $X_\pm$. In compactifications of M-theory, modes localized only on $X_+ \times \mathbb{S}^1_{e,+}$ or $X_- \times \mathbb{S}^1_{e,-}$ give rise to subsectors with enhanced $\mathcal{N} = 2$ supersymmetry in four dimensions. These subsectors are coupled such that they mutually only preserve $\mathcal{N} = 1$ supersymmetry, and we may think of the parameter T which controls the length of the cylindrical region as the inverse of their coupling [43, 46].

As both $X_\pm \times \mathbb{S}^1_{e,\pm}$ are fibered by K3 surfaces and the gluing acts separately on the fiber and base, J is (topologically) fibered by K3 surfaces as well. The base of this fibration is a three-sphere S^3 glued together from two solid tori. We can hence think of the local models associated with TCS G_2-manifolds as describing an ALE space which is cut out from the K3 fiber over a base space M_3 which is S^3. To engineer non-abelian gauge groups, every ALE fiber of the local geometry and hence every K3 fiber of the associated compact G_2-manifold must be singular. It is straightforward to construct aCyl Calabi-Yau threefolds in which every K3 fiber has a singularity of ADE type and the work of [45, 46] suggests that gluing such singular three-folds indeed results in a singular G_2-manifold.

Let us consider this in more detail. Denote the image of

$$\rho_\pm : H^2(Z_\pm, \mathbb{Z}) \to H^2(S^0_\pm, \mathbb{Z}) \tag{8.5}$$

by $N_\pm$. The Donaldson matching implies an idenfication of $H^2(S_+^0, \mathbb{Z}) \simeq H^2(S_-^0, \mathbb{Z})$. Using this map, every element of

$$\mathfrak{g} = N_+ \cap N_- \,, \tag{8.6}$$

gives rise to an associated harmonic two-form on J: the Poincaré dual cycle to such a form is algebraic for both S_+ and S_-, so that its fibration over the whole base S^3 of J is trivial and it sweeps out a five-cycle, which is Poincaré dual to a two-form on J. The number of independent such two-forms on J is simply given by the rank of $\mathfrak{g}$ [38]. In compactifications of M-theory on J, there are hence rank($\mathfrak{g}$) massless $U(1)$ vectors from the Kaluza-Klein reduction of the three-form C_3[1].

The hyper-Kähler structure on $S_\pm^0$ is forced by the Donaldson matching to be such that the integral of both $\Omega_\pm^{2,0}$ and $\omega_\pm$ vanishes for every cycle contained in $\mathfrak{g}$. This means that whenever there is a root, i.e., a lattice vector of length -2, contained in $\mathfrak{g}$, the K3 fibers $S_\pm^0$ are singular. As $\mathfrak{g}$ sits inside of the polarizing lattices[2] of the algebraic families $X_\pm$, this implies that every single K3 fiber has a singularity. The type of singularity can be read of by finding the sublattice $\mathfrak{g}_{\mathrm{root}} \subset \mathfrak{g}$ generated by the roots of $\mathfrak{g}$. This sublattice must be a (sum of) ADE root lattice(s) and its type determines the corresponding singularity and the resulting simply-laced[3] non-abelian gauge group upon compactification of M-theory.

The matter loci in these models arise as the degeneration loci of the singular K3-fibration i.e., where the singularity worsens. This happens over points in $\mathbb{P}_\pm^1$, each of which gets multiplied with a circle in the TCS construction. This implies that in M-theory compactification on a TCS manifold J, matter is localized along circles. This is true at least in the Kovalev

---

[1]There are in general further massless $U(1)$ vectors associated with classes in the kernel of $\rho_\pm$ [38], which associated with the irreducible components of reducible fibers of the K3 fibrations on $Z_\pm$.

[2]The polarizing lattice of a family of K3 surfaces is the sublattice of $H^2(K3, \mathbb{Z})$ which is orthogonal to $\Omega^{2,0}$ for all members of the family.

[3]While this data is sufficient to find the singularities associated with simply-laced gauge groups, it is slightly more tricky to find non-simply laced gauge groups. Their emergence in TCS G_2-manifolds parallels their emergence in F-theory [121] in that the exceptional divisors of resolutions of ADE singularities of $S_\pm$ may globally become a single divisor in $X_\pm$ [45]. In terms of lattice data, this can be expressed by saying that a cycle of self-intersection $n < -2$ contained in $\mathfrak{g}$ can force an ADE singularity in every fiber if it is a linear combination of -2 curves in S_+ or S_- which are all in the polarizing lattices of the families S_+ and S_-. The difference between the polarizing lattices and $N_\pm$ determines the 'folding' of the ADE Dynkin diagram.

(stretched neck) limit in which the metric on the J is well approximated by the metrics on each of the building blocks, which can be thought of as being contained inside J (more precisely, the products $X_\pm \times \mathbb{S}^1_\pm$ are in J).

8.2 Higgs Bundles of TCS G_2-manifolds

We start by considering the local models of the two building blocks individually. As the discussion is the same for both sides, we will drop the $\pm$ subscripts. The first step is to replace the K3 fibration with a local ALE model. The precise details of this local limit depends on the ADE group corresponding to the type of ADE singularity, and are well known in the literature [122, 123]. Besides an ADE singularity, every ALE fiber contains a number of compact cycles, the volumes of which vary over the base. Such cycles may collapse over points in the base $\mathbb{C}$. At these loci the singularity present in the generic fiber is enhanced and matter is localized. Let

$$\sigma \in H_2(S, \mathbb{Z}) \tag{8.7}$$

be such cycle which vanishes at (some) of the corresponding points in the base $\mathbb{C}$. Let us denote the hyper-Kähler triple by $\Theta = (\omega_I, \omega_J, \omega_K)$. In terms of (8.4) the hyper-Kähler structure is simply

$$\omega = \omega_I$$
$$\Omega^{2,0} = \omega_J + i\omega_K. \tag{8.8}$$

After taking the local limit and integrating over σ we get a meromorphic function ϕ on $\mathbb{C}$:

$$\phi = \int_\sigma \Theta, \tag{8.9}$$

with zeros precisely where σ shrinks to zero volume. The poles and zeros of ϕ are located away from ∞. Moreover, we can identify ϕ with the meromorphic (1,0)-form as $\phi\,dz$. Since the base $\mathbb{C}$ is contractible $\phi = df$, where f is now a Morse function with critical points of index 1 and singular loci corresponding to the poles of ϕ. After taking a product with the circle we trivially get a Morse-Bott function.

If (unit) charges are placed at points $a_i \in \mathbb{C}$, the function ϕ will be of the form

$$\phi(z) = \sum_{i=1}^{n} \frac{1}{z - a_i}\,. \tag{8.10}$$

Therefore ϕ can have at most $n - 1$ critical loci, which is generically the case. If we impose charge conservation on each side, there can be at most $n - 2$ critical loci of ϕ.

With this information let us now consider how the Higgs bundle for TCS manifolds. After gluing $\mathbb{C}_+ \times \mathbb{S}^1_{e,+}$ with $\mathbb{C}_- \times \mathbb{S}^1_{e,-}$, the base manifold is $M_3 = S^3$. In the Kovalev limit, the critical locus of the harmonic Morse-Bott function f consists of a disjoint union of m circles of Morse index 1. As before, we may engineer such an f by an appropriate configuration of charges Γ on S^3. On $\mathbb{C}_\pm \times \mathbb{S}^1_\pm$, these charges will simply be given by a collection of points on $\mathbb{C}_\pm$ times the circle $\mathbb{S}^1_\pm$.

From the above discussion we only need the simple observation that matter loci in TCS G_2-manifold, at least in the Kovalev limit, are circles. Suppose that there are m matter circles and no points. Using the results of section 5.5 we see that the Morse-Bott complex is

$$C^1 = \Omega^0(\mathbb{S}^1)^m\,, \qquad C^2 = \Omega^1(\mathbb{S}^1)^m\,, \tag{8.11}$$

and the cohomology gives just

$$H^1(\mathcal{M}_3, \Sigma_-) \cong \mathbb{R}^m\,, \qquad H^2(\mathcal{M}_3, \Sigma_-) \cong \mathbb{R}^m\,. \tag{8.12}$$

We find that every perturbative ground state constitutes a true ground state, the Morse-Bott function f is thus perfect. As each circle gives rise to a pair of chiral and conjugate-chiral zero modes upon Kaluza-Klein reduction, the spectrum associated to this Higgs field configuration $\phi = df$ is non-chiral

$$\chi(\mathcal{M}_3, \mathbf{R}_q) = 0\,. \tag{8.13}$$

We can use this result to derive constraints on the function f. By the above results the relative Euler characteristic $\chi(\mathcal{M}_3, \Sigma_-) = 0$ vanishes and by Lefschetz duality we find that

this implies $\chi(\mathcal{M}_3, \Sigma_+) = 0$. We obtain the topological constraint

$$\chi(\mathcal{M}_3) = \chi(\Sigma_+) = \chi(\Sigma_-) = 0\,. \tag{8.14}$$

There has been a recent attempt to modify the TCS construction to yield singular G_2-manifolds with codimension 6 singularities by Chen [81]. Instead of smooth bulding blocks Chen takes the Z_+ building block to be a threefold with isolated nodal singularities, which means that the non-compact aCyl G_2-manifold $X_+ \times \mathbb{S}^1_{e+}$ has singularities in codimension 6. However, the standard TCS gluing argument does not work in this case; rather it is conjectured [81] that if circles of nodal singularities are replaced by pairs of isolated conical singularities it is possible to glue to a G_2-manifold with conical singularities using a modified version of the connected sum construction. In terms of the local model, the collapse of circles into points corresponds to deforming the Morse-Bott function to a generic Morse function, where the same collapse of critical circles to critical points occurs (recall that critical points correspond precisely to isolated singularities of the total space of the G_2-manifold). However, even if this conjecture is true, such G_2-manifold will still give rise to a non-chiral spectrum by the arguments above.

Finally, let us discuss the spectral covers for a TCS G_2-manifold which is given to us in terms of building blocks $X_\pm$ and a gluing map

$$\gamma: \quad S^0_+ \to S^0_-\,, \tag{8.15}$$

where $S_\pm$ have ADE singularities over $U_\pm \subset \mathbb{C}_\pm$. This gluing of the K3 fibers in the TCS geometry also implies a consistent gluing map for the ALE-fibrations associated with the local model[4]. In general, to be able to glue two given ALE-fibrations together, the two ALE-spaces need to be of the same type, $\tilde{G}_+ = \tilde{G}_-$, and furthermore the periods of the ALE-fibers must satisfy a matching condition. By Torelli theorem for ALE-spaces [124], the structure of an ALE-space is completely determined by the periods of the hyper-Kähler

---

[4]Here we assume the existence of a complete metric for the local model.
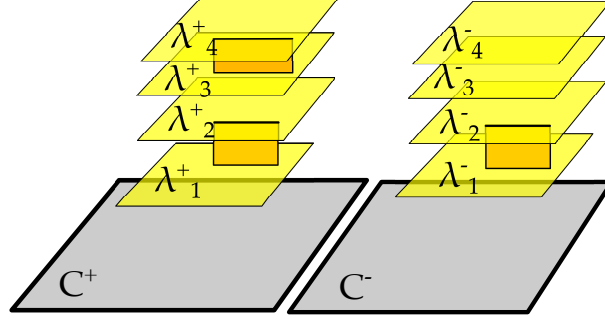
Figure 8.2: Each of the building blocks $X_\pm$ defines a spectral cover over $\mathbb{C}_\pm$, and these are then glued to a spectral cover over S^3. In the example shown here, the cover on $\mathbb{C}_+$ factors into two components and the cover on $\mathbb{C}_-$ factors into three components. These covers are glued such that the resulting spectral cover over S^3 has two components with two sheets each. Hence the resulting model has $G_\perp = S[U(2) \times U(2)]$ and there is a single unbroken $U(1)$.

structure forms over the 2-cycles in the root lattice of the algebra of $\widetilde{G}$. Explicitly, the matching condition is

$$\int_{\sigma_j} \omega_{I,+} = \int_{\sigma_j} \omega_{J,-} \,, \qquad \int_{\sigma_j} \omega_{J,+} = \int_{\sigma_j} \omega_{J,-} \,, \qquad \int_{\sigma_j} \omega_{K,+} = -\int_{\sigma_j} \omega_{K,-} \,, \qquad (8.16)$$

where σ_j are the 2-cycles generating the root lattice. Note that this implies that the non-abelian part of the group G, i.e., the type if ADE singularity, must be the same on both sides.

Each $X_\pm$ furthermore has a local model, which is a Higgs bundle $\phi_{(\pm)}$ over $\mathbb{C}_\pm$, and a corresponding spectral cover $\mathcal{C}_{(\pm)}$. The asymptotic values the Higgs fields $\phi_{(\pm),0}$ are similarly related by

$$\phi_{(+),0} = \gamma^* \phi_{(-),0} \,, \qquad (8.17)$$

which induces a gluing of the spectral covers.

Let us explain the origin of $U(1)$ gauge symmetries in glued spectral covers. Each cover $\mathcal{C}_{(\pm)}$ can have a factorization structure, which defines two-forms (five-cycles) and locally $U(1)$ symmetries. This can be detected by the restriction of the map (8.5) to the ALE-fibrations over $\mathbb{C}_\pm$. Factorization of the spectral cover $\mathcal{C}$ over S^3 after gluing $\mathcal{C}_{(\pm)}$ can likewise be detected by (8.6), and only those two-forms in the image that lie in the intersection will

globally give rise to a two-form and thereby a $U(1)$ symmetry. An example is shown in figure 8.2, where $\mathcal{C}_{(\pm)} \to \mathbb{C}_\pm$ each is a four-sheeted cover. However $\mathcal{C}_{(\pm)}$ is factored into two (three), and thus locally gives one (two) $U(1)$ symmetries. The gluing is such that the spectral cover $\mathcal{C} \to S^3$ has only two factors, and thus only gives rise to a single $U(1)$ symmetry. The scale at which the other $U(1)$ is broken is set by the size of the neck region of the TCS-construction.

Besides an analysis via Higgs bundles, the matter spectrum of M-theory on TCS G_2-manifolds can also be found using a purely geometric reasoning. The geometry in the vicinity of each matter locus is that of a Calabi-Yau threefold times a circle. The local Calabi-Yau geometry is that of a fibration of an ADE singularity over $\mathbb{C}$ with a further degeneration at a point. Using the usual dictionary between singularities and gauge theory for M-theory or type IIA on Calabi-Yau threefolds, the Cartan generators and weight vectors can be identified with exceptional divisors and curves in the resolved Calabi-Yau geometry [15, 97, 125, 126]. Our analysis of Higgs bundles now implies that the multiplicities must be such that each matter locus gives rise to a single vector-like pair of representations. Furthermore, we may determine the $U(1)$ charges by simply integrating the two-forms in $\mathfrak{g}$ which give rise to the $U(1)$s over the exceptional curves of the resolution associated with the matter.

8.3 Deformation of TCS Higgs Bundles

Given the local model for TCS G_2-manifolds we now consider the behavior of the physics under deformations of the Morse-Bott function. We have seen above that circular critical loci arise in the non-generic $\mathbb{S}^1$-invariant distributions of charges in S^3 which are present in the Kovalev limit. The natural question is what happens if this invariance in is broken by a slight deformation. The strategy we will use to describe deformations is to exploit the construction of Morse(-Bott) functions in terms of charge distributions. For every charge distribution ρ, there is an associated Morse-Bott function, which in turn lifts to an ALE-fibration, our local model of a G_2-manifold. For every deformation of the charge distribution there is
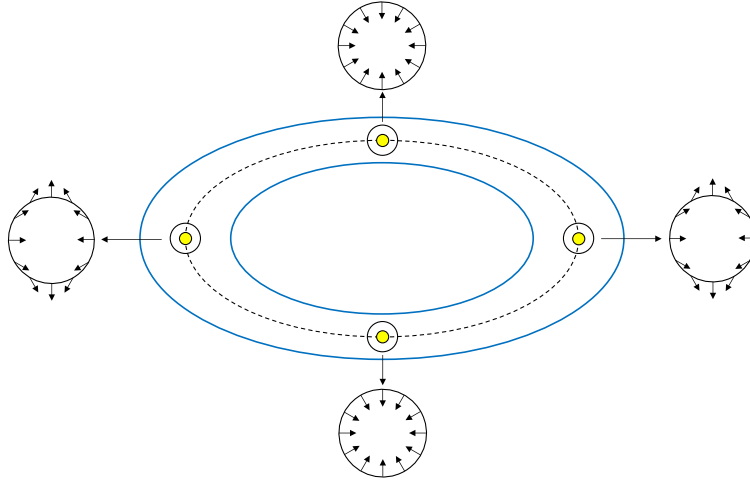
Figure 8.3: Two homogeneously negatively charged coplanar circles which have been stretched to ellipses. On the ellipse which is equidistant to the two charge loci, the electric field only vanishes at the four points marked as black dots. To find the Morse index, consider the small circles (coplanar to the ellipses) around these points and the restriction of the electric field to these circles. The Morse index of the points near the vertices of the ellipse is 2 and while those near the co-vertices have a Morse index of 1. As before, the critical loci are shown in yellow, and the charges in blue.

hence an associated deformation of the local model. Note that this deformation might be trivial: contrary to the number of deformations of Higgs bundles or the deformations of G_2-manifolds, which are finite in number, there are infinitely many deformations of any given charge configuration.

A configuration of charges which produces the Morse-Bott function associated with a TCS G_2-manifold in the Kovalev limit must of course be finely tuned, as a generic configuration of charges will always result in critical loci of dimension zero. Let us discuss this in a simple example – see figure 8.3: consider a charge distribution of two equally charged coplanar and cocentric circles in $\mathbb{R}^3$. This setup has rotational symmetry and correspondingly the critical locus is another coplanar and concentric circle. A generic deformation will destroy the rotational symmetry and lead to critical points instead of a circle. Consider e.g., deforming the charges to ellipses while preserving coplanarity. This collapses the critical locus to two points of Morse index 1 near the vertices of the ellipses and two points of index

2 near the co-vertices.

More generally, the function f will become Morse with isolated critical points for a generic deformation. However, since the topology of $\Sigma_\pm$ does not change, we still have

$$\chi(\mathcal{M}_3, \Sigma_-) = 0\,. \tag{8.18}$$

Physically this means that any deformation of f will give rise to chiral spectrum if under the deformation the topology of Σ_- remains unchanged. Denoting the number of points with Morse index i by m_i, the Morse inequalities for manifolds with boundary imply

$$\chi(\mathcal{M}_3, \Sigma_-) = m_2 - m_1 = 0\,. \tag{8.19}$$

Equally, every deformation of the local model of a TCS G_2-manifold that has an associated charge distribution which consists of a number of circles will satisfy $n_\pm = l_\pm$, so that the resulting spectrum is seen to be non-chiral.

8.4 Chirality and Singular Transitions

It is not at all surprising that TCS G_2-manifolds do not give rise to chiral spectra and that small deformations do not change the chiral index. However the result we have found already has fairly interesting geometrical implications: for a generic small deformation of a TCS G_2-manifold, the loci at which matter is localized are no longer one-dimensional but become point-like. This of course implies that the product structure of $X_\pm \times \mathbb{S}^1_{e,\pm}$ must be broken and the periods of the hyper-Kähler triplet on the K3 fiber must have a non-trivial dependence along $\mathbb{S}^1_{e,\pm}$. Although such small deformations will not yield G_2-manifolds giving rise to chiral spectra, the crucial ingredient, which are point-like singularities, is already present for small deformations of TCS G_2-manifolds.

Engineering the ALE-fibration from a Morse function which in turn is determined by a configuration of charges allows us to make the key observation for how to deform TCS G_2-manifolds to situation with chiral spectra: we need to make a transition after which $n_\pm = l_\pm$ no longer holds. The simplest way to do so is to bring two circles of equal charge
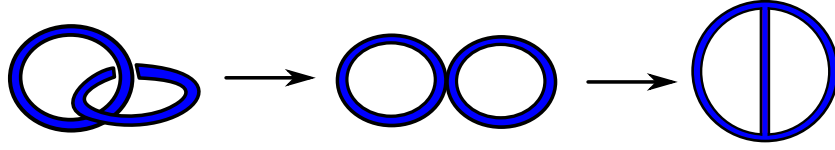
Figure 8.4: A transition of the charge configuration which results in a transition between a non-chiral and a chiral spectrum. Starting from a TCS configuration of charges deforming the configuration to one that results in a chiral spectrum.

together and then deform them to an object with $l = 2$. For TCS G_2-manifolds, there are essentially two different ways to achieve this.

The first option is to take e.g., a positive charge on $\mathbb{C}_+$ and another positive charge on $\mathbb{C}_-$, bring them together, and fuse them as shown in figure 8.4. As now $l_+ - n_+ = 1$ while $l_- - n_- = 0$, the resulting spectrum must be chiral. In a generic situation in which f is Morse, i.e., f only has isolated critical points, the critical locus of f hence consists of an odd number of points now. As we started from a non-chiral configuration with an even number of critical points, this implies that some of the critical points must have fused. As the circles of positive charge we have fused originated from different ends of the TCS G_2-manifold we started from, the critical points which have fused must likewise originate from different ends. Geometrically, these critical points are nothing but degeneration loci of the K3 fibration of the G_2-manifold, so that we have effectively taken specific singular fibers of the K3 fibration into what used to be cylindrical region of the TCS and collided them. As expected from our earlier statement about the absence of chiral spectra in TCS G_2-manifolds, this signifies a definite departure from the TCS set-up, where the K3-fibration must be constant in the cylinder region.

In fact, the type of transition we have just sketched can also be anticipated from the heterotic duals of TCS G_2-manifolds, which are given by compactifications on the Schoen Calabi-Yau threefold with different vector bundles [45]. Such models always have non-chiral spectra and a singular transition connecting the Schoen Calabi-Yau threefold to a different Calabi-Yau threefold (together with appropriate vector bundles) is needed to find a chiral

spectrum. The Schoen Calabi-Yau threefold can be described as a fiber product of two dP_9s, and it allows singular transitions in which a singular fiber of one dP_9 is collided with a singular fiber of the other dP_9. As discussed in [45, 47], the duality to a TCS G_2-manifold implies that the singular fibers of these two dP_9s are separated into disjoint regions of the common $\mathbb{P}^1$ base. A collison between singular fibers from both ends translates to a collision of singular K3 fibers coming from the two separate ends X_+ and X_- of the dual TCS G_2-manifold.

The second option is to change the charge configuration corresponding to a TCS G_2-manifold by colliding two circles of equal charge which are both located in the same building block. The picture of such a deformation will be similar to the one in figure 8.4, however initially the charged circles will be unlinked. Again, it is clear that this signals a departure from a TCS G_2-manifold (and must result in a singular transition on the heterotic side as well): after the transition e.g., $X_+ \times \mathbb{S}^1_{e,+}$ must become a non-compact G_2-manifold without the structure of a product.

Chapter 9
Higgs Bundles with Non-Split Spectral Covers

We now turn to colored SQMs probing Higgs bundles with non-split spectral covers. These covers are branched and were discussed in chapter 3, they are the spectral covers generically encountered in F-theory constructions [13, 15, 94, 99, 100, 127–132]. Here we explore the Morse-theoretic consequences of the presence of branch sheets and find that previously distinct copies of Witten's SQM combine into a single SQM whose target space is now topologically an irreducible component of the spectral cover. Consequently the cohomology of the supercharge $\mathcal{Q}$ on M_3 computes topological properties for the spectral cover components $\mathcal{C}_k$ rather than those of the base manifold M_3. We discuss how to count zero modes in these models and determine the gauge symmetry of the associated 4d physics. We further com-
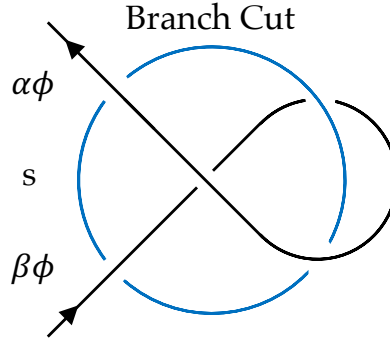
Figure 9.1: Sketch of a flow line (black) encircling a branch cut (blue). The incoming flow is determined by the Morse 1-form $\alpha^I \phi_I$ and the monodromy action associated to the branch circle is given by $s = -1$, then the outgoing flow is determined by $\beta^I \phi_I$. The two Witten SQMs associated to the roots α, β are coupled and combine to a single SQM.

ment on turning on flat abelian connections A and how these generically lift zero modes. As in chapter 3 we specialize to $M_3 = S^3$. To distinguish the eigenvalues of the Higgs field from the color fermions we denote the first by Λ and latter by λ in this chapter.

9.1 Combination of Witten SQMs

We consider the Lagrangian (6.28) with a Higgs field $\phi = \operatorname{diag}(\Lambda_K) \in \Omega^1(S^3, \mathfrak{g}_{\mathrm{ADE}})$ solving the sourced BPS equations (3.9) whose associated n-sheeted spectral cover is irreducible and cyclically branched as described in section 3.5. For concreteness we furthermore restrict to Lie algebras $\mathfrak{g}_{\mathrm{ADE}} = \mathfrak{su}(n)$. The topology of such covers is fixed by the pairs (L_i, F_i) where $L_i = \partial F_i \subset M_3$ denotes the links of the branch locus and $F_i \subset M_3$ a choice of Seifert surfaces together with a cyclic monodromy action $s \in S_n$.

We begin analysing the 1-particle sector of the colored SQM. The notion of perturbative ground states and the flow equations between these are identical to the case of non-split spectral covers, but the global structure of flow lines is altered. Along a path linking the branch locus the eigenvalues of the Higgs field are interchanged according to the monodromy action which is given by

$$\phi \quad \rightarrow \quad g\phi g^{-1}, \qquad g \in SU(n), \tag{9.1}$$

where the element g is determined by the monodromy element s. A particle following the flow line set by a sum of Higgs field eigenvalues $\alpha^I \phi_I$ follows a different combination of eigenvalues $\beta^I \phi_I$ after circling the branch locus and changes color. We have depicted this process in figure 9.1. The color change is determined by the monodromy action

$$E^\alpha \quad \to \quad g E^\alpha g^{-1}, \tag{9.2}$$

and looping around the branch locus multiple times we find an orbit of generators

$$E^{[\alpha]} = \left\{ g^k E^\alpha g^{-k} \mid k = 0, \ldots, n-1 \right\}. \tag{9.3}$$

For a standard choice of Cartan-Weyl basis E^α conjugation by g^k acts as a permutation of the roots α and we find an associated orbit of colors $[\alpha]$ to the action (9.3).

The eigenvalue 1-forms of the Higgs field can be distinguished on the simply connected subspace $S^3 \setminus \cup_i F_i$ and while flowing in $S^3 \setminus \cup_i F_i$ the particle is of definite color. Traversing the Seifert surfaces F_i the particle changes color according to (9.2). This leads to an interpretation of the Seifert surfaces as defects in the colored SQM. The wave functions of particles of definite color need not extend smoothly across the Seifert surfaces in $S^3 \setminus \cup_i F_i$ but rather they are required to glue smoothly to a wave function profile on $S^3 \setminus \cup_i F_i$ associated with a color prescribed by the monodromy action (9.2). Equivalently, they must glue exactly as the eigenvalues of the Higgs field in (3.21). By this effect particles of color α evolve identically to an uncolored particle probing n copies of $S^3 \setminus \cup_i L_i$. Each copy is associated with a color $\beta \in [\alpha]$ and the potential governing the particle is determined in the respective copy by the 1-form $\beta^I \phi_I$. Due to (3.21) this gives a well-defined potential on the n-fold glued space (3.18) which is topologically the spectral cover $\mathcal{C}$. With this the correspondence (6.34) is altered to

$$
\begin{aligned}
E^{[\alpha]} \subset \mathfrak{su}(n) \quad &\leftrightarrow \quad \text{Witten's SQM on } \mathcal{C} \text{ with supercharge } \mathcal{Q} = d + \Phi_{[\alpha]} \wedge, \\
H^I \in \mathfrak{su}(n) \quad &\leftrightarrow \quad \text{Witten's SQM on } M_3 \text{ with supercharge } \mathcal{Q} = d.
\end{aligned}
\tag{9.4}
$$

Here the 1-form $\Phi_{[\alpha]} \in \Omega^1(\mathcal{C})$ is defined by gluing the 1-forms $\beta^I \phi_I$ across the gluing factors given in (3.18).

The branch cuts of the Higgs field or equivalently its Seifert surface defects break the gauge symmetry to the stabilizer $\mathrm{Stab}(\phi)$ which consists of gauge transformations leaving ϕ invariant. They are generated by the generators H of the maximal torus of the gauge group which satisfy

$$gHg^{-1} = H \, . \tag{9.5}$$

For the n-sheeted irreducible coverings discussed in this section all of the gauge symmetry is broken. More general Higgs fields whose spectral covers have $N + 1$ irreducible components have their gauge group broken to $U(1)^N$. This may enhance to include factors of $SU(k)$ if k eigenvalues of the Higgs field take the same value.

9.2 Monodromies and Partial Higgsing

We are interested in preserving some of the gauge symmetry and non-split Higgs field backgrounds whose spectral cover (3.1) has multiple components. The eigenvalues Λ_K associated with each irreducible component of the cover can be activated successively whereby we can focus on Higgs fields where n eigenvalues have been set to vanish and m have been activated to trace out an irreducible m-sheeted cover.

We begin by consider a Higgs field background valued in the Lie algebra $\mathfrak{su}(n + m)$ for which m eigenvalues are turned on as described in section 3.5. This naively realizes a partial Higgsing of the gauge symmetry from $SU(n + m)$ to $SU(n) \times U(1)^m$ as discussed in section 6.5.2. The adjoint representation breaks into representations of $SU(n) \times U(1)^m$ as

$$
\begin{aligned}
\mathrm{Ad}\, SU(n + m) \quad \rightarrow \quad & (\mathrm{Ad}\, SU(n) \otimes \mathbf{1}) \oplus (\mathbf{1} \otimes \mathrm{Ad}\, U(1)^m) \\
& \oplus \sum_{i=1}^{m} (\mathbf{n}_{Q_i} \oplus \overline{\mathbf{n}}_{-Q_i}) \oplus \sum_{j=1}^{m^2 - m} \mathbf{1}_{Q_j} \, .
\end{aligned}
\tag{9.6}
$$

Here we denote the fundamental representation of $SU(n)$ by $\mathbf{n}$ and both Q_i, Q_j are charge vectors of $U(1)^k$. There are m pairs of the fundamental representation of $SU(n)$ and $m(m - 1)$ trivial representations charged under $U(1)^k$.

Monodromy effects (9.5) now break the gauge symmetry to $SU(n) \times U(1)$ and the colored SQM now groups the representations in (9.6) into representations of this reduced gauge

symmetry. The m pairs of fundamental representations $\mathbf{n}_{Q_i}, \overline{\mathbf{n}}_{-Q_i}$ belong to the same monodromy orbit of colors with length m (9.3) and combine to a single pair of fundamental representations $\mathbf{n}_+, \overline{\mathbf{n}}_-$ of the gauge symmetry $SU(n) \times U(1)$. Similarly the $m(m-1)$ trivial representations are grouped into $(m-1)$ trivial representations which are uncharged under the new gauge group. The m representations $\mathrm{Ad}\, U(1)^m$ combine to $\mathrm{Ad}\, U(1)$. The latter follows from the common geometric origin of the Higgs field ϕ and the connection A. The gauge fields valued in $\mathrm{Ad}\, U(1)^m$ are in correspondence with the m activated Higgs field eigenvalues. They are constrained to glue in the same way as the eigenvalues (3.21) across the branch sheets and are not independent. Summarizing we find that the monodromy effects lead to following representation content

$$
\begin{aligned}
&(\mathrm{Ad}\, SU(n) \otimes \mathbf{1}) \oplus (\mathbf{1} \otimes \mathrm{Ad}\, U(1)^m) \oplus \sum_{j=1}^{m^2-m} \mathbf{1}_{Q_j} \oplus \sum_{i=1}^{m} (\mathbf{n}_{Q_i} \oplus \overline{\mathbf{n}}_{-Q_i}) \\
\rightarrow \quad &(\mathrm{Ad}\, SU(n) \otimes \mathbf{1}) \oplus (\mathbf{1} \otimes \mathrm{Ad}\, U(1)) \oplus \sum_{k=1}^{m-1} \mathbf{1}_0^{(k)} \oplus (\mathbf{n}_+ \oplus \overline{\mathbf{n}}_-)
\end{aligned}
\tag{9.7}
$$

of the reduced gauge symmetry group $SU(n) \times U(1)$. The raised superscript $\mathbf{1}_0^{(k)}$ is introduced to distinguish the $m-1$ uncharged trivial representation.

We check these results by considering the circle reduction of M-theory on the ALE geometry set by the Higgs field background to the IIA set-up. This is given by $n+m$ D6-branes of which m have been Higgsed leaving a stack of n coincident branes. The m D6-branes recombine into a single D6-brane which explains the gauge symmetry reduction to $SU(n) \times U(1)$. Further this interpretations explains the single pair of fundamental representations $\mathbf{n}_+, \overline{\mathbf{n}}_-$ which correspond to the open string sector between the stack of n D6-branes and the recombined, Higgsed D6-brane. The modes in the uncharged trivial representations originate from the self-intersection of the Higgsed D6-brane.

The colored SQM now further determines a simplification of the cohomology groups $H_{\mathcal{Q}}^*(S^3, \mathfrak{g}_{\mathrm{ADE}})$ with $\mathfrak{g}_{\mathrm{ADE}} = \mathfrak{su}(n+m)$ which determine the 4d spectrum (2.45). The spectral cover is the union of n copies of the zero section in T^*S^3 and the Higgsed eigenvalues which

sweep out the irreducible 3-manifold $\mathcal{C} \subset T^*S^3$ given topologically by

$$\mathcal{C} = \left[S^3 \setminus \left(\bigcup_i F_i \right) \right]_1 \# \dots \# \left[S^3 \setminus \left(\bigcup_i F_i \right) \right]_m \setminus (\cup_i L_i). \tag{9.8}$$

We discuss the zero mode counting for each summand of (9.7) in turn. The fields transforming in $\mathrm{Ad}\, SU(n) \otimes \mathbf{1}$ are not effected by the Higgs field background and the relevant zero modes in the reduction on M_3 are counted by the de Rham cohomology groups $H^*_{\mathrm{dR}}(S^3, \mathbb{R})$. The fields transforming in $\mathbf{1} \otimes \mathrm{Ad}\, U(1)$ commute with the Higgs field, but, as explained above, zero modes are counted by the de Rham cohomology groups $H^*_{\mathrm{dR}}(\mathcal{C}, \mathbb{R})$. The fields transforming in the $m-1$ uncharged trivial representations $\mathbf{1}^{(k)}$ are similarly effected by the branch cuts. Such representations resulted from combining m charged representations $\mathbf{1}_{Q_j}$ and the relevant Higgs field for each of these is given by $Q_j^I \phi_I$. The charge vectors Q_j are nothing but the roots α_j of $\mathfrak{su}(m)$ and the glued representations $\mathbf{1}_{Q_j}$ precisely fit into a color orbit of the monodromy action (9.2). The sum $\sum_{k=1}^{m-1} \mathbf{1}^{(k)} = \sum_{[\alpha]} \mathbf{1}^{[\alpha]}$ in (9.7) is equivalently expressed as a sum over color orbits. The m 1-forms $Q_j^I \phi_I$ associated with the color orbit $[\alpha]$ glue across the m factors in (9.8) to the 1-form $\Phi_{[\alpha]}$ on the gluing space $\mathcal{C}$. As a consequence zero modes are counted by the Novikov cohomology groups $H^*_{\mathrm{Nov.}}(\mathcal{C}, \Phi_{[\alpha]})$. The fields transforming in $\mathbf{n}_+$ are identically argued to be counted by $H^*_{\mathrm{Nov.}}(\mathcal{C}, \Phi_{[\beta]})$ where β is a positive root of $\mathfrak{su}(n+m)$ that is neither a root of the subalgebras $\mathfrak{su}(n)$ or $\mathfrak{su}(m)$. Of course there are many different (precisely nm) such roots but due to the degeneracy explained in section 6.5.2 all such roots yield the same 1-form $\Phi_{[\beta]}$. Zero modes transforming in $\bar{\mathbf{n}}_-$ are simply counted by the groups $H^*_{\mathrm{Nov.}}(\mathcal{C}, -\Phi_{[\beta]})$. Due to its distinguished role we denote $\Phi_{[\beta]}$ simply by Φ.

We can now generalize (7.9) for partial Higgsings with non-split spectral covers. For the Lie algebra $\mathfrak{g} = \mathfrak{su}(n+m)$ and monodromy orbits $[\alpha]$ of $\mathfrak{su}(m)$ we have, counting with

multiplicities,

$$
H^*_{\mathcal{Q}}(S^3, \mathfrak{g}) = \left(\bigoplus_{i=1}^{n^2-1} H^*_{\mathrm{dR}}(S^3, \mathbb{R}) \right) \oplus H^*_{\mathrm{dR}}(\mathcal{C}, \mathbb{R})
$$
$$
\oplus \left(\bigoplus_{[\alpha]} H^*_{\mathrm{Nov.}}(\mathcal{C}, \Phi_{[\alpha]}) \right) \oplus \left(\bigoplus_{k=1}^{m} [H^*_{\mathrm{Nov.}}(\mathcal{C}, \Phi) \oplus H^*_{\mathrm{Nov.}}(\mathcal{C}, -\Phi)] \right).
$$

$$(9.9)$$

More generally we can consider other ADE gauge groups and turn on Higgs fields similarly as above. Consider for example the gauge symmetry breaking $E_8 \to SU(5)_{\mathrm{GUT}} \times SU(5)_\perp$ where the Higgs field is turned on along $SU(5)_\perp$. Such a breaking is described by a five sheeted spectral cover of $SU(5)_\perp$ traced out by the non-vanishing eigenvalues of the Higgs field. The Higgsing is a special case of

$$
\begin{aligned}
E_8 &\to SU(5)_{\mathrm{GUT}} \times SU(5)_\perp \\
\mathbf{248} &\to (\mathbf{24}, \mathbf{1}) \oplus (\mathbf{1}, \mathbf{24}) \oplus (\mathbf{10}, \mathbf{5}) \oplus (\overline{\mathbf{5}}, \mathbf{10}) \oplus (\overline{\mathbf{10}}, \overline{\mathbf{5}}) \oplus (\mathbf{5}, \overline{\mathbf{10}}),
\end{aligned}
$$

$$(9.10)$$

for which $SU(5)_\perp$ is further reduced to $U(1)$ when taking the eigenvalues of the Higgs field to trace out an irreducible 5-fold covering. The representations of $SU(5)_{\mathrm{GUT}}$ follow from orbits of the Weyl group action S_5 on the representations in (9.10) of $SU(5)_\perp$. The Higgs field breaks $SU(5)_\perp$ naively to $S[U(1)^5]$, the spectrum transforming under $SU(5)_{\mathrm{GUT}} \times U(1)$ then follows as in (9.7). We normalize the $U(1)$ charge of the fundamental representations $\mathbf{5}$ to unity and then find following spectrum transforming under the gauge symmetry $SU(5)_{\mathrm{GUT}} \times U(1)$

$$
\mathbf{24}_0 \oplus \left(\mathbf{1}_0 \oplus \sum_{k=1}^{4} \mathbf{1}_0^{(k)} \right) \oplus \mathbf{10}_{+1} \oplus \overline{\mathbf{10}}_{-1} \oplus 2 \times \overline{\mathbf{5}}_{+2} \oplus 2 \times \mathbf{5}_{-2}.
$$

$$(9.11)$$

The zero modes of $\mathcal{Q}$ transforming in each representation are again characterized by a Higgs field on the space (9.8) constructed via gluing. For example the matter curves (here points) of $(\mathbf{10}, \mathbf{5})$ in (9.10) give matter transforming in the anti-symmetric representation of $SU(5)_{\mathrm{GUT}}$ which localizes at $\Lambda_K = 0$ for the $K = 1, \ldots, 5$ eigenvalues of the Higgs field. The eigenvalues Λ_K glue to a 1-form Λ on $\mathcal{C}$ as in (3.21). The massless matter transforming in $\mathbf{10}_{+1}$ of (9.11) is therefore counted by $H^*_{\mathrm{Nov.}}(\mathcal{C}, \Lambda)$. Similarly the massless matter in $(\overline{\mathbf{5}}, \mathbf{10})$ localizes at $\Lambda_K + \Lambda_L = 0$ with $K > L$. The monodromy action groups these ten 1-forms into

Figure 9.2: The picture locally shows the four D6-branes which are IIA realization of the Higgs field (9.12). The D6-branes labeled by $\pm\Lambda$ are connected by branch sheets and along a closed path linking a branch cut locus S_i^1 the components of the combined D6-brane interchange. By (a,b,c) we label three open string sectors and their image when transported around the branch locus. The Chan-Paton factors of the string determine to which root of the Lie algebra $\mathfrak{su}(4)$ it is associated. The pairs of roots (9.21)-(9.24) are now understood as the open string sectors which are mapped onto another by the monodromy action.

two groups of five 1-forms which glue to the 1-forms $\Lambda_{\mathrm{as}}^{(1)}, \Lambda_{\mathrm{as}}^{(2)}$ on $\mathcal{C}$. The matter transforming in the two representations $\overline{\mathbf{5}}_{+2}$ are therefore counted by $H_{\mathrm{Nov.}}^*(\mathcal{C}, \Lambda_{\mathrm{as}}^{(i)})$ with $i = 1, 2$.

9.3 Example: 2-sheeted Covers and Monodromy

We give an explicit example of the effects discussed in the previous sections. Consider the family of two-sheeted covers (3.14) constructed in section 3.4 and embed these two sheets sheets $(\Lambda, -\Lambda)$ into an $\mathfrak{su}(4)$ valued Higgs field ϕ on $M_3 = S^3$ as

$$\phi = \mathrm{diag}(0, 0, \Lambda, -\Lambda) \,. \tag{9.12}$$

Here Λ is a 1-form with branch loci along a collection of circles $\cup_i S_i^1$ defined on $S^3 \setminus \cup_i D_i$ where D_i are disks realizing the branch sheets and bound by the branch locus $\partial D_i = S_i^1$. With respect to the Cartan basis

$$H^1 = \mathrm{diag}(1, -1, 0, 0) \,, \qquad H^2 = \mathrm{diag}(0, 1, -1, 0) \,, \qquad H^3 = \mathrm{diag}(0, 0, 1, -1) \,, \tag{9.13}$$

consider the six positive roots

$$\alpha_1 = (2, -1, 0) \,, \qquad \alpha_2 = (-1, 2, -1) \,, \qquad \alpha_3 = (0, -1, 2) \,, \tag{9.14}$$

$$\alpha_4 = (1, 1, -1) \,, \qquad \alpha_5 = (-1, 1, 1) \,, \qquad \alpha_6 = (1, 0, 1) \,. \tag{9.15}$$

When traversing a closed path linking one of the circles S_i^1 the third and fourth sheet of the spectral cover are interchanged, i.e., the Higgs field ϕ returns to (9.1)

$$\phi \to -\phi = g\phi g^{-1}, \qquad g = \begin{pmatrix} 1 & 0 & 0 & 0 \\ 0 & 1 & 0 & 0 \\ 0 & 0 & 0 & 1 \\ 0 & 0 & -1 & 0 \end{pmatrix} \in SU(4), \tag{9.16}$$

which realizes a $\mathbb{Z}_2$ monodromy action. The gauge group is broken to $SU(2) \times U(1)$. The supercharge $\mathcal{Q} = d + [\phi\wedge, \cdot]$ preserves the standard complexified Lie algebra generators E^{α_i} associated with the roots (9.14) and restricts to each of the respective subspaces, in the notation of (6.32), to

$$\mathcal{Q}^{(\alpha_1)} = d, \qquad \mathcal{Q}^{(\alpha_2)} = d - \Lambda\wedge, \qquad \mathcal{Q}^{(\alpha_3)} = d + 2\Lambda\wedge, \tag{9.17}$$

$$\mathcal{Q}^{(\alpha_4)} = d - \Lambda\wedge, \qquad \mathcal{Q}^{(\alpha_5)} = d + \Lambda\wedge, \qquad \mathcal{Q}^{(\alpha_6)} = d + \Lambda \wedge. \tag{9.18}$$

The gauge transformation (9.16) determines which copies of Witten's SQM associated with different roots of $\mathfrak{su}(4)$ combine across the branch sheets. The conjugation of (9.16) acts on the positive generators of $\mathfrak{su}(4)$ as

$$g E^{\alpha_1} g^{-1} = E^{\alpha_1}, \qquad g E^{\alpha_2} g^{-1} = -E^{\alpha_5}, \qquad g E^{\alpha_3} g^{-1} = -(E^{\alpha_3})^T = -E^{-\alpha_3}, \tag{9.19}$$

$$g E^{\alpha_4} g^{-1} = -E^{\alpha_6}, \qquad g E^{\alpha_5} g^{-1} = E^{\alpha_2}, \qquad g E^{\alpha_6} g^{-1} = E^{\alpha_4}, \tag{9.20}$$

and the roots (9.14) and (9.15) together with their negative copies are grouped into the color orbits

$$[\alpha_1] = \{\alpha_1\}, \qquad\qquad [-\alpha_1] = \{-\alpha_1\}, \qquad\qquad \big(\text{Ad}\, SU(2)\big) \tag{9.21}$$

$$[\alpha_2] = \{\alpha_2, \alpha_5\}, \qquad\qquad [\alpha_4] = \{\alpha_4, \alpha_6\}, \qquad\qquad (\mathbf{n}_+) \tag{9.22}$$

$$[-\alpha_2] = \{-\alpha_2, -\alpha_5\}, \qquad [-\alpha_4] = \{-\alpha_4, -\alpha_6\}, \qquad (\overline{\mathbf{n}}_-) \tag{9.23}$$

$$[\alpha_3] = \{\alpha_3, -\alpha_3\} \qquad\qquad\qquad\qquad\qquad\qquad (\mathbf{1}_0). \tag{9.24}$$

The twelve SQMs naively associated with the roots of $\mathfrak{su}(4)$ in (6.34) (and their negative copies) consequently combine across the branch sheets to SQMs associated with the color orbits (9.21)-(9.24). The generators $E^{\pm\alpha_1}$ commute with the Higgs field and give free SQMs

mapping into S^3. The remaining color orbits contain two roots and are over (9.4) in correspondence with SQMs mapping into the target space

$$\mathcal{C} = \left(S^3 \setminus D\right)_1 \# \left(S^3 \setminus D\right)_2 \setminus L, \qquad D = \bigcup_{i=1}^{N} D_i, \qquad L = \bigcup_{i=1}^{N} S_i^1, \qquad (9.25)$$

whose metric is inherited from the gluing factors. Each gluing component is associated with one of the roots in of the pairs (9.22)-(9.24). The 1-forms $\Lambda, -\Lambda$ glue to a single harmonic 1-form Φ on $\mathcal{C}$ and consequently the supercharges (9.17), (9.18) combine in pairs to give the supercharges of the SQMs mapping into (9.25).

We briefly comment on the IIA string theory interpretation of the above effects. In the type IIA set-up associated with the Higgs field (9.12) we locally have four D6-branes of which two have combined to a connected object corresponding to the spectral cover component $\mathcal{C}$. The transformations (9.19) are then understood as open string sectors identified by the monodromy action. For instance, an open strings locally connecting the first and third D6-branes are found to connect the first and fourth D6-brane when transported around the branch locus. We depict this interpretation in figure 9.2.

The monodromy orbits already fix the representation content (9.7) transforming under $SU(2) \times U(1)$ which here reads

$$\mathrm{Ad}\, SU(2)_0 \oplus \mathrm{Ad}\, U(1) \oplus \mathbf{1}_0 \oplus \mathbf{2}_+ \oplus \mathbf{2}_-, \qquad (9.26)$$

where the roots associated with each representation are as given in (9.21)-(9.24). In figure 9.2 the open string sectors corresponding to $\mathbf{2}_+, \mathbf{2}_-, \mathbf{1}_0$ are marked with (a, b, c) respectively. The reflective symmetry $\theta \to \pi - \theta$ of the set-up, we refer to section 3.4, requires all instanton effects potentially lifting perturbative ground states to come in pairs and cancel. All perturbative ground states are therefore ground states of the colored SQM and their count determines the cohomologies in (9.9). These are localized at the zero of the Higgs field, counted in (3.17), and therefore the Novikov cohomology groups evaluate to

$$H_{\mathrm{Nov.}}^*(\mathcal{C}, \Phi) = \left\{0, \mathbb{R}^{l-2}, \mathbb{R}^{l-2}, 0\right\}, \qquad (9.27)$$

where l is the number of disks participating in the gluing construction (9.25). The Novikov groups for the 1-form $\Phi_{[\alpha_3]} = 2\Phi$ on $\mathcal{C}$ of the color orbit $[\alpha_3]$ also evaluate to (9.27).

Part III
4d $\mathcal{N} = 1$ from 6d $\mathcal{N} = (2,0)$ and Confinement

This part of the thesis is devoted to the study of confinement in a large class of 4d $\mathcal{N} = 1$ theories. We begin by reviewing the definition of confinement that we use here, background on 6d $\mathcal{N} = (2,0)$ theories relevant for this thesis part and their geometric construction in IIB string theory is laid out in section 10. A vacuum r of a quantum field theory (QFT) $\mathfrak{T}$ is called confining if the vacuum expectation value (vev) of some genuine[1] line operator in $\mathfrak{T}$ exhibits area law in r. This is correlated with the existence of confining strings in the spectrum which can end on such line operators and are responsible for giving rise to the linear potential that gives rise to the area law. A classic example is provided by 4d $\mathcal{N} = 1$ pure Super-Yang-Mills (SYM) theory with gauge group $SU(n)$. This theory has n vacua and in each vacuum, the Wilson line operator in the fundamental representation of $SU(n)$ exhibits area law. Thus, each vacuum is confining.

Confinement can be characterized in terms of the 1-form symmetry group $\mathcal{O}$ of $\mathfrak{T}$ [57], which captures equivalence classes of line operators with two line operators L_1 and L_2 considered to be in the same class if there exists a local operator living at the junction of L_1 and L_2. For the theories that are studied in this thesis part, these equivalence classes form an abelian group Λ under OPE and characterize different charges under the 1-form symmetry group $\mathcal{O} = \widehat{\Lambda}$, which is the Pontryagin dual of Λ. If a line operator L_1 shows area or perimeter law, then another line operator L_2 in the same equivalence class shows the same law. Thus confinement can be characterized by dividing Λ into two subsets: those showing area law and those showing perimeter law. Furthermore, the classes exhibiting perimeter law form a subgroup Λ_r of Λ which depends on the vacuum r under consideration [133].

---

[1] A non-genuine line operator is one which lives at the boundaries or corners of higher-dimensional extended operators. A genuine line operator exists independently of any higher-dimensional extended operator.

Consider a line operator L that exhibits perimeter law in vacuum r. Then, any element of the 1-form symmetry group $\mathcal{O}$ under which L is non-trivially charged is spontaneously broken in the vacuum r, because we can set the vev of L to a non-zero constant by introducing a counter-term along the location of L, which cancels the perimeter dependence [57, 134]. Thus, the 1-form symmetry group $\mathcal{O}_r$ preserved in vacuum r can be written as[2]

$$
\mathcal{O}_r = \widehat{\left(\frac{\Lambda}{\Lambda_r} \right)} \subseteq \widehat{\Lambda} = \mathcal{O} \, . \tag{9.28}
$$

In other words, the data of the preserved 1-form symmetry group $\mathcal{O}_r$ is equivalent to the data of the set $\Lambda - \Lambda_r$ of line operators that exhibit area law. The confining strings are charged under $\mathcal{O}_r$ and their charges take values in its Pontryagin dual Λ/Λ_r.

The goal of this thesis part is to study confinement in $\mathcal{N} = 1$ deformations of 4d $\mathcal{N} = 2$ Class S theories [55], i.e., those 4d $\mathcal{N} = 2$ theories that can be obtained via compactification of the 6d $\mathcal{N} = (2,0)$ theories on Riemann surfaces with a partial topological twist. We only consider those Class S theories that can be obtained by compactifying 6d $\mathcal{N} = (2,0)$ theory of A_{n-1} type on a Riemann surface with untwisted punctures and no closed twist lines [135]. It should be noted that, though in practice we will largely consider such Class S constructions with irregular punctures, our considerations apply to general Class S set-ups.

Much like the 4d $\mathcal{N} = 2$ Class S theories have a description in terms of Higgs bundles that are solutions to a Hitchin system [77], their $\mathcal{N} = 1$ deformations are similarly related to a set of BPS equations, which form a generalized Hitchin-like system, involving two Higgs fields. Akin to the spectral curve (or the Seiberg-Witten curve) in the $\mathcal{N} = 2$ case, one can associate a spectral curve, known as the $\mathcal{N} = 1$ curve, to the generalized Hitchin system [79, 136]. The $\mathcal{N} = 1$ curve has appeared in various forms in the literature [52, 71–73, 78, 79, 136–151]. The $\mathcal{N} = 1$ deformation is realized by turning on singular behaviors of the second Higgs field at the locations of the punctures on the Riemann surface, which we dub as a "rotation" of the involved punctures. The profile of the second Higgs field is solved in terms of its asymptotic behavior by the generalized Hitchin system, which also constrains the profile of the $\mathcal{N} = 2$

---

[2]Hats denote Pontryagin duals, i.e., $\widehat{\Lambda} := \mathrm{Hom}(\Lambda, U(1))$.

Higgs field. Ultimately, the different solutions for the two Higgs field capture $\mathcal{N} = 1$ vacua of the deformed theory.

One can also study a generalization of the above set-up, where one starts with a topological twist that only preserves 4d $\mathcal{N} = 1$ supersymmetry. The BPS equations are a generalized Hitchin system, where the two Higgs fields are now on an equal footing and can have singularities at mutually distinct locations on the Riemann surface. One can again associate an $\mathcal{N} = 1$ curve to a vacuum of the resulting 4d $\mathcal{N} = 1$ theory, which now does not have an interpretation as a deformation of a 4d $\mathcal{N} = 2$ Class S theory. In M-theory, the two twists are distinguished as follows: the Class S construction is obtained by wrapping M5-branes on the UV curve embedded in a local K3-surface. The $\mathcal{N} = 1$ twists arise by instead embedding the curve into a local Calabi-Yau threefold. These set-ups are discussed in sections 13.3 and 13.4.

The 1-form symmetry group $\mathcal{O}$ of a Class S theory is encoded in the 1-cycles of the punctured Riemann surface as discussed in detail in [3] (which is based on [64], also see [66,70] and the study of line operators in [152]), which we summarize in our context in chapter 11.1 and section 13.2. In a similar spirit, we argue in section 13.5 that the preserved 1-form symmetry group $\mathcal{O}_r$ in a vacuum r is encoded in the 1-cycles of the $\mathcal{N} = 1$ curve Σ_r associated to the vacuum r. Our work can thus be viewed as a part of the recent surge of activity in the study of generalized symmetries of QFTs via compactifications of string theory and higher-dimensional QFTs [3, 58–60, 62, 65, 66, 70, 153–157].

To explain and test our framework we first consider pure $\mathcal{N} = 1$ SYM as well as an extension to the set-up studied in Cachazo-Seiberg-Witten (CSW) [71–73], which corresponds to turning on a superpotential for the adjoint chiral superfield that lives in the $\mathcal{N} = 2$ vector multiplet. Both instances have well-documented confining vacua and we use them to test our general framework and to showcase how to go from the $\mathcal{N} = 1$ curve to the area/perimeter law of line operators.

The most exciting application of this work is to the realm of non-Lagrangian theories –

which are ubiquitous in Class S constructions. For these the standard tool set for analyzing confinement from a Lagrangian point of view is unavailable. We identify, in section 16, a family of $\mathcal{N} = 1$ theories, and show that this class of theories exhibits confinement! We argue – based on the curve and associated line operators that these theories have confining vacua. Clearly numerous generalizations of this can be considered, opening up a vast arena for studying confinement in theories with no apparent Lagrangian.

The plan of this thesis part is as follows:

In chapter 12 we will whet the appetite of the reader by discussing in detail the $\mathfrak{su}(2)$ SYM theory and its confining vacua using the Class S and $\mathcal{N} = 1$ perspective.

The main conceptual background will be explained in chapter 13, which includes the $\mathcal{N} = 1$ curve and associated Hitchin system. We then apply this general approach to two well-known instances of theories with confining vacua: in chapter 14 we study the $\mathcal{N} = 1$ curves for 4d $\mathcal{N} = 1$ $\mathfrak{su}(n)$ SYM , and use it to recover the well-known properties of confinement in this model. In chapter 15, we discuss the CSW model, whose confinement properties are also well-known in the literature. These two models provide extensive consistency checks of our proposed method of computing confinement, and also for testing our methodology.

In chapter 16, it comes time to reap the rewards as we use our method to find an infinite class of non-Lagrangian 4d $\mathcal{N} = 1$ theories that contain confining vacua. The simplest theory in this class can be described as an $\mathcal{N} = 1$ deformation of the $\mathcal{N} = 2$ asymptotically conformal theory obtained by gauging $\mathfrak{su}(3)^3$ flavor symmetry subgroup of the famous E_6 Minahan-Nemeschansky theory (or the T_3 trinion theory) [158]. Other theories in this class can be described as $\mathcal{N} = 1$ deformations of $\mathcal{N} = 2$ asymptotically conformal theories obtained by gauging $\mathfrak{su}(n)^n$ flavor symmetry group of the 4d $\mathcal{N} = 2$ SCFT obtained by compactifying A_{n-1} $\mathcal{N} = (2,0)$ theory on a sphere with n maximal regular untwisted punctures.

Summary of notation in figures of v- and w-curves.

- The pictures show the UV curve parametrized by t and the branch cuts for v, w as n-fold cover over it.

- Punctures and branch points are denoted by stars and crosses, respectively.

- Branch lines are labelled by a monodromy element in the symmetric group S_n.

- Cyclic permutation $(123\cdots n) \to (234\cdots n1)$ is denoted by a.

- Transposition of ij is denoted by b_{ij}.

- Dashed lines are associated with $\mathbb{Z}_2$ branch cuts and solid oriented lines are associated with $\mathbb{Z}_{n>2}$ branch cuts.

- Branch lines are oriented such that the labelled monodromy takes action along a closed path $\gamma(\tau)$ when the cross product of the oriented line with the vector $\dot{\gamma}$ points out of the page.

- The circle $|t| = 1$ is located at the vertical equator with $t = 1$ on the front and $t = -1$ on the back.

Chapter 10
6d $\mathcal{N} = (2,0)$ SCFTs from IIB

We review 6d $\mathcal{N} = (2,0)$ superconformal field theories following [159, 160]. In this thesis two equivalent perspectives are taken on such theories with gauge algebra of type A_n. In M-theory these theories arise as the world volume theory of a stack of n M5-branes. By M/F-theory duality these are equally described as IIB string theory on an ADE singularity of type A_n. The latter allows for immediate generalization to 6d $\mathcal{N} = (2,0)$ with gauge algebras of type D and E. In this section we elaborate the more general geometric construction and classification. The presented structures are intrinsic to the 6d theory.

Consider IIB string theory on an ADE singularity. To understand the physics we resolve the singularity and study its properties in the limit of collapsing vanishing cycles. For concreteness consider $\mathbb{C}^2/\mathbb{Z}_2$. A minimal resolution of this A_1 singularity, as discussed in section 1.2, gives the local Calabi-Yau two-fold $\mathcal{O}_{\mathbb{P}^1}(-2)$ with resolution divisor $\mathbb{P}^1$. The effective physics on this smooth geometry derives from a Kaluza-Klein reduction of IIB supergravity and gives a 6d theory with gravity decoupled. This geometry preserves half of the 32 supercharges, with the unbroken 16 supercharges assembling into two spinors of identical chirality, we have $\mathcal{N} = (2,0)$ supersymmetry. The Kaluza-Klein reduction of the chiral four-form wrapped on $\mathbb{P}^1$ gives a two-form B with anti-self dual field strength. The metric modulus controlling the size of the $\mathbb{P}^1$ descends to a bosonic field. This field and the two-form are part of the $\mathcal{N} = (2,0)$ tensor multiplet. The chiral four-form of IIB string theory couples to D3-branes. Wrapping D3-branes on the divisor $\mathbb{P}^1$ gives a dynamical string in 6d, which couples to the two-form B and whose tension is set by the volume of $\mathbb{P}^1$. On the other hand wrapping the D3-brane on the non-compact two-cycle in $\mathcal{O}_{\mathbb{P}^1}(-2)$ gives a non-dynamical string of infinite tension in 6d, which we refer to as a surface operator. This non-compact two-cycle is constructed by taking the torsional one-cycle in the asymptotic boundary $\partial\mathcal{O}_{\mathbb{P}^1}(-2) = S^3/\mathbb{Z}_2$ and fibering it over a radial direction. Often, $\partial\mathcal{O}_{\mathbb{P}^1}(-2)$ and $\mathbb{P}^1$ are referred to as link and bolt.

Now we collapse the $\mathbb{P}^1$ [161, 162]. The dynamical strings become tensionless, the non-dynamical strings are essentially unaffected. The resulting theory is 6d SCFT of type $\mathfrak{g} = A_1$.

Now consider more general set-ups with an arbitrary number of $\mathbb{P}^1$'s contained inside a local Calbabi-Yau two-fold. The Calabi-Yau condition requires these curves Σ_i to be (-2) curves. This collection of (-2) curves can only be contracted if its intersection matrix $A_{ij} = \Sigma_i \cap \Sigma_j$ is negative definite with off-diagonal entries either zero or one. These are precisely the Cartan matrices of type ADE. One finds that 6d $\mathcal{N} = (2,0)$ SCFTs are labelled by an ADE gauge algebra $\mathfrak{g}$.

Now consider IIB string theory on the resolution $B = \widetilde{\mathbb{C}^2/\Gamma_{\text{ADE}}}$. The charge lattice of

the massive dynamical strings is given by the compactly supported homology group $\Lambda = H_2^c(B, \mathbb{Z})$ generated by the Σ_i. The dual lattice Λ^* is associated with the non-compact two-cycles and characterizes the charge lattice of the non-dynamical strings. The pairing between these two lattices is interpreted physically as a Dirac pairing [163]. Surface defects engineered from D3-branes on non-compact curves are thus labelled by their charge, a wrapped non-compact surface in $H_2^{\mathrm{nc}}(B, \mathbb{Z})$ and the supersymmetry they preserve.

The intersection pairing on Λ gives a map $\Lambda^* \to \Lambda$. The defect group D is now given by [160]

$$D = \Lambda^*/\Lambda . \tag{10.1}$$

For the A_1 example above we clearly have $\Lambda^* \cong \mathbb{Z}$ and $\Lambda \cong 2\mathbb{Z}$ giving $D = \mathbb{Z}_2$. More generally D computes to the abelianization of the ADE group Γ. The defect group characterizes the charges of the surface operators which can not be screened by dynamical particles.

Whenever the defect group D is non-trivial the 6d $\mathcal{N} = (2,0)$ theory is a relative quantum field theory [66, 164]. Theories of ADE type are relative to a three-form abelian Chern-Simons theory in 7d with level matrix given by the Cartan matrix of the corresponding Lie algebra. This means, that if the 6d theory is defined on M_6, the 7d theory is defined on M_7 with $M_7 = M_6 \times I$. The 6d theory can be interpreted as a topological boundary condition of the 7d Chern-Simons theory [66]. For this consider the 7d theory compactified on the interval I and choose boundary conditions at one end while coupling to the 6d theory at the other. After compactification, the final absolute 6d theory has a group of genuine surface operators and non-genuine surface operators constrained to live at the ends of topological three-dimensional operators generating the 2-form symmetry. The genuine surface operators are acted on by an anomalous 2-form global symmetry which is matched by the 7d theory to render the coupled 6d/7d system anomaly free. Genuine surface operators are determined by a choice of polarization and are mutually local.

In the following sections we will expand both on the above geometric picture and its M-theory counterpart for theories with gauge algebra of type A. We study the higher form

symmetries and defect groups as they descend to 4d theories with $\mathcal{N} = 1, 2$ supersymmetry by compactification on Riemann surfaces.

Chapter 11
1-form Symmetries in 4d $\mathcal{N} = 2$ Class S

In this section we study the 1-form symmetries for 4d $\mathcal{N} = 2$ theories of class S. We establish the construction and properties of line operators and the preserved higher form symmetries in the absence and presence of regular punctures. Further we consider a geometric IIB dual interpretation of the set-up.

We briefly give some background on higher form symmetries [57]. A q-form global symmetry in d dimensional space-time is realized by an operator $U_g(S)$ associated with a $(d - q - 1)$-dimensional closed submanifold S of space-time and labelled by a group element $g \in G$. Operators compose according to group multiplication

$$U_g(S)U_{g'}(S) = U_{gg'}(S) \,. \tag{11.1}$$

Further these operators are topological and correlation functions do not change under small deformations of their supports. Operators $V(S)$ charged under the associated symmetry are supported on a closed q-dimensional submanifolds T. The operators supported on S, T satisfy the equal time commutator

$$U(S)V(T) = g(V)^{S \cdot T} V(T)U(S) \tag{11.2}$$

where S, T are now contained in the same spacial slice with $S \cdot T$ denoting their intersection and $g(V)$ characterizing the charge/phase of the extended operator $V(T)$ under the symmetry generated by $U(S)$. This relation holds at unequal times with $S \cdot T$ replaced by the linking number $l(S, T)$.

In following sections we discuss 1-form symmetries in 4d and 2-form symmetries in 6d.

$\mathfrak{g}$	$Z(\mathcal{G})$	$\widehat{Z}(\mathcal{G})$	$\langle \cdot, \cdot \rangle$
A_{n-1}	$\mathbb{Z}_n$	$\mathbb{Z}_n$	$\langle f, f \rangle = \frac{1}{n}$
D_{4n}	$\mathbb{Z}_2 \times \mathbb{Z}_2$	$\mathbb{Z}_2 \times \mathbb{Z}_2$	$\langle s, s \rangle = 0, \quad \langle c, c \rangle = 0, \quad \langle s, c \rangle = \frac{1}{2}$
D_{4n+1}	$\mathbb{Z}_4$	$\mathbb{Z}_4$	$\langle s, s \rangle = \frac{3}{4}$
D_{4n+2}	$\mathbb{Z}_2 \times \mathbb{Z}_2$	$\mathbb{Z}_2 \times \mathbb{Z}_2$	$\langle s, s \rangle = \frac{1}{2}, \quad \langle c, c \rangle = \frac{1}{2}, \quad \langle s, c \rangle = 0$
D_{4n+3}	$\mathbb{Z}_4$	$\mathbb{Z}_4$	$\langle s, s \rangle = \frac{1}{4}$
E_6	$\mathbb{Z}_3$	$\mathbb{Z}_3$	$\langle f, f \rangle = \frac{2}{3}$
E_7	$\mathbb{Z}_2$	$\mathbb{Z}_2$	$\langle f, f \rangle = \frac{1}{2}$
E_8	0	0	$-$

Table 11.1: For the ADE Lie algebras $\mathfrak{g}$ we denote by $\mathcal{G}$ the simply-connected Lie group, and list the center $Z(\mathcal{G})$, the Pontryagin dual group to the center $\widehat{Z}(\mathcal{G})$, and the bihomomorphism $\langle \cdot, \cdot \rangle$. E_8 has a trivial center group, which has been denoted by 0 since we use an additive notation for the group multiplication law throughout this chapter. We denote a generator of $\widehat{Z}(\mathcal{G})$ for $\mathfrak{g} = A_{n-1}, E_6, E_7$ as f; a generator of $\widehat{Z}(\mathcal{G})$ for $\mathfrak{g} = D_{2n+1}$ as s; and generators of $\widehat{Z}(\mathcal{G}) \simeq \mathbb{Z}_2 \times \mathbb{Z}_2$ for $\mathfrak{g} = D_{2n}$ as s, c. We also define $v := s + c$ for $\mathfrak{g} = D_{2n}$.

11.1   Surface Operators and Outer Automorphisms in 6d $(2, 0)$

6d $\mathcal{N} = (2, 0)$ SCFTs are relative QFTs classified by a simple Lie algebra $\mathfrak{g}$ of ADE type. Such a theory contains surface defect operators of dimension 2. Modulo screening by dynamical objects, these operators can be classified by the Pontryagin dual $\widehat{Z}(\mathcal{G})$ of the center $Z(\mathcal{G})$ of the simply connected group $\mathcal{G}$ associated to $\mathfrak{g}$, which are summarized in table 11.1. The Pontryagin dual $\widehat{Z}(\mathcal{G}) := \mathrm{Hom}(Z(\mathcal{G}), \mathbb{R}/\mathbb{Z})$ of a finite abelian center group is isomorphic to the center group itself.

These surface operators are not all mutually local. Consider a correlation function containing two surface operators $\alpha, \beta \in \widehat{Z}(G)$. As α is moved around β, the correlation function is transformed by a phase factor[1]

$$\exp\big(2\pi i \langle \alpha, \beta \rangle\big) \tag{11.3}$$

---

[1]Notice (in the following equation) that we define the pairing with a negative sign as compared to the standard choice, which can be found for example in [66].

with a bihomomorphism

$$\langle \cdot, \cdot \rangle : \quad \widehat{Z}(\mathcal{G}) \times \widehat{Z}(\mathcal{G}) \;\to\; \mathbb{R}/\mathbb{Z} \,. \tag{11.4}$$

The bihomomorphism can be specified by providing its values on the generators of $\widehat{Z}(G)$ [66]. These are also listed in table 11.1.

The $(2,0)$ theory admits a discrete 0-form symmetry which can be identified with the group of outer-automorphisms $\mathcal{O}_{\mathfrak{g}}$ of $\mathfrak{g}$, which are

$$\mathcal{O}_{\mathfrak{g}} = \mathbb{Z}_2 \tag{11.5}$$

for $\mathfrak{g} = A_{n \geq 2}, D_{n \geq 5}, E_6$, and

$$\mathcal{O}_{D_4} = S_3 \,, \tag{11.6}$$

namely the group formed by permutations of three objects. $\mathcal{O}_{\mathfrak{g}}$ is trivial for E_7 and E_8. The outer-automorphisms act on representations of $\mathfrak{g}$, and hence on $\widehat{Z}(\mathcal{G})$. For $\mathfrak{g} = A_n, D_{2n+1}, E_6$, the non-trivial element of $\mathcal{O}_{\mathfrak{g}} = \mathbb{Z}_2$ acts by sending the generator of $\widehat{Z}(\mathcal{G})$ to its inverse. For $\mathfrak{g} = D_{2n}$ and $n \geq 3$, the non-trivial element of $\mathcal{O}_{\mathfrak{g}} = \mathbb{Z}_2$ acts by exchanging the two chosen generators s, c of $\widehat{Z}(\mathcal{G}) \simeq \mathbb{Z}_2 \times \mathbb{Z}_2$. For $\mathfrak{g} = D_4$, we write

$$\mathcal{O}_{D_4} = S_3 \simeq \mathbb{Z}_3 \rtimes \mathbb{Z}_2 \tag{11.7}$$

and choose generators $a \in \mathbb{Z}_3$ and $b \in \mathbb{Z}_2$, which act as follows

$$
\begin{aligned}
a : & \quad s \to v, \quad v \to c, \quad c \to s \\
b : & \quad s \to c, \quad c \to s, \quad v \to v \,.
\end{aligned}
\tag{11.8}
$$

11.2   Compactifications without Punctures

In this chapter we consider compactifications of 6d $(2,0)$ theories on a Riemann surface $\mathcal{C}_g$ of genus g without any punctures. If there are no other ingredients involved in the compactification, such a compactification is called an *untwisted* compactification. On the other hand, we can also consider *twisted* compactifications which means the following. The outer-automorphism 0-form symmetry in 6d $(2,0)$ theory discussed in the last section is

generated by topological operators of codimension-1 in the 6d theory. Inserting such a topological operators along a cycle of the Riemann surface gives rise to a "codimension-0 object" in the 4d theory, which means that the resulting 4d theory itself is different from the 4d theory arising when no such topological operators are inserted. Further discussion on twisted compactification is omitted here, but can be found in [3].

Twisted and untwisted compactifications can equivalently be distinguished in the Higgs bundle description of the compactification. Here the insertion of topological operators along twist lines gives rise to an action on the Higgs field by an outer automorphism o across these. The insertions alter the gauge group of the effective 4d $\mathcal{N} = 2$ theory and have a geometric interpretation in the IIB dual description as we explain in more detail in section 11.4. In this geometric picture we are further able to justify the key assumption that regular untwisted punctures are irrelevant in determining the defect group, which we also argue for in section 11.3.

11.2.1 Untwisted Compactifications

Let us compactify a $(2, 0)$ theory on a Riemann surface $\mathcal{C}_g$ of genus g without any punctures or twists. This gives rise to a relative 4d $\mathcal{N} = 2$ theory with a set of line defects descending from the elements of $\widehat{Z}(\mathcal{G})$ wrapped along various cycles of $\mathcal{C}_g$. That is, the set $\mathcal{L}$ of 4d line defects (modulo screening) can be identified with

$$\mathcal{L} = H_1(\mathcal{C}_g, \widehat{Z}) \simeq H_1(\mathcal{C}_g, \mathbb{Z}) \otimes \widehat{Z} \,. \tag{11.9}$$

These line defects are not all mutually local. The violation of mutual locality between two elements $a \otimes \alpha, b \otimes \beta \in H_1(\mathcal{C}_g, \mathbb{Z}) \otimes \widehat{Z} \simeq H_1(\mathcal{C}_g, \widehat{Z})$ is captured by the phase

$$\exp\big(2\pi i \langle \alpha, \beta \rangle \langle a, b \rangle \big) \,, \tag{11.10}$$

where $\langle a, b \rangle$ is the intersection pairing on $H_1(\mathcal{C}_g, \mathbb{Z})$. This gives rise to a pairing on $H_1(\mathcal{C}_g, \widehat{Z})$ which is the natural combination of the intersection pairing and the bihomomorphism (11.4)

$$\langle \cdot, \cdot \rangle : \quad H_1(\mathcal{C}_g, \widehat{Z}) \times H_1(\mathcal{C}_g, \widehat{Z}) \to \mathbb{R}/\mathbb{Z}$$

$$\langle a \otimes \alpha, b \otimes \beta \rangle = \langle a, b \rangle \langle \alpha, \beta \rangle \,. \tag{11.11}$$

We can specify an absolute 4d $\mathcal{N} = 2$ theory by choosing a maximal set of line operators

$$\Lambda \subset H_1(\mathcal{C}_g, \widehat{Z}) \,, \tag{11.12}$$

which are all mutually local, i.e., the phase (11.10) is trivial for any two elements in Λ. Such a set Λ is also referred to as a 'maximal isotropic subgroup' or as a 'polarization' in what follows. The 1-form symmetry of the absolute 4d $\mathcal{N} = 2$ theory can then be identified with the Pontryagin dual $\widehat{\Lambda}$ of Λ.

Once we choose a set of A and B cycles on $\mathcal{C}_g$, we can decompose

$$H_1(\mathcal{C}_g, \widehat{Z}) \simeq \widehat{Z}_A^g \times \widehat{Z}_B^g \,, \tag{11.13}$$

where $\widehat{Z}_A^g$ is the contribution of A-cycles, and $\widehat{Z}_B^g$ is the contribution of B-cycles. Moreover, $\widehat{Z}_A^g$ and $\widehat{Z}_B^g$ are maximal isotropic sublattices, and hence provide canonical choices of Λ once a choice of A and B cycles has been made.

Example: When $(2,0)$ theory of type $\mathfrak{g}$ is compactified on a torus, we obtain 4d $\mathcal{N} = 4$ SYM with gauge algebra $\mathfrak{g}$. Choosing an A-cycle and a B-cycle, we write

$$H_1(T^2, \widehat{Z}) \simeq \widehat{Z}_A \times \widehat{Z}_B \,. \tag{11.14}$$

We assume without loss of generality that the A-cycle is much shorter than the B-cycle, this specifies the electromagnetic duality frame in which the W-bosons become light. Then, $\widehat{Z}_A$ can be identified as the set of 4d Wilson line operators, and $\widehat{Z}_B$ can be identified as the set of 4d 't Hooft line operators. Choosing $\Lambda = \widehat{Z}_A$, we obtain 4d $\mathcal{N} = 4$ SYM with gauge group $\mathcal{G}$. On the other hand, choosing $\Lambda = \widehat{Z}_B$, we obtain 4d $\mathcal{N} = 4$ SYM with gauge group $\mathcal{G}/Z(\mathcal{G})$ and all discrete theta parameters turned off. In these cases, we have 1-form symmetry

$$\widehat{\Lambda} \simeq Z(\mathcal{G}) \,, \tag{11.15}$$

which matches with the 1-form symmetry obtained using the Lagrangian description of 4d $\mathcal{N} = 4$ SYM: when the gauge group is $\mathcal{G}$, this is the electric 1-form symmetry; and then the gauge group is $\mathcal{G}/Z(\mathcal{G})$, this is the magnetic 1-form symmetry.

Other choices of global forms of the gauge group and discrete theta angles are obtained by choosing other polarizations. For concreteness, consider the case of $\mathfrak{g} = \mathfrak{su}(4)$. In this case, $\widehat{Z}_A \simeq \widehat{Z}_B \simeq \mathbb{Z}_4$. The $PSU(4)$ theory with a discrete theta parameter $n \in \{0, 1, 2, 3\}$ turned on is obtained by choosing Λ to be the sublattice generated by the element $(n, 1) \in \mathbb{Z}_4 \times \mathbb{Z}_4 \simeq \widehat{Z}_A \times \widehat{Z}_B$ (where we have represented $\mathbb{Z}_4$ as the additive group $\mathbb{Z}/4\mathbb{Z}$). Any such choice leads to the 1-form symmetry

$$\widehat{\Lambda} \simeq \mathbb{Z}_4 \,. \tag{11.16}$$

If we choose the polarization Λ generated by elements $(0, 2)$ and $(2, 0)$ in $\mathbb{Z}_4 \times \mathbb{Z}_4$, then we obtain the $SO(6) \simeq SU(4)/\mathbb{Z}_2$ theory with the discrete theta parameter turned off. In this case the 1-form symmetry is

$$\widehat{\Lambda} \simeq \mathbb{Z}_2 \times \mathbb{Z}_2 \,. \tag{11.17}$$

From the point of view of the Lagrangian description, the two $\mathbb{Z}_2$ factors are electric and magnetic 1-form symmetries respectively. The remaining $\mathfrak{su}(4)$ theory has $SO(6)$ gauge group and a discrete theta parameter turned on. This is obtained by choosing Λ to be generated by the element $(1, 2) \in \mathbb{Z}_4 \times \mathbb{Z}_4 \simeq \widehat{Z}_A \times \widehat{Z}_B$, and the 1-form symmetry group of the theory is

$$\widehat{\Lambda} \simeq \mathbb{Z}_4 \,. \tag{11.18}$$

Example: Consider compactifying A_1 $(2, 0)$ theory on $\mathcal{C}_g$ with $g \geq 2$. In an S-duality frame, in which A-cycles are much shorter than B-cycles, we obtain the following Lagrangian 4d

$\mathcal{N} = 2$ theory

$$
\begin{array}{ccccccccccc}
 & & \tfrac{1}{2}\mathsf{F} & & & & & & & \tfrac{1}{2}\mathsf{F} & \\
 & & | & & & & & & & | & \\
\mathfrak{so}(3) \!-\!\!\!-\! & \mathfrak{su}(2) \!-\!\!\!-\! & \mathfrak{so}(4) \!-\!\!\!-\! & \mathfrak{su}(2) \!-\!\!\!-\! & \mathfrak{so}(4) & -\cdots- & \mathfrak{so}(4) \!-\!\!\!-\! & \mathfrak{su}(2) \!-\!\!\!-\! & \mathfrak{so}(3)
\end{array}
$$

$$\tag{11.19}$$

where we have a total of $2g - 1$ nodes. Each node describes a gauge algebra and an edge between two nodes denotes a half-bifundamental[2] between the two nodes. An edge connecting an $\mathfrak{su}(2)$ node to a node labeled $\tfrac{1}{2}\mathsf{F}$ implies that the corresponding $\mathfrak{su}(2)$ gauge algebra carries an extra half-hyper charged in fundamental rep. If we choose $\Lambda = (\mathbb{Z}/2\mathbb{Z})^g_A$, we obtain the 4d theory with all the gauge groups being simply connected. In this case, we have 1-form symmetry

$$\widehat{\Lambda} \simeq \mathbb{Z}_2^g \,, \tag{11.20}$$

which can be easily matched with the above Lagrangian description with all the gauge groups chosen to be the simply connected ones. A $\mathbb{Z}_2$ factor arises from each of the g number of $\mathfrak{so}(n)$ nodes (where $n = 3, 4$ and the corresponding gauge group is $\mathrm{Spin}(n)$). This $\mathbb{Z}_2$ is the subgroup of the center of $\mathrm{Spin}(n)$ that acts trivially on the fundamental representation of $\mathfrak{so}(n)$ as defined in the above footnote.

11.3 Compactifications with Regular Punctures

Regular punctures are a special set of punctures defined by the condition that the Hitchin field has (at most) a simple pole at the location of the puncture. These punctures can be either *untwisted* or *twisted*. Twisted regular punctures arise at the ends of twist lines, and hence the Hitchin field transforms by the action of the corresponding outer-automorphism as one encircles a twisted regular puncture. On the other hand, untwisted punctures do *not* live at the ends of non-trivial twist lines, and correspondingly the Hitchin field does

---

[2]Here, for ease of notation, we are using the convention that the fundamental representation of $\mathfrak{so}(n)$ is the n-dimensional vector representation. So, the fundamental representation for $\mathfrak{so}(3)$ is not the fundamental representation for $\mathfrak{su}(2)$, but rather the adjoint representation. Similarly, the fundamental representation of $\mathfrak{so}(4)$ is the $(2, 2)$ rep of $\mathfrak{su}(2) \oplus \mathfrak{su}(2) \simeq \mathfrak{so}(4)$.

Untwisted Puncture   Twisted Puncture

Figure 11.1:   A twisted puncture lives at the end of a non-trivial twist line t, while an untwisted puncture does not live at the end of a non-trivial twist line.

not pick up the action of any non-trivial outer automorphism as one encircles an untwisted regular puncture. See figure 11.1. We restrict the presentation to regular puncture and avoid complications due to twist lines which are irrelevant for the content presented in chapters going forward.

Moreover, we further omit a special subset of regular punctures. The punctures in this subset are referred to as *atypical* punctures. In the presence of atypical regular punctures, the number of simple factors in the gauge algebra arising in a degeneration limit of the Riemann surface is not equal to the dimension of the moduli space of the Riemann surface [165–167] (see also [135]). We call a regular puncture which is not atypical a *typical* puncture. An atypical regular puncture can be resolved into some number of typical regular punctures. Throughout this chapter a regular puncture always refers to a *typical* regular puncture.

In this chapter, we consider compactifications of 6d $\mathcal{N} = (2,0)$ theories on a Riemann surface C_g with an arbitrary number of (untwisted and twisted) regular punctures, and an arbitrary number of closed twist lines (which do not have end-points).

11.3.1   Untwisted Regular Punctures

Let $\mathcal{L}$ be the set of 4d line operators (modulo screening) when a $(2,0)$ theory is compactified on a Riemann surface $\mathcal{C}_g$ without any punctures, but possibly in the presence of closed twist lines. The set $\mathcal{L}$ (and Dirac pairing on it) was determined in the last few sections. Now, insert n regular untwisted punctures on $\mathcal{C}_g$. We propose that the set of 4d line operators modulo flavor charges (and screening) can again be identified with $\mathcal{L}$. Moreover, an absolute

4d $\mathcal{N} = 2$ theory is obtained by choosing a maximal isotropic subgroup

$$\Lambda \subset \mathcal{L} \tag{11.21}$$

and the 1-form symmetry of such an absolute 4d $\mathcal{N} = 2$ theory can be identified with $\widehat{\Lambda}$. In other words, regular untwisted punctures turn out to be irrelevant for the considerations of this paper. In the rest of this section, we substantiate this proposal by studying some examples. This behavior is in stark contrast with the irregular punctures of type $\mathcal{P}_0$ which play a major role in the constructions of chapter 12 and beyond.

Sphere with 4 regular untwisted punctures: As a few examples, we can obtain the following 4d $\mathcal{N} = 2$ gauge theories by compactifying $(2,0)$ theories on a sphere with 4 regular untwisted punctures[3]:

- $\mathfrak{su}(n) + 2n\mathsf{F}$ by compactifying A_{n-1} $(2,0)$ theory.

- $\mathfrak{so}(8) + 2\mathsf{F} + 2\mathsf{S} + 2\mathsf{C}$, $\mathfrak{so}(8) + 4\mathsf{S} + 2\mathsf{C}$, $\mathfrak{so}(8) + 4\mathsf{S} + \mathsf{C} + \mathsf{F}$ by compactifying D_4 $(2,0)$ theory [168].

- $\mathfrak{so}(9) + 3\mathsf{S} + \mathsf{F}$, $\mathfrak{so}(10) + 4\mathsf{S}$, $\mathfrak{so}(10) + 2\mathsf{S} + 4\mathsf{F}$ by compactifying D_5 $(2,0)$ theory [168].

- $\mathfrak{so}(11) + \mathsf{S} + 5\mathsf{F}$, $\mathfrak{so}(11) + \frac{3}{2}\mathsf{S} + 3\mathsf{F}$, $\mathfrak{so}(12) + \mathsf{S} + \frac{1}{2}\mathsf{C} + 4\mathsf{F}$, $\mathfrak{so}(12) + \mathsf{S} + 6\mathsf{F}$, $\mathfrak{so}(12) + \frac{3}{2}\mathsf{S} + \frac{1}{2}\mathsf{C} + 2\mathsf{F}$ by compactifying D_6 $(2,0)$ theory [168].

- $\mathfrak{su}(4) + 2\Lambda^2 + 4\mathsf{F}$, $\mathfrak{sp}(2) + 6\mathsf{F}$ by compactifying A_3 $(2,0)$ theory [56].

For this case $\mathcal{L}$ is trivial, which is what is expected from the 4d gauge theory description as it can be checked that the line operators (modulo screening and flavor charges) form a trivial set in all of the above gauge theories. Consequently, the 1-form symmetry is also trivial for all of these theories, and the gauge group must be the simply connected one.

---

[3]The notation $\mathfrak{g}_i + \sum n_i \mathsf{R}_i$ denotes a 4d $\mathcal{N} = 2$ gauge theory with gauge algebra $\mathfrak{g}$ along with n_i full hypers in irrep R_i. If n_i is half-integral, it means that there is an additional half-hyper in R_i along with $\lfloor n_i \rfloor$ number of full hypers in R_i. F denotes fundamental irrep for $\mathfrak{su}(n)$ and $\mathfrak{sp}(n)$, and vector irrep for $\mathfrak{so}(n)$. S denotes spinor irreps for $\mathfrak{so}(n)$ and C denotes co-spinor irrep for $\mathfrak{so}(2n)$. Λ^2 denotes 2-index antisymmetric irrep for $\mathfrak{su}(n)$ and $\mathfrak{sp}(n)$.

Torus with 1 regular untwisted puncture and twisted line: We can obtain the following 4d $\mathcal{N} = 2$ gauge theories by compactifying $(2,0)$ theories on a torus with 1 regular untwisted puncture and a twisted line wrapped along a non-trivial cycle[4]:

- $\mathfrak{su}(2n) + \mathsf{S}^2 + \mathsf{\Lambda}^2$ by compactifying A_{2n-1} $(2,0)$ theory.

- $\mathfrak{su}(2n+1) + \mathsf{S}^2 + \mathsf{\Lambda}^2$ by compactifying A_{2n} $(2,0)$ theory.

In the former case, we have

$$\mathcal{L} \simeq \mathbb{Z}_2 \times \mathbb{Z}_2 \,, \tag{11.22}$$

which can be matched with the 4d gauge theory expectation. For a pure $\mathfrak{su}(2n)$ gauge theory, the set of Wilson lines (modulo screening) is $\mathbb{Z}_{2n}$ with generator W being the Wilson line in fundamental rep of $\mathfrak{su}(2n)$. The set of 't Hooft lines (modulo screening) is also $\mathbb{Z}_{2n}$ with generator H. The Dirac pairing between W and H is $\langle W, H \rangle = \frac{1}{2n}$. Now we add in the matter. The hypermultiplets in $\S^2$ and $\mathsf{\Lambda}^2$ screen $2W$, and thus the set of Wilson lines (modulo screening and flavor charges) can be identified with $\mathbb{Z}_2$, generated by W. On the other hand, the 't Hooft lines must be mutually local with $2W$, and hence the set of 't Hooft lines (modulo screening and flavor charges) can be identified with $\mathbb{Z}_2$, generated by nH. Thus, we verify the prediction (11.22). Choosing the polarization Λ to be the $\mathbb{Z}_2$ generated by W leads to gauge group $SU(2n)$. Choosing Λ to be the $\mathbb{Z}_2$ generated by nH or $W + nH$ leads to gauge group $SU(2n)/\mathbb{Z}_2$ with discrete theta parameter turned off or on respectively. In all these cases, the 1-form symmetry is

$$\widehat{\Lambda} \simeq \mathbb{Z}_2 \,. \tag{11.23}$$

In the latter case, $\mathcal{L}$ is trivial. Correspondingly, the set of line operators in the gauge theory (modulo screening and flavor charges) is trivial. The set of Wilson lines is trivial because $2W$ is a generator of $\mathbb{Z}_{2n+1}$, and the set of 't Hooft lines is trivial because they need to be mutually local with W (as W is screened). There is no 1-form symmetry, and the gauge group must be the simply connected $SU(2n+1)$.

---

[4]S^2 denotes the 2-index symmetric representation of $\mathfrak{su}(n)$.

Torus with k regular untwisted punctures: 4d $\mathcal{N} = 2$ $\mathfrak{su}(n)^k$ necklace quiver can be obtained by compactifying A_{n-1} $(2,0)$ theory on a torus with k regular untwisted punctures. In this case,

$$\mathcal{L} \simeq \widehat{Z}_A \times \widehat{Z}_B \simeq \mathbb{Z}_n^A \times \mathbb{Z}_n^B \,, \qquad (11.24)$$

which can be verified from the 4d gauge theory description. For example, choosing all gauge groups to be $SU(n)$ corresponds to choosing one of the two $\mathbb{Z}_n$ factors as the polarization. The 1-form symmetry is then predicted to be

$$\widehat{\Lambda} \simeq \mathbb{Z}_n \,, \qquad (11.25)$$

which can be identified as the diagonal subgroup of the $\mathbb{Z}_n^k$ center of the gauge group $SU(n)^k$.

$\mathcal{C}_g$ **with n regular untwisted punctures**: Consider compactifying A_1 $(2,0)$ theory on $\mathcal{C}_g$ in the presence of n regular untwisted punctures [55]. According to our proposal, we predict

$$\mathcal{L} \simeq \mathbb{Z}_2^g \times \mathbb{Z}_2^g \,. \qquad (11.26)$$

There are a number of degeneration limits which lead to a variety of S-dual weakly-coupled 4d conformal gauge theories. The predicted answer for $\mathcal{L}$ and the pairing on it can be verified from the point of view of any of these 4d gauge theories. For example, one such degeneration limit (which exists for $n \geq 2$) leads to the following 4d gauge theory

$$(11.27)$$

where an edge between two $\mathfrak{su}(2)$ gauge algebras denotes a full hyper in bifundamental, while an between an $\mathfrak{su}(2)$ and an $\mathfrak{so}(n)$ gauge algebra denotes a half-hyper in bifundamental (see earlier discussion for our slightly non-standard definition of fundamental of $\mathfrak{so}(3)$ and $\mathfrak{so}(4)$). The edge between a node labeled $n\mathsf{F}$ and a node labeled $\mathfrak{su}(2)$ denotes that the

corresponding $\mathfrak{su}(2)$ gauge algebras carries n extra hypers in fundamental representation, where n is allowed to be a half-integer to account for half-hypers in fundamental. Choosing a particular $\Lambda \simeq \mathbb{Z}_2^g \subset \mathcal{L}$ corresponds to choosing all the gauge groups to be simply connected. The 1-form symmetry is predicted to be $\widehat{\Lambda} \simeq \mathbb{Z}_2^g$ for this choice, which can be verified easily from the 4d gauge theory description. A $\mathbb{Z}_2$ factor arises as the subgroup of the center of each $\mathrm{Spin}(n)$ (where $n = 3, 4$) gauge group that leaves the vector rep of $\mathrm{Spin}(n)$ invariant.

Example and Comparison with 6d $(1,0)$ on T^2: The last class of example has an alternative realization in terms of a 6d $(1,0)$ on T^2 [169, 170]: For $g = 1$ and $n = 2$ the A_1 theory on $\mathcal{C}_{1,2}$ has defect group $\mathcal{L} = \mathbb{Z}_2 \times \mathbb{Z}_2$. We can alternatively think of this as the compactification of the 6d (1,0) theory that is the $SU(2) - SU(2)$ conformal matter theory of rank 2, i.e., 2 M5-branes probing $\mathbb{C}^2/\mathbb{Z}_2$. The 6d theory has a tensor branch geometry, which has two non-compact curves, with $SU(2)$ singularities, sandwiching a (-2)-curve, with $SU(2)$ gauge group. The defect group given by $\mathbb{Z}_2$, and the dimensional reduction of this on T^2, results in $\mathcal{L}_A = \mathcal{L}_B = \mathbb{Z}_2$. More generally, 2 M5-branes probing a $\mathbb{Z}_k$ singularity results in a 'hybrid' class S theory, where an A_1-trinion is glued to an A_{k-1} one (see (2.6) in [170]). The tensor branch-geometry changes simply to $SU(k)$ groups both on the non-compact curves as well as on the (-2)-curve, thus leaving the defect group, and the expected 1-form symmetry unchanged.

11.4   1-Form Symmetries from Type IIB Realization

11.4.1   Class S from Type IIB

Class S theories can also have a realization in terms of a dual, Type IIB compactification, using geometric field theory methods, developed for general $\mathcal{N} = 2$ theories, predating class S [171]. Type IIB on a canonical singularity gives rise to $\mathcal{N} = 2$ SCFTs, and more generally can provide a way to engineer gauge theories. The Calabi-Yau X geometries that realize class S theories, can be constructed as ALE-fibrations over a curve

$$\widetilde{\mathbb{C}^2/\Gamma_{\mathrm{ADE}}} \hookrightarrow X \to \mathcal{C}_{g,n} \,, \tag{11.28}$$

where the resolutions parametrized for the ALE-fiber are encoded in a Higgs field φ. The Higgs field φ is a meromorphic 1-form valued in the respective ADE Lie algebra $\mathfrak{g}$ and enters into a Higgs bundle [77, 172]. We consider the 6d $(2,0)$ theory of type ADE on $\mathcal{C}_{g,n}$, with the standard topological twist that retains $\mathcal{N} = 2$ supersymmetry in 4d, i.e., $SO(5) \to SU(2) \times U(1)_R$ and $SO(6) \to SO(4) \times U(1)_L$ twisting the $U(1)_L$ by combining it with the $U(1)_R$ R-symmetry transformation. The scalars give rise to the $(1,0)$ and $(0,1)$ forms φ and $\bar{\varphi}$. These define together with the gauge field components (along the curve) the Higgs bundle, satisfying the Hitchin equations when describing supersymmetric vacua. The spectral equation defines the SW curve inside the co-tangent bundle of $\mathcal{C}_{g,n}$

$$\det(\varphi - \lambda \, \mathrm{Id}) = 0 \,. \tag{11.29}$$

We assume that the Higgs bundle is diagonalizable, i.e., $\varphi = \mathrm{diag}(\lambda_1, \cdots, \lambda_r)$. The spectral data encodes a local Calabi-Yau, which defines an ALE-fibration over C. Each sheet is labeled by a fundamental weight of $\mathfrak{g}$. For simplicity let us focus on the A_{N-1} case. There are N sheets, associated to the L_i, $i = 1, \cdots, N$ fundamental weights, with the simple roots realized as $\alpha_i = L_i - L_{i+1}$. The Higgs field eigenvalues λ_i encode the volumes of the rational curve in the ALE-fibration, where each simple root is associated to a rational curve $\mathbb{P}^1_i$, whose volume is determined by

$$\int_{\mathbb{P}^1_i} \Omega = \lambda_i - \lambda_{i+1} \,. \tag{11.30}$$

When $\lambda_i = 0$ for all i, the full $SU(N)$ symmetry is restored. More precisely, the spectral curve allows us to construct three-cycles as follows: if b_α are the branch points of the spectral curve, where two sheets of the cover collide, we can construct an S^3 by considering the ALE-fiber over the line $\ell_{\alpha,\beta}$ connecting two branch-points in C. At each of the branch-points a 2-sphere collapses, and thus we obtain an S^3. These three-spheres are Lagrangian and give rise in IIB to the gauge fields in 4d. Other three-cycles with the topology of $S^2 \times S^1$ are obtained by considering the rational curves fibered over closed 1-cycles in the base.
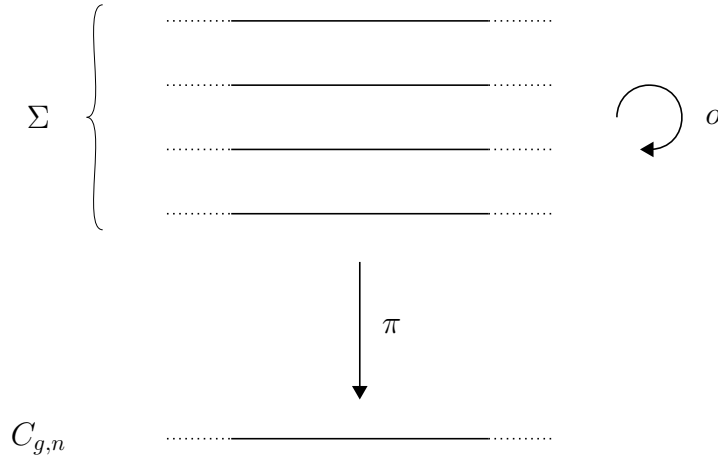
Figure 11.2: The outer automorphism (11.31) acting on the spectral cover.

Regular, untwisted punctures correspond to simple poles of φ. In the ALE-fibration, this maps to sending the volumes of (some) $\mathbb{P}^1$s to infinity. In class S regular, untwisted punctures are further labelled by a Young diagram [55], which is a pictorial representation of a partition of $N = \sum n_i h_i$. It is a finite collection of boxes with row lengths of non-increasing order. Listing the number of boxes in each row gives the partition where n_i is the multiplicity of the box of height h_i in the Young diagram. The flavor symmetry is $G_F = S(\prod_i U(n_i))$. E.g. the full punctures corresponding to the partition 1^N the flavor symmetry is $SU(N)$, corresponds to sending all N sheets to infinity with the same rate, parameterized by the residue of the pole of φ.

Open and closed twist lines alter the global structure of the ALE geometry. Open twist lines are inserted between punctures and closed twist lines are wrapped along a 1-cycle B of the base $\mathcal{C}$, both are labelled by an element o of the outer automorphism group. When encircling a puncture or traversing a 1-cycle intersecting B the Higgs field is acted on the by the outer automorphism o, see figure 11.2. In the ALE-fibration, rational curves $\mathbb{P}^1$ locally sweeping out distinct three-cycles are identified reducing the total number of 3-cycles in X. The Poincaré dual of these three-cycles are used to expand the supergravity four-form and construct the gauge bosons of the effective 4d theory. The gauge algebra of the theory is therefore determined by the initial choice of ADE gauge group and twist line structure.

Example: Consider the 6d $(2,0)$ A_{2n-1} theory compactified on the torus $\mathcal{C}_g = T^2$ with a closed b twist line along the B cycle. The spectral cover Σ is a $2n$-sheeted cover of the torus T^2. Each sheet can be thought of as associated to a fundamental weight L_i, $i = 1, \cdots, 2n$, and the outer automorphism acts as

$$o: \qquad L_i \longleftrightarrow -L_{2n+1-i}, \tag{11.31}$$

which induces an action on the simple roots $\alpha_i = L_i - L_{i+1} \leftrightarrow \alpha_{2n-i}$. The root α_n is fixed. There are n 3-cycles, one for each orbit of the outer automorphism on the $\mathbb{P}^1$ fibers which determine the root system of the 4d gauge algebra. These 3-cycles intersect linearly with the 3-cycle corresponding to the fixed $\mathbb{P}^1$ lying at the end of this chain. The root originating from this $\mathbb{P}^1$ is shorter than than the remaining $n-1$ roots and we find the roots system of type B_n. Overall we find the gauge group to reduce from $SU(2n)$ to $\mathrm{Spin}(2n+1)$ when introducing the twist line, the center of $\mathrm{Spin}(2n+1)$ is $\mathbb{Z}_2$.

11.4.2 Line operators from IIB

The line operators in this context are realized in terms of wrapped D3-branes, on non-compact three-cycles, modulo screening by particles, which are D3-branes wrapped on compact three-cycles. To study these, consider the analog arguments as in [58–60]. In relative homology, where ∂X is the boundary link 5-fold of the Calabi-Yau three-fold, the line operators are thereby realized in terms of

$$\mathcal{L} = \frac{H_3(X, \partial X, \mathbb{Z})}{H_3(X, \mathbb{Z})}. \tag{11.32}$$

Chasing this through the long exact sequence in relative homology,

$$\cdots \longrightarrow H_3(X, \mathbb{Z}) \xrightarrow{q} H_3(X, \partial X, \mathbb{Z}) \xrightarrow{\partial} H_2(\partial X, \mathbb{Z}) \xrightarrow{\iota} H_2(X, \mathbb{Z}) \longrightarrow \cdots, \tag{11.33}$$

we find that

$$\mathcal{L} = \frac{H_3(X, \partial X, \mathbb{Z})}{H_3(X, \mathbb{Z})} = \frac{H_3(X, \partial X, \mathbb{Z})}{\mathrm{Im}(q)} = \mathrm{Im}(\partial) = \mathrm{Ker}(\iota). \tag{11.34}$$

In particular we can write it as

$$\mathcal{L} = \{\ell \in H_2(\partial X, \mathbb{Z}) | \; \ell \text{ is a 2-cycle in } \partial X \text{ which becomes trivial in } X\}. \tag{11.35}$$

The pairing on $\mathcal{L}$ governing the mutual non-locality of 4d line operators descends straightforwardly from the linking pairing on $H_2(\partial X, \mathbb{Z})$.

The boundary ∂X receives contributions B_F and B_k from the fibers and punctures respectively

$$\partial X_{C_{g,n}} = B_F \cup \bigcup_{k=1}^{n} B_k\,, \tag{11.36}$$

where the topology of B_k is given by

$$\widetilde{\mathbb{C}^2/\Gamma_{\text{ADE}}} \; \hookrightarrow \; B_k \; \rightarrow \; S^1\,, \tag{11.37}$$

and the topology of B_F is given by

$$S^3/\Gamma_{\text{ADE}} \; \hookrightarrow \; B_F \; \rightarrow \; \mathcal{C}_{g,n}\,. \tag{11.38}$$

The contribution of (11.38) part of $\partial X_{\mathcal{C}_{g,n}}$ to $H_2(\partial X_{\mathcal{C}_{g,n}}, \mathbb{Z})$ is obtained by choosing an element $\alpha \in H_1(S^3/\Gamma_{\text{ADE}})$, which is then fibered over a loop L in $\mathcal{C}_{g,n}$. We have

$$H_1(S^3/\Gamma_{\text{ADE}}, \mathbb{Z}) \simeq \widehat{Z}(\mathcal{G})\,, \tag{11.39}$$

where $\mathcal{G}$ is the simply connected Lie group associated to the ADE Lie algebra $\mathfrak{g}$ associated to Γ_{ADE}. Moreover, an outer-automorphism of $\mathfrak{g}$ acts on $H_1(S^3/\Gamma_{\text{ADE}}, \mathbb{Z})$ in precisely the same way as it acts on $\widehat{Z}(\mathcal{G})$. When the loop L crosses an outer-automorphism twist line o, α is transformed to $o \cdot \alpha$. Moreover, any such element $(\alpha, L) \in H_2(B_F, \mathbb{Z}) \subset H_2(\partial X, \mathbb{Z})$ is clearly trivial, when embedded into X since α is contractible when embedded into $\mathbb{C}^2/\Gamma_{\text{ADE}}$. Thus, contributions of type (α, L) give rise to a non-trivial subgroup

$$\mathcal{L}_F \subseteq \mathcal{L}\,, \tag{11.40}$$
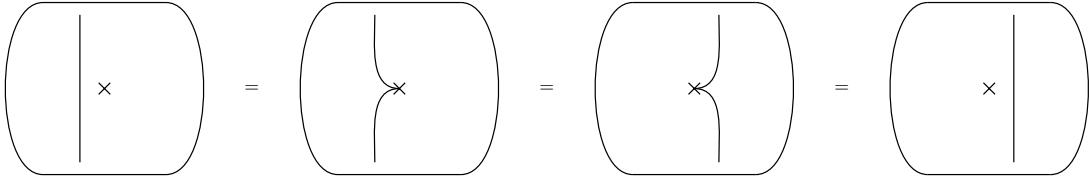
where $\mathcal{L}$ is defined in (11.35).

Figure 11.3: Consider an untwisted regular puncture and a boundary cycle $(L, \alpha) \in H_2(B_F, \mathbb{Z})$, with $\alpha \in H_1(S^3/\Gamma_{\mathrm{ADE}})$. We illustrate how the untwisted puncture does not affect this contribution to the defect group. Left: A line L, associated to (L, α). Right: A line L' associated to (L', α). Center-left: Limiting configuration as L is moved towards an untwisted regular puncture. Center-right: Limiting configuration as L' is moved towards the puncture.

Now, notice that the above contributions of the kind (α, L) are precisely the contributions we have been considering throughout the paper. Let us label the group of line operators obtained using the earlier considerations in the paper as $\mathcal{L}_0$. Then we clearly have

$$\mathcal{L}_0 \subseteq \mathcal{L}_F. \tag{11.41}$$

Thus, the only way for our previous calculation $\mathcal{L}_0$ and the Type IIB calculation $\mathcal{L}$ to match is if

$$\mathcal{L}_0 = \mathcal{L}_F = \mathcal{L}. \tag{11.42}$$

In the rest of this subsection, we justify this equality.

First thing we need to show is that the contribution of all boundary components B_k to $\mathcal{L}$ is trivial. Indeed, the only 2-cycles in B_k are the exceptional $\mathbb{P}^1$s in $\widetilde{\mathbb{C}^2/\Gamma_{\mathrm{ADE}}}$, but none of these 2-cycles is trivial when embedded into X, and hence do not contribute to $\mathcal{L}$.

Next, we need to show that (L, α) and (L', α) give rise to the same element in $H_2(\partial X, \mathbb{Z})$ if L' is obtained from L by passing it over an untwisted regular puncture. Consider the limiting configuration of L approaching an untwisted regular puncture k, say from the left in figure 11.3. We hit the boundary component B_k at a particular point $p \in S^1$. The fiber component α embeds into the fiber $\left(\widetilde{\mathbb{C}^2/\Gamma_{\mathrm{ADE}}}\right)_p$ of B_k at p via the inclusion map

$$\iota_p: \qquad S^3/\Gamma_{\mathrm{ADE}} \hookrightarrow \left(\widetilde{\mathbb{C}^2/\Gamma_{\mathrm{ADE}}}\right)_p. \tag{11.43}$$
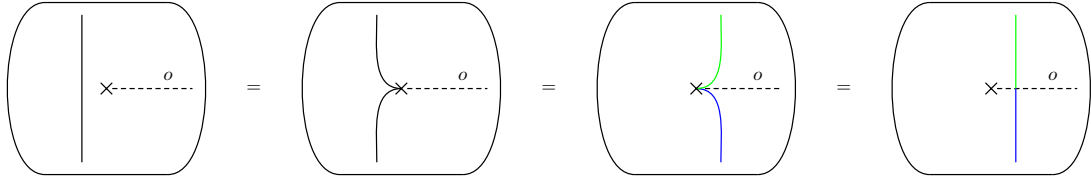
Figure 11.4: Consider again $(L, \alpha), (L', \alpha) \in H_2(B_F, \mathbb{Z})$ with $\alpha \in H_1(S^3/\Gamma_{\text{ADE}})$. Left: A line L associated to (L, α). Right: A line L' associated to (L', α) along the blue subsegment and $o \cdot \alpha$ along the green subsegment. Center-left: Limiting configuration as L is moved towards an untwisted regular puncture. Center-right: Limiting configuration as L' is moved towards the puncture. The central equality only holds for $\alpha = o \cdot \alpha$.

Similarly, the limiting configuration of L' approaching an untwisted regular puncture k, say from the right in figure 11.3, hits the boundary component B_k at a particular point $p' \in S^1$. The fiber component α embeds into the fiber $\left(\widetilde{\mathbb{C}^2/\Gamma_{\text{ADE}}}\right)_{p'}$ of B_k at p' via the inclusion map described above. Since the two embeddings of α into $\left(\widetilde{\mathbb{C}^2/\Gamma_{\text{ADE}}}\right)_p$ and $\left(\widetilde{\mathbb{C}^2/\Gamma_{\text{ADE}}}\right)_{p'}$ respectively are homotopic to each other, we deduce that $(L, \alpha) = (L', \alpha)$ as elements of $H_2(\partial X, \mathbb{Z})$.

Finally, we need to show that (L, α) and (L', α) give rise to the same element in $H_2(\partial X, \mathbb{Z})$ if L' is obtained from L by passing it over an twisted regular puncture, as long as α is left invariant by the action of the outer-automorphism associated to the twist line emanating from the twisted regular puncture. The argument proceeds exactly as in the untwisted case since the twist line is immaterial if α is left invariant by the corresponding outer-automorphism action. On the other hand, if α is not left invariant by the outer-automorphism, then L' needs to be divided into two sub-rays (denoted by blue and green respectively in figure 11.4) with α inserted along the blue sub-ray and $o \cdot \alpha$ inserted along the green sub-ray. In particular, there is no consistent limiting configuration as L' approaches the puncture, and the above argument fails. Thus, L and L' give rise to different elements of $H_2(\partial X, \mathbb{Z})$ (and hence $\mathcal{L}$) if α is acted upon by the twist line emanating from the regular puncture.

The above argument can be viewed as a justification of our key assumption used in the earlier parts of the paper: If L is a loop surrounding a regular (untwisted or twisted) puncture

carrying an element $\alpha \in \widehat{Z}(\mathcal{G})$ left invariant by the twist line emanating from the puncture, then such a loop is trivial in $\mathcal{L}$. As an alternative approach one might consider arguing that closing an untwisted regular puncture does not change the defect group. It would be interesting to develop this point of view. Here we note, that in the geometric descriptions one could argue as follows: regular punctures characterize base points at which fibral $\mathbb{P}^1$'s both decompactify and potentially braid when approaching the puncture. For line operators the decompactification of cycles is immaterial. We can therefore rescale Higgs field with a factor of the base coordinate z preserving the braiding structure. This completely removes regular punctures. In other words, regular punctures can be filled in from the perspective of line operators and do not contribute to the defect group. It would be interesting to develop the precise dictionary, and to expand it to include irregular punctures.

Generically the above procedure can be applied to any canonical singularity. E.g. even in the case of general irregular punctures, which realize Argyres Douglas theories, that do not necessarily admit a Lagrangian description. The theories of type $\mathrm{AD}[G, G']$ have a realization in terms of Type IIB on a canonical singularity and for $\mathrm{AD}[G, G']$ theories, the 1-form symmetries are non-trivial only for $G = A_N$ with $N > 1$ and $G' = D, E$ type, see [59, 60]. These results should provide further insights into computing the one-form symmetry for irregular punctures more generally.

Chapter 12
Appetizer: Confinement in $\mathfrak{su}(2)$ $\mathcal{N} = 1$ SYM Theory

In this section, we discuss confinement in $\mathcal{N} = 1$ pure super-Yang-Mills (SYM) theories with gauge algebra $\mathfrak{su}(2)$. As we review in section 12.1, there are three such theories: one with gauge group $SU(2)$ and two with gauge group $SO(3)$. The two theories with gauge group $SO(3)$ are distinguished by a discrete theta parameter, and correspondingly are referred to as $SO(3)_+$ and $SO(3)_-$ theories. All these theories have two massive vacua. Both of these

vacua are confining for the $SU(2)$ theory, while only one of them is confining for the $SO(3)_\pm$ theories.

In section 12.2, we discuss a construction of these 4d $\mathcal{N} = 1$ theories involving compactification of the 6d A_1 $\mathcal{N} = (2, 0)$ theory. The construction involves transitioning through 4d $\mathcal{N} = 2$ pure SYM theories with gauge algebra $\mathfrak{su}(2)$. Compactifying the 6d theory on a sphere with two irregular punctures provides a Class S construction for these 4d $\mathcal{N} = 2$ theories. One can then further "rotate" one of the punctures to softly break $\mathcal{N} = 2$ supersymmetry to $\mathcal{N} = 1$. Field theoretically, this corresponds to adding a small superpotential proportional to the Coulomb branch (CB) parameter u to the 4d $\mathcal{N} = 2$ theories (viewed as $\mathcal{N} = 1$ theories). As is well-known, all the CB vacua are lifted under this deformation, except the monopole and dyon points, giving rise to two massive vacua. As the rotation parameter is taken to infinity, these theories reduce to the pure $\mathfrak{su}(2)$ $\mathcal{N} = 1$ SYM theories, with the above two vacua being identified as the vacua of the pure $\mathcal{N} = 1$ theories.

We then proceed in section 12.3 to explain the above field theory results about confinement from the point of view of this compactification and properties of the 6d $\mathcal{N} = (2, 0)$ theory.

12.1   Result from Field Theory

In this subsection, we review the discussion in [133, 173] about confinement in pure $\mathfrak{su}(2)$ $\mathcal{N} = 1$ SYM theories. A massive vacuum is called confining if a non-trivial subgroup of the 1-form symmetry group of the theory is left *unbroken* in that vacuum [57]. Thus we need to study the 1-form symmetry group in the $SU(2), SO(3)_\pm$ versions of the theory, and its spontaneous breaking in each of the two vacua.

The 1-form symmetry group acts on the line operators in the theory. For pure $\mathfrak{su}(2)$ gauge theories, the set $\mathcal{L}$ of line operators modulo screenings forms a group

$$\mathcal{L} \simeq \mathbb{Z}_2 \times \mathbb{Z}_2 \tag{12.1}$$

under fusion. The two $\mathbb{Z}_2$ factors are generated by a fundamental Wilson line W and a 't Hooft line H, with their sum $W + H$ (the sum operation represents fusion) being a dyonic Wilson-'t Hooft line operator.

These line operators are not all mutually local with respect to the Dirac pairing. For example, if W is taken around H, or if H is taken around W, then the correlation function changes sign. This non-locality is captured in a $\mathbb{Z}_2$ valued pairing defined on $\mathcal{L}$ as follows

$$\langle W, W \rangle = 0$$

$$\langle H, H \rangle = 0 \tag{12.2}$$

$$\langle W, H \rangle = \frac{1}{2}\,.$$

The change in phase of a correlation function as an element $\alpha \in \mathcal{L}$ is taken around $\beta \in \mathcal{L}$ is then

$$\exp\big(2\pi i \langle \alpha, \beta \rangle\big)\,. \tag{12.3}$$

This means that not all the line operators in $\mathcal{L}$ are genuine line operators. If $\alpha, \beta \in \mathcal{L}$ are such that $\langle \alpha, \beta \rangle \neq 0$, then either α or β lives at the boundary of a topological surface operator which acts on the other line operator, and this action is responsible for producing the phase (12.3). Thus specifying a theory $\mathfrak{T}$ (also called as an "absolute" theory) specifies a maximal subgroup Λ of mutually commuting line operators in $\mathcal{L}$ which are genuine in $\mathfrak{T}$. The line operators in $\mathcal{L} - \Lambda$ are non-genuine line operators of $\mathfrak{T}$.

Consequently, a theory can only contain one out of W, H and $W + H$ in its spectrum of genuine line operators. Choosing W to lie in the spectrum gives rise to a pure 4d gauge theory with gauge group $SU(2)$. On the other hand, choosing H or $W + H$ give rise to pure 4d gauge theories with gauge group $SO(3)$. The two $SO(3)$ theories are differentiated by a discrete theta parameter[1]. The theory containing H is called the $SO(3)_+$ theory and the theory containing $W + H$ is called the $SO(3)_-$ theory.

---

[1]The $SO(3)_+$ theory is obtained from the $SU(2)$ theory by gauging its $\mathbb{Z}_2$ 1-form symmetry, while the $SO(3)_-$ theory is obtained by gauging the diagonal $\mathbb{Z}_2$ 1-form symmetry of the $SU(2)$ theory stacked with an SPT phase for the $\mathbb{Z}_2$ 1-form symmetry. After gauging, the SPT phase is understood as a discrete theta-like parameter which when added to the Lagrangian of the $SO(3)_+$ theory leads to the $SO(3)_-$ theory and vice versa. The above construction in terms of the $SU(2)$ theory allows us to call the $SO(3)_+$ theory as the theory with discrete theta parameter "turned off", and the $SO(3)_-$ theory as the theory with discrete theta parameter "turned on".

The 1-form symmetry in each of these three theories is $\mathbb{Z}_2$. The charged operator is the non-trivial element of $\mathcal{L}$ lying in the spectrum of genuine line operators of the theory. Notice, for future purposes, that the above analysis regarding $\mathcal{L}$, different global forms of the gauge group, discrete theta parameters and 1-form symmetry is independent of the amount of supersymmetry. In particular, it applies equally well to pure 4d $\mathfrak{su}(2)$ SYM theories with $\mathcal{N} = 1$ and $\mathcal{N} = 2$ supersymmetry.

To probe confinement in 4d $\mathfrak{su}(2)$ pure $\mathcal{N} = 1$ SYM theories, we realize them as deformations of 4d $\mathfrak{su}(2)$ pure $\mathcal{N} = 2$ SYM theories. Let us deform the $\mathcal{N} = 2$ theory by a superpotential $\mu \text{Tr} \phi^2$ where μ is a mass parameter and ϕ is an $\mathcal{N} = 1$ adjoint chiral superfield inside the $\mathcal{N} = 2$ vector multiplet. For $\mu \ll \Lambda_{\mathcal{N}=2}$ the superpotential is represented as μU where U is an $\mathcal{N} = 1$ chiral superfield whose scalar component corresponds to the CB modulus u. It is well-known [174] that this superpotential lifts the entire CB except for the monopole and dyon points, and thus the theory has two massive vacua, which we refer to as the monopole vacuum and the dyon vacuum respectively. The superpotential leads to condensation of monopoles at the monopole point and the condensation of dyons (whose charges align with $W + H$) at the dyon point. This has the following consequence for confinement in the three theories:

- For the $SU(2)$ theory, since the charge of the chosen line operator W does not align with the charges of condensing monopoles or dyons, W exhibits area law in both vacua. Hence, both vacua are confining and preserve the $\mathbb{Z}_2$ 1-form symmetry.

- For the $SO(3)_+$ theory in the monopole vacuum, the charge of the chosen line operator H aligns with the charge of condensing monopoles, and hence H exhibits perimeter law in the monopole vacuum. On the other hand, the charge of H does not align with the charge of condensing dyons in the dyon vacuum, and hence H exhibits area law in the dyon vacuum. Thus, the monopole vacuum is not confining and spontaneously breaks the $\mathbb{Z}_2$ 1-form symmetry, while the dyon vacuum is confining and preserves the $\mathbb{Z}_2$ 1-form symmetry.

- For the $SO(3)_-$ theory in the dyon vacuum, the charge of the chosen line operator $W+H$ aligns with the charge of condensing dyons, and hence $W+H$ exhibits perimeter law in the dyon vacuum. On the other hand, the charge of $W+H$ does not align with the charge of condensing monopoles in the monopole vacuum, and hence $W + H$ exhibits area law in the monopole vacuum. Thus, the dyon vacuum is not confining and spontaneously breaks the $\mathbb{Z}_2$ 1-form symmetry, while the monopole vacuum is confining and preserves the $\mathbb{Z}_2$ 1-form symmetry.

In a confining vacuum there are massive confining strings which are charged under the 1-form symmetry, while in a non-confining vacuum there are no such strings.

For $\mu \gg \Lambda_{\mathcal{N}=2}$ we can rely on the UV description of the $\mathcal{N} = 2$ theory to integrate out Φ thus leading to the pure $\mathcal{N} = 1$ SYM theory at low-energies, which is expected to admit two massive vacua. This ties in neatly with the two vacua found for $\mu \ll \Lambda_{\mathcal{N}=2}$ and suggests that there is no phase transition as we vary $\mu/\Lambda_{\mathcal{N}=2}$. Moreover, we are lead to the prediction that both the vacua of the $SU(2)$ pure $\mathcal{N} = 1$ SYM are confining, while for the $SO(3)_{\pm}$ pure $\mathcal{N} = 1$ SYM only one of the vacua is confining.

12.2 Construction from 6d A_1 $\mathcal{N} = (2,0)$ Theory

The pure $\mathcal{N} = 2$ theory admits a Hanany-Witten type brane construction in terms of NS5 and D4 branes in Type IIA superstring theory [8, 175], which is shown in figure 12.1. This allows us to read off the Seiberg-Witten curve (SW curve) of the theory

$$v^2 = \frac{\Lambda^2}{t} + u + \Lambda^2 t, \tag{12.4}$$

where we have used the notation of [175] and we have shortened $\Lambda_{\mathcal{N}=2}$ used in the previous subsection to Λ.

Now, following [55, 77], one can use the above SW curve to phrase the construction of the pure $\mathcal{N} = 2$ theory as a compactification of 6d A_1 $\mathcal{N} = (2,0)$ superconformal field theory (SCFT). The $(2,0)$ theory contains a chiral operator[2] that we denote as $\mathrm{Tr}\Phi^2$ which

---

[2]It should be noted that while $\mathrm{Tr}\Phi^2$ is a genuine local operator in the 6d theory, Φ is not.
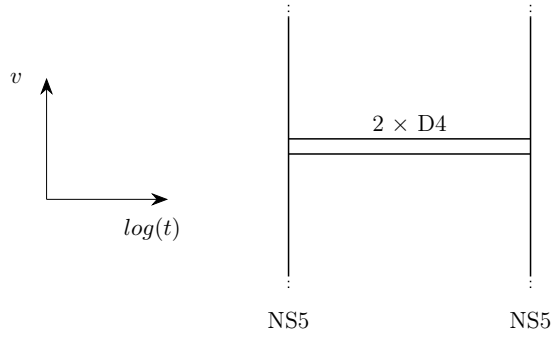
Figure 12.1: The Hanany-Witten setup realizing in Type IIA string theory the pure $\mathcal{N} = 2$ $\mathfrak{su}(2)$ SYM theories.

transforms in an irreducible representation of the $\mathfrak{so}(5)_R$ symmetry. Vevs of this chiral operator parametrize the moduli space of supersymmetric vacua of the $(2,0)$ theory.

To construct the pure 4d $\mathcal{N} = 2$ theory, we need to compactify the A_1 $(2,0)$ theory on a sphere $\mathcal{C}$ with two punctures whose coordinate is t and the punctures are located at $t = 0, \infty$. $\mathcal{C}$ is the UV curve for this Class S construction. We need to perform a topological twist along $\mathcal{C}$ which decomposes $\mathfrak{so}(5)_R \to \mathfrak{so}(3)_R \oplus \mathfrak{so}(2)_R$ and identifies $\mathfrak{so}(2)_R$ with the $\mathfrak{so}(2)$ holonomy group of $\mathcal{C}$, while identifying $\mathfrak{so}(3)_R$ as the R-symmetry of the descendant 4d $\mathcal{N} = 2$ theory. This decomposes $\mathrm{Tr}\Phi^2$ into various operators, out of which we single out an operator $\mathrm{Tr}\phi^2$ which is charged only under the $\mathfrak{so}(2)_R$ subalgebra of $\mathfrak{so}(5)_R$ and transforms as a quadratic differential on $\mathcal{C}$ due to the twist. The vevs

$$\phi_2 := \langle \mathrm{Tr}\phi^2 \rangle \tag{12.5}$$

are quadratic meromorphic differentials on $\mathcal{C}$ and parametrize the CB of the resulting 4d $\mathcal{N} = 2$ theory. To fully specify the space of $\phi_2(t)$, we need to specify their behavior at the punctures $t = 0, \infty$. This can be read off by identifying the SW curve as

$$\phi_2 = \frac{v^2}{t^2} dt^2 = \left(\frac{\Lambda^2}{t^3} + \frac{u}{t^2} + \frac{\Lambda^2}{t} \right) dt^2 \,, \tag{12.6}$$

from which follows that ϕ_2 has poles of order 3 at both punctures. The corresponding Higgs field ϕ has a pole of order $\frac{3}{2}$ at each puncture. Since this is higher-order singularity than a simple pole of order 1, it is called as an *irregular* singularity of the Higgs field. Thus, the 4d
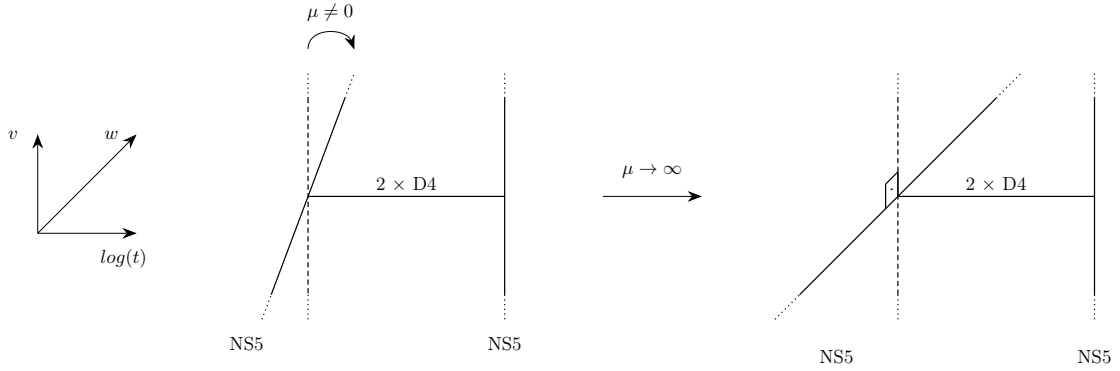
Figure 12.2: Rotation of the branes in the Hanany-Witten setup, which results in breaking $\mathcal{N} = 2$ to $\mathcal{N} = 1$ supersymmetry. Again we show the construction for $\mathfrak{su}(2)$ pure SYM.

pure $\mathfrak{su}(2)$ $\mathcal{N} = 2$ SYM is constructed by compactifying the 6d A_1 $(2,0)$ theory on a sphere with two irregular punctures where the Higgs field has a pole of order $\frac{3}{2}$ at each puncture.

Now, to reach the 4d $\mathcal{N} = 1$ SYM theory, we would like to deform the 4d $\mathcal{N} = 2$ SYM theory by the superpotential discussed in the previous subsection. In the Type IIA brane construction, this corresponds to rotating one of the NS5 branes in two of the transverse directions denoted by a complex coordinate w [52, 138, 176]. The $\mu \to \infty$ limit which leads to the 4d $\mathcal{N} = 1$ SYM theory is obtained when the NS5 brane has been completely rotated. See figure 12.2.

To achieve this deformation from the point of view of the 6d A_1 $(2,0)$ theory, we start by choosing an $\mathfrak{so}(2)_w$ inside $\mathfrak{so}(3)_R$ which corresponds to choosing an operator $\mathrm{Tr}\varphi^2$ inside $\mathrm{Tr}\Phi^2$ which is charged only under $\mathfrak{so}(2)_w$ subalgebra of $\mathfrak{so}(5)_R$. Then we turn on vevs

$$\varphi_2 := \langle \mathrm{Tr}\varphi^2 \rangle \,, \tag{12.7}$$

which are meromorphic functions on $\mathcal{C}$. Since $\mathrm{Tr}\varphi^2$ is charged under $\mathfrak{so}(3)_R$, its vevs break the $\mathcal{N} = 2$ R-symmetry in 4d, and hence the resulting theory only has 4d $\mathcal{N} = 1$ supersymmetry. The asymptotic values of the Higgs field[3] φ are

$$\begin{aligned} \varphi &\sim \mu V \quad \text{as } t \to \infty \\ \varphi &\sim c \qquad \text{as } t \to 0 \end{aligned}, \tag{12.8}$$

---

[3]Notice that the Higgs field φ is a function on $\mathcal{C}$, while the Higgs field ϕ is a 1-form.

where c is a constant and V is a Higgs field defined via

$$V \frac{dt}{t} = \phi \,.$$ (12.9)

Thus φ has a singularity only at $t = \infty$ but not at $t = 0$, which encodes the fact that we are "rotating" the puncture at $t = \infty$ but not the puncture at $t = 0$.

Turning on vevs for $\mathrm{Tr}\phi^2$ and $\mathrm{Tr}\varphi^2$ also turns on vevs for operator $\mathrm{Tr}\phi\varphi$ sitting inside $\mathrm{Tr}\Phi^2$, which is charged under both $\mathfrak{so}(2)_R$ and $\mathfrak{so}(2)_w$. The vevs

$$(\phi\varphi)_2 := \langle \mathrm{Tr}\phi\varphi \rangle$$ (12.10)

are meromorphic 1-forms on $\mathcal{C}$ due to the topological twist.

The SW curve can now be transformed to an "$\mathcal{N} = 1$ curve" specified by

$$\begin{aligned} v^2 \frac{dt^2}{t^2} &= \phi_2 \\ w^2 &= \varphi_2 \\ vw \frac{dt}{t} &= (\phi\varphi)_2 \end{aligned}$$ (12.11)

with $(t, v, w) \in \mathbb{C}^* \times \mathbb{C} \times \mathbb{C}$, which is a 2-fold cover of the UV curve $\mathcal{C}$. In particular, the last equation in the above set of equations combines the double covers associated to v and w into a single double cover. This equation can be imposed because ϕ and φ are simultaneously diagonalizable and hence $\mathrm{Tr}(\phi\varphi)$ defines a consistent profile for $vw\frac{dt}{t}$.

It turns out that the set of equations (12.11) is consistent only for two values of the CB parameter u [136]. To see this, we first write down the most general form of w^2 compatible with the boundary condition (12.8)

$$w^2 = \mu^2 \Lambda^2 t + c \,.$$ (12.12)

Now the well-defined-ness of vw requires us to impose that the product of (12.4) and (12.12) is a perfect square, that is

$$v^2 w^2 = \frac{\left(\Lambda^2 t^2 + ut + \Lambda^2\right)\left(\mu^2 \Lambda^2 t + c\right)}{t} = \frac{P^2(t)}{Q^2(t)} \,.$$ (12.13)
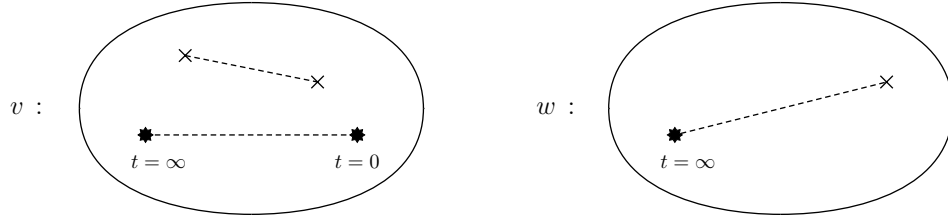
Figure 12.3: The figure displays the sheet structures of v-curve and w-curve over the UV curve $\mathcal{C}$ with the coordinate t. A star denotes a singular point where the corresponding curve escapes to infinity, $\times$ denotes a non-singular branch-point, and the dashed lines denote branch cuts.

Keeping Λ fixed, the only way to achieve the perfect square condition is by requiring

$$c = 0$$
$$u = \pm 2\Lambda^2$$

$$(12.14)$$

Thus, we rediscover that after a rotation only two vacua survive, which are the monopole and the dyon points in the $\mathcal{N} = 2$ CB. The $\mathcal{N} = 1$ curves for these two vacua are

$$v^2 = \Lambda^2 \left(\frac{1}{t} \pm 2 + t \right)$$
$$w^2 = \mu^2 \Lambda^2 t$$
$$vw = \mu \Lambda^2 (t \pm 1)$$

$$(12.15)$$

The perfect square condition, which is equivalent to vw being well-defined, can be understood in a more topological/group-theoretical way that will be very useful for further generalizations in later chapters. If we only consider (12.4) and (12.12), we find that in general there are 4 values of (v, w) associated to a fixed value of t. That is, we are describing two separate double covers v, w of the UV curve $\mathcal{C}$ parametrized by t. Instead, we would like to combine these two double covers into a single double cover of $\mathcal{C}$, and the combined curve is the $\mathcal{N} = 1$ curve we are after. We can represent the sheet structures of the two double covers (12.4) and (12.12) in terms of branch points and the branch lines (i.e., branch cuts) joining them, as shown in figure 12.3.

To combine these two double covers, we need to move the branch points and potentially collide them such that the resulting branch structure of the two double covers is the same. One such possible movement of branch points is shown in figure 12.4. From the point of
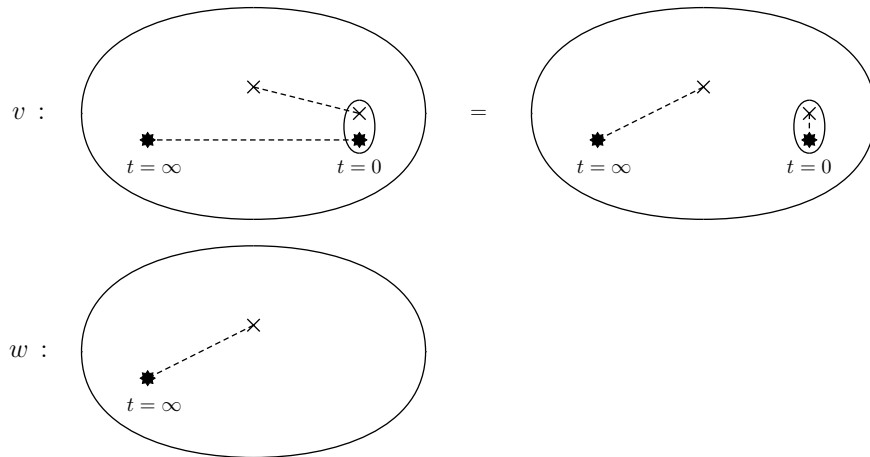
Figure 12.4: A possible movement and collision of branch points that ensures that the branch structures of v and w curves coincide. However, as explained in the text, this branch structure is not possible.
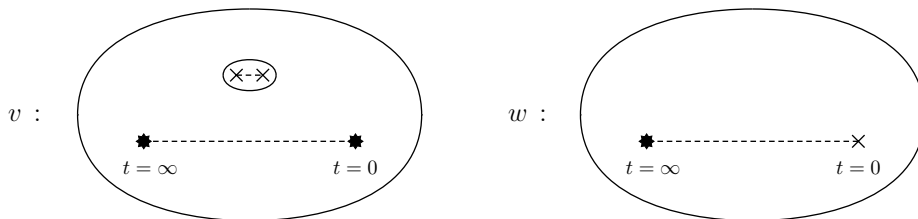

Figure 12.5: A possible movement and collision of branch points that ensures that the branch structures of v and w curves coincide. This configuration gives rise to a consistent $\mathcal{N} = 1$ curve.

view of (12.4), this movement requires that $t = 0$ is a root of $\Lambda^2 t^2 + ut + \Lambda^2$ which is not possible for a fixed Λ, and requires us to change our starting $\mathcal{N} = 2$ theory. Thus, we reject this movement of branch points.

However, there is another possible movement of the branch points which results in the same branch structure for the two double covers. See figure 12.5. From the point of view of (12.4), this movement requires colliding the two branch points of $\Lambda^2 t^2 + ut + \Lambda^2$; and from the point of view of (12.12), this movement requires sending the branch point of (12.12) located at finite t to be moved to $t = 0$. Thus, this movement enforces precisely the conditions (12.14) which lead to the $\mathcal{N} = 1$ curve (12.15).

Now, even though both the $\mathcal{N} = 1$ curves (12.15) have the same structure of branch points, they have different structure of branch lines. This can be seen easily by analyzing
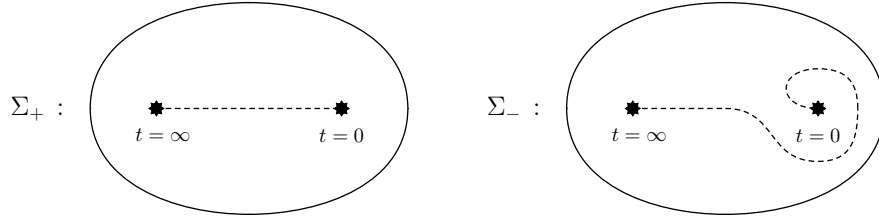
Figure 12.6: Branch-cut structure for the two $\mathcal{N} = 1$ curves for $\mathfrak{su}(2)$ SYM. The figures show the projections of the $\mathcal{N} = 1$ curves onto the UV curve (parametrized by t). The right hand figure is related to the left by a Dehn twist. These two curves characterize the two vacua of the theory.

the behavior of vw as $t \to 0$. In this limit we can write

$$vw = \pm \mu \Lambda^2 \,. \tag{12.16}$$

So, for a fixed asymptotic value of v, the two curves have asymptotic values of w having

opposite signs. From the equation $w^2 = \mu^2 \Lambda^2 t$, we see that we can change the sign of

asymptotic value of w by encircling once the $t = 0$ point. Thus, the branch cuts of the two

$\mathcal{N} = 1$ curves (seen as double covers of $\mathcal{C}$) are related by a Dehn twist around the puncture

at $t = 0$. If we choose to represent the branch cut for the $\mathcal{N} = 1$ curve (12.15) with plus

sign as in the left side of figure 12.6, then the branch cut for the $\mathcal{N} = 1$ curve (12.15) with

minus sign is as shown on the right side of figure 12.6.

Taking an appropriate $\mu \to \infty$ limit of (12.15) leads to $\mathcal{N} = 1$ curves for the two vacua

of pure $\mathfrak{su}(2)$ $\mathcal{N} = 1$ SYM [138]. Under this limit, the following quantities are kept fixed

$$\Lambda^3_{\mathcal{N}=1} := \mu \Lambda^2$$
$$\widetilde{t} := \mu t \tag{12.17}$$

and after the limit we obtain the following $\mathcal{N} = 1$ curves

$$v^2 = \frac{\Lambda^3_{\mathcal{N}=1}}{\widetilde{t}}$$
$$w^2 = \Lambda^3_{\mathcal{N}=1} \widetilde{t} \cdot \tag{12.18}$$
$$vw = \pm \Lambda^3_{\mathcal{N}=1}$$

Notice that the structure of branch points and cuts of the above two $\mathcal{N} = 1$ curves (viewed

as double covers of the $\widetilde{t}$ plane) is exactly the same as in figure 12.6, i.e., the structure of

branch points and cuts is left unchanged in the $\mu \to \infty$ limit.

12.3 Confinement from the 6d Construction

In this subsection, we apply our results from [3], and first discuss how the group of line operators $\mathcal{L}$ (12.1) is encoded in the cycles on the UV curve $\mathcal{C}$. Different theories $SU(2)$ and $SO(3)_{\pm}$ correspond to different subgroups Λ of $\mathcal{L}$. The 1-form symmetry group is then identified with the Pontryagin dual $\widehat{\Lambda}$ of Λ. Let $\mathcal{I}_r \subseteq \mathcal{L}$ be defined as

$$\mathcal{I}_r = \{\text{projections of 1-cycles on the } \mathcal{N}=1 \text{ curve } \Sigma_r \text{ for vacuum } r \text{ onto } \mathcal{C}\}. \quad (12.19)$$

Then we propose that the 1-form symmetry group $\mathcal{O}_r$ preserved in the vacuum r can be identified with

$$\mathcal{O}_r = \left(\widehat{\frac{\Lambda}{\mathcal{I}_r|_\Lambda}}\right) \subseteq \widehat{\Lambda}. \quad (12.20)$$

where $\mathcal{I}_r|_\Lambda := \mathcal{I}_r \cap \Lambda$ and a hat on top of a group denotes the Pontryagin dual of that group. If $\mathcal{O}_r$ is trivial, then the vacuum r is not confining. On the other hand, if $\mathcal{O}_r$ is non-trivial then the vacuum r is confining.

The group $\mathcal{L}$ in the 4d $\mathcal{N}=2$ $\mathfrak{su}(2)$ SYM theory descends from a similar group $\widehat{Z} \simeq \mathbb{Z}_2$ formed by dimension-2 surface operators (modulo screenings) in the 6d A_1 $(2,0)$ theory. Let us denote the non-trivial element of $\widehat{Z}$ by f, which is non-local with itself

$$\langle f, f \rangle = \frac{1}{2}, \quad (12.21)$$

As proposed in [3], after compactifying on $\mathcal{C}$, the set $\mathcal{L}$ (12.1) descends from $\widehat{Z}$ as shown in figure 12.7. Compactifying f on the cycle W (which encircles both punctures) leads to the element named $W \in \mathcal{L}$, and compactifying f on the cycle H (which extends between the two punctures) leads to the element named $H \in \mathcal{L}$. The pairing (12.2) on $\mathcal{L}$ is obtained by combining the pairing (12.21) on $\widehat{Z}$ with the intersection pairing on $\mathcal{C}$.

As we discussed earlier, the various global forms of the gauge group are distinguished as follows, where $[W]$ denotes the subgroup generated by $W \in \mathcal{L}$, etc:

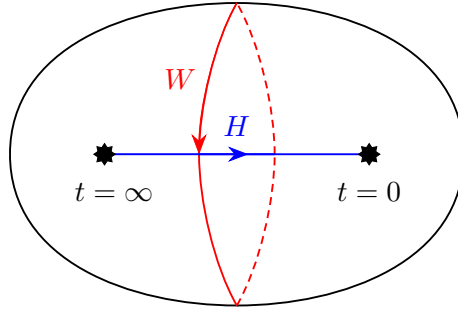- $SU(2)$ theory is obtained by choosing $\Lambda = [W] \subset \mathcal{L}$,

Figure 12.7: The Wilson (W, red) and 't Hooft (H, blue) lines in the Class S realization of the 4d $\mathcal{N} = 2$ $\mathfrak{su}(2)$ pure SYM theories.

- $SO(3)_+$ theory is obtained by choosing $\Lambda = [H] \subset \mathcal{L}$,

- $SO(3)_-$ theory is obtained by choosing $\Lambda = [W + H] \subset \mathcal{L}$.

As we deform the $\mathcal{N} = 2$ theory, the sets Λ and $\mathcal{L}$ remain same. That is, our encoding of Λ and $\mathcal{L}$ into the UV curve $\mathcal{C}$ should hold even after rotating one of the punctures. This should continue to hold even as we take the limit $\mu \to \infty$, with the role of $\mathcal{C}$ played by the $\widetilde{t}$-plane.

We can now study the subgroups $\mathcal{I}_r$ for the two vacua obtained after the deformation. For the vacuum $r = +$ with the plus sign in (12.15), this is encoded in the left side of figure 12.6 which depicts the projection of the corresponding $\mathcal{N} = 1$ curve Σ_+ onto $\mathcal{C}$. Because of the branch cut extending between the two punctures, one must go around a puncture twice to obtain a cycle on Σ_+. This cycle projects to $2W \equiv 0 \in \mathcal{L}$. Traveling from one puncture to the other along one side of the branch cut, we obtain another cycle on Σ_+ which projects to $H \in \mathcal{L}$. Thus, we find that

$$\mathcal{I}_+ = [H] . \tag{12.22}$$

For the vacuum $r = -$ with the minus sign in (12.15), $\mathcal{I}_-$ is encoded in the right side of figure 12.6 which depicts the projection of the corresponding $\mathcal{N} = 1$ curve Σ_- onto $\mathcal{C}$. Again, because of the branch cut, one must go around a puncture twice to obtain a cycle on Σ_- which projects to $2W \equiv 0 \in \mathcal{L}$. On the other hand, traveling from one puncture to the other along one side of the branch cut, now we obtain a cycle on Σ_- which projects to $W + H \in \mathcal{L}$.

Thus, we find that

$$\mathcal{I}_- = [W + H].\tag{12.23}$$

From these, we readily compute for the $SU(2)$ theory the 1-form symmetry that is preserved in each of the vacua is

$$\begin{aligned}\mathcal{O}_+ &\simeq \mathbb{Z}_2\\\mathcal{O}_- &\simeq \mathbb{Z}_2\end{aligned}.\tag{12.24}$$

That is, both vacua $r = \pm$ are confining for the $SU(2)$ theory. For the $SO(3)_+$ theory, we find

$$\begin{aligned}\mathcal{O}_+ &\simeq 0\\\mathcal{O}_- &\simeq \mathbb{Z}_2\end{aligned}.\tag{12.25}$$

That is, the monopole vacuum $r = +$ is not confining, while the dyon vacuum $r = -$ is confining. For the $SO(3)_-$ theory, we find

$$\begin{aligned}\mathcal{O}_+ &\simeq \mathbb{Z}_2\\\mathcal{O}_- &\simeq 0\end{aligned}.\tag{12.26}$$

That is, the monopole vacuum $r = +$ is confining, while the dyon vacuum $r = -$ is not confining. Thus, our proposal (12.20) recovers the field theory results discussed in section 12.1.

Since the branch structure (over the $\widetilde{t}$-plane) of the $\mathcal{N} = 1$ curves (12.18) in the $\mu \to \infty$ limit is also described by the figure 12.6, the above results about $\mathcal{O}_\pm$ remain the same even after the $\mu \to \infty$ limit.

Chapter 13
$\mathcal{N} = 1$ Hitchin Systems and Confinement

13.1 Confinement, 1-form Symmetries, and Relative and Absolute Theories

The vacua of distinct absolute theories agree and are thefore independent of the choice of polarization Λ and so the vacua can be associated to the relative 4d theory. A vacuum r of a relative theory divides line operators in $\mathcal{L}$ into two distinct sets: those showing perimeter

law and those showing area law. The subset of line operators exhibiting perimeter law form

a subgroup $\mathcal{I}_r \subseteq \mathcal{L}$. For an absolute QFT having (genuine) line operators specified by a

polarization Λ, the subgroup $\Lambda_r := \mathcal{I}_r \cap \Lambda \subseteq \Lambda$ of line operators show perimeter law. Then,

the vacuum r preserves a subgroup

$$\mathcal{O}_r := \widehat{\left(\frac{\Lambda}{\Lambda_r}\right)} \subseteq \widehat{\Lambda} \tag{13.1}$$

of the 1-form symmetry group $\widehat{\Lambda}$. If $\mathcal{O}_r$ is trivial, it is said that the vacuum r is not confining.

On the other hand, if $\mathcal{O}_r$ is non-trivial, the vacuum r is said to be *confining*. Moreover, if

$\mathcal{O}_r \simeq \mathbb{Z}_t$, then t is called the *confinement index* of the vacuum r [72, 177].

13.2 1-form Symmetry for A_{n-1} Class S Theories

The class of 4d theories we study in this thesis are related to 4d $\mathcal{N} = 2$ theories of Class S

obtained by compactifying 6d A_{n-1} $(2,0)$ SCFT on a punctured Riemann surface $\mathcal{C}_g$ of genus

g with arbitrary (untwisted) punctures but without any outer-automorphism twists. The

line operators $\mathcal{L}$ in this class of theories arise by wrapping dimension-2 surface operators

along 1-cycles of $\mathcal{C}_g$. For A_{n-1} $(2,0)$ theory, the dimension-2 surface operators modulo

screenings form a group $\widehat{Z} \simeq \mathbb{Z}_n$. The group $\widehat{Z}$ carries a non-trivial pairing $\langle \cdot, \cdot \rangle$ capturing

the non-locality between the dimension-2 surface operators. Choosing a generator $f \in \widehat{Z}$,

this pairing can be written as

$$\langle f, f \rangle = \frac{1}{n} . \tag{13.2}$$

Thus the $(2,0)$ theory is a relative QFT in the language of section 13.1. Its compactification

on $\mathcal{C}_g$ gives rise to a *relative* 4d $\mathcal{N} = 2$ Class S theory.

Apriori, the possible ways of wrapping dimension-2 operators along 1-cycles of $\mathcal{C}_g$ are

described by $H_1(\mathcal{C}_g, \widehat{Z}, *)$, which is the homology group of 1-cycles (with coefficients in

$\widehat{Z}$) that are allowed to end on punctures, indicated by $*$. See figure 13.1. On the other

hand, let $H_1(\mathcal{C}_g, \widehat{Z})$ denote the homology group of 1-cycles (with coefficients in $\widehat{Z}$) that do

not end on punctures. Clearly $H_1(\mathcal{C}_g, \widehat{Z}) \subseteq H_1(\mathcal{C}_g, \widehat{Z}, *)$. Now, it is not possible for all
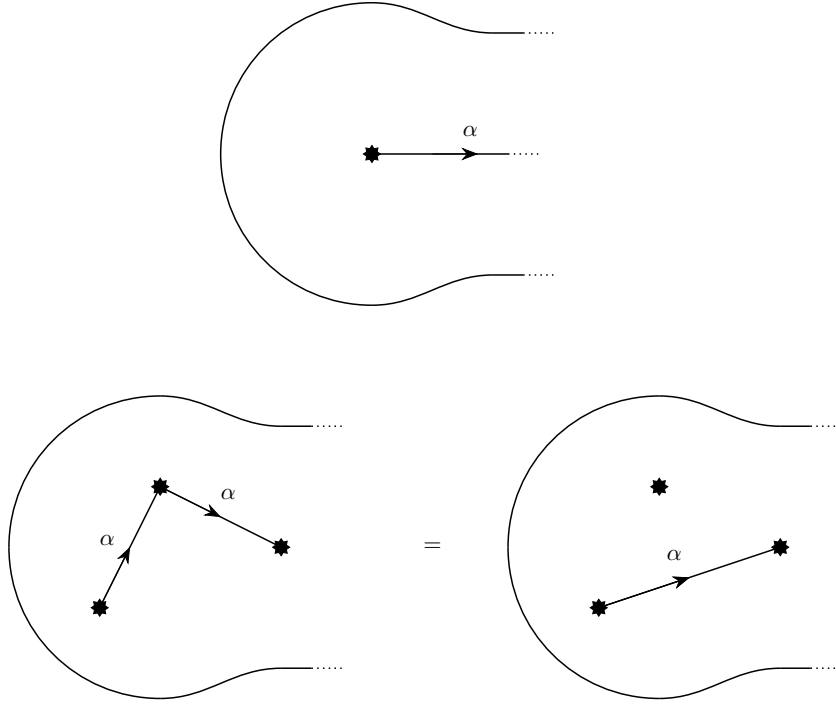
Figure 13.1: Top: The cycles in $H_1(\mathcal{C}_g, \widehat{Z}, *)$ are allowed to end on punctures. α denotes some element of $\widehat{Z}$. Bottom: Composition rule for cycles that end on punctures.

dimension-2 operators to end on every puncture. Given a specific puncture p of type $\mathcal{P}$, only a subgroup $Z_\mathcal{P} \subseteq \widehat{Z}$ of dimension-2 surface operators can end at p. So, let $\mathcal{S}$ be the subgroup of $H_1(\mathcal{C}_g, \widehat{Z}, *)$ such that the coefficient $\alpha \in \widehat{Z}$ associated to a 1-cycle in $\mathcal{S}$ ending at a puncture of type $\mathcal{P}$ is such that $\alpha \in Z_\mathcal{P}$. See figure 13.2. The physical interpretation of $\mathcal{S}$ is the subgroup of 1-cycles that can be wrapped by the dimension-2 operators.

$\mathcal{S}$ is not straightforwardly identified with the group $\mathcal{L}$ of 4d line operators, as $\mathcal{S}$ also captures flavor charges of 4d line operators but the flavor charges are not part of the data tracked by $\mathcal{L}$. The data of flavor charges is modded out by modding out certain elements of $\mathcal{S}$ resulting in a projection map

$$\pi : \qquad \mathcal{S} \to \mathcal{L} . \tag{13.3}$$

The elements of $\mathcal{S}$ that are modded are described as follows. Consider a 1-cycle L_p encircling a puncture p of type $\mathcal{P}$. Wrapping dimension-2 surface operators along L_p we generate a subgroup $\bar{Z}_p \simeq \widehat{Z}$ of $\mathcal{S}$. Then, depending on the type $\mathcal{P}$ of the puncture p, a subgroup
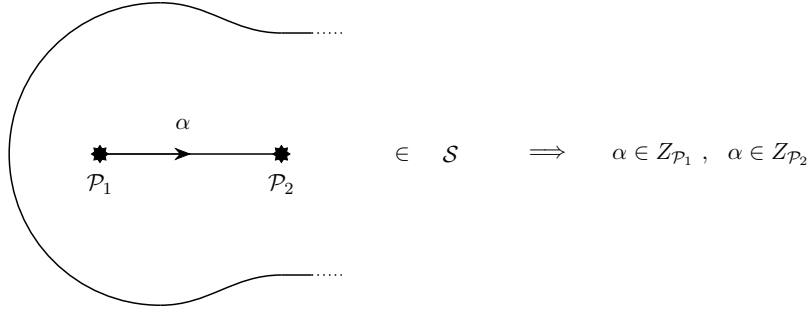
Figure 13.2:   If a 1-cycle in $\mathcal{S}$ carrying $\alpha \in \widehat{Z}$ ends on punctures of types $\mathcal{P}_1$ and $\mathcal{P}_2$, then we must have $\alpha \in Z_{\mathcal{P}_1}$ and $\alpha \in Z_{\mathcal{P}_2}$.

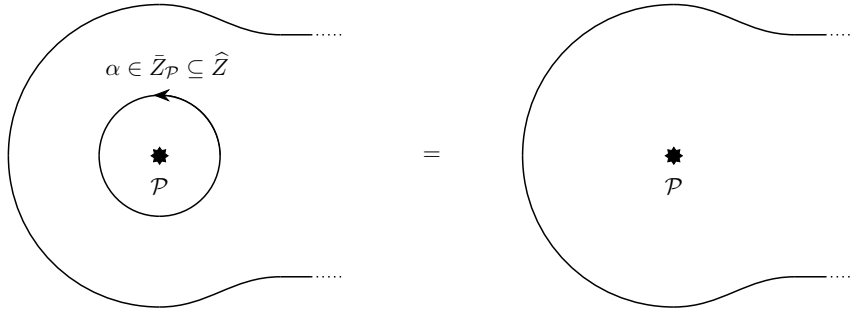Figure 13.3:   A 1-cycle surrounding a puncture of type $\mathcal{P}$ and carrying $\alpha \in \bar{Z}_{\mathcal{P}} \subseteq \widehat{Z}$ is trivial in $\mathcal{L}$.

$\bar{Z}_{\mathcal{P},p} \subseteq \bar{Z}_p \subseteq \mathcal{S}$ is modded out where $\bar{Z}_{\mathcal{P},p} \simeq \bar{Z}_{\mathcal{P}}$ and $\bar{Z}_{\mathcal{P}}$ is a subgroup of dimension-2 operators $\widehat{Z}$. See figure 13.3.

The pairing on $\mathcal{L}$ can be determined in terms of pairing on $\widehat{Z}$ and the intersection pairing of 1-cycles. First of all, combining these two pairings we obtain a pairing on $H_1(\mathcal{C}_g, \widehat{Z}, *) \simeq H_1(\mathcal{C}_g, \mathbb{Z}, *) \otimes \widehat{Z}$. For two elements $a \otimes \alpha, b \otimes \beta \in H_1(\mathcal{C}_g, \mathbb{Z}, *) \otimes \widehat{Z}$ the pairing is written as

$$\langle a \otimes \alpha, b \otimes \beta \rangle = \langle a, b \rangle \langle \alpha, \beta \rangle, \tag{13.4}$$

with $\langle a, b \rangle$ determined using the intersection pairing and $\langle \alpha, \beta \rangle$ determined using the pairing on $\widehat{Z}$. The above pairing is then extended by linearity to all of $H_1(\mathcal{C}_g, \widehat{Z}, *)$. Since $\mathcal{S} \subseteq H_1(\mathcal{C}_g, \widehat{Z}, *)$, we obtain a pairing on $\mathcal{S}$ by simply restricting the pairing on $H_1(\mathcal{C}_g, \widehat{Z}, *)$. Now we would like to push-forward the pairing on $\mathcal{S}$ to a pairing on $\mathcal{L}$ using the projection map (13.3). This can only be done consistently if

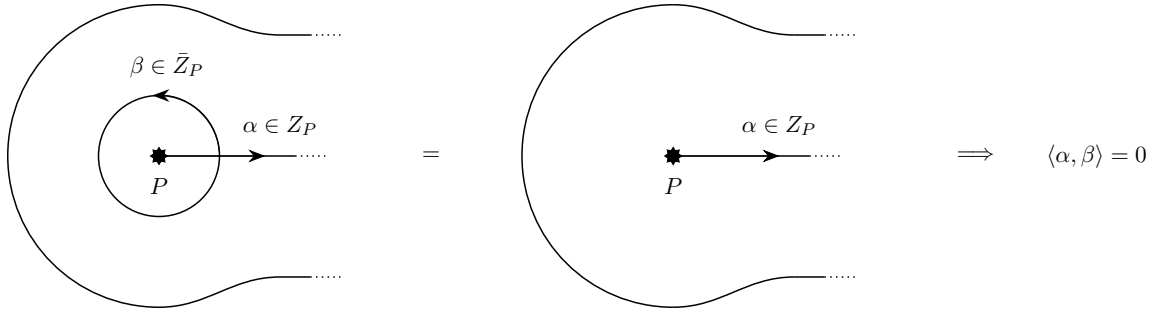$$\langle \alpha, \beta \rangle = 0 \tag{13.5}$$

Figure 13.4: A consistent pairing on $\mathcal{L}$ exists only if the mutual pairing between elements of $\bar{Z}_{\mathcal{P}}$ and $Z_{\mathcal{P}}$ vanishes.

for all $\alpha \in Z_{\mathcal{P}} \subseteq \widehat{Z}$ and $\beta \in \bar{Z}_{\mathcal{P}} \subseteq \widehat{Z}$, and for all $\mathcal{P}$. See figure 13.4. Thus, the well-definedness of pairing on $\mathcal{L}$ imposes the above constraint on the subgroups $Z_{\mathcal{P}}, \bar{Z}_{\mathcal{P}}$ for all puncture types $\mathcal{P}$. Once this condition is satisfied, we obtain a pairing on $\mathcal{L}$ as a push-forward of (13.4).

This determines $\mathcal{L}$ and pairing $\langle \cdot, \cdot \rangle$ on $\mathcal{L}$ for the relative Class S theory arising from the above compactification. As discussed in section 13.1, an absolute Class S theory arising from this compactification chooses a maximal subgroup $\Lambda \subset \mathcal{L}$ such that the pairing restricted to Λ is trivial. The 1-form symmetry of such an absolute Class S theory is $\widehat{\Lambda}$ which is the Pontryagin dual of Λ.

13.2.1 Data Associated to Various Punctures

Let us now collect information about $Z_{\mathcal{P}}, \bar{Z}_{\mathcal{P}}$ for various types of punctures that can arise in untwisted compactifications of 6d A_{n-1} $(2,0)$ theory. The punctures can be divided into two types: the regular punctures for which the $\mathcal{N} = 2$ Hitchin field ϕ has at most a simple pole, and the irregular punctures for which ϕ has higher-order poles.

For regular punctures, it was argued in [3] that in this case we have[1]

$$Z_{\mathcal{P}} = 0 \subset \widehat{Z}$$
$$\bar{Z}_{\mathcal{P}} = \widehat{Z}$$
(13.6)

The constraint (13.5) is trivially satisfied. In other words, no element of $\widehat{Z}$ can end on a regular puncture and all elements of $\widehat{Z}$ are trivial when inserted along a loop encircling a regular puncture.

More interesting values for $Z_{\mathcal{P}}$ and $\bar{Z}_{\mathcal{P}}$ occur for irregular punctures. For general irregular punctures, this information about $Z_{\mathcal{P}}, \bar{Z}_{\mathcal{P}}$ is not known. However, this information can be deduced using Lagrangian field theory for a special class of irregular punctures that can be constructed using Hanany-Witten type brane constructions in Type IIA superstring theory. Consider a brane configuration of the form shown in figure 13.5, where the following inequalities are satisfied

$$n_1 \leq n - 1$$
$$n + n_2 \leq 2n_1$$
$$n_{i-1} + n_{i+1} \leq 2n_i \qquad \text{for} \quad 2 \leq i \leq k - 1$$
$$n_{k-1} \geq 2 \,.$$
(13.7)

At $t = 0$, this constructs an irregular puncture for A_{n-1} $(2, 0)$ theory which we call to be of type $\mathcal{P}_{n_1, n_2, \cdots, n_k}$.

Let us first consider a sphere with two punctures of type $\mathcal{P}_0$. This corresponds to the brane configuration shown in figure 13.6. The resulting 4d $\mathcal{N} = 2$ theory can be read from the brane configuration to be pure SYM theory with gauge algebra $\mathfrak{su}(n)$. This theory has

$$\mathcal{L} \simeq \mathbb{Z}_n^W \times \mathbb{Z}_n^H$$
(13.8)

---

[1]A first-principles way to see that this must be the case is to realize the puncture as a boundary condition of 5d $\mathcal{N} = 2$ $\mathfrak{su}(n)$ SYM theory. A surface operator of the 6d theory wrapping a loop encircling the puncture becomes a gauge Wilson line of the 5d theory. For a regular puncture, the associated boundary condition is such that the 5d dynamical gauge field becomes a background gauge field at the 4d boundary. Consequently, every gauge Wilson line of the 5d theory reduces to a flavor Wilson line at the 4d boundary, which does not contribute to $\mathcal{L}$ and hence $\bar{Z}_{\mathcal{P}} = \widehat{Z}$. $Z_{\mathcal{P}} = 0$ is now fixed by (13.5).
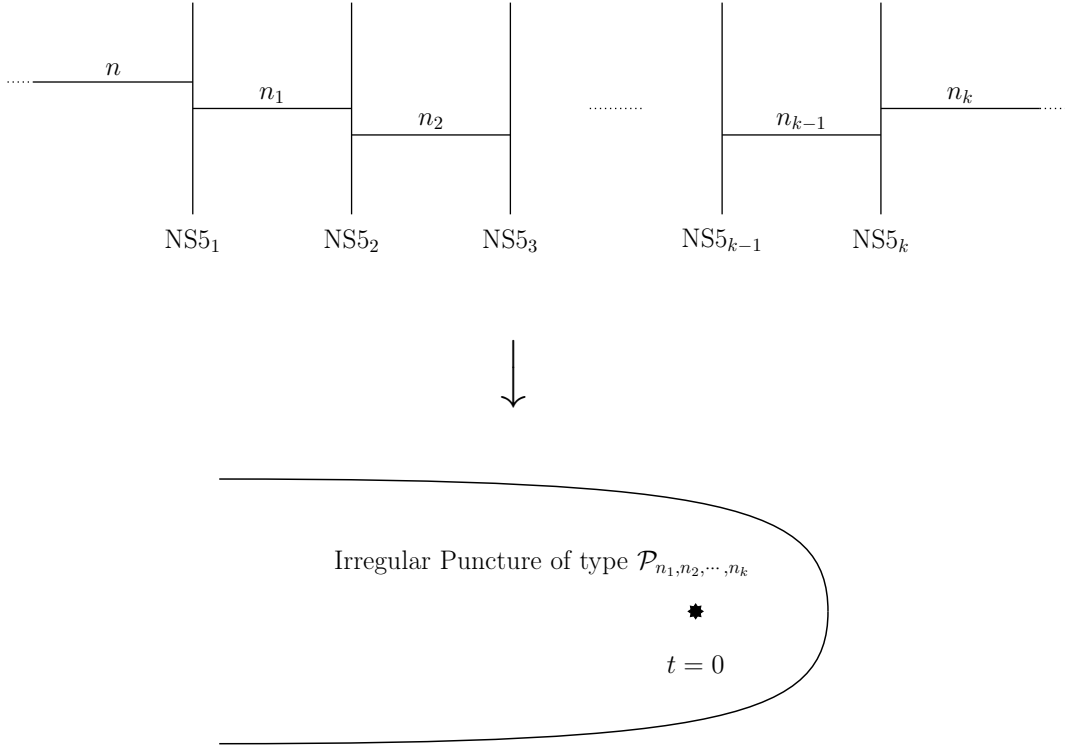
Figure 13.5: Top: $k \geq 1$ parallel NS5 branes in Type IIA superstring theory with D4 branes stretched between them. All the branes share a common 4-dimensional spacetime, and the preserved supersymmetry is $\mathcal{N} = 2$. Here, n, n_i denote numbers of D4 branes. The stacks of n D4 branes on the left and n_k D4 branes on the right are semi-infinite. Bottom: If $n_1 < n$, then the above brane construction can be associated to an irregular puncture of A_{n-1} $(2,0)$ theory compactified on a cigar parametrized by a complex coordinate t with the puncture being located at $t = 0$. This puncture is referred to be of the type $\mathcal{P}_{n_1, n_2, \cdots, n_k}$.

with the sub-factor $\mathbb{Z}_n^W$ arising from Wilson lines and the sub-factor $\mathbb{Z}_n^H$ arising from 't Hooft lines. The pairing on $\mathcal{L}$ is

$$\langle W_g, H_g \rangle = \frac{1}{n} \, , \tag{13.9}$$

where W_g is a generator of $\mathbb{Z}_n^W$ and H_g is a generator of $\mathbb{Z}_n^H$. On the other hand, as can be seen from figure 13.7, we also have

$$H_1(\mathcal{C}_g, \widehat{Z}, *) \simeq \mathbb{Z}_n^W \times \mathbb{Z}_n^H \, , \tag{13.10}$$

where $\mathbb{Z}_n^W$ sub-factor is generated by wrapping $f \in \widehat{Z} \simeq \mathbb{Z}_n$ along the cycle denoted W in the figure 13.7, and $\mathbb{Z}_n^H$ sub-factor is generated by wrapping $f \in \widehat{Z} \simeq \mathbb{Z}_n$ along the cycle
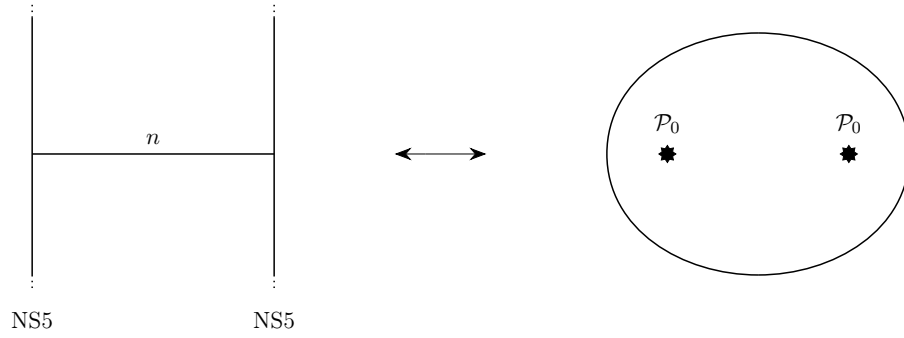
Figure 13.6: The Type IIA brane construction associated to 6d A_{n-1} $(2,0)$ theory compactified on a sphere with 2 irregular punctures of type $\mathcal{P}_0$.
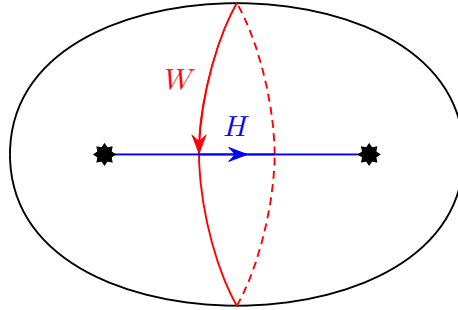
Figure 13.7: The generators W and H of 1-cycles on a 2-punctured sphere. The intersection number between them is $\langle W, H \rangle = 1$.

denoted H. We can read the pairing between the generators of $\mathbb{Z}_n^W$ and $\mathbb{Z}_n^H$ to be

$$\langle W \otimes f, H \otimes f \rangle = \frac{1}{n} \,. \tag{13.11}$$

Matching with the gauge theory results (13.8), (13.9) we find that

$$\mathcal{L} = \mathcal{S} = H_1(\mathcal{C}_g, \widehat{Z}, *) \,, \tag{13.12}$$

which implies that for a puncture of type $\mathcal{P} = \mathcal{P}_0$ the associated data is

$$Z_\mathcal{P} = \widehat{Z}$$
$$\bar{Z}_\mathcal{P} = 0 \,, \tag{13.13}$$

which also trivially satisfies (13.5). In other words, every element of $\widehat{Z}$ can end on a type $\mathcal{P}_0$ irregular puncture and no element of $\widehat{Z}$ is trivial, when inserted along a loop encircling a type $\mathcal{P}_0$ irregular puncture.

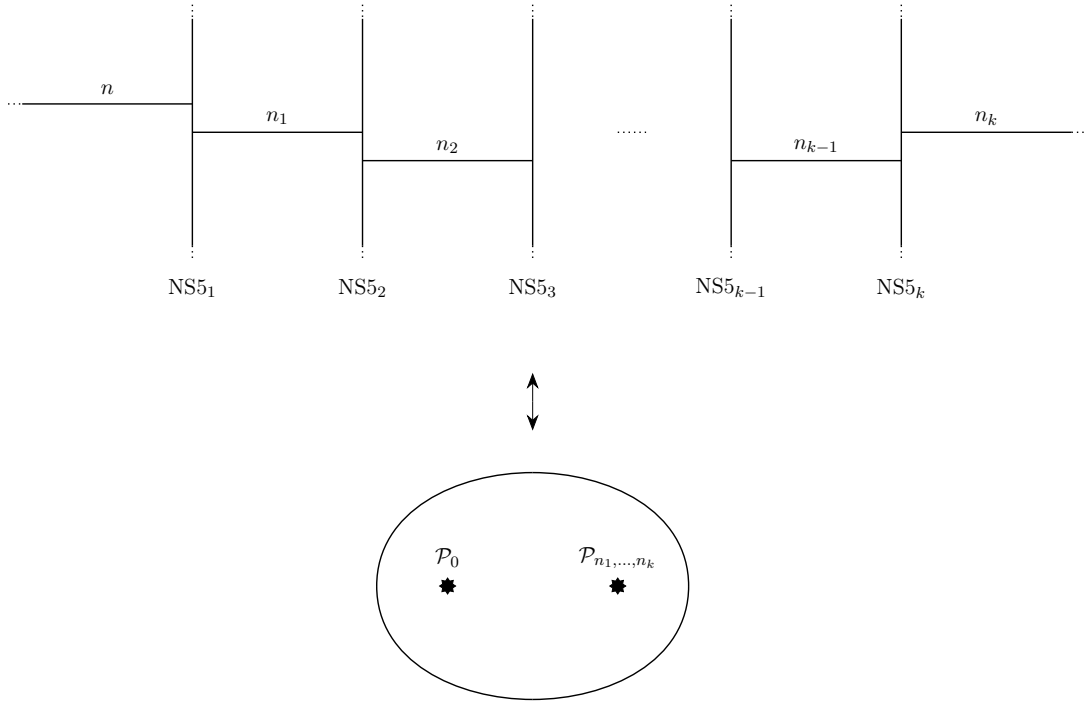Figure 13.8: The Type IIA brane construction associated to 6d A_{n-1} $(2,0)$ theory compactified on a sphere with 2 irregular punctures, one of type $\mathcal{P}_0$, and the other of type $\mathcal{P}_{n_1,n_2,\cdots,n_k}$.

Now let us consider a sphere with a puncture of type $\mathcal{P}_0$ and a puncture of general type $\mathcal{P}_{n_1,n_2,\cdots,n_k}$. This corresponds to the brane configuration shown in figure 13.8. The resulting 4d $\mathcal{N}=2$ theory is the following quiver

$$\mathfrak{su}(n) \rule[0.5ex]{2em}{0.4pt} \mathfrak{su}(n_1) \rule[0.5ex]{2em}{0.4pt} \mathfrak{su}(n_2) - \cdots - \mathfrak{su}(n_{k-1}) \rule[0.5ex]{2em}{0.4pt} n_k\mathsf{F} \quad , \tag{13.14}$$

where there is a bifundamental hyper for any two adjacent gauge algebras, plus n_k fundamental hypers for $\mathfrak{su}(n_{k-1})$. For $n_k > 0$, all electric charges for all $\mathfrak{su}(n_i)$ are screened by the fundamentals and bifundamentals. This implies that there are no magnetic charges that are simultaneously unscreened and mutually local with all the electric charges. Thus, using the Lagrangian description we find that

$$\mathcal{L} = 0 \tag{13.15}$$

for $n_k > 0$. This implies that any element of $\widehat{Z}$ wrapped along the 1-cycle W must be trivial in $\mathcal{L}$. We know that this triviality does not arise at the location of $\mathcal{P}_0$ puncture. So it must

be the case that for a puncture of type $\mathcal{P} = \mathcal{P}_{n_1, n_2, \cdots, n_k}$ with $n_k > 0$, we have

$$\bar{Z}_{\mathcal{P}} = \widehat{Z}. \tag{13.16}$$

Moreover, for (13.15) to hold, it should not be possible to insert any element of $\widehat{Z}$ along the 1-cycle H. Since there are no restrictions on the elements of $\widehat{Z}$ that can end on a puncture of type $\mathcal{P}_0$, we learn that for a puncture of type $\mathcal{P} = \mathcal{P}_{n_1, n_2, \cdots, n_k}$ with $n_k > 0$, we have

$$Z_{\mathcal{P}} = 0. \tag{13.17}$$

Notice that this is just as for regular punctures, and the constraint (13.5) is trivially satisfied.

Now let us consider the $n_k = 0$ case. Before accounting for bifundamental matter the electric charges form $\mathbb{Z}_n \times \prod_{i=1}^{k-1} \mathbb{Z}_{n_i}$ group. Let W be the generator of $\mathbb{Z}_n$ sub-factor and W_i be the generators for $\mathbb{Z}_{n_i}$ sub-factors. Accounting for the bifundamentals, we obtain the relations $W_i = W$ for all i. Thus, we have

$$\gcd(n, n_1, n_2, \cdots, n_{k-1})W = 0 \tag{13.18}$$

and the contribution of Wilson operators to $\mathcal{L}$ is $\mathbb{Z}_{\gcd(n, n_1, n_2, \cdots, n_{k-1})}$. Similarly, before accounting for the bifundamental matter, the magnetic charges also form $\mathbb{Z}_n \times \prod_{i=1}^{k-1} \mathbb{Z}_{n_i}$ group. Let H be the generator of $\mathbb{Z}_n$ sub-factor and H_i be the generators for $\mathbb{Z}_{n_i}$ sub-factors. The subgroup mutually local with the bifundamentals is spanned by

$$\frac{n}{\gcd(n, n_1, n_2, \cdots, n_{k-1})}H + \sum_{i=1}^{k-1} \frac{n_i}{\gcd(n, n_1, n_2, \cdots, n_{k-1})}H_i. \tag{13.19}$$

Thus, the contribution of 't Hooft operators to $\mathcal{L}$ is also $\mathbb{Z}_{\gcd(n, n_1, n_2, \cdots, n_{k-1})}$. In total, we have

$$\mathcal{L} \simeq \mathbb{Z}_{\gcd(n, n_1, n_2, \cdots, n_{k-1})}^{W} \times \mathbb{Z}_{\gcd(n, n_1, n_2, \cdots, n_{k-1})}^{H}. \tag{13.20}$$

From this, we read that for an irregular puncture of type $\mathcal{P} = \mathcal{P}_{n_1, n_2, \cdots, n_{k-1}, 0}$, we have

$$\begin{aligned} Z_{\mathcal{P}} &= \left[\frac{n}{\gcd(n, n_1, n_2, \cdots, n_{k-1})} f \right] \subseteq \widehat{Z} \\ \bar{Z}_{\mathcal{P}} &= \left[\gcd(n, n_1, n_2, \cdots, n_{k-1}) f \right] \subseteq \widehat{Z} \end{aligned}, \tag{13.21}$$

where $[\alpha]$ denotes the subgroup of $\widehat{Z}$ generated by $\alpha \in \widehat{Z}$. The pairing between the generators of $Z_\mathcal{P}$ and $\bar{Z}_\mathcal{P}$ is

$$\left\langle \frac{n}{\gcd(n,n_1,n_2,\cdots,n_{k-1})}f \ , \ \gcd(n,n_1,n_2,\cdots,n_{k-1})f \right\rangle = 0 \qquad (13.22)$$

as required by the constraint (13.5).

13.3 Rotation and $\mathcal{N}=1$ Higgs Bundles

We next discuss constructions of $\mathcal{N}=1$ theories by compactification of 6d $(2,0)$ theories on a Riemann surface with a partial topological twist. This includes both general $\mathcal{N}=1$ theories, and the $\mathcal{N}=1$ theories of interest that can be obtained by deforming $\mathcal{N}=2$ theories of Class S. Along the way, we would encounter key notions of generalized Hitchin system and $\mathcal{N}=1$ curve which characterize vacua of these $\mathcal{N}=1$ theories.

13.3.1 Topological Twists for 4d $\mathcal{N}=2$ and $\mathcal{N}=1$

Start with 6d $(2,0)$ theory of type $\mathfrak{g}=A,D,E$ compactified on a Riemann surface $\mathcal{C}_{g,n}$ of genus g, with n punctures. We want to perform a partial topological twist along $\mathcal{C}$ which preserves at least 4d $\mathcal{N}=1$ supersymmetry as discussed in [147]. The global symmetries of the 6d theory are the local Lorentz and R-symmetry $\mathfrak{so}(6)_L \oplus \mathfrak{so}(5)_R$ which are broken to $\mathfrak{so}(4)_L \oplus \mathfrak{u}(1)_L \oplus \mathfrak{so}(5)_R$ by the background $M_4 \times \mathcal{C}$. To preserve $\mathcal{N}=2$ supersymmetry, we would decompose the R-symmetry as $\mathfrak{so}(5)_R \to \mathfrak{su}(2)_R \oplus \mathfrak{u}(1)_1$ and twist $\mathfrak{u}(1)_L$ by $\mathfrak{u}(1)_1$. For a more general twist that in general preserves $\mathcal{N}=1$ supersymmetry, we further reduce $\mathfrak{su}(2)_R$ to $\mathfrak{u}(1)_2$ and both $\mathfrak{u}(1)_1$ and $\mathfrak{u}(1)_2$ are used to twist $\mathfrak{u}(1)_L$. The supercharges Q and scalars[2] Φ decompose as

$$
\begin{aligned}
\mathfrak{so}(6)_L \oplus \mathfrak{so}(5)_R \quad &\to \quad (\mathfrak{so}(4)_L \oplus \mathfrak{u}(1)_L) \oplus (\mathfrak{u}(1)_1 \oplus \mathfrak{u}(1)_2) \\
Q: \quad (\mathbf{4},\mathbf{4}) \quad &\to \quad ((\mathbf{2},\mathbf{1})_{+1} \oplus (\mathbf{1},\mathbf{2})_{-1}) \otimes (\mathbf{1}_{++} \oplus \mathbf{1}_{+-} \oplus \mathbf{1}_{-+} \oplus \mathbf{1}_{--}) \quad . \quad (13.23) \\
\Phi: \quad (\mathbf{1},\mathbf{5}) \quad &\to \quad \mathbf{1}_0 \otimes (\mathbf{1}_{2,0} \oplus \mathbf{1}_{-2,0} \oplus \mathbf{1}_{0,2} \oplus \mathbf{1}_{0,0} \oplus \mathbf{1}_{0,-2}) .
\end{aligned}
$$

---

[2]These scalars are not genuine local operators in the 6d $(2,0)$ SCFT, but the Casimirs built out of these scalars are genuine local operators in the 6d theory.

The twists giving $\mathcal{N} = 1$ supersymmetry are parametrized by an integer parameter α which sets the charge q_{tw} of the preserved diagonal combinination of the three $\mathfrak{u}(1)$ factors

$$q_{\text{tw}} = q_L + (1 - \alpha)q_1 + \alpha q_2 \,. \tag{13.24}$$

For $\alpha = 0, 1$, we recover the usual $\mathcal{N} = 2$ twist. For other values of α, only 4 supercharges are preserved and hence the twist is $\mathcal{N} = 1$. It should be noted that one can obtain $\mathcal{N} = 1$ supersymmetry from the $\mathcal{N} = 2$ twist, as we discuss below.

The scalars Φ of the 6d theory transform with charges $q_{\text{tw}} = \pm 2(1 - \alpha), \pm 2\alpha, 0$. The twisted scalars carrying charges $\pm 2\alpha$ and $\pm 2(1 - \alpha)$ are sections of two line bundles $\mathcal{L}_1$ and $\mathcal{L}_2$ with

$$\deg(\mathcal{L}_1) + \deg(\mathcal{L}_2) = \deg(K_{\mathcal{C}}) \,, \tag{13.25}$$

where $K_{\mathcal{C}}$ is the canonical line bundle on $\mathcal{C}$. We denote these by ϕ and φ respectively.

The above setup preserves 4d $\mathcal{N} = 1$ supersymmetry for $\alpha \neq 0, 1$ since the twist only preserves a maximum of 4 supercharges. But for $\alpha = 0, 1$ one can have either 4d $\mathcal{N} = 1$ or 4d $\mathcal{N} = 2$ supersymmetry. To understand this, without loss of generality, consider the case $\alpha = 0$, for which ϕ must be singular, and hence non-zero, but φ (which is a function on $\mathcal{C}$) can be zero or non-zero. For zero φ, we inherit $\mathfrak{su}(2)_R \subset \mathfrak{so}(5)_R$ R-symmetry in 4d and thus 4d $\mathcal{N} = 2$ supersymmetry. On the other hand, if φ is non-zero, then the $\mathfrak{su}(2)_R$ R-symmetry is broken by the non-zero profile of φ, and we only obtain 4d $\mathcal{N} = 1$ supersymmetry.

13.3.2 Generalized Hitchin System and Rotation of Codim-2 Defects

The profiles of ϕ, φ over $\mathcal{C}$ satisfy a set of BPS equations that were determined in [79] and yield what is known as the $\mathcal{N} = 1$ Hitchin system

$$\bar{D}\phi = \bar{D}\varphi = 0$$

$$[\phi, \varphi] = 0 \tag{13.26}$$

$$F + [\varphi, \varphi^*] + [\phi, \phi^*] = 0 \,.$$

Here the star denotes conjugation and F abbreviates the field strength of a connection on $\mathcal{C}$. In this thesis, we always restrict ourselves to the special case where the Higgs fields ϕ and

φ are diagonalizable (at each point in $\mathcal{C}$), and therefore the third BPS equation in (13.26) imposes $F = 0$.

The punctures on $\mathcal{C}$ are characterized by singularities of the two Higgs fields ϕ, φ. From the point of view of the 6d $(2, 0)$ theory, punctures with different singularities are identified as different codimension-2 defects inserted along the locations of punctures. Such defects preserve 4d $\mathcal{N} = 1$ supersymmetry in general. In the standard $\mathcal{N} = 2$ Class S case, we have $\alpha = 0$ and $\varphi = 0$. The codimension-2 defects are then characterized by singularities of ϕ and preserve a mutual $\mathcal{N} = 2$ supersymmetry. Now, one can "rotate" such an $\mathcal{N} = 2$ codimension-2 defect to an $\mathcal{N} = 1$ codimension-2 defect[3] by turning on a singular φ at the location of the corresponding puncture. As we will discuss in section 13.4, the second equation in (13.26) allows us to write the behavior of φ near the defect, placed at $t = 0$, as

$$\varphi \sim \sum_{k=0}^{m} \frac{r_k}{t^{b_k}} \phi_\zeta^k \,, \tag{13.27}$$

where ϕ_ζ is the contraction of ϕ with a holomorphic vector field ζ that is non-singular at $t = 0$, and $b_k \in \mathbb{Z}$. Let the most singular piece of ϕ_ζ be of order t^{-q} for some $q > 0$. Let

$$S = \{k \in \{0, 1, 2, \cdots, m\} :\ b_k + kq > 0\} \,. \tag{13.28}$$

The terms in the sum (13.27) that correspond to $k \in S$ capture the singular pieces of φ near p. Consequently, r_k for $k \in S$ are interpreted as deformation parameters rotating the codimension-2 defect. We refer to a puncture associated to a rotated codimension-2 defect as a rotated puncture.

13.3.3   Rotation of a 4d $\mathcal{N} = 2$ to a 4d $\mathcal{N} = 1$ Theory

Consider a situation in which all the punctures on $\mathcal{C}$ are rotated punctures. If we replace all the rotated punctures by their unrotated versions, and take a zero area limit of $\mathcal{C}$, then we obtain a (not necessarily conformal) 4d $\mathcal{N} = 2$ Class S theory which is UV complete in

---

[3]It is also possible that the resulting defect actually preserves an $\mathcal{N} = 2$ supersymmetry but it would be a different $\mathcal{N} = 2$ supersymmetry than the $\mathcal{N} = 2$ supersymmetry preserved by the unrotated defect. That is, in such a situation, inserting both the rotated and unrotated defects would only preserve $\mathcal{N} = 1$ supersymmetry.

4d. In a similar way, from the original situation having rotated punctures, one would want to obtain a UV complete 4d $\mathcal{N} = 1$ theory by taking the zero area limit of $\mathcal{C}$. For small non-zero area A, the compactified 6d system can be described at energy scales $E \ll 1/A$ by 4d $\mathcal{N} = 2$ Class S theory deformed by rotation parameters $r_k \in S$ coming from each puncture, defined at a cutoff scale $1/A$. In general, these parameters may contain relevant, marginal and irrelevant deformation parameters of the 4d $\mathcal{N} = 2$ Class S theory. If all the deformation parameters are relevant or marginal, then one can consistently take a zero area limit, thus lifting the cutoff and obtaining a UV complete 4d $\mathcal{N} = 1$ theory which is defined as relevant and marginal deformation of the initial 4d $\mathcal{N} = 2$ Class S theory. However, on the other hand, if any of the rotation parameters is irrelevant, then one runs into the usual issues of non-renormalizability and it is not clear if the zero area limit can be consistently taken, and if it can be taken then what the resulting 4d $\mathcal{N} = 1$ theory is. Irrespective of these subtleties, we can still study the confinement properties of the 4d $\mathcal{N} = 1$ theory with a cutoff imposed by the area of $\mathcal{C}$, as it is not impacted by the cutoff and the precise details of 4d UV completion (if it exists). We will study examples of both kinds of situations later.

In either case, different profiles on $\mathcal{C}$ of ϕ, φ satisfying the generalized Hitchin equations (13.26) (for a fixed structure of singularities) characterize different 4d vacua. For a 4d $\mathcal{N} = 2$ Class S theory, we have $\varphi = 0$ and the various profiles of ϕ form a moduli space which can be identified with the Coulomb branch (CB) of vacua of the 4d $\mathcal{N} = 2$ theory. After an $\mathcal{N} = 1$ rotation which switches on a non-zero φ, only a subset of profiles of ϕ satisfy the second condition in (13.26). This means that the CB vacua corresponding to other profiles of ϕ are lifted by the $\mathcal{N} = 1$ deformation, and the CB vacua corresponding to the profiles of ϕ that satisfy (13.26) remain as vacua of the resulting 4d $\mathcal{N} = 1$ theory (which may have a UV cutoff as discussed above). It should be noted that there can also be other vacua arising from the Higgs branch of the unrotated 4d $\mathcal{N} = 2$ theory, which we do not study here.

13.4 The $\mathcal{N} = 1$ Curve

13.4.1 Spectral Curve

To a generic-enough profile of diagonalizable ϕ, φ satisfying (13.26), one can associate an $\mathcal{N} = 1$ curve which lives in $\mathcal{L}_1 \oplus \mathcal{L}_2$ and is an N-sheeted cover of $\mathcal{C}$. We start by picking two generic meromorphic sections ζ and η of $\mathcal{L}_1^{-1}$ and $\mathcal{L}_2^{-1}$ respectively. The contractions

$$\phi_\zeta \equiv \phi(\zeta), \qquad \varphi_\eta \equiv \varphi(\eta) \tag{13.29}$$

are meromorphic functions on $\mathcal{C}$. By the second equation in (13.26), the Higgs fields φ_η and ϕ_ζ commute. If at generic points on the curve $\mathcal{C}$ the eigenvalue spectrum of ϕ_ζ and φ_η are distinct, then each Higgs field can be expressed as a polynomial of the other Higgs field

$$\varphi_\eta = \mathcal{R}(\phi_\zeta) = \sum_k r_k(t) \phi_\zeta^k$$
$$\phi_\zeta = \mathcal{S}(\varphi_\eta) = \sum_k s_k(t) \varphi_\eta^k . \tag{13.30}$$

By the first BPS equation in (13.26) the coefficient functions r_k, s_k are meromorphic functions on the compact curve $\mathcal{C}$. We diagonalize (13.30) and find

$$w = \mathcal{R}(v) = \sum_k r_k(t) v^k$$
$$v = \mathcal{S}(w) = \sum_k s_k(t) w^k , \tag{13.31}$$

solved by pairs of eigenvalues (w, v) of $(\varphi_\eta, \phi_\zeta)$.

The above pairing of eigenvalues allows us to combine the spectral covers associated to φ_η, ϕ_ζ into a single N-sheeted cover $\Sigma \subset \mathcal{L}_1 \oplus \mathcal{L}_2$ of $\mathcal{C}$ known as the $\mathcal{N} = 1$ curve. In more detail, the two characteristic equations[4]

$$\det(v - \phi_\zeta) = 0$$
$$\det(w - \varphi_\eta) = 0 \tag{13.32}$$

for φ_η and ϕ_ζ define two spectral covers

$$\mathcal{P}(v) = \sum_l p_l(t) v^l = 0 , \qquad \mathcal{Q}(w) = \sum_l q_l(t) w^l = 0 . \tag{13.33}$$

---

[4]To write down the characteristic equations, we represent ϕ_ζ, φ_η as matrices acting in the fundamental representation, vector representation, $\mathbf{27}$, $\mathbf{56}$ and $\mathbf{248}$ for the Lie algebras A_n, D_n, E_6, E_7 and E_8 respectively.

The coefficients p_l, q_l are again meromorphic functions. Each spectral curve (13.33) is an N-sheeted covering of $\mathcal{C}$ with the number of sheets N depending on the type $\mathfrak{g} = A, D, E$ of the $(2,0)$ theory. Consider the monodromy of the N sheets of $\mathcal{P}(v)$ around a branch point $p \in \mathcal{C}$ or around a cycle $C \in H_1(\mathcal{C})$, which is given by some element of the permutation group S_N permuting the N sheets. Now, the monodromy of $\mathcal{Q}(w)$ around p or C must be the same as the sheets (which are described by the eigenvalues) of $\mathcal{P}(v)$ and $\mathcal{Q}(w)$ are paired. Thus, the monodromies of $\mathcal{P}(v)$ must match the monodromies of $\mathcal{Q}(w)$. Furthermore, the pairs (v, w) define a *combined* N-fold cover $\widetilde{\Sigma} \subset \mathcal{O}_\mathcal{C} \oplus \mathcal{O}_\mathcal{C}$ of $\mathcal{C}$ whose monodromies match the monodromies of $\mathcal{P}(v)$ and $\mathcal{Q}(w)$. The $\mathcal{N} = 1$ curve $\Sigma \subset \mathcal{L}_1 \oplus \mathcal{L}_2$ is then identified as the N-sheeted cover of $\mathcal{C}$ spanned by pairs $(v\zeta^{-1}, w\eta^{-1})$. The $\mathcal{N} = 1$ curve Σ can also be thought of as being cut out by

$$\det(\lambda - \phi) = 0\,, \qquad \det(\sigma - \varphi) = 0\,, \qquad \det(\lambda\sigma - \phi\varphi) = 0\,, \qquad (13.34)$$

where $\lambda \in \mathcal{L}_1$ and $\sigma \in \mathcal{L}_2$.

In conclusion, for each vacuum r of a 4d $\mathcal{N} = 1$ theory that can be characterized by profiles ϕ_r, φ_r of $\mathcal{N} = 1$ Higgs fields satisfying at least one of the equations[5] (13.31), we can associate a curve $\Sigma_r \subset \mathcal{L}_1 \oplus \mathcal{L}_2$ which is an N-fold cover of $\mathcal{C}$.

13.4.2   Algorithm for Determining the $\mathcal{N} = 1$ Curve

In this thesis, we focus on the study of the $\mathcal{N} = 1$ curves with $\alpha = 0$ with $\varphi \neq 0$, and in particular those cases which can be understood as "rotations" of standard $\mathcal{N} = 2$ Class S setups. For these cases, we provide an algorithm to determine the $\mathcal{N} = 1$ curves for those vacua of the $\mathcal{N} = 1$ theory (obtained after rotation) that arise from the $\mathcal{N} = 2$ Coulomb branch:

1. Unrotated Theory: Choose an $\mathcal{N} = 2$ Class S theory (which need not be conformal) by specifying the singularities of ϕ at the locations of punctures. We can determine the profile of ϕ away from the punctures by using holomorphicity. Different profiles

---

[5]Later, we will see an example where only one of the two equations in (13.31) is satisfied, but not both.

of ϕ parameterize Coulomb branch of $\mathcal{N}=2$ vacua, and the Seiberg-Witten (SW) curve associated to each vacuum is obtained by inserting the corresponding profile of ϕ into the characteristic equation $\det(\lambda-\phi)=0$. The SW curve is an N-sheeted cover $\mathcal{P}(\lambda)=0$ of the UV curve $\mathcal{C}_{g,n}$.

2. Rotation: Fix the singularities of φ at each puncture p. This can be done by specifying $r_k^{(p)}$ and $b_k^{(p)}$ arising in (13.27) for $k \in S$. This determines the deformation parameters used to deform the Class S $\mathcal{N}=2$ theory chosen above. Write down the generic meromorphic profile of φ having singularities determined by the above imposed boundary conditions. This generic profile determines another N-sheeted cover $\mathcal{Q}(w)=0$ of $\mathcal{C}_{g,n}$ via the characteristic equation $\det(w-\varphi)=0$.

3. Topological Factorization: Determine all possible topological degenerations by moving and colliding the branch points of both the N-sheeted covers $\mathcal{P}(\lambda)$ and $\mathcal{Q}(w)$ of $\mathcal{C}$, such that the monodromies for $\mathcal{P}(\lambda), \mathcal{Q}(w)$ match after the degeneration. Each such topological degeneration determines a potential factorization of the discriminants of $\mathcal{P}(\lambda), \mathcal{Q}(w)$ as N-sheeted covers of $\mathcal{C}$.

4. "Holomorphic" Factorization: After determining all possible topological degenerations for which monodromies of $\mathcal{P}(\lambda), \mathcal{Q}(w)$ match, one needs to check that the corresponding potential factorizations of the discriminants of $\mathcal{P}(\lambda), \mathcal{Q}(w)$ are realizable without changing the singularities of ϕ, φ which defined the parent $\mathcal{N}=2$ theory and its $\mathcal{N}=1$ rotation. If this is possible, then one also needs to check that all the monodromies are as determined by the topological degeneration. If the monodromies also match, then the CB moduli for which the factorization is possible determine a vacuum of the descendant $\mathcal{N}=1$ theory. It is possible that one finds multiple possible choices of CB parameters for a fixed topological degeneration leading to multiple $\mathcal{N}=1$ vacua whose corresponding $\mathcal{N}=1$ curves have the same set of branch points and monodromies. However, the branch lines connecting the branch points for these different vacua might

be topologically distinct from each other. This difference reflects in the difference of the images of the map (13.36) for these different vacua, that we discuss in the next subsection.

13.5 Confinement from the $\mathcal{N} = 1$ Curve

Consider a relative 4d $\mathcal{N} = 1$ theory that has been obtained as a rotation of a relative 4d $\mathcal{N} = 2$ Class S theory of above type. We propose that the defect group $\mathcal{L}$ of line operators remains invariant under the rotation. Thus, $\mathcal{L}$ for the resulting 4d $\mathcal{N} = 1$ theory is the same as for the 4d $\mathcal{N} = 2$ theory determined in section 13.2.

Consider a vacuum r of the 4d $\mathcal{N} = 1$ theory that descends from a Coulomb branch vacuum of the parent 4d $\mathcal{N} = 2$ theory. As we discussed in the previous subsection, if certain conditions are met, we can associate to this vacuum r an $\mathcal{N} = 1$ curve $\Sigma_r \subset T^*\mathcal{C} \times \mathbb{C}$ which is an N-fold cover of $\mathcal{C}$ characterized by a projection map

$$\pi^r : \qquad \Sigma_r \to \mathcal{C} \, . \tag{13.35}$$

We can use this map to define a pushforward map

$$\pi_*^r : \qquad H_1(\Sigma_r, \widehat{Z}, *) \to H_1(\mathcal{C}, \widehat{Z}, *) \tag{13.36}$$

from 1-cycles on Σ_r (that are allowed to end on punctures) to 1-cycles on $\mathcal{C}$ (that are allowed to end on punctures). We further argue (see below) that the line operators $\mathcal{I}_r \subseteq \mathcal{L}$ that exhibit perimeter law can be identified with

$$\mathcal{I}_r = \pi_* \left(\mathcal{S} \cap \pi_*^r \left(H_1(\Sigma_r, \widehat{Z}, *) \right) \right), \tag{13.37}$$

where π is the projection map from $\mathcal{S}$ to $\mathcal{L}$ defined in (13.3), and π_* is the associated pushforward.

As discussed in section 13.1, an absolute 4d $\mathcal{N} = 1$ theory specifies a polarization $\Lambda \subset \mathcal{L}$, and then the preserved 1-form symmetry group $\mathcal{O}_r$ for this absolute theory in the vacuum r is determined to be

$$\mathcal{O}_r = \widehat{\left(\frac{\Lambda}{\Lambda_r} \right)}, \tag{13.38}$$

where $\Lambda_r := \mathcal{I}_r \cap \Lambda$.

Our argument for (13.37) is a generalization of the argument appearing in [52] where confinement for $\mathcal{N} = 1$ SYM was studied in this setup, which can be understood as a compactification of M-theory as follows. We can realize a CB vacuum of the 4d $\mathcal{N} = 2$ Class S theory before rotation as M-theory compactified on $T^*\mathcal{C}$ with M5-branes wrapping a curve $\Sigma \subset T^*\mathcal{C}$, which is identified as the SW curve for that vacuum. Σ is an n-fold cover of $\mathcal{C}$ under the projection map $T^*\mathcal{C} \to \mathcal{C}$ and is cut out by the characteristic equation $\det(\lambda - \phi) = 0$, where ϕ is the $\mathcal{N} = 2$ Higgs field discussed above and λ is a coordinate along the fiber of $T^*\mathcal{C}$. Once we rotate the $\mathcal{N} = 2$ theory to $\mathcal{N} = 1$, then a vacuum r of the resulting $\mathcal{N} = 1$ theory is realized by M5-branes wrapping a curve $\Sigma_r \subset T^*\mathcal{C} \times \mathbb{C}$, which is identified as the $\mathcal{N} = 1$ curve associated to that vacuum. The projection of Σ_r to $T^*\mathcal{C}$ is cut out by the characteristic equation $\det(\lambda - \phi) = 0$ and the projection of Σ_r to $\mathbb{C}$ is cut out by the characteristic equation $\det(w - \varphi) = 0$, where φ is the other Higgs field discussed above and w is a coordinate along $\mathbb{C}$.

To study confinement, we study the charges of confining strings in this setup. The confining strings are realized by compactifying M2-branes along 1-cycles of $Y = T^*\mathcal{C} \times \mathbb{C}$. A crucial addition to the argument of [52] is that we need to also include 1-cycles in Y whose projections onto $\mathcal{C}$ contain 1-cycles included in $H_1(\mathcal{C}, \mathbb{Z}, *)$ (see section 13.2) which end at punctures of $\mathcal{C}$. After including such 1-cycles we obtain a homology group $H_1(Y, \mathbb{Z}, *)$, which is isomorphic to $H_1(\mathcal{C}, \mathbb{Z}, *)$ under the projection map. Thus, as a first step, the possible charges of confining strings are characterized by $H_1(Y, \mathbb{Z}, *) \simeq H_1(\mathcal{C}, \mathbb{Z}, *)$. Now, we need to account for the fact that M2-branes can end on M5-branes, which implies that M2-branes characterized by different elements of $H_1(Y, \mathbb{Z}, *)$ can be related by topological moves, which split and join the M2-branes along the M5 brane locus Σ_r. All such identifications are captured by the fact that a confining string arising from an element $i_* H_1(\Sigma_r, \mathbb{Z}, *) \subseteq H_1(Y, \mathbb{Z}, *)$ is topologically equivalent to a trivial string and hence must have trivial charge. Here $i : \Sigma_r \hookrightarrow Y$ denotes the inclusion map and i_* denotes the associated pushforward map
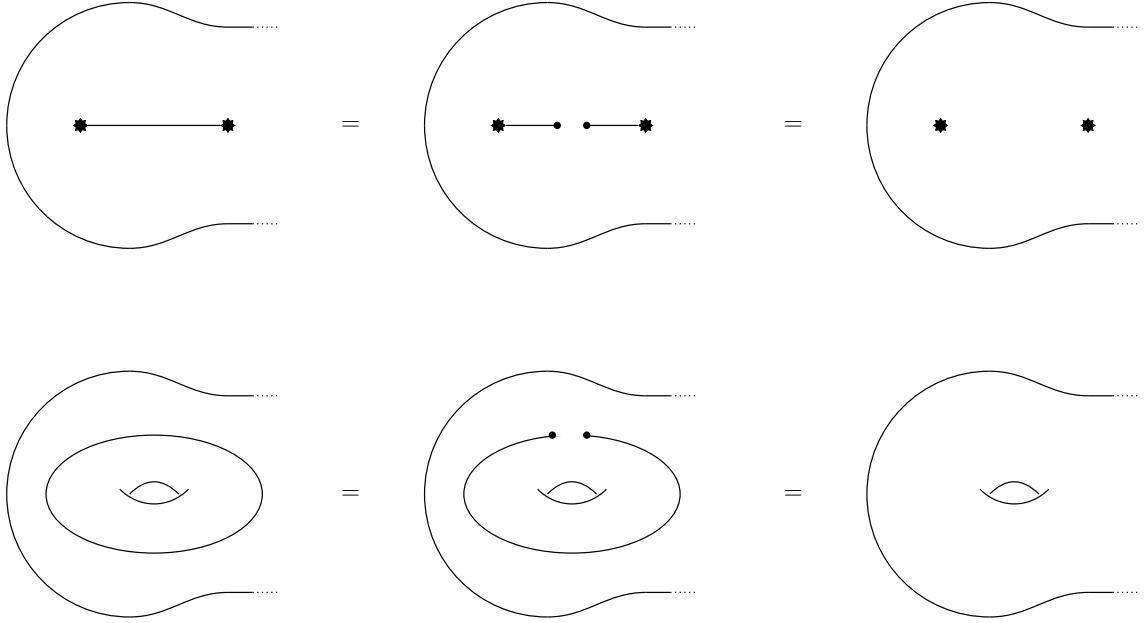
Figure 13.9:   The figure shows various configurations of M2-branes wrapping 1-chains inside M5-branes. An M5-branes is depicted as a surface, which shows a local region of Σ_r. In the top-left configuration, we consider an M2 brane stretched between two punctures on Σ_r. The subsequent configurations depict that we can get rid of this M2 brane by splitting it into two by creating its end-points (shown with a black dot) on the M5 brane. Similarly, in the bottom-left configuration, we consider an M2 brane wrapping a compact 1-cycle on Σ_r. As shown in the subsequent configurations, we can get rid of this M2 brane again by creating its end-points on the M5 brane.

which embeds the cycles of Σ_r into Y. See figures 13.9 and 13.10.

We can use this fact to constrain the possible charges of confining strings to lie in

$$\frac{H_1(Y, \mathbb{Z}_n, *)}{i_* H_1(\Sigma_r, \mathbb{Z}_n, *)}, \tag{13.39}$$

since any cycle of the form nC with $C \in H_1(Y, \mathbb{Z}, *) \simeq H_1(\mathcal{C}, \mathbb{Z}, *)$ lies in $i_* H_1(\Sigma_r, \mathbb{Z}, *)$ because Σ is an n-fold cover of $\mathcal{C}$. In other words, at this step, the possible charges of confining strings are characterized by modding out $H_1(\mathcal{C}, \widehat{Z}, *)$ by the image of $H_1(\Sigma_r, \widehat{Z}, *)$ under the projection map (13.35)

$$\frac{H_1(\mathcal{C}, \widehat{Z}, *)}{\pi_*^r H_1(\Sigma_r, \widehat{Z}, *)}, \tag{13.40}$$

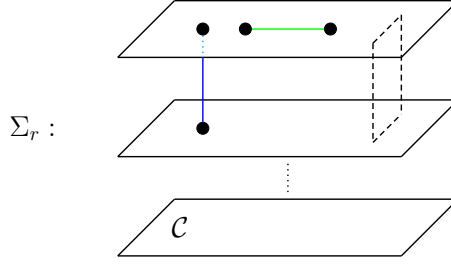where $\widehat{Z} \simeq \mathbb{Z}_n$.

Figure 13.10: The $\mathcal{N} = 1$ curve $\Sigma_r \subset Y$ as a covering of the UV curve $\mathcal{C}$. The dashed sheet denotes a branch cut connecting two sheets. The green and blue line segments denote 1-cycles wrapped by M2-branes and give rise to potential confining strings. The green cycle is contained in the M5 brane locus and is of the type depicted in figure 13.9. The confining strings associated to it are trivial and uncharged under the 1-form symmetry. The blue cycle stretches between the sheets, is contained in Y, and is an element of the relative homology group $H_1(Y, \Sigma_r)$. These are *charged* under the 1-form symmetry.

We can further reduce the set of possible charges by recalling that different punctures allow different subgroups of $\widehat{Z}$ to end on them. As we discussed in section 13.2, this means that the allowed charges of line operators take values in a subgroup $\mathcal{S}$ of $H_1(\mathcal{C}, \widehat{Z}, *)$. Consequently, at this step, the possible charges of confining strings are characterized by

$$\frac{\mathcal{S}}{\mathcal{S} \cap \pi_*^r \left(H_1(\Sigma_r, \widehat{Z}, *) \right)} . \tag{13.41}$$

Finally, we take into account the fact that not all charges in $\mathcal{S}$ are independent charges of line operators. As discussed in section 13.2, we need to mod out a subgroup of $\mathcal{S}$ to obtain the true group of charges $\mathcal{L}$ of line operators, resulting in a projection map $\pi : \mathcal{S} \to \mathcal{L}$. Thus, finally the possible charges of confining strings are characterized by

$$\frac{\mathcal{L}}{\mathcal{I}_r} \tag{13.42}$$

with $\mathcal{I}_r$ given in (13.37). Once we choose an absolute theory with charges of line operators specified by subgroup $\Lambda \subset \mathcal{L}$ fixing the 1-form symmetry group $\mathcal{O} = \widehat{\Lambda}$, the confining strings are chosen to have charges

$$\frac{\Lambda}{\mathcal{I}_r \cap \Lambda} \tag{13.43}$$

176

and the preserved 1-form symmetry group is $\mathcal{O}_r \subseteq \mathcal{O}$ where $\mathcal{O}_r$ is the Pontryagin dual of the above group formed by charges of confining strings.

Chapter 14
Confinement in 4d $\mathcal{N} = 1$ SYM

In this section we consider the well studied case of 4d $\mathcal{N} = 1$ $\mathfrak{su}(n)$ SYM and determine the 1-form symmetry groups and their spontaneous breakings in various vacua for various global forms of the gauge group and discrete theta parameters. We do so using the machinery developed in chapter 13, and in particular using our main proposal in section 13.5 about reading off confinement from the $\mathcal{N} = 1$ curve. This problem was previously studied field-theoretically in [133] without using the modern language of 1-form symmetry and its spontaneous breaking. We enhance their description at various points by providing explicit results for the UV 1-form symmetry groups for various polarizations and the preserved 1-form symmetry groups in various vacua for various polarizations. Our main purpose is to use this example as a test ground to verify and demonstrate our more general prescription.

We begin with a Class S construction of 4d $\mathcal{N} = 2$ $\mathfrak{su}(n)$ SYM discussed in section 13.2, where the defect group $\mathcal{L}$ of the theory was also discussed. We then perform a rotation μ of the 4d $\mathcal{N} = 2$ theory such that 4d $\mathcal{N} = 1$ SYM is obtained as the $\mu \to \infty$ limit. Following the algorithm of section 13.4.2, we determine various $\mathcal{N} = 1$ vacua and their corresponding $\mathcal{N} = 1$ curves for finite μ. Then we use the topological structure of $\mathcal{N} = 1$ curves to determine the group $\mathcal{I}_r$ of line operators showing perimeter law in each vacuum r. This allows us to present our main result, i.e., the computation of the preserved 1-form symmetry group $\mathcal{O}_r$ in the vacuum r (for various choices of polarization Λ). These results remain unchanged as we take the limit $\mu \to \infty$ and recover pure 4d $\mathcal{N} = 1$ $\mathfrak{su}(n)$ SYM theory.

14.1 $\mathcal{N} = 2$ Curve and Line Operators

A Class S construction of 4d $\mathcal{N} = 2$ $\mathfrak{su}(n)$ SYM was discussed in section 13.2. It involves compactifying 6d A_{n-1} $(2,0)$ theory on a compactification manifold $\mathcal{C}$ which is a sphere with two punctures, both of type $\mathcal{P}_0$ (see figure 13.6). As discussed there, the defect group $\mathcal{L}$ is identified with the group of 1-cycles $H_1(\mathcal{C}, \widehat{Z}, *)$

$$\mathcal{L} = H_1(\mathcal{C}, \widehat{Z}, *) \cong \mathbb{Z}_n^W \times \mathbb{Z}_n^H \tag{14.1}$$

with coefficients in $\widehat{Z} \cong \mathbb{Z}_n$. The factors labelled W, H are associated with the Wilson and 't Hooft lines of the field theory and geometrically with the 1-cycles encircling a puncture and running between the punctures respectively, as depicted in figure 13.7 in section 13.2.

The SW curve is [175]

$$\mathcal{P}(v) = P_n(v) - \Lambda^n \left(t + \frac{1}{t} \right) = 0 \,, \tag{14.2}$$

where $(v, t) \in \mathbb{C} \times \mathbb{C}^*$ with $P_n(v) = v^n + u_2 v^{n-2} + \cdots + u_n$ where u_k are combinations of CB parameters. The SW differential is $\lambda = v\,dt/t$. The dynamically generated scale is denoted $\Lambda_{\mathcal{N}=2} \equiv \Lambda$. The asymptotics of the Higgs field approaching the punctures at $t = 0, \infty$ can be derived from (14.2) and are taken to define the Higgs field ϕ profile characterizing punctures of type $\mathcal{P}_0$. At the two $\mathcal{P}_0$ punctures $t = 0, \infty$ the Higgs field $\phi = \phi_\zeta (dt/t)$ therefore diverges as

$$
\begin{aligned}
t \to 0 : &\qquad \phi_\zeta \sim \frac{\Lambda}{t^{1/n}} \mathrm{diag}\left(1, \omega, \omega^2, \cdots, \omega^{n-1}\right) + \cdots \\
t \to \infty : &\qquad \phi_\zeta \sim \Lambda t^{1/n} \mathrm{diag}\left(1, \omega, \omega^2, \cdots, \omega^{n-1}\right) + \cdots \,,
\end{aligned}
\tag{14.3}
$$

with the n-th root of unity $\omega = \exp(2\pi i/n)$. We have made the choice $\zeta = t\partial_t$ for which the coordinate $v = \lambda(\zeta) = x^8 + ix^9$ has the interpretation of two flat space-time coordinates in the weakly coupled IIA brane picture (see figure 13.6).

14.2 Constraints from Rotation

We rotate to $\mathcal{N} = 1$ by turning on the Higgs field φ subject to the boundary conditions

$$t \to \infty : \qquad \varphi \to \mu \phi_\zeta \,. \tag{14.4}$$

The puncture at $t = 0$ is not rotated and φ is required to be regular everywhere except $t = \infty$. At $t = \infty$ we therefore prescribe the asymptotics

$$t \to \infty : \qquad \varphi \sim \mu \Lambda t^{1/n} \mathrm{diag}\left(1, \omega, \omega^2, \cdots, \omega^{n-1}\right) + \cdots . \tag{14.5}$$

This constitutes a boundary value problem with bulk equations given by the BPS equations (13.26). Field theoretically, we are turning on a superpotential $W(\Phi) = \frac{\mu}{2} \mathrm{Tr}\,\Phi^2$ in the $\mathcal{N} = 2$ $\mathfrak{su}(n)$ SYM theory, where Φ is an $\mathcal{N} = 1$ chiral multiplet living inside the $\mathcal{N} = 2$ vector multiplet. This deformation has been studied before and one expects only those points in $\mathcal{N} = 2$ Coulomb branch to survive, where all A-cycles of the SW curve (14.2) pinch to develop a nodal singularity. It is known that there are n such points. Thus, we expect the existence of n solutions to (13.26) corresponding to the n points of the $\mathcal{N} = 2$ CB that are not lifted by the deformation (14.4).

Using (14.5), we deduce that

$$\begin{aligned} \mathrm{Tr}\,\varphi^k &= c_k \qquad 2 \leq k \leq n - 1 \\ \mathrm{Tr}\,\varphi^n &= n\mu^n \Lambda^n t + c_n \end{aligned} \tag{14.6}$$

The above form of the Casimirs is valid over the whole sphere $\mathcal{C}$ for some constants c_i. Thus we can write the spectral equation $\det(w - \varphi) = 0$ as

$$\mathcal{Q}(w) = w^n - \sum_{k=2}^{n} c_k w^{n-k} - \mu^n \Lambda^n t = 0 , \tag{14.7}$$

for some constants c_i.

14.3 Topological Factorization

As discussed in section 13.4, the solutions to the $\mathcal{N} = 1$ BPS equations (13.26) are curves $\Sigma_r \subset K_C \oplus \mathcal{O}_C(0)$ constituting n-fold coverings of $\mathcal{C}$. They are parametrized by λ, w and combine the spectral curves of the Higgs fields ϕ, φ into a single covering. Contracting with $\zeta = t\partial_t$ we equivalently study the n-fold coverings parametrized by v, w for the Higgs fields ϕ_ζ, φ. Crucially, the branch cut structures of the coordinates v, w are required to match as otherwise the sheets of the spectral curves for ϕ_ζ, φ can not be consistently combined into an

n-fold covering. This allows us to describe a set of curves, which are topologically consistent, thereby improving on the constraints in section 14.2. Which of these also holomorphically satisfy the BPS-equations is then determined by computation with an ansatz derived from the branch cut structure of the candidate curves.

We begin by deriving the generic branch cut structures for the coordinate v from the SW curve (14.2) and for the coordinate w from the curve (14.7). The coordinate v has in total two $\mathbb{Z}_n$ branch cuts emanating from the punctures at $t = 0, \infty$. The coordinate w has a single $\mathbb{Z}_n$ branch cut emanating from the rotated puncture at $t = \infty$. The number of branch points for each cover is given by the degree in t of the respective discriminants

$$\deg \Delta(\mathcal{P}, v) = 2n - 2\,, \qquad \deg \Delta(\mathcal{Q}, w) = n - 1\,. \tag{14.8}$$

Here $\Delta(\mathcal{P}, v)$ denotes the discriminant of the polynomial $\mathcal{P}$ with respect to the variable v. The branch points are given by the roots of (14.8). In the generic case, the discriminants (14.8) have isolated zeros and are associated with monodromy actions of order 2.

The SW curve is symmetric with respect to $t \to 1/t$ and the $2n - 2$ branch points come in pairs with identical monodromy action. We denote the cyclic permutation of the n sheets as $a \in S_n$ and the transposition of the i-th and j-th sheet by $b_{i,j} \in S_n$. The generic branch cut structure for the coordinates (v, w) can be described as:

$$(14.9)$$
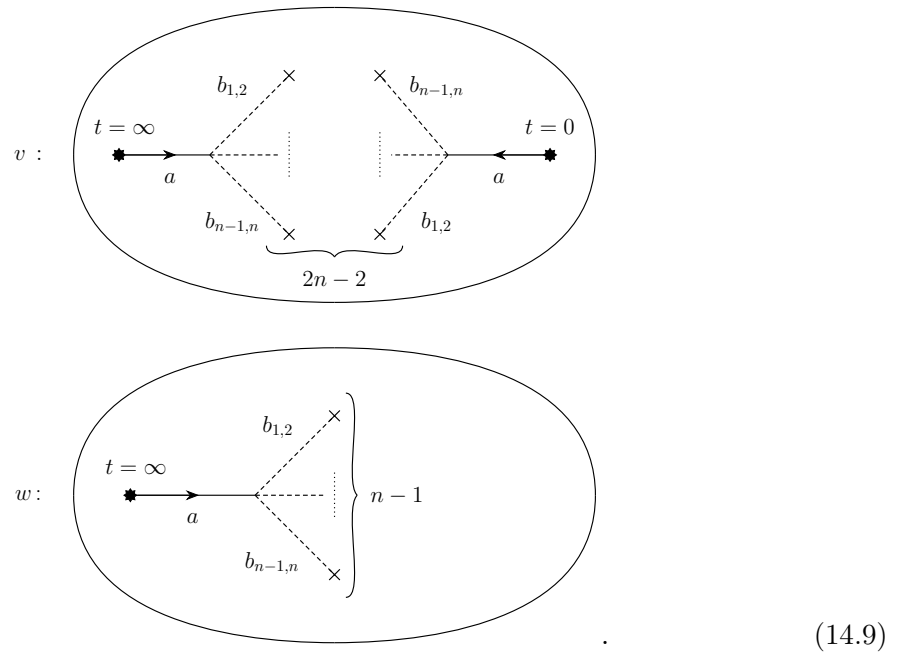
Now we implement the topological factorization condition. The CB moduli u_k and constants c_k must be tuned such that the branch cut structures of v, w coincide. The $n-1$ $\mathbb{Z}_2$-valued branch points of w must collide at $t=0$ to match the $\mathbb{Z}_n$ branch point of $\mathcal{P}(v)$ at $t=0$. After implementing this, the branch cut structures of v and w can be described as:

$$(14.10)$$
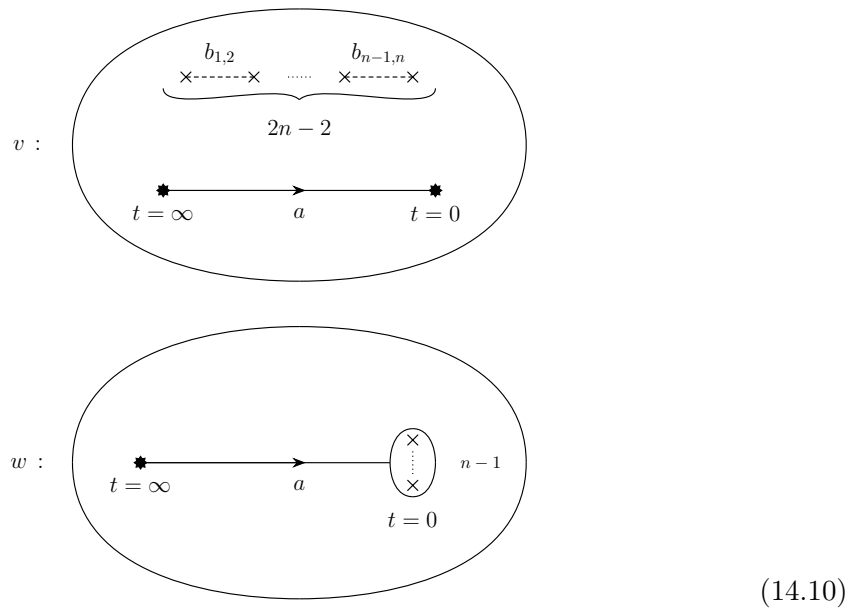
where we have rearranged the branch cuts for v to match with branch cuts of w at $t=0$ and $t=\infty$, and we have denoted the collision of $n-1$ branch points by a circle surrounding

the points. Since there are no more branch points for w, the v curve cannot have any monodromy at $t \neq 0, \infty$ either. Thus, we find that the $2n - 2$ $\mathbb{Z}_2$-valued branch points of v must collide in pairs, eliminating all branch cuts not terminating at punctures. The final configurations for v and w are as follows:

$$\tag{14.11}$$

Here we have denoted the collision of branch points by a circle enclosing them.

14.4 Holomorphic Factorization

The topology (14.11) for $\mathcal{P}(v), \mathcal{Q}(w)$ constrains the coefficients u_k, c_k in (14.2) and (14.7). It is known [142, 178] that the degeneration for v in (14.11) fixes the CB parameters such that $P_n^{(r)}(v) = 2\Lambda^n T_n^{(r)}(v/2\Lambda)$ with $T_n^{(r)}(x) = T_n(e^{2\pi i r/2n}x)$ where T_n is the n-th Chebyshev polynomial of the first kind. Due to the Weyl invariance $v \to -v$ this gives in total n physically distinct solutions. On the other hand, the degeneration for w in (14.11) fixes all $c_i = 0$, otherwise the n sheets for $\mathcal{Q}(w)$ cannot come together at $t = 0$. With this we find n distinct solutions for $\mathcal{P}(v), \mathcal{Q}(w)$ associated to the topological degeneration (14.11) at finite values of μ to be

$$P_n^{(r)}(v) - \Lambda^n \left(t + \frac{1}{t} \right) = 0 \,, \qquad w^n = \mu^n \Lambda^n t \tag{14.12}$$

parametrized by $r = 0, \ldots, n-1$. We solve these equations for v. First, for $r = 0$, we find $v = \Lambda \left(t^{1/n} + t^{-1/n} \right)$ which follows from the properties of the Chebyshev polynomials. For general r, we send $v \to v e^{2\pi i r / 2n}$ followed by a coordinate transformation $e^{\pi i r} t \to t$. This gives

$$v = \Lambda \left(t^{1/n} + \omega^r t^{-1/n} \right) , \tag{14.13}$$

where $\omega = \exp(2\pi i / n)$. We can pair the n values of v with n values of w by requiring

$$vw = \mu \Lambda^2 \left(t^{2/n} + \omega^r \right) . \tag{14.14}$$

Overall we find

$$\begin{aligned} v &= \Lambda \left(t^{1/n} + \omega^r t^{-1/n} \right) \\ w &= \mu \Lambda t^{1/n} \end{aligned} , \tag{14.15}$$

where the n different values of $t^{1/n}$ parametrize the n sheets of the $\mathcal{N} = 1$ curve Σ_r. In total, we have n different $\mathcal{N} = 1$ curves corresponding to the n different vacua of the rotated $\mathcal{N} = 1$ theory. The curves of these n vacua are related via Dehn twists. Consider the pairing condition (14.13) near $t = 0$ where it reads $vw = \mu \Lambda^2 \omega^r$. Going between the r-th and $(r+1)$-th vaccum the pairing between the sheets is cyclically permuted. From $w = \mu \Lambda t^{1/n}$ we see that this shift can be realized by circling once around origin. It follows that the branch cuts of curves associated with neighbouring vacua are related by a Dehn twist and we therefore depict the branch cut structure of the curve Σ_r as:

$$\tag{14.16}$$
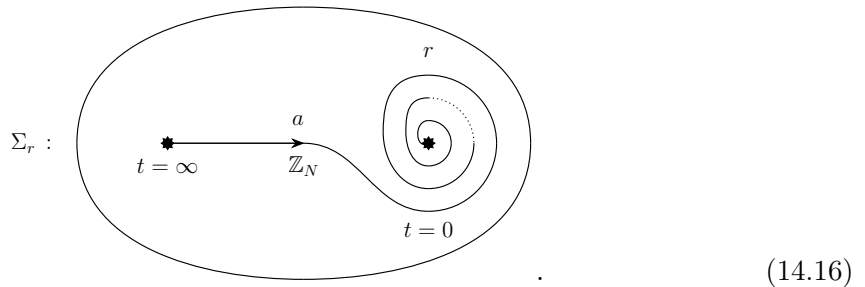
The v-curve becomes singular and displays double points at those points in the CB that admit rotation (14.11). These singularities are removed in the $\mathcal{N} = 1$ curve as the double points are resolved to two points with distinct w-coordinates. The difference of the value

for w between these points encodes the vev of glueball superfield [52, 138, 140]. We redefine the coordinates to make this dimensionally manifest

$$v \;\to\; v/\Lambda\,, \qquad w \;\to\; w\Lambda\,, \tag{14.17}$$

and introduce the $\mathcal{N}=1$ strong coupling scale $\Lambda^3_{\mathcal{N}=1} = \mu\Lambda^2$. The new coordinates (v, w) carry charges $(0, 2)$ under the $\mathbb{Z}_{2N}$ R-symmetry and are of mass dimension $(0, 3)$. The former now makes the cyclic rotation between the sheets paired in (14.16) clear, as the vacua are manifestly rotated into each other by the R-symmetry. Further we make the redefinition $v \to v - t^{1/n}$ and find

$$v^n = t\,, \qquad w^n = \Lambda^{3n}_{\mathcal{N}=1}t\,, \qquad vw = \Lambda^3_{\mathcal{N}=1}\omega^r \tag{14.18}$$

giving the n curves described in [175]. Taking the limit $\mu \to \infty$ keeping $\Lambda_{\mathcal{N}=1}$ constant we are left with 4d $\mathcal{N}=1$ $\mathfrak{su}(n)$ SYM [138]. Crucially the branch cut structure of the associated $\mathcal{N}=1$ curves is not altered from (14.16) which correctly captures the topology of the $\mathcal{N}=1$ curves associated with each SYM vacuum.

14.5 Line Operators and Confinement from the Curve

To discuss 1-form symmetry preserved in each of the n vacua, we need to first choose a polarization $\Lambda \subset \mathcal{L}$ which determines the 1-form symmetry group $\widehat{\Lambda}$ of the absolute UV theory. Recall that for pure $\mathfrak{su}(n)$ SYM we have

$$\mathcal{L} \simeq \mathbb{Z}_n \times \mathbb{Z}_n\,. \tag{14.19}$$

The two factors are generated by W and H, respectively, with the pairing

$$\langle W, W \rangle = \langle H, H \rangle = 0\,, \qquad \langle W, H \rangle = \frac{1}{n}\,. \tag{14.20}$$

Let us choose Λ such that it contains Wilson line operators ikW with $i \in \{0, 1, \cdots, l-1\}$ where $1 \le k, l \le n$ are integers such that $kl = n$. Then the gauge group of the corresponding absolute theory is

$$G = SU(n)/\mathbb{Z}_k\,. \tag{14.21}$$

where $\mathbb{Z}_k$ is the order k subgroup of the center $\mathbb{Z}_n$ of the simply connected group $SU(n)$ associated to the gauge algebra $\mathfrak{g} = \mathfrak{su}(n)$. To make Λ maximal, we can add to it the line operator $lH + mW$ where $m \in \{0, 1, \cdots, k-1\}$ is known as the discrete theta parameter associated to the absolute theory. Then

$$\Lambda = [kW, lH + mW] \subset \mathcal{L} \tag{14.22}$$

is the subgroup of $\mathcal{L}$ generated by kW and $lH + mW$.

The group structure of polarisation Λ can be obtained by computing the Smith normal form of the following matrix associated to the generators of Λ

$$M_{klm} = \begin{pmatrix} k & 0 \\ m & l \end{pmatrix}. \tag{14.23}$$

A diagonal matrix D is the Smith normal form of M_{klm} if we find invertible integral matrices S, T such that if $SM_{klm}T = D$. The form of D is fixed to be $D = \mathrm{diag}(d, N/d)$. We find that $d = \gcd(k, l, m)$ and correspondingly

$$\Lambda \cong \mathbb{Z}_d \times \mathbb{Z}_{n/d} \tag{14.24}$$

is the group structure of Λ.

Now we compute the line operators $\mathcal{I}_r$ exhibiting perimeter law in vacuum r from the topological structure (14.16) of the associated $\mathcal{N} = 1$ curve Σ_r. We can see that we need to encircle a puncture n times to obtain a cycle on Σ_r implying that nW exhibits perimeter law, but $nW = 0$ in $\mathcal{L}$. On the other hand, following the branch cut, we see that $H + rW$ exhibits perimeter law, which is a non-trivial element of $\mathcal{L}$. Thus, $\mathcal{I}_r = [H + rW]$ is the subgroup of $\mathcal{L}$ generated by $H + rW$. The intersection $\Lambda_r = \mathcal{I}_r \cap \Lambda$ determines the line operators of the chosen absolute theory that exhibit perimeter law and we can compute it to be

$$\Lambda_r \cong \mathbb{Z}_{b_r}, \tag{14.25}$$

where $b_r = \gcd(k, m - lr)$. The 1-form symmetry group $\mathcal{O}_r$ preserved in r-th vacuum is now given by the Pontryagin dual of Λ/Λ_r and crucially depends on the embedding $\iota_r : \Lambda_r \cong \mathbb{Z}_{b_r} \hookrightarrow \mathbb{Z}_d \times \mathbb{Z}_{n/d} \cong \Lambda$.

To compute $\mathcal{O}_r$ we denote the order $d, n/d$ generators of Λ by F, G respectively. Then we have the relation of bases $(F, G) = DT^{-1}(W, H)$. From (14.25) we find the generator of Λ_r to be $B_r = (n/b_r)(H + rW)$. We expand this generator as $B_r = p_r F + q_r G$ with coefficients $(p_r, q_r) \in \mathbb{Z}_d \times \mathbb{Z}_{n/d}$. These coefficients follow in turn from $(p_r, q_r) = (n/b_r)(r, 1)TD^{-1}$. The quotient Λ/Λ_r is computed using the Smith normal form (SNF) of the matrix

$$M_r = \begin{pmatrix} d & 0 \\ 0 & n/d \\ p_r & q_r \end{pmatrix} \xrightarrow{\text{SNF}} \begin{pmatrix} s_r & 0 \\ 0 & t_r \\ 0 & 0 \end{pmatrix}. \tag{14.26}$$

With this we find the 1-form symmetry group of the r-th vacuum to be

$$\mathcal{O}_r = \mathbb{Z}_{s_r} \times \mathbb{Z}_{t_r}, \tag{14.27}$$

where the integers s_r, t_r can be computed form the minors of M_r and are given by

$$s_r = \gcd\left(d, \frac{n}{d}, p_r, q_r\right), \qquad t_r = \gcd\left(n, \frac{np_r}{d}, dq_r\right). \tag{14.28}$$

Note that even if s_r, t_r agree for two different vacua they are physically distinct if the associated embeddings $\iota_r : \mathbb{Z}_{b_r} \hookrightarrow \mathbb{Z}_d \times \mathbb{Z}_{n/d}$ differ. The embedding ι_r is determined by $B_r \in \Lambda$, that is the confining properties of two vacua r_1, r_2 differ if and only if $B_{r_1} \neq B_{r_2}$.

Before ending with two examples we give a simplification of the formula (14.27) for the case of $d = 1$ often encountered at low rank. In this case $s_r = 1$ and from $p_r = 0$ and $q_r = n/b_r$ it follows

$$d = 1: \qquad \mathcal{O}_r = \mathbb{Z}_{t_r} \tag{14.29}$$

with $t_r = \gcd(n, n/b_r) = n/b_r = n/\gcd(k, m - lr)$.

Example: Consider the gauge algebra $\mathfrak{su}(4)$. There are seven different choices for the spectrum of line operators [133]

$$\begin{aligned}
SU(4) &: & \Lambda &= \mathbb{Z}_4 = [W] \\
SU(4)/\mathbb{Z}_2 &: & \begin{cases} SO(6)_+ : & \Lambda = \mathbb{Z}_2^{(1)} \times \mathbb{Z}_2^{(2)} = [2W, 2H] \\ SO(6)_- : & \Lambda = \mathbb{Z}_4 = [W + 2H] \end{cases} & \\
SU(4)/\mathbb{Z}_4 &: & \begin{cases} \left(SU(4)/\mathbb{Z}_4\right)_0 : & \Lambda = \mathbb{Z}_4 = [H] \\ \left(SU(4)/\mathbb{Z}_4\right)_1 : & \Lambda = \mathbb{Z}_4 = [W + H] \\ \left(SU(4)/\mathbb{Z}_4\right)_2 : & \Lambda = \mathbb{Z}_4 = [2W + H] \\ \left(SU(4)/\mathbb{Z}_4\right)_3 : & \Lambda = \mathbb{Z}_4 = [3W + H]. \end{cases} &
\end{aligned} \tag{14.30}$$

The line operators exhibiting perimeter law in each vacuum are given by the intersection $\mathcal{I}_r \cap \Lambda$ and computed mod 4 for $r = 0, 1, 2, 3$ respectively to be

$$
\begin{aligned}
SU(4) &: \quad \mathcal{I}_r \cap \Lambda = 0, 0, 0, 0 \\
SO(6)_+ &: \quad \mathcal{I}_r \cap \Lambda = [2H], [2W + 2H], [2H], [2W + 2H] \\
SO(6)_- &: \quad \mathcal{I}_r \cap \Lambda = 0, 0, 0, 0 \\
\left(SU(4)/\mathbb{Z}_4\right)_0 &: \quad \mathcal{I}_r \cap \Lambda = [H], 0, [2H], 0 \\
\left(SU(4)/\mathbb{Z}_4\right)_1 &: \quad \mathcal{I}_r \cap \Lambda = 0, [W + H], 0, [2W + 2H] \\
\left(SU(4)/\mathbb{Z}_4\right)_2 &: \quad \mathcal{I}_r \cap \Lambda = [2H], 0, [2W + H], 0 \\
\left(SU(4)/\mathbb{Z}_4\right)_3 &: \quad \mathcal{I}_r \cap \Lambda = 0, [2W + 2H], 0, [3W + H] \,.
\end{aligned}
\tag{14.31}
$$

The 1-form symmetry preserved in each vacuum is given by the Pontryagin dual of the quotient $\Lambda / (\mathcal{I}_r \cap \Lambda)$

$$
\begin{aligned}
SU(4) &: \quad \mathcal{O}_r = \mathbb{Z}_4 \\
SO(6)_+ &: \quad \mathcal{O}_r = \mathbb{Z}_2^{(1)}, \mathbb{Z}_2^{(3)}, \mathbb{Z}_2^{(1)}, \mathbb{Z}_2^{(3)} \\
SO(6)_- &: \quad \mathcal{O}_r = \mathbb{Z}_4 \\
\left(SU(4)/\mathbb{Z}_4\right)_0 &: \quad \mathcal{O}_r = 0, \mathbb{Z}_4, \mathbb{Z}_2, \mathbb{Z}_4 \\
\left(SU(4)/\mathbb{Z}_4\right)_1 &: \quad \mathcal{O}_r = \mathbb{Z}_4, 0, \mathbb{Z}_4, \mathbb{Z}_2 \\
\left(SU(4)/\mathbb{Z}_4\right)_2 &: \quad \mathcal{O}_r = \mathbb{Z}_2, \mathbb{Z}_4, 0, \mathbb{Z}_4 \\
\left(SU(4)/\mathbb{Z}_4\right)_3 &: \quad \mathcal{O}_r = \mathbb{Z}_4, \mathbb{Z}_2, \mathbb{Z}_4, 0 \,.
\end{aligned}
\tag{14.32}
$$

Here $\mathbb{Z}_2^{(3)}$ is the diagonal subgroup of $\mathbb{Z}_2^{(1)} \times \mathbb{Z}_2^{(2)}$. The 1-form symmetries of $\left(SU(4)/\mathbb{Z}_4\right)_k$ are cyclic permutations of each other induced by shifts of the theta angle $\theta \to \theta + 2\pi$.

Note that the $SO(6)_+$ theory is obtained from the $SU(4)$ theory by gauging the $\mathbb{Z}_2$ subgroup of the $\mathbb{Z}_4$ 1-form symmetry of the $SU(4)$ theory. The resulting $\mathbb{Z}_2 \times \mathbb{Z}_2$ 1-form symmetry thus has a mixed anomaly [179], which is captured by the Bockstein of the extension $1 \to \mathbb{Z}_2 \to \mathbb{Z}_4 \to \mathbb{Z}_2 \to 1$. It would be interesting to see this anomaly from a direct reduction starting with the 6d anomaly polynomial.

Example: Consider the gauge algebra $\mathfrak{su}(12)$ with the polariztation $\Lambda = [6W, 4W + 2H]$. Using (14.24) we find $\Lambda \cong \mathbb{Z}_2 \times \mathbb{Z}_6$. The generators of each factor are $(F, G) = (6H, 4H + 2W)$. There are 12 vacua labelled by $r = 0, \ldots, 11$ and with respect to the basis F, G the generators of Λ_r have the coordinates

$$\left(\begin{array}{c|cccccccccccc} r & 0 & 1 & 2 & 3 & 4 & 5 & 6 & 7 & 8 & 9 & 10 & 11 \\ \hline p_r & 1 & 1 & 1 & 1 & 1 & 1 & 1 & 1 & 1 & 1 & 1 & 1 \\ q_r & 0 & 3 & 2 & 3 & 0 & 5 & 0 & 3 & 2 & 3 & 0 & 2 \end{array} \right) . \tag{14.33}$$

The 1-form symmetry $\mathcal{O}_r$ preserved in each vacuum now follows from appending the columns of (14.33) as a row to the diagonal matrix $\mathrm{diag}(2, 6)$ and computing the diagonal entries of its Smith normal form. The 1-form symmetries preserved in each vacuum are isomorphic to:

$$\begin{array}{c|cccccccccccc} r & 0 & 1 & 2 & 3 & 4 & 5 & 6 & 7 & 8 & 9 & 10 & 11 \\ \hline \mathcal{O}_r & \mathbb{Z}_6 & \mathbb{Z}_6 & \mathbb{Z}_2 & \mathbb{Z}_6 & \mathbb{Z}_6 & \mathbb{Z}_2 & \mathbb{Z}_6 & \mathbb{Z}_6 & \mathbb{Z}_2 & \mathbb{Z}_6 & \mathbb{Z}_6 & \mathbb{Z}_2 \end{array} . \tag{14.34}$$

The set of line operators displaying perimeter and area law differ for vacua with distinct (p_r, q_r) even if their confinement indices agree. As in the previous example, there is a mixed 1-form symmetry anomaly associated to the extension $1 \to \mathbb{Z}_6 \to \mathbb{Z}_{12} \to \mathbb{Z}_2 \to 1$ [180].

Chapter 15
Confinement Index in the Cachazo-Seiberg-Witten Set-up

In this section we consider another rotation of $\mathcal{N} = 2$ SYM with gauge algebra $\mathfrak{g} = \mathfrak{su}(n)$. This rotation corresponds to turning on a generic tree-level cubic superpotential for the $\mathcal{N} = 1$ adjoint chiral multiplet living in the $\mathcal{N} = 2$ vector multiplet

$$W(\Phi) = \frac{g}{3} \operatorname{Tr} \Phi^3 + \frac{\mu}{2} \operatorname{Tr} \Phi^2 . \tag{15.1}$$

We also briefly discuss rotations corresponding to generic superpotentials of higher order

$$W(\Phi) = \sum_{i=2}^{k} \frac{g_i}{i} \operatorname{Tr} \Phi^i , \tag{15.2}$$

for $k \leq n$, which are analyzed similarly. Properties of confinement were discussed in great detail for the latter case by Cachazo, Seiberg, Witten in [72]. Here we concentrate mainly on cubic superpotentials. Note that the mass dimension of g_i is negative for $i \geq 4$, so the higher order superpotentials are non-renormalizable and the resulting $\mathcal{N} = 1$ theory needs a UV cutoff to be well-defined (see the related discussion in section 13.3.3).

Field theoretically the confining properties of the theory after turning on these superpotentials was studied in [72], which we briefly review before turning to the main discussion deriving these properties from $\mathcal{N} = 1$ curves. Classical vacua are given by diagonal configurations of Φ with eigenvalues extremizing the superpotential. Classical vacua are therefore labelled by $k - 1$ integers $(n_1, n_2, \cdots, n_{k-1})$ (such that $n_1 + n_2 + \cdots + n_{k-1} = n$) counting the number of eigenvalues fixed to the $k - 1$ different critical points of the superpotential. In such a vacuum the gauge symmetry is broken as

$$\mathfrak{su}(n) \quad \rightarrow \quad \mathfrak{su}(n_1) \oplus \mathfrak{su}(n_2) \oplus \cdots \oplus \mathfrak{su}(n_{k-1}) \oplus \mathfrak{u}(1)^{k-2} \,. \tag{15.3}$$

At low energies the non-abelian factors decouple and individually confine, and the system settles in one of $n_1 n_2 \cdots n_{k-1}$ quantum vacua, leaving an abelian gauge theory. We label these vacua by integers $(r_1, r_2, \cdots, r_{k-1})$ where $r_i \in \{0, \ldots, n_i - 1\}$. The Wilson and 't Hooft lines W_i, H_i of each non-abelian factor $\mathfrak{su}(n_i)$ are identified as Wilson and 't Hooft lines W, H of the initial $\mathfrak{su}(n)$, which can be used to read the confining properties. We expect $n_i W_i, H_i + r_i W_i$ for each i to exhibit perimeter law, implying perimeter laws for $n_i W, H + r_i W$ for each i. Thus the set of lines exhibiting perimeter law in vacuum $(r_1, r_2, \cdots, r_{k-1})$ can be written as

$$\mathcal{I}_{r_1, r_2, \cdots, r_{k-1}} = [H + r_1 W, \gcd(n_1, n_2, \cdots, n_{k-1}, r_1 - r_2, r_2 - r_3, \cdots, r_{k-2} - r_{k-1}) W] \tag{15.4}$$

which is a subgroup of $\mathcal{L} \simeq \mathbb{Z}_n^W \times \mathbb{Z}_n^H$. The confining properties of each vacuum can now be determined once one chooses a polarization. For instance, if one chooses the purely electric polarization $\Lambda = \mathbb{Z}_n^W$, then the 1-form symmetry group preserved in vac-

uum $(r_1, r_2, \cdots, r_{k-1})$ is

$$\mathcal{O}_{r_1, r_2, \cdots, r_{k-1}} = \mathbb{Z}_t ; \qquad t = \gcd(n_1, n_2, \cdots, n_{k-1}, r_1 - r_2, r_2 - r_3, \cdots, r_{k-2} - r_{k-1}), \quad (15.5)$$

where t is known as the confinement index of the vacuum.

15.1 Constraints from Rotation to $\mathcal{N} = 1$

The starting point is the Seiberg-Witten curve for $\mathfrak{g} = \mathfrak{su}(n)$ $\mathcal{N} = 2$ SYM

$$\mathcal{P}(v) = \det(v - \phi_\zeta) = P_n(v) - \Lambda^n \left(t + \frac{1}{t} \right) = 0 . \tag{15.6}$$

Here ϕ_ζ denotes the contraction of the Higgs field ϕ with the vector $\zeta = t\partial_t$ and $P_n(v) = v^n + \sum_{i=2}^n u_i v^{n-i}$ with the u_i parametrizing the CB. Irregular punctures of type $\mathcal{P}_0$ are located at $t = 0, \infty$. The cubic superpotential (15.1) can be turned on by rotating the puncture at $t = \infty$ such that the Higgs field φ is subject to the boundary conditions

$$t \to \infty : \qquad \varphi \to g\phi_\zeta^2 + \mu\phi_\zeta . \tag{15.7}$$

The asymptotics of the Higgs field ϕ at the puncture $t = \infty$ read

$$t \to \infty : \qquad \phi_\zeta = \Lambda t^{1/n} \mathrm{diag} \left(1, \omega, \omega^2, \cdots, \omega^{n-1} \right) + \dots , \tag{15.8}$$

at the puncture $t = \infty$, which follows from (15.6). Here $\omega = \exp(2\pi i/n)$. The eigenvalues of ϕ_ζ grow as $\Lambda|t|^{1/n}$ whereby those of φ grow as $g\Lambda^2|t|^{2/n}$ as $t \to \infty$. This restricts the w-curve $\mathcal{Q}(w) = \det(w - \varphi) = 0$ to take the form

$$\mathcal{Q}(w) = w^n + bt^2 + t \sum_{k=0}^{\lfloor n/2 \rfloor} d_k w^k + \sum_{k=0}^{n-1} c_k w^k \tag{15.9}$$

for some complex constants b, c_k, d_k. The boundary condition (15.7) fixes the terms of maximal growth $\mathcal{O}(t^2)$, i.e., the coefficients $b, d_{n/2}$ or b when n is even or odd respectively. This follows by substituting the asymptotics (15.8) into the boundary condition (15.7) and collecting all terms of the w-curve which do not receive contributions from the lower order terms. For even n we find

$$\mathcal{Q}(w) = \left(w^{n/2} - g^{n/2}\Lambda^n t \right)^2 + t \sum_{k=0}^{n/2-1} d_k w^k + \sum_{k=0}^{n-1} c_k w^k , \tag{15.10}$$

while for odd n we have

$$\mathcal{Q}(w) = w^n - g^n \Lambda^{2n} t^2 + t \sum_{k=0}^{(n-1)/2} d_k w^k + \sum_{k=0}^{n-1} c_k w^k \,. \tag{15.11}$$

This form of the w-curve follows purely from the prescribed behavior of φ at the puncture $t = \infty$. We can improve on this ansatz for even n with $n_1 = n_2$ and $r_1 = r_2$ where a spontaneously broken R-symmetry is restored. While select, these cases display interesting screening effects, as seen from the confinement index (15.5). We finish this section with a discussion of this symmetry enhancement before improving on the above Ansätze by prescribing branch points and cuts away from the punctures.

The superpotential (15.1) has two critical points associated to $\mathfrak{su}(n_1)$ and $\mathfrak{su}(n_2)$ gauge algebras arising at low energies. The exchange of these two critical points is an R-symmetry of the theory[1] which acts on the quantum vacua by $n_1 \leftrightarrow n_2$ and $r_1 \leftrightarrow r_2$. Thus, this symmetry is spontaneously preserved only in the vacua characterized by $n_1 = n_2$ and $r_1 = r_2$. The symmetry changes the sign of v while leaving w invariant and we therefore expect the eigenvalues of φ to come in identical pairs. The w-curve must only have double roots and this improves the ansatz (15.10) to

$$\mathcal{Q}(w) = \left(w^{n/2} - g^{n/2} \Lambda^n t + \sum_{k=0}^{n/2-1} e_k w^k \right)^2 , \tag{15.12}$$

introducing the complex constants e_k. The sheets of the v-curve on the other hand must come in pairs related by the symmetry $v \leftrightarrow -v$, in particular there must be an involutive renumbering of the sheets which leaves the branch cuts structure invariant. The v-curve is an n-fold cover of the UV curve and the w-curve is an n-fold cover which degenerated to an $(n/2)$-fold cover as seen from the perfect square (15.12). We call latter as the reduced w-curve. By the above the branch cut structure of the reduced w-curve is the $\mathbb{Z}_2$ quotient of that of the v-curve.

---

[1] To see this, shift $v \to v - \mu/2g$ for which we have $W'(v) = gv^2 - \mu^2/4g$. The symmetry is now implemented by $v \to -v$ which changes the sign of the superpotential, and hence the symmetry is an R-symmetry.

15.2 Topological Factorization

We begin by determining the ramification structure of the generic v- and w-curves from (15.6) and (15.10) or (15.11). The v-curve has two $\mathbb{Z}_n$ branch cuts emanating from the punctures at $t = 0, \infty$. Further there are $\deg \Delta(\mathcal{P}, v) = 2n - 2$ branch points terminating $\mathbb{Z}_2$ branch cuts. The w curves (15.10), (15.11) have a single $\mathbb{Z}_n$ branch cut emanating from the rotated puncture at $t = \infty$. The discriminant $\Delta(\mathcal{Q}, w)$ has order

$$\deg \Delta(\mathcal{Q}, w) = \begin{cases} 2n - 3, & n \text{ even and } r_1 \neq r_2 \text{ whenever } n_1 = n_2 \\ 2n - 2, & n \text{ odd}, \end{cases} \tag{15.13}$$

which is equal to the number of branch points terminating $\mathbb{Z}_2$ branch cuts. The generic branch cut structure therefore takes the form

$$\tag{15.14}$$
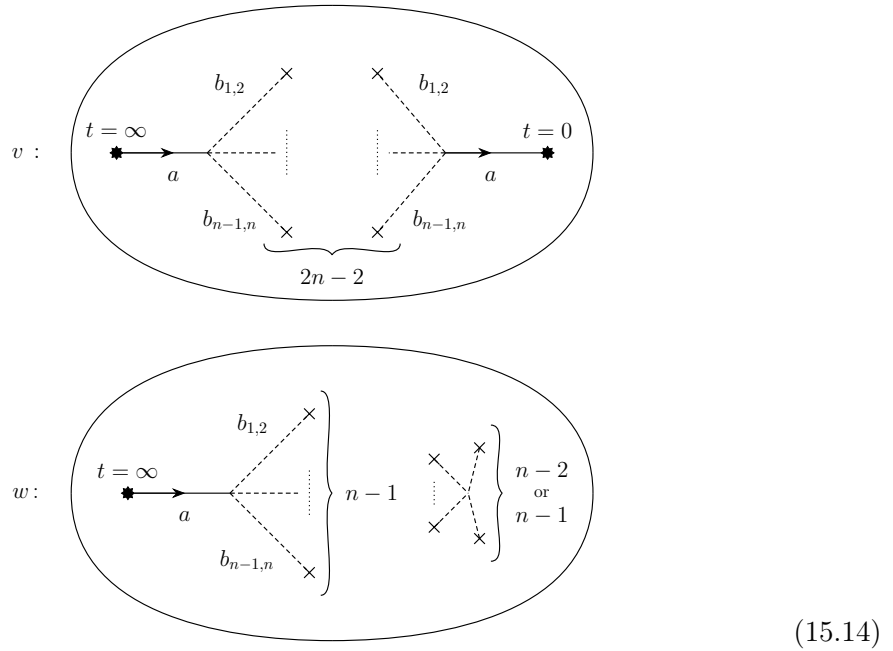
with $n - 2$ and $n - 1$ branch points not connected to $t = \infty$ in the w-curve for n even and odd respectively. When n is even and $n_1 = n_2$ and $r_1 = r_2$ the w-curve takes the form (15.12). We remove the doubling up of roots by considering the $(n/2)$-fold cover $\mathcal{Q}^{1/2}(w) = 0$ for which we find to have the branch cut structure:

$$, \qquad (15.15)$$

where $\tilde{a}$ denotes the cyclic permutation of the $n/2$ sheets and $\tilde{b}_{ij}$ a transposition of the i-th and j-th sheet.

We now implement the factorization condition topologically. The gauge symmetry breaking to $\mathfrak{su}(n_1) \oplus \mathfrak{su}(n_2) \oplus \mathfrak{u}(1)$ demands the presence of $n_1 + n_2 - 2 = n - 2$ mutually local massless monopoles. We need to restrict to the CB sublocus on which the SW curve degenerates to genus one (here φ can be turned on). Therefore this condition is addressed at the level of the v-curve and met by colliding all but one pair of branch points of the v-curve, which are related by the $t \leftrightarrow 1/t$, at $t = \pm 1$. When n is even/odd there are three/two possibilities for the number of branch points colliding in at $t = \pm 1$. This follows from considering the limit $\Lambda \to 0$, which does not change the topology of the SW curve (or the $\mathcal{N} = 1$ curve after rotation). In this limit the dynamics of the $\mathfrak{su}(n_i)$ factors decouple and each subsector is described by its own SW curve $\mathcal{P}_{n_i} = P_{n_i}(v) - \Lambda^{n_i}(t + 1/t) = 0$. The polynomials $P_{n_i}(v)$ are the Chebyshev polynomials. The discriminant of these SW curves then takes the form

$$\Delta(\mathcal{P}_{n_i}, v) \sim (t+1)^{2k_{i,-}}(t-1)^{2k_{i,+}} , \qquad (15.16)$$

where $k_{i,-} = k_{i,+} + 1 = n_i/2$ and $k_{i,-} = k_{i,+} = (n_i - 1)/2$ for even and odd n_i, respectively For example when $n_i = 2, 3, 4$ we have $k_{i,-} = 1, 1, 2$ and $k_{i,+} = 0, 1, 1$ respectively. Here $k_{i,\pm}$ denotes the number of branch points collided at $t = \pm 1$. Naively this suggests that a given partition $n = n_1 + n_2$ fixes the number of branch points collided at $t = \pm 1$ to $k_\pm = k_{1,\pm} + k_{2,\pm}$. However taking the chiral symmetry $t \to -t$ and $\Lambda^n \to -\Lambda^n$ of the $\mathfrak{su}(n)$ theory into account we find that for every factorization of the discriminant $\Delta(\mathcal{P}, v)$ characterized by (k_+, k_-) there must also exist one with (k_-, k_+) in the $\mathcal{N} = 2$ CB as the

chiral symmetry maps $k_+ \leftrightarrow k_-$. Therefore the discriminant of the rank n SW curve takes one of the three possible forms

$$\Delta(\mathcal{P}, v) \sim \begin{cases} (t+1)^{n/2}(t-1)^{n/2-1} \\ (t+1)^{n/2}(t-1)^{n/2} \\ (t+1)^{n/2-1}(t-1)^{n/2} \end{cases} \tag{15.17}$$

for even n, while taking one of the two forms

$$\Delta(\mathcal{P}, v) \sim \begin{cases} (t+1)^{(n-3)/2+1}(t-1)^{(n-3)/2} \\ (t+1)^{(n-3)/2}(t-1)^{(n-3)/2+1} \end{cases} \tag{15.18}$$

for odd n along loci of complex dimension one in the $\mathcal{N} = 2$ CB at which the gauge symmetry enhances to $\mathfrak{su}(n_1) \oplus \mathfrak{su}(n_2) \oplus \mathfrak{u}(1)$. These loci are not irreducible in general. However, in low rank examples with gauge algebra $\mathfrak{g} = \mathfrak{su}(3), \mathfrak{su}(4)$ we have precisely $2, 3$ such irreducible subloci characterized by (15.18), (15.17), respectively.

When the unbroken gauge symmetry is $\mathfrak{su}(n_1) \oplus \mathfrak{su}(n_2) \oplus \mathfrak{u}(1)$ the deformed $\mathcal{N} = 1$ gauge theory has $n_1 n_2$ vacua. Each such vacuum is associated with an $\mathcal{N} = 1$ curve which in turn follows from a rotation of the v-curve described above. Different v-curves are related by partial Dehn twists, which result from movements of branch-points on the base curve. This follows again from studying the topology of the SW curve in the limit $\Lambda \to 0$, where the dynamics of the $\mathfrak{su}(n_i)$ factors decouple. There are $n_i - 1$ massless monopoles associated with each factor and correspondingly $n_i - 1$ pairs of branch points colliding at $t = \pm 1$. These are in correspondence with a subset of the branch points of the full $\mathfrak{su}(n)$ theory. The problem essentially factorizes and we can determine for each $\mathfrak{su}(n_i)$ the set of branchpoint movements associated to different Dehn twists, and then superpose them.

We therefore need to understand the movement of the branch points for the Chebyshev polynomials when going between the monopole points of the $\mathfrak{su}(n_i)$ SW curve via the phase rotation $v \to e^{\pi i / n_i} v$. These are precisely the Dehn twists discussed in chapter 14.

Consider the v-curve preparing the rotation to the vacuum labelled $(r_1, r_2) = (0, 0)$ with the integer double (n_1, n_2). We have the branch cut structure

$$, \tag{15.19}$$

where b_{n_1} and b_{n_2} act via cyclic permutation on the first n_1 and last n_2 sheets respectively, i.e., the central branch lines are commuting and of monodromy type $\mathbb{Z}_{n_1}$ and $\mathbb{Z}_{n_2}$. The branch lines connecting to $t = c, 1/c$ are $\mathbb{Z}_2$ branch lines. For clarity we depict (15.19) once more, now labelling the branch cuts by their monodromy subgroups

$$. \tag{15.20}$$

From (15.19) we generate a total of $n_1 n_2$ branch cut structures, labelled by integers (r_1, r_2), by wrapping the $\mathbb{Z}_{n_1}$ and $\mathbb{Z}_{n_2}$ branch lines r_1 and r_2 times around the vertical equator of the UV curve respectively. We call the move individually increasing or decreasing r_1, r_2 by one a positive or negative partial Dehn twist respectively, while the move simultaneously increasing or decreasing r_1, r_2 by one is referred to as an overall positive or negative Dehn twist respectively. For instance, the $(1, 0)$ and $(0, 1)$ configurations respectively are

$$(15.21)$$

where the dotted lines depict a branch cut wrapping around the twice punctured sphere C. Wrapping the $\mathbb{Z}_{n_i}$ branch line n_i times around the sphere the n_i loops can be stacked and trivialize, i.e., we have the equivalence of configurations $(r_1, r_2) \sim (r_1+n_1, r_2) \sim (r_1, r_2+n_2)$ for a given partition $n = n_1+n_2$. Therefore we restrict to the labels to run as $r_i = 0, \ldots, n_i-1$ and for every partition $n = n_1 + n_2$ we therefore have $n_1 n_2$ branch cut structures of the type

$$(15.22)$$

We turn to the w-curve. The branch points of the generic w-curve (15.14) must be moved to match the branch cut structure of the v-curve (15.22). The v-curve has a $\mathbb{Z}_n$ branch line terminating at $t = 0$. The w-curve is therefore required to have a branch point at $t = 0$ similarly terminating a $\mathbb{Z}_n$ branch line. This follows by colliding branch points on the lhs of (15.14) at $t = 0$. This move is realized by setting $c_k = 0$ in (15.10) and (15.11) improving

the ansätze for the w-curve to

$$\mathcal{Q}(w) = w^n + g^n \Lambda^{2n} t^2 - 2g^{n/2} \Lambda^n w^{n/2} t + \sum_{k=0}^{n/2-1} d_k w^k t \qquad (15.23)$$

for even n and to

$$\mathcal{Q}(w) = w^n - g^n \Lambda^{2n} t^2 + \sum_{k=0}^{\lceil n/2 \rceil - 1} d_k w^k t \qquad (15.24)$$

for odd n as otherwise total ramification at $t = 0$ is not possible. For cases with $n_1 = n_2$ and $r_1 = r_2$ this move sets $e_k = 0$ in (15.12) which fully fixes the curve to

$$\mathcal{Q}(w) = \left(w^{n/2} - g^{n/2} \Lambda^n t \right)^2. \qquad (15.25)$$

The remaining $\lceil n/2 \rceil$ complex constants d_k in (15.23) and (15.24) are determined, up to discrete choices, by colliding all but a pair of the $n - 2$ or $n - 1$ branch points shown on the rhs in (15.14) and moving the two unpaired branch points to $t = c, 1/c$. The former fixes $\lceil n/2 \rceil - 2$ parameters and the latter the remaining 2. For a given v-curve with branch points at $t = c, 1/c$ we must pick the w-curve with the same branch cut structures of this discrete set of solutions. This finally determines the unique w-curve to a given v-curve, both share the branch cut structure shown in (15.22). In the cases with $n_1 = n_2$ and $r_1 = r_2$ the w-curve (15.15) however simply takes the form
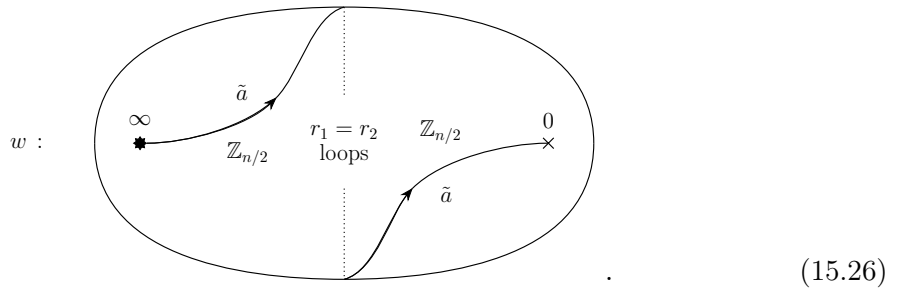
$$\qquad (15.26)$$

This w-curve is the $\mathbb{Z}_2$ quotient of the corresponding v-curve (15.22) via identification of the sheets related through the unbroken $\mathbb{Z}_2$ R-symmetry.

The $\mathcal{N} = 1$ curve is now the diagonal of the v, w-curves. If both curves are given by (15.22) the $\mathcal{N} = 1$ curve is given by the n pairs (v_i, w_i) sweeping out its i-th sheet. For

the cases with $n_1 = n_2$ and $r_1 = r_2$ with v-curve (15.22) and w-curve (15.26), the $\mathbb{Z}_2$ R-symmetry maps the j-th sheet of the v-curve to the $\tilde{j}$-th sheet where we number the sheets as $j = 1, \ldots, n/2$ and $\tilde{j} = n/2 + 1, \ldots, n$. The $\mathcal{N} = 1$ curve in these cases is given by the two sets of $n/2$ pairs (v_j, w_j) and $(v_{\tilde{j}}, w_j)$. In both cases the $\mathcal{N} = 1$ curve is an n-fold cover of the UV curve.

15.3   Line Operators, Confinement and Higher-order Superpotentials

Consider the CSW $\mathcal{N} = 1$ curve associated to the (r_1, r_2) vacuum for partition $n = n_1 + n_2$ given by

$$\text{(15.27)}$$

We now determine, using the curve (15.27) and following the procedure of section 13.5, the set $\mathcal{I}_{r_1,r_2}$ of line operators that would exhibit perimeter law in the $\mathcal{N} = 1$ vacuum described by the curve (15.27). The central $\mathbb{Z}_{n_1}, \mathbb{Z}_{n_2}$ monodromy actions commute and act on a disjoint set of sheets. Starting from a point lying along the equator and on the sheet acted upon by the $\mathbb{Z}_{n_i}$ action, we return to the same sheet if we go around the equator n_i times. Thus $n_i W \in \mathcal{I}_{r_1,r_2}$ for $i = 1, 2$. Now, start from the puncture at infinity from a sheet acted upon by the $\mathbb{Z}_{n_1}$ action, and follow the $\mathbb{Z}_n, \mathbb{Z}_{n_1}$ branch cuts to reach the puncture at $t = 0$. On this path, one is allowed to cross the $\mathbb{Z}_{n_2}$ branch cut, but not the $\mathbb{Z}_n, \mathbb{Z}_{n_1}, \mathbb{Z}_2$ branch cuts. Since $\mathbb{Z}_{n_2}$ does not act on this sheet, one remains on the same sheet and obtains a cycle on the $\mathcal{N} = 1$ curve Σ_{r_1,r_2} which projects to the cycle $H + r_1 W$ on the UV curve $\mathcal{C}$. Similarly, there is a cycle on Σ_{r_1,r_2} which projects onto the cycle $H + r_2 W$ on $\mathcal{C}$. Thus, in total,

$$\mathcal{I}_{(r_1,r_2)} = [n_1 W, n_2 W, H + r_1 W, H + r_2 W] = [H + r_1 W, \gcd(n_1, n_2, r_1 - r_2) W] \quad (15.28)$$

matching the field theory expectation (15.4).

In a similar fashion, one can study the theory deformed by a general higher-order super-potential (15.2). This deformation can be achieved by performing the rotation

$$t \to \infty : \qquad \varphi \to \sum_{i=2}^{k} g_i \phi_\zeta^{i-1} \,. \qquad (15.29)$$

Consider a vacuum specified by the partition $n_1 + n_2 + \cdots + n_{k-1} = n$ and integers $(r_1, r_2, \cdots, r_{k-1})$ with $r_i \in \{0, \ldots, n_i - 1\}$. The $\mathcal{N} = 1$ curve $\Sigma_{r_1, r_2, \cdots, r_{k-1}}$ has the following branch cut structure
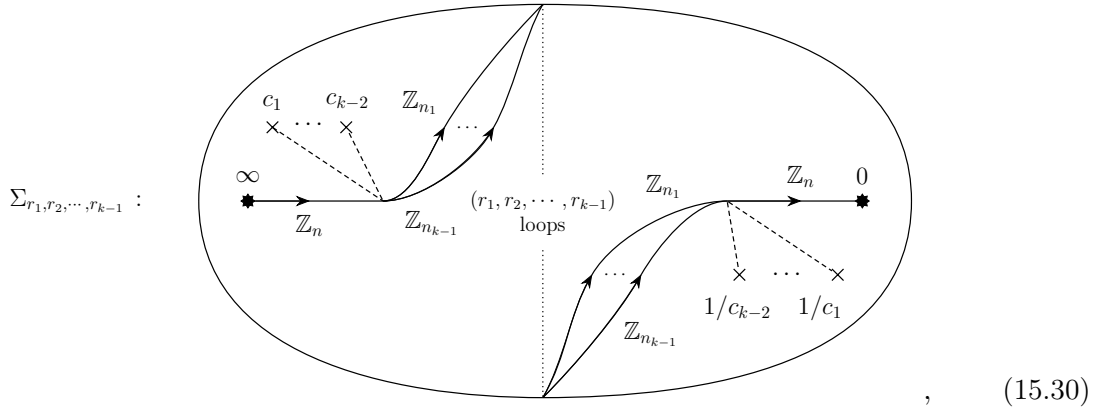
where dashed lines carry (in general, different) $\mathbb{Z}_2$ monodromies whose associated branch cuts combine with the $\mathbb{Z}_n$ branch line and split it into $\mathbb{Z}_{n_i}$ branch lines with each $\mathbb{Z}_{n_i}$ acting on mutually different n_i number of sheets. The $\mathbb{Z}_{n_i}$ branch line wraps the sphere r_i number of times along the equator. The branch points at c_i and $1/c_i$ carry the same $\mathbb{Z}_2$ monodromy.

Let us study the cycles on this $\mathcal{N} = 1$ curve. If we start at a point on equator and along a sheet acted upon by the $\mathbb{Z}_{n_i}$ line, then traversing the equator n_i times brings us back to the same sheet. Thus $n_i W$ exhibits perimeter law for each i. Moreover, starting at $t = \infty$ along a sheet acted upon by $\mathbb{Z}_{n_i}$ and running along the $\mathbb{Z}_n$ branch line and $\mathbb{Z}_{n_i}$ branch line to reach $t = 0$, we obtain the cycle $H + r_i W$, which implies that the associated line exhibits perimeter law. The full set of line operators exhibiting perimeter law can be written as

$$\mathcal{I}_{r_1, r_2, \cdots, r_{k-1}} = [H + r_1 W, \gcd(n_1, n_2, \cdots, n_{k-1}, r_1 - r_2, r_2 - r_3, \cdots, r_{k-2} - r_{k-1})W] \quad (15.31)$$

matching the field theory expectation (15.4).

Chapter 16
Confinement in Non-Lagrangian Theories

Because of the lack of available tools, confinement is typically studied only in Lagrangian theories. The main advantage of the method outlined in this thesis part is that it allows to study confinement for $\mathcal{N} = 1$ deformations of Class S theories, which are typically non-Lagrangian. Thus, in this section, we discuss a class of non-Lagrangian theories and apply our method to show that they contain vacua exhibiting confinement.

We discuss an infinite class of such theories. The simplest theory in this class is related to the famous E_6 Minahan-Nemeschansky theory. More precisely, it is an $\mathcal{N} = 1$ deformation of the asymptotically conformal 4d $\mathcal{N} = 2$ theory obtained by gauging an $\mathfrak{su}(3)^3$ subalgebra of the $\mathfrak{e}_6$ flavor algebra of the E_6 Minahan-Nemeschansky SCFT. Other examples in the class are $\mathcal{N} = 1$ deformations of the asymptotically conformal 4d $\mathcal{N} = 2$ theory obtained by gauging $\mathfrak{su}(n)^n$ flavor symmetry of the 4d $\mathcal{N} = 2$ SCFT obtained by gluing $n - 2$ copies of T_n trinions, or in other words, the 4d $\mathcal{N} = 2$ SCFT obtained by compactifying A_{n-1} $(2,0)$ theory on a sphere with n maximal regular untwisted punctures.

The first few subsections are devoted to the $n = 3$ example, while the last subsection discusses briefly the generalization to general n.

16.1 The 4d $\mathcal{N} = 2$ Set-up: Sphere with three $\mathcal{P}_0$ Punctures

Consider compactification of 6d $\mathcal{N} = (2,0)$ theory of type A_{n-1} on a sphere with three irregular punctures of type $\mathcal{P}_0$. We will refer to these theories by $\mathfrak{P}_{n,3}$, and more generally we define

$$\mathfrak{P}_{n,\alpha} = \text{6d } (2,0) \ A_{n-1} \text{ theory on a sphere with } \alpha \text{ irregular } \mathcal{P}_0 \text{ punctures}. \qquad (16.1)$$

Though our interest is in the case $n = 3$, we keep n general in this subsection. This constructs a 4d $\mathcal{N} = 2$ theory described by a quiver of the form

$$\mathfrak{P}_{n,3}: \qquad\qquad T_n \tag{16.2}$$

i.e., the T_n theory with its $\mathfrak{su}(n)^3$ flavor symmetry gauged and no additional matter. For $n = 3$, the T_3 theory is the same as the E_6 Minahan-Nemeschansky theory.

Placing the punctures at $t = 0, 1, \infty$ the v-curve takes the form

$$\mathcal{P}(v) = v^n - \sum_{k=1}^{n-2} \frac{P_{n-k}(t)v^k}{(t-1)^{n-k}} - \frac{P_{n+3}(t)}{t(t-1)^{n+1}} = 0, \tag{16.3}$$

where the polynomials $P_k(t)$ are polynomial of degree k. These contain

$$3 + 3(n-1) + \frac{(n-2)(n-1)}{2} \tag{16.4}$$

complex parameters with $3(n-1)$ of them being the CB parameters associated to the three $\mathfrak{su}(n)$ gauge algebras, $(n-2)(n-1)/2$ of them being the CB parameters associated to the T_n theory, and 3 of them being mass parameters associated to the strong-coupling scales of the three $\mathfrak{su}(n)$ gauge algebras which can be identified via the asymptotics

$$t \to 0: \qquad \phi_\zeta \sim \Lambda_0 \, t^{-1/n} \mathrm{diag}\left(1, \omega, \omega^2, \cdots, \omega^{n-1}\right) + \cdots$$

$$t \to 1: \qquad \phi_\zeta \sim \Lambda_1 \, (t-1)^{-(n+1)/n} \mathrm{diag}\left(1, \omega, \omega^2, \cdots, \omega^{n-1}\right) + \cdots. \tag{16.5}$$

$$t \to \infty: \qquad \phi_\zeta \sim \Lambda_\infty \, t^{1/n} \mathrm{diag}\left(1, \omega, \omega^2, \cdots, \omega^{n-1}\right) + \cdots$$

From this we learn

$$\Lambda_0^n = (-1)^{n+1} P_{n+3}(0), \qquad \Lambda_1^n = (-1)^{n+1} P_{n+3}(1), \qquad \Lambda_\infty^n = \left.\frac{P_{n+3}(t)}{t^{n+3}}\right|_{t=\infty}. \tag{16.6}$$

Let us now turn to the study of the defect group of line operators in this 4d $\mathcal{N} = 2$ theory. Inserting the surface defect $f \in \widehat{Z} \simeq \mathbb{Z}_n$ along the cycles encircling the three punctures gives rise to three line operators W_i, and inserting f along cycles stretching between the three punctures gives rise to line operators H_{ij}, as shown below

$$. \tag{16.7}$$

W_i can be identified with the Wilson line associated to $\mathfrak{su}(n)_i$ and H_{ij} can be identifed with 't Hooft line $H_i - H_j$ where H_i is the 't Hooft line associated to $\mathfrak{su}(n)_i$. These lines are not independent but sum to zero

$$W_1 + W_2 + W_3 = 0\,, \qquad H_{21} + H_{32} + H_{13} = 0\,. \tag{16.8}$$

Thus the defect group is

$$\mathcal{L} = \{W_i, H_{jk}\} / \{W_1 + W_2 + W_3 = 0, H_{21} + H_{32} + H_{13} = 0\}\,. \tag{16.9}$$

The pairing on these line operators is

$$\langle W_i, H_{ij} \rangle = 1/n\,, \qquad \langle W_j, H_{ij} \rangle = -1/n\,, \tag{16.10}$$

and zero otherwise. One can choose various polarizations, but we will be particularly concerned with the purely electric polarization $\Lambda = \{W_i\} / \{W_1 + W_2 + W_3 = 0\}$ which corresponds to choosing the global form of the gauge symmetry groups to be $SU(n)_i$ for each i. The 1-form symmetry group for this polarization is $\widehat{\Lambda} \simeq \mathbb{Z}_n \times \mathbb{Z}_n$.

16.2 Rotating to $\mathcal{N} = 1$: $\mathfrak{P}_{3,3}$

We now deform the $n = 3$ version of the above discussed $\mathcal{N} = 2$ theory to $\mathcal{N} = 1$, which is the theory $\mathfrak{P}_{3,3}$ defined in (16.1). We do this by rotating the two punctures at $t = 0, \infty$. The specific form of the rotation is discussed later. This rotation is only possible at certain points in the CB of $\mathcal{N} = 2$ vacua, whose branch cut structure we first discuss. At a generic point in the CB, the v-curve (16.3) has 12 branch points of $\mathbb{Z}_2$ monodromy. Thus, we can

represent the branch cut structure as

$$\tag{16.11}$$
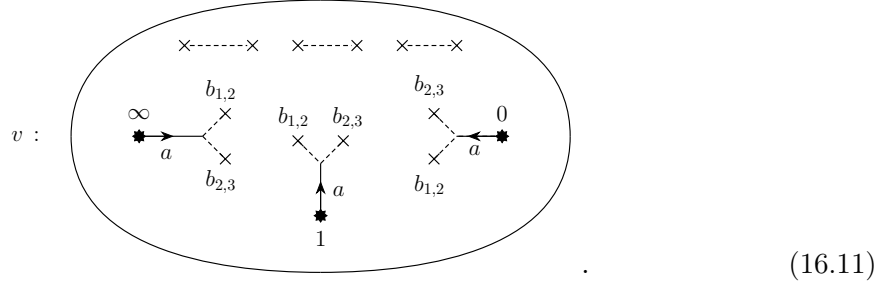
The CB vacua that survive are obtained by colliding the two sets of 6 branch points together at $t = t_1, t_2$ with the v-curve being The v-curve after taking the above limit is written as

$$v^3 - \Lambda^3 \frac{(t - t_1)^3 (t - t_2)^3}{t(t-1)^4} = 0 \,. \tag{16.12}$$

From this we see that all the CB parameters have been fixed, and the scale Λ and the locations t_1, t_2 of collided branch points are determined in terms of Λ_i computed in (16.6). There is no monodromy as one encircles the two points t_1 and t_2, while the three punctures still have a $\mathbb{Z}_3$ monodromy. Thus the branch cut structure has to be

$$\tag{16.13}$$
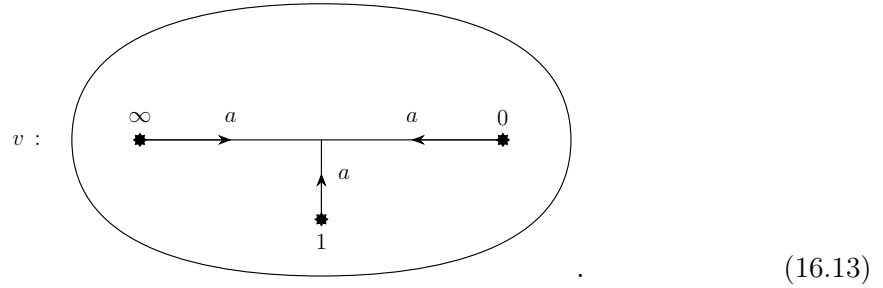
The rotation that we perform is specified by the boundary conditions

$$t \to 0: \qquad \varphi \to \mu_0 \phi_\zeta$$

$$\tag{16.14}$$

$$t \to \infty: \qquad \varphi \to \mu_\infty \phi_\zeta \,.$$

The generic w-curve compatible with these asymptotics is

$$w^3 - \sum_{k=0}^{1} c_{3-k} w^k - \frac{d_0}{t} - d_\infty t = 0 \,, \tag{16.15}$$

for some complex constants c_2, c_3, d_0, d_∞. The associated branch cut structure can be displayed as

$$(16.16)$$
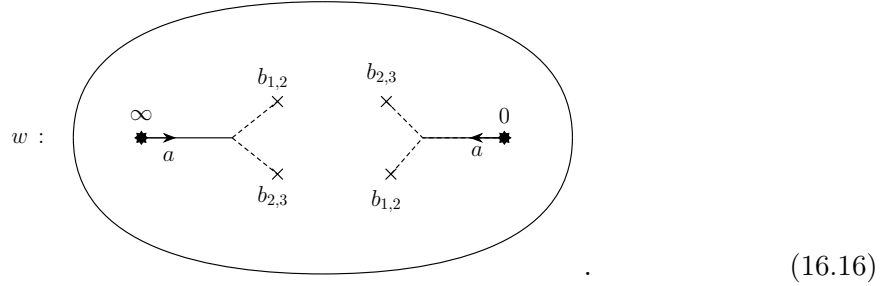
The w-curve (16.15) has the symmetry

$$t \leftrightarrow d_0/td_\infty \,, \qquad (16.17)$$

which pairs branch points of identical $\mathbb{Z}_2$ monodromy. To match the $\mathbb{Z}_3$ monodromy of the v-curve about $t = 1$ we need to collide 2 branch points of the w-curve with $\mathbb{Z}_2$ monodromy at $t = 1$. Necessarily the remaining 2 branch points collide at $t = d_0/d_\infty \equiv d$. The point $t = 1$ is a branch point and necessarily fully ramified, i.e., all sheets must come together at $w = 0$. Thus we require that substitution of $t = 1$ into the w-curve (16.15) results in the equation $w^3 = 0$. This implies $c_3 = d_0 + d_\infty$ with c_2 vanishing. Further we have

$$
\begin{aligned}
t \to 0: &\quad w^3 \to \mu_0^3 v^3 = \mu_0^3 \Lambda_0^3/t + \ldots \\
t \to \infty: &\quad w^3 \to \mu_\infty^3 v^3 = \mu_\infty^3 \Lambda_\infty^3 t + \ldots
\end{aligned}
\qquad (16.18)
$$

from which $d_0 = \mu_0^3 \Lambda_0^3$ and $d_\infty = \mu_\infty^3 \Lambda_\infty^3$ follow. The w-curves potentially matched by the v-curve simplify to

$$w^3 - \mu_0^3 \Lambda_0^3 \left(1 - \frac{1}{t}\right) - \mu_\infty^3 \Lambda_\infty^3 \left(1 - t\right) = 0 \,. \qquad (16.19)$$

The structure of this curve is determined by two disjoint branch cuts of $\mathbb{Z}_3$ monodromy and takes the form

$$(16.20)$$

We further take the limit $d = 1$, which constrains the two parameters μ_0, μ_∞ in terms of

each other (and Λ_i) and the final w-curve is then

$$(16.21)$$

In equations, the w-curve becomes

$$w^3 - \mu^3 \Lambda^3 \left(t + \frac{1}{t} - 2 \right) = 0 \, , \tag{16.22}$$

where $\mu^3 = -\mu_\infty^3$.

The $\mathcal{N} = 1$ curve is specified by the diagonal combination of (16.13) and (16.21). The

cycles on the $\mathcal{N} = 1$ curves project to H_{ij} and $3W_i$. Thus H_{ij} show perimeter law while W_i

show area law. Thus, in the electric polarization Λ, the preserved 1-form symmetry group

in this vacuum is

$$\mathcal{O} = \widehat{\Lambda} \simeq \mathbb{Z}_3 \times \mathbb{Z}_3 \, . \tag{16.23}$$

That is, akin to the case of a vacuum of $\mathcal{N} = 1$ SYM in electric polarization, no element of

the 1-form symmetry group is broken in this vacuum.

16.3 Generalizations: $\mathfrak{P}_{n,n}$

The above discussed example falls into an infinite class of theories which contain similar

confining vacua. The $\mathcal{N} = 2$ theory $\mathfrak{P}_{n,\alpha=n}$, defined in (16.1), that we begin with is obtained

by compactifying A_{n-1} $(2,0)$ theory on a sphere with n irregular punctures of type $\mathcal{P}_0$.

Notice that the number of punctures is correlated to the type of $(2,0)$ theory. This $\mathcal{N} = 2$

theory $\mathfrak{P}_{n,n}$ can be understood as being obtained by gauging the $\mathfrak{su}(n)^n$ flavor symmetry

algebra of the 4d $\mathcal{N} = 2$ SCFT $\mathfrak{S}_n$ obtained by compactifying A_{n-1} $(2,0)$ theory on a sphere

with n maximal regular punctures. Each $\mathfrak{su}(n)$ factor in the resulting $\mathfrak{su}(n)^n$ gauge algebra

has non-vanishing beta function such that the associated gauge couplings asymptote to zero in the UV. Thus, the 4d $\mathcal{N} = 2$ theory $\mathfrak{P}_{n,n}$ under consideration asymptotes in the UV to the 4d $\mathcal{N} = 2$ SCFT $\mathfrak{S}_n$ described above.

If we label the punctures by $i \in \{1, 2, \cdots, n\}$, then the un-screened line operators can be written as W_i, H_{ij}, where W_i arises by wrapping the surface defect f along a loop encircling the i-th puncture, and H_{ij} arises by wrapping f along a 1-cycle going from puncture j to puncture i. We can write the defect group as

$$\mathcal{L} = \mathcal{L}_W \times \mathcal{L}_H \,, \tag{16.24}$$

such that

$$\mathcal{L}_W = \{W_i\} / \left\{\sum W_i = 0\right\} \simeq \mathbb{Z}_n^{n-1} \tag{16.25}$$

and

$$\mathcal{L}_W = \{H_{i+1,i}, H_{1n}\} / \left\{\sum H_{i+1,i} + H_{1n} = 0\right\} \simeq \mathbb{Z}_n^{n-1} \,. \tag{16.26}$$

The non-trivial pairings are

$$\langle W_i, H_{ij}\rangle = 1/n \,, \qquad \langle W_j, H_{ij}\rangle = -1/n \,. \tag{16.27}$$

We call the polarization $\Lambda = \mathcal{L}_W$ as the electric polarization.

Let the punctures be located at $t = 0, \infty, 1, p_1, p_2, \cdots, p_{n-3}$. We rotate all punctures except the one located at $t = 1$ such that the asymptotics of φ are

$$t \to 0 : \qquad \varphi \to \mu_0 \phi_\zeta$$

$$t \to \infty : \qquad \varphi \to \mu_\infty \phi_\zeta \,. \tag{16.28}$$

$$t \to p_i : \qquad \varphi \to \mu_i \phi_\zeta \,.$$

We take specific limits of the v and w curves such that they become

$$v^n - \frac{\Lambda^n(t - t_{n-2}^v)^n(t - t_{n-1}^v)^n}{t(t-1)^{n+1}} \prod_{i=1}^{n-3} \frac{(t - t_i^v)^n}{(t - p_i)^{n+1}} = 0$$

$$w^n - \frac{d^n(t-1)^{n-1}}{t} \prod_{i=1}^{n-3} \frac{(t - t_i^w)^n}{(t - p_i)^{n+1}} = 0 \,, \tag{16.29}$$

where Λ, t_i^v capture the strong coupling scales associated to $\mathfrak{su}(n)^n$ gauge algebra and d, t_i^w capture the rotation parameters μ_i. Since we have $n-1$ number of μ_i but only $n-2$ number of parameters d, t_i^w, there is a constraint the rotation parameters have to satisfy for the vacuum described by the above solution to exist. From the above expressions, we see that there is no monodromy around t_i^v for the v-curve, and there is no monodromy around t_i^w for the w-curve. On the other hand, there is a $\mathbb{Z}_n$ monodromy around $p_i, 1, 0, \infty$ for both v and w curves. Thus, we can write the branch structure of the $\mathcal{N} = 1$ curve Σ as

$$ \tag{16.30} $$

From this curve we see that H_{ij} show perimeter law, while W_i show area law. It should be noted though that some combinations of W_i also show perimeter law. For example, pick a positive integer k that divides n. Choose any set S_k comprising of k punctures. Then the line operator

$$ \frac{n}{k} \sum_{i \in S_k} W_i \tag{16.31} $$

shows perimeter law. In any case, since W_i show area law, this vacuum exhibits non-trivial confinement for the electric polarization $\Lambda = \mathcal{L}_W$. The preserved 1-form symmetry group depends on the divisors of n. If n is prime, then the preserved 1-form symmetry group is easily computed to be

$$ \mathcal{O} = \widehat{\Lambda} \simeq \mathbb{Z}_n^{n-1} \,. \tag{16.32} $$

Clearly this class of non-Lagrangian confining theories deserve further investigation. In a similar way, using the methods described in this this part, one can construct a large number of other classes of examples of $\mathcal{N} = 1$ theories that contain confining vacua.

Part IV
Final Remarks

Chapter 17
Conclusion and Outlook

In this thesis we studied two interesting construction of 4d $\mathcal{N} = 1$ gauge theories in M-theory. The first involved an ALE-fibered G_2-manifold, with base M_3, which engineered a partially twisted 7d SYM theory on M_3. The 4d gauge theory then followed from compactification of the 7d theory on M_3. Different BPS configurations in 7d give rise to distinct minimally supersymmetric theories in 4d and are described by solutions to the Higgs bundle

$$D_A\phi = *j\,, \qquad D_A^\dagger\phi = \rho\,, \qquad F_A = i[\phi,\phi]\,, \tag{17.1}$$

on M_3 with gauge covariant connection D_A, one-form Higgs field ϕ and one-form and function source terms j, ρ respectively, all ADE-valued. The metric-independent BPS equations are equivalent to the flatness of the complex connection $\mathcal{D} = d + \phi + iA$ which, together with the twisted field content, allowed us to rephrase the compactification integrals as amplitudes of a colored supersymmetric quantum mechanics with supercharge $\mathcal{Q} = \mathcal{D}$.

Solutions to (17.1) are geometric for trivial connections $D_A = d$ and conjectured to lift to ALE-fibered G_2-manifolds[1]. In this setting the colored SQM was interpreted to descend from M2-branes probing the G_2-manifold. We studied the 4d physics of such solutions and considered the Higgs bundles resulting from TCS G_2-manifolds which solved (17.1) with

---

[1]These and related constructions are treated in the mathematics literature for smooth geometries in [36, 90, 181] and exploring the mathematics of the singular ALE-fibrations discussed in this thesis is a very interesting and fundamental open problem.

$j = 0$. Deformations of these Higgs bundles were given by altering the sources ρ with chirality of the final 4d spectrum depending on the topology of their support $\mathrm{supp}\, \rho$.

The presented results suggest many interesting research directions. First, the local model techniques laid out have potential for the analysis of a recently described family of G_2-manifolds [182]. These are described as circle bundles over hyper-conifolds with geometric structures generalizing the Bryant-Salamon cone [51] based on theorems presented in [183]. These theories also have interesting IR duals derived from an open/closed string duality generalizing arguments of [31]. The IR physics of these models is unexplored yet should permit an analysis similar to the one presented in [32, 50]. Similarly interesting would be the study of possible domain walls in such theories.

Second, local $Spin(7)$-manifolds, recently analysed in [117, 184], also permit a description in terms of a Higgs bundle over a four-dimensional base M_4 given by

$$D_A \phi_{\mathrm{SD}} = 0 \,, \qquad F_{\mathrm{SD}} + \phi_{\mathrm{SD}} \times \phi_{\mathrm{SD}} = 0 \tag{17.2}$$

with the self-dual two-form Higgs field ϕ_{SD}, the self-dual part F_{SD} of the curvature F of the gauge covariant connection D_A and $(\phi_{\mathrm{SD}} \times \phi_{\mathrm{SD}})_{ij} = [(\phi_{\mathrm{SD}})_{ik}, (\phi_{\mathrm{SD}})_{jl}]g^{kl}/4$. In this setting, M2-brane probes were touched on in [184], but the non-perturbative aspects of matter in the resulting 3d $\mathcal{N} = 1$ theory are not fully understood. Here the SQM must map into the signature complex of M_4 and understanding its generalization is expected to yield an additional tool for the study of these vacua.

Third, 4d theories with minimal supersymmetry can also be constructed in F-theory [11]. The Higgs bundle associated to these models is defined on a Kähler surface S

$$F_A^{(0,2)} = F_A^{(2,0)} = 0 \,, \qquad \bar{\partial}_A \varphi = \partial_A \bar{\varphi} = 0 \,, \qquad \omega \wedge F_A + \frac{i}{2}[\varphi, \bar{\varphi}] = 0 \tag{17.3}$$

with complex (2,0)-form Higgs field φ and Kähler form ω. The overlap between sets of 4d $\mathcal{N} = 1$ theories engineered by (17.1) and (17.3) is unclear and determining it an interesting open problem. Analysis of this will possibly involve a third formulation employing the

Heterotic string, studied in [49, 185] with the above Higgs bundles replaced by the Hull-Strominger system. Equivalently, this problem can be phrased as the problem of how Higgs bundles map through string dualities.

The second part of this thesis studied deformations of 4d $\mathcal{N} = 2$ theories to $\mathcal{N} = 1$ and derives string theoretic diagnostics for their confinement. These deformations rotate the spectral curve of the $\mathcal{N} = 2$ theory into the $\mathcal{N} = 1$ curve, which is the diagonal spectral curve of the Higgs field pair (ϕ, φ). These solve a Higgs bundle described by

$$\bar{\partial}_A \phi = \bar{\partial}_A \varphi = 0 \,, \qquad [\phi, \varphi] = 0 \,, \qquad F_A + [\varphi, \varphi^*] + [\phi, \phi^*] = 0 \,, \tag{17.4}$$

defined on the Riemann surface $\mathcal{C}$ with 1-form and 0-form Higgs fields ϕ, φ respectively and gauge connection A. We gave a topologically motivated method for solving (17.4) and characterized the line operators exhibiting perimeter and area law in each $\mathcal{N} = 1$ vacuum purely from the associated $\mathcal{N} = 1$ curve. In particular this approach extends to non-Lagrangian theories which we demonstrated by giving an infinite family of such theories containing confining vacua. We further studied the interplay between punctures and line operators. Regular punctures were found to be undetected by line operators unlike punctures of type $\mathcal{P}_{n_1, \ldots, n_k}$. However, both types of punctures themselves did not contribute to the one-form symmetry, i.e., the defect theory of the puncture did not have a one-form symmetry.

Again, the result presented in this thesis lead to multiple open questions. Starting with 4d $\mathcal{N} = 2$ theories of class S many irregular punctures remain unexplored. These often result from collisions and degenerations [186] of simpler punctures and understanding how properties relating to higher form symmetries are affected by such processes is an unsolved problem. One possible approach for analysis of such situations consists of bootstrapping rules from Lagrangian examples. Alternatively, the geometric picture, presented in chapter 11.1, is expected to yield a more direct, top-down analysis. However, this view point is far from fully developed and establishing the class S dictionary in terms of ALE-fibered Calabi-Yau three-folds is a necessarily preceding and very interesting line of research. These

questions extend by rotation to the $\mathcal{N} = 1$ setting discussed in part III of this thesis. We note that we have studied a very small subset of $\mathcal{N} = 1$ theories and heavily relied on class S methods for their analysis. Taking the point of view that an $\mathcal{N} = 1$ theory is defined by an $\mathcal{N} = 1$ curve together with a choice of polarization we can ask if we can extend our analysis to a larger class of theories. For example, a simple, yet new, generalization we expect in reach are theories for which the punctures of the w-curve are not a subset of those of the v-curve. Another example would be $\mathcal{N} = 1$ deformations of twisted D-type. This class of theories not only exhibits 1-form symmetry but extends these to a 2-group symmetry. It is an open problem how to extract these higher group structures from the $\mathcal{N} = 1$ curve.

Many properties studied here were topological in nature and are expected to hold even if supersymmetry is broken completely. Such configurations have been studied in [187] and warrant further attention. Of interest are also 4d $\mathcal{N} = 1$ SCFTs of the type described in [147]. These theories, being SCFTs, do not confine, rather the interesting physics lies in their known holographic dual description which relates to their higher form symmetries following [68].

Finally, we also mention the study of lower dimensional theories embedded into 4d $\mathcal{N} = 1$ theories, e.g., as domain wall theories [188]. Anomaly inflow for higher form symmetries constrain the modes trapped on the domain walls [57] and using methods presented in this text we expect to derive a string theoretic understanding of such effects whereby non-Lagrangian set-ups become accessible.

Bibliography

[1] Andreas P. Braun, Sebastjan Cizel, Max Hübner, and Sakura Schäfer-Nameki. Higgs Bundles for M-theory on G_2-Manifolds. *JHEP*, 03:199, 2018.

[2] Max Hubner. Local G$_2$-manifolds, Higgs bundles and a colored quantum mechanics. *JHEP*, 05:002, 2021.

[3] Lakshya Bhardwaj, Max Hubner, and Sakura Schafer-Nameki. 1-form Symmetries of 4d N=2 Class S Theories. 2 2021.

[4] Lakshya Bhardwaj, Max Hubner, and Sakura Schafer-Nameki. Liberating Confinement from Lagrangians: 1-form Symmetries and Lines in 4d $\mathcal{N} = 1$ from 6d $\mathcal{N} = (2,0)$. 6 2021.

[5] P. Candelas, Gary T. Horowitz, Andrew Strominger, and Edward Witten. Vacuum Configurations for Superstrings. *Nucl. Phys. B*, 258:46–74, 1985.

[6] Sheldon H. Katz, Albrecht Klemm, and Cumrun Vafa. Geometric engineering of quantum field theories. *Nucl. Phys. B*, 497:173–195, 1997.

[7] Sheldon H. Katz and Cumrun Vafa. Geometric engineering of N=1 quantum field theories. *Nucl. Phys. B*, 497:196–204, 1997.

[8] Amihay Hanany and Edward Witten. Type IIB superstrings, BPS monopoles, and three-dimensional gauge dynamics. *Nucl. Phys. B*, 492:152–190, 1997.

[9] Bobby Samir Acharya. N=1 heterotic / M theory duality and Joyce manifolds. *Nucl. Phys.*, B475:579–596, 1996.

[10] Bobby Samir Acharya. On Realizing N=1 superYang-Mills in M theory. 11 2000.

[11] Chris Beasley, Jonathan J. Heckman, and Cumrun Vafa. GUTs and Exceptional Branes in F-theory - I. *JHEP*, 01:058, 2009.

[12] Chris Beasley, Jonathan J. Heckman, and Cumrun Vafa. GUTs and Exceptional Branes in F-theory - II: Experimental Predictions. *JHEP*, 01:059, 2009.

[13] Ron Donagi and Martijn Wijnholt. Model Building with F-Theory. *Adv. Theor. Math. Phys.*, 15(5):1237–1317, 2011.

[14] Andreas P. Braun, Andres Collinucci, and Roberto Valandro. G-flux in F-theory and algebraic cycles. *Nucl. Phys.*, B856:129–179, 2012.

[15] Joseph Marsano and Sakura Schafer-Nameki. Yukawas, G-flux, and Spectral Covers from Resolved Calabi-Yau's. *JHEP*, 11:098, 2011.

[16] Sven Krause, Christoph Mayrhofer, and Timo Weigand. G_4 flux, chiral matter and singularity resolution in F-theory compactifications. *Nucl. Phys.*, B858:1–47, 2012.

[17] Thomas W. Grimm and Hirotaka Hayashi. F-theory fluxes, Chirality and Chern-Simons theories. *JHEP*, 03:027, 2012.

[18] Bobby Samir Acharya and Sergei Gukov. M theory and singularities of exceptional holonomy manifolds. *Phys. Rept.*, 392:121–189, 2004.

[19] Jonathan J. Heckman, David R. Morrison, and Cumrun Vafa. On the Classification of 6D SCFTs and Generalized ADE Orbifolds. *JHEP*, 05:028, 2014. [Erratum: JHEP06,017(2015)].

[20] Jonathan J. Heckman, David R. Morrison, Tom Rudelius, and Cumrun Vafa. Atomic Classification of 6D SCFTs. *Fortsch. Phys.*, 63:468–530, 2015.

[21] Lakshya Bhardwaj. Classification of 6d $\mathcal{N} = (1,0)$ gauge theories. *JHEP*, 11:002, 2015.

[22] Lakshya Bhardwaj and Patrick Jefferson. Classifying 5d SCFTs via 6d SCFTs: Rank one. 2018.

[23] Lakshya Bhardwaj and Patrick Jefferson. Classifying 5d SCFTs via 6d SCFTs: Arbitrary rank. 2018.

[24] Fabio Apruzzi, Craig Lawrie, Ling Lin, Sakura Schafer-Nameki, and Yi-Nan Wang. 5d Superconformal Field Theories and Graphs. *Phys.Lett.*, B800:135077, 2019.

[25] Fabio Apruzzi, Craig Lawrie, Ling Lin, Sakura Schafer-Nameki, and Yi-Nan Wang. Fibers add Flavor, Part I: Classification of 5d SCFTs, Flavor Symmetries and BPS States. *JHEP*, 11:068, 2019.

[26] Fabio Apruzzi, Craig Lawrie, Ling Lin, Sakura Schäfer-Nameki, and Yi-Nan Wang. Fibers add Flavor, Part II: 5d SCFTs, Gauge Theories, and Dualities. 2019.

[27] Cumrun Vafa. The String landscape and the swampland. 9 2005.

[28] Hirosi Ooguri and Cumrun Vafa. On the Geometry of the String Landscape and the Swampland. *Nucl. Phys. B*, 766:21–33, 2007.

[29] Nima Arkani-Hamed, Lubos Motl, Alberto Nicolis, and Cumrun Vafa. The String landscape, black holes and gravity as the weakest force. *JHEP*, 06:060, 2007.

[30] Tom Banks and Nathan Seiberg. Symmetries and Strings in Field Theory and Gravity. *Phys. Rev. D*, 83:084019, 2011.

[31] Michael Atiyah, Juan Martin Maldacena, and Cumrun Vafa. An M theory flop as a large N duality. *J. Math. Phys.*, 42:3209–3220, 2001.

[32] Michael Atiyah and Edward Witten. M theory dynamics on a manifold of G(2) holonomy. *Adv. Theor. Math. Phys.*, 6:1–106, 2003.

[33] Edward Witten. Anomaly cancellation on G(2) manifolds. 2001.

[34] Bobby Samir Acharya and Edward Witten. Chiral fermions from manifolds of G(2) holonomy. 2001.

[35] Dominic D. Joyce. Compact riemannian 7-manifolds with holonomy g_2. i. *J. Differential Geom.*, 43(2):291–328, 1996.

[36] D. Joyce and Spiro Karigiannis. A new construction of compact torsion-free g_2-manifolds by gluing families of eguchi-hanson spaces. *arXiv: Differential Geometry*, 2017.

[37] Alexei Kovalev. Twisted connected sums and special Riemannian holonomy. *J. Reine Angew. Math.*, 565:125–160, 2003.

[38] Alessio Corti, Mark Haskins, Johannes Nordström, and Tommaso Pacini. G$_2$-manifolds and associative submanifolds via semi-Fano 3-folds. *Duke Math. J.*, 164(10):1971–2092, 2015.

[39] Alessio Corti, Mark Haskins, Johannes Nordström, and Tommaso Pacini. Asymptotically cylindrical Calabi-Yau 3-folds from weak Fano 3-folds. *Geom. Topol.*, 17(4):1955–2059, 2013.

[40] James Halverson and David R. Morrison. The landscape of M-theory compactifications on seven-manifolds with G$_2$ holonomy. *JHEP*, 04:047, 2015.

[41] James Halverson and David R. Morrison. On gauge enhancement and singular limits in G$_2$ compactifications of M-theory. *JHEP*, 04:100, 2016.

[42] Andreas P. Braun. Tops as building blocks for G$_2$ manifolds. *JHEP*, 10:083, 2017.

[43] Thaisa C. da C. Guio, Hans Jockers, Albrecht Klemm, and Hung-Yu Yeh. Effective Action from M-Theory on Twisted Connected Sum G$_2$-Manifolds. *Commun. Math. Phys.*, 359(2):535–601, 2018.

[44] Andreas P. Braun and Michele Del Zotto. Mirror Symmetry for G_2-Manifolds: Twisted Connected Sums and Dual Tops. *JHEP*, 05:080, 2017.

[45] Andreas P. Braun and Sakura Schafer-Nameki. Compact, Singular G_2-Holonomy Manifolds and M/Heterotic/F-Theory Duality. *JHEP*, 04:126, 2018.

[46] Andreas P. Braun and Michele Del Zotto. Towards Generalized Mirror Symmetry for Twisted Connected Sum G_2 Manifolds. *JHEP*, 03:082, 2018.

[47] Andreas P. Braun, Michele Del Zotto, James Halverson, Magdalena Larfors, David R. Morrison, and Sakura Schafer-Nameki. Infinitely Many M2-instanton Corrections to M-theory on G_2-manifolds. 2018.

[48] Bobby Samir Acharya, Andreas P. Braun, Eirik Eik Svanes, and Roberto Valandro. Counting Associatives in Compact G_2 Orbifolds. 2018.

[49] Tony Pantev and Martijn Wijnholt. Hitchin's Equations and M-Theory Phenomenology. *J. Geom. Phys.*, 61:1223–1247, 2011.

[50] Bobby Samir Acharya. Confining strings from G(2) holonomy space-times. 1 2001.

[51] Robert L. Bryant and Simon M. Salamon. On the construction of some complete metrics with exceptional holonomy. *Duke Math. J.*, 58(3):829–850, 06 1989.

[52] Edward Witten. Branes and the dynamics of QCD. *Nucl. Phys. B*, 507:658–690, 1997.

[53] Edward Witten. Some comments on string dynamics. In *STRINGS 95: Future Perspectives in String Theory*, 7 1995.

[54] Nathan Seiberg. Five-dimensional SUSY field theories, nontrivial fixed points and string dynamics. *Phys. Lett.*, B388:753–760, 1996.

[55] Davide Gaiotto. N=2 dualities. *JHEP*, 08:034, 2012.

[56] Oscar Chacaltana and Jacques Distler. Tinkertoys for Gaiotto Duality. *JHEP*, 11:099, 2010.

[57] Davide Gaiotto, Anton Kapustin, Nathan Seiberg, and Brian Willett. Generalized Global Symmetries. *JHEP*, 02:172, 2015.

[58] David R. Morrison, Sakura Schafer-Nameki, and Brian Willett. Higher-Form Symmetries in 5d. *JHEP*, 09:024, 2020.

[59] Federica Albertini, Michele Del Zotto, Iñaki García Etxebarria, and Saghar S. Hosseini. Higher Form Symmetries and M-theory. *JHEP*, 12:203, 2020.

[60] Cyril Closset, Sakura Schafer-Nameki, and Yi-Nan Wang. Coulomb and Higgs Branches from Canonical Singularities: Part 0. 7 2020.

[61] Pietro Benetti Genolini and Luigi Tizzano. Instantons, Symmetries and Anomalies in Five Dimensions. 9 2020.

[62] Lakshya Bhardwaj and Sakura Schafer-Nameki. Higher-form symmetries of $6d$ and $5d$ theories. 8 2020.

[63] Matthew Buican and Hongliang Jiang. 1-Form Symmetry, Isolated N=2 SCFTs, and Calabi-Yau Threefolds. 6 2021.

[64] Yuji Tachikawa. On the 6d origin of discrete additional data of 4d gauge theories. *JHEP*, 05:020, 2014.

[65] Julius Eckhard, Heeyeon Kim, Sakura Schafer-Nameki, and Brian Willett. Higher-Form Symmetries, Bethe Vacua, and the 3d-3d Correspondence. *JHEP*, 01:101, 2020.

[66] Sergei Gukov, Po-Shen Hsin, and Du Pei. Generalized Global Symmetries of $T[M]$ Theories. I. 10 2020.

[67] Edward Witten. AdS / CFT correspondence and topological field theory. *JHEP*, 12:012, 1998.

[68] Fabio Apruzzi, Marieke van Beest, Dewi S. W. Gould, and Sakura Schäfer-Nameki. Holography, 1-Form Symmetries, and Confinement. 4 2021.

[69] Oren Bergman, Yuji Tachikawa, and Gabi Zafrir. Generalized symmetries and holography in ABJM-type theories. *JHEP*, 07:077, 2020.

[70] Ibrahima Bah, Federico Bonetti, and Ruben Minasian. Discrete and higher-form symmetries in SCFTs from wrapped M5-branes. *JHEP*, 03:196, 2021.

[71] Freddy Cachazo, Michael R. Douglas, Nathan Seiberg, and Edward Witten. Chiral rings and anomalies in supersymmetric gauge theory. *JHEP*, 12:071, 2002.

[72] Freddy Cachazo, Nathan Seiberg, and Edward Witten. Phases of N=1 supersymmetric gauge theories and matrices. *JHEP*, 02:042, 2003.

[73] Freddy Cachazo, Nathan Seiberg, and Edward Witten. Chiral rings and phases of supersymmetric gauge theories. *JHEP*, 04:018, 2003.

[74] S. Elitzur, A. Forge, A. Giveon, Kenneth A. Intriligator, and E. Rabinovici. Massless monopoles via confining phase superpotentials. *Phys. Lett. B*, 379:121–125, 1996.

[75] N. J. Hitchin. The self-duality equations on a riemann surface. *Proc. Lond. Math. Soc., III. Ser*, 1987.

[76] Carlos Simpson. Higgs bundles and local systems. *Publications Mathématiques de l'IHÉS*, 75:5–95, 1992.

[77] Davide Gaiotto, Gregory W. Moore, and Andrew Neitzke. Wall-crossing, Hitchin Systems, and the WKB Approximation. 7 2009.

[78] Dan Xie and Kazuya Yonekura. Generalized Hitchin system, Spectral curve and $\mathcal{N}=1$ dynamics. *JHEP*, 01:001, 2014.

[79] Dan Xie. M5 brane and four dimensional N = 1 theories I. *JHEP*, 04:154, 2014.

[80] Bobby Samir Acharya. M theory, Joyce orbifolds and superYang-Mills. *Adv. Theor. Math. Phys.*, 3:227–248, 1999.

[81] Gao Chen. G_2 manifolds with nodal singularities along circles. 2018.

[82] D.D. Joyce. *Compact Manifolds with Special Holonomy*. Oxford mathematical monographs. Oxford University Press, 2000.

[83] Patrick Du Val. On isolated singularities of surfaces which do not affect the conditions of adjunction (part i.). *Mathematical Proceedings of the Cambridge Philosophical Society*, 30(4):453–459, 1934.

[84] Patrick Du Val. On isolated singularities of surfaces which do not affect the conditions of adjunction (part ii.). *Mathematical Proceedings of the Cambridge Philosophical Society*, 30(4):460–465, 1934.

[85] Patrick Du Val. On isolated singularities of surfaces which do not affect the conditions of adjunction (part iii.). *Mathematical Proceedings of the Cambridge Philosophical Society*, 30(4):483–491, 1934.

[86] P. B. Kronheimer. The construction of ale spaces as hyper-kähler quotients. *J. Differential Geom.*, 29(3):665–683, 1989.

[87] Edward Witten. Branes, Instantons, And Taub-NUT Spaces. *JHEP*, 06:067, 2009.

[88] N. J. Hitchin, A. Karlhede, U. Lindström, and M. Roček. Hyperkähler metrics and supersymmetry. *Communications in Mathematical Physics*, 108(4):535–589, Dec 1987.

[89] S.W. Hawking. Gravitational instantons. *Physics Letters A*, 60(2):81 – 83, 1977.

[90] Rodrigo Barbosa, Mirjam Cvetič, Jonathan J. Heckman, Craig Lawrie, Ethan Torres, and Gianluca Zoccarato. T-Branes and G_2 Backgrounds. 2019.

[91] R.P. Thomas and Shing-Tung Yau. Special Lagrangians, stable bundles and mean curvature flow. *Commun. Anal. Geom.*, 10:1075–1113, 2002.

[92] J. Erdmenger, Z. Guralnik, R. Helling, and I. Kirsch. A World volume perspective on the recombination of intersecting branes. *JHEP*, 04:064, 2004.

[93] Hirosi Ooguri and Cumrun Vafa. Knot invariants and topological strings. *Nucl. Phys. B*, 577:419–438, 2000.

[94] Ron Donagi and Martijn Wijnholt. Higgs Bundles and UV Completion in F-Theory. *Commun. Math. Phys.*, 326:287–327, 2014.

[95] Jonathan J. Heckman, Craig Lawrie, Ling Lin, and Gianluca Zoccarato. F-theory and Dark Energy. 2018.

[96] P. B. Kronheimer. The construction of ALE spaces as hyper-Kähler quotients. *J. Differential Geom.*, 29(3):665–683, 1989.

[97] Sheldon H. Katz and Cumrun Vafa. Matter from geometry. *Nucl. Phys.*, B497:146–154, 1997.

[98] Edward Witten. Deconstruction, G(2) holonomy, and doublet triplet splitting. In *Supersymmetry and unification of fundamental interactions. Proceedings, 10th International Conference, SUSY'02, Hamburg, Germany, June 17-23, 2002*, pages 472–491, 2001.

[99] Joseph Marsano, Natalia Saulina, and Sakura Schafer-Nameki. Monodromies, Fluxes, and Compact Three-Generation F-theory GUTs. *JHEP*, 08:046, 2009.

[100] Joseph Marsano, Natalia Saulina, and Sakura Schafer-Nameki. Compact F-theory GUTs with U(1) (PQ). *JHEP*, 04:095, 2010.

[101] W.B.Raymond Lickorish. *An Introduction to Knot Theory*. Number 978-1-4612-0691-0 in Graduate texts in mathematics. Springer, 1997.

[102] C. Livingston and A. H. Moore. KnotInfo: Table of Knot Invariants. `http://www.indiana.edu/~knotinfo`.

[103] The Knot Atlas. `http://katlas.org/`.

[104] Sergio Cecotti, Clay Cordova, and Cumrun Vafa. Braids, Walls, and Mirrors. 2011.

[105] Kung Ching Chang and Jiaquan Liu. A cohomology complex for manifolds with boundary. *Topol. Methods Nonlinear Anal.*, 5(2):325–340, 1995.

[106] Claude Godbillon. *Éléments de topologie algébrique*. Hermann, 1971.

[107] Edward Witten. Supersymmetry and Morse theory. *J. Diff. Geom.*, 17(4):661–692, 1982.

[108] Kentaro Hori, Sheldon Katz, Albrecht Klemm, Rahul Pandharipande, Richard Thomas, Cumrun Vafa, Ravi Vakil, and Eric Zaslow. *Mirror symmetry*, volume 1

of *Clay Mathematics Monographs*. American Mathematical Society, Providence, RI; Clay Mathematics Institute, Cambridge, MA, 2003. With a preface by Vafa.

[109] J. Milnor. *Morse theory*. Based on lecture notes by M. Spivak and R. Wells. Annals of Mathematics Studies, No. 51. Princeton University Press, Princeton, N.J., 1963.

[110] Davide Gaiotto, Gregory W. Moore, and Edward Witten. Algebra of the Infrared: String Field Theoretic Structures in Massive $\mathcal{N} = (2,2)$ Field Theory In Two Dimensions. 2015.

[111] M. Farber. *Topology of closed one-forms*. Number 108 in Mathematical surveys and monographs. American Mathematical Society, Providence, RI, January 2004.

[112] Jeffrey A. Harvey and Gregory W. Moore. Superpotentials and membrane instantons. 1999.

[113] Chris Beasley and Edward Witten. Residues and world sheet instantons. *JHEP*, 10:065, 2003.

[114] D. M. Austin and P. J. Braam. Morse-Bott theory and equivariant cohomology. In *The Floer memorial volume*, volume 133 of *Progr. Math.*, pages 123–183. Birkhäuser, Basel, 1995.

[115] Luis Alvarez-Gaumé and Edward Witten. Gravitational anomalies. *Nuclear Physics B*, 234(2):269 – 330, 1984.

[116] Rachel Heloise Rietdijk. *Applications of supersymmetric quantum mechanics*. PhD thesis, Amsterdam U., 1992.

[117] Mirjam Cvetic, Jonathan J. Heckman, Thomas B. Rochais, Ethan Torres, and Gianluca Zoccarato. Geometric Unification of Higgs Bundle Vacua. 3 2020.

[118] F. Guedira and A. Lichnerowicz. Géométrie des algèbres de lie locales de kirilov. *J. Math. Pures et Appl.*, pages 407–484, 1984.

[119] S. P. Novikov. Multivalued functions and functionals. an analogue of the morse theory. *Dokl. Akad. Nauk SSSR*, pages 31–35.

[120] Kenji Fukaya. Morse homotopy and its quantization. *Geometry and Topology*, 1997.

[121] M. Bershadsky, Kenneth A. Intriligator, S. Kachru, David R. Morrison, V. Sadov, and Cumrun Vafa. Geometric singularities and enhanced gauge symmetries. *Nucl. Phys.*, B481:215–252, 1996.

[122] W. Lerche and N. P. Warner. Exceptional SW geometry from ALE fibrations. *Phys. Lett.*, B423:79–86, 1998.

[123] Marco Billo, Frederik Denef, Pietro Fre, Igor Pesando, Walter Troost, Antoine Van Proeyen, and Daniela Zanon. The Rigid limit in special Kahler geometry: From K3 fibrations to special Riemann surfaces: A Detailed case study. *Class. Quant. Grav.*, 15:2083–2152, 1998.

[124] P. B. Kronheimer. A Torelli type theorem for gravitational instantons. *J. Diff. Geom.*, 29(3):685–697, 1989.

[125] Kenneth A. Intriligator, David R. Morrison, and Nathan Seiberg. Five-dimensional supersymmetric gauge theories and degenerations of Calabi-Yau spaces. *Nucl. Phys.*, B497:56–100, 1997.

[126] David R. Morrison and Washington Taylor. Matter and singularities. *JHEP*, 01:022, 2012.

[127] Ron Y. Donagi. Spectral covers. 1993.

[128] Robert Friedman, John Morgan, and Edward Witten. Vector bundles and F theory. *Commun. Math. Phys.*, 187:679–743, 1997.

[129] Hirotaka Hayashi, Radu Tatar, Yukinobu Toda, Taizan Watari, and Masahito Ya-
mazaki. New Aspects of Heterotic–F Theory Duality. *Nucl. Phys.*, B806:224–299,
2009.

[130] Ralph Blumenhagen, Thomas W. Grimm, Benjamin Jurke, and Timo Weigand. Global
F-theory GUTs. *Nucl. Phys.*, B829:325–369, 2010.

[131] Hirotaka Hayashi, Teruhiko Kawano, Radu Tatar, and Taizan Watari. Codimension-3
Singularities and Yukawa Couplings in F-theory. *Nucl. Phys.*, B823:47–115, 2009.

[132] Hirotaka Hayashi, Teruhiko Kawano, Yoichi Tsuchiya, and Taizan Watari. More on
Dimension-4 Proton Decay Problem in F-theory – Spectral Surface, Discriminant Lo-
cus and Monodromy. *Nucl. Phys.*, B840:304–348, 2010.

[133] Ofer Aharony, Nathan Seiberg, and Yuji Tachikawa. Reading between the lines of
four-dimensional gauge theories. *JHEP*, 08:115, 2013.

[134] Clay Córdova and Kantaro Ohmori. Anomaly Obstructions to Symmetry Preserving
Gapped Phases. 10 2019.

[135] Yuji Tachikawa. Six-dimensional D(N) theory and four-dimensional SO-USp quivers.
JHEP, 07:067, 2009.

[136] Giulio Bonelli, Simone Giacomelli, Kazunobu Maruyoshi, and Alessandro Tanzini.
N=1 Geometries via M-theory. *JHEP*, 10:227, 2013.

[137] Kenneth A. Intriligator and N. Seiberg. Lectures on supersymmetric gauge theories
and electric-magnetic duality. *Nucl. Phys. B Proc. Suppl.*, 45BC:1–28, 1996.

[138] Kentaro Hori, Hirosi Ooguri, and Yaron Oz. Strong coupling dynamics of four-
dimensional N=1 gauge theories from M theory five-brane. *Adv. Theor. Math. Phys.*,
1:1–52, 1998.

[139] A. Brandhuber, N. Itzhaki, V. Kaplunovsky, J. Sonnenschein, and S. Yankielowicz. Comments on the M theory approach to N=1 SQCD and brane dynamics. *Phys. Lett. B*, 410:27–35, 1997.

[140] Jan de Boer and Yaron Oz. Monopole condensation and confining phase of N=1 gauge theories via M theory five-brane. *Nucl. Phys. B*, 511:155–196, 1998.

[141] Amit Giveon and Oskar Pelc. M theory, type IIA string and 4-D N=1 SUSY SU(N(L)) x SU(N(R)) gauge theory. *Nucl. Phys. B*, 512:103–147, 1998.

[142] F. Cachazo, Kenneth A. Intriligator, and Cumrun Vafa. A Large N duality via a geometric transition. *Nucl. Phys. B*, 603:3–41, 2001.

[143] Freddy Cachazo and Cumrun Vafa. N=1 and N=2 geometry from fluxes. 6 2002.

[144] Robbert Dijkgraaf and Cumrun Vafa. Matrix models, topological strings, and supersymmetric gauge theories. *Nucl. Phys. B*, 644:3–20, 2002.

[145] Robbert Dijkgraaf and Cumrun Vafa. On geometry and matrix models. *Nucl. Phys. B*, 644:21–39, 2002.

[146] Robbert Dijkgraaf and Cumrun Vafa. A Perturbative window into nonperturbative physics. 8 2002.

[147] Ibrahima Bah, Christopher Beem, Nikolay Bobev, and Brian Wecht. Four-Dimensional SCFTs from M5-Branes. *JHEP*, 06:005, 2012.

[148] Davide Gaiotto, Sergei Gukov, and Nathan Seiberg. Surface Defects and Resolvents. *JHEP*, 09:070, 2013.

[149] Kazunobu Maruyoshi, Yuji Tachikawa, Wenbin Yan, and Kazuya Yonekura. $\mathcal{N} = 1$ dynamics with T_N theory. *JHEP*, 10:010, 2013.

[150] Kazuya Yonekura. Supersymmetric gauge theory, (2,0) theory and twisted 5d Super-Yang-Mills. *JHEP*, 01:142, 2014.

[151] Dan Xie. N=1 Curve. 9 2014.

[152] Nadav Drukker, David R. Morrison, and Takuya Okuda. Loop operators and S-duality from curves on Riemann surfaces. *JHEP*, 09:031, 2009.

[153] I Garcia Etxebarria, Ben Heidenreich, and Diego Regalado. IIB flux non-commutativity and the global structure of field theories. *JHEP*, 10:169, 2019.

[154] Michele Del Zotto, Inaki Garcia Etxebarria, and Saghar S. Hosseini. Higher form symmetries of Argyres-Douglas theories. *JHEP*, 10:056, 2020.

[155] Fabio Apruzzi, Lakshya Bhardwaj, Jihwan Oh, and Sakura Schafer-Nameki. The Global Form of Flavor Symmetries and 2-Group Symmetries in 5d SCFTs. 5 2021.

[156] Lakshya Bhardwaj. Global Form of Flavor Symmetry Groups in 4d N=2 Theories of Class S. 5 2021.

[157] Mirjam Cvetic, Markus Dierigl, Ling Lin, and Hao Y. Zhang. Higher-Form Symmetries and Their Anomalies in M-/F-Theory Duality. 6 2021.

[158] Joseph A. Minahan and Dennis Nemeschansky. An N=2 superconformal fixed point with E(6) global symmetry. *Nucl. Phys. B*, 482:142–152, 1996.

[159] Jonathan J. Heckman and Tom Rudelius. Top Down Approach to 6D SCFTs. *J. Phys. A*, 52(9):093001, 2019.

[160] Michele Del Zotto, Jonathan J. Heckman, Daniel S. Park, and Tom Rudelius. On the Defect Group of a 6D SCFT. *Lett. Math. Phys.*, 106(6):765–786, 2016.

[161] Lance J. Dixon, Jeffrey A. Harvey, C. Vafa, and Edward Witten. Strings on Orbifolds. *Nucl. Phys. B*, 261:678–686, 1985.

[162] Lance J. Dixon, Jeffrey A. Harvey, C. Vafa, and Edward Witten. Strings on Orbifolds. 2. *Nucl. Phys. B*, 274:285–314, 1986.

[163] Stanley Deser, A. Gomberoff, M. Henneaux, and C. Teitelboim. P-brane dyons and electric magnetic duality. *Nucl. Phys. B*, 520:179–204, 1998.

[164] Daniel S. Freed and Constantin Teleman. Relative quantum field theory. *Commun. Math. Phys.*, 326:459–476, 2014.

[165] Oscar Chacaltana, Jacques Distler, and Yuji Tachikawa. Gaiotto duality for the twisted A_{2N-1} series. *JHEP*, 05:075, 2015.

[166] Oscar Chacaltana, Jacques Distler, and Anderson Trimm. Tinkertoys for the Twisted D-Series. *JHEP*, 04:173, 2015.

[167] Oscar Chacaltana, Jacques Distler, and Anderson Trimm. Tinkertoys for the Z3-twisted D4 Theory. 1 2016.

[168] Oscar Chacaltana and Jacques Distler. Tinkertoys for the D_N series. *JHEP*, 02:110, 2013.

[169] Kantaro Ohmori, Hiroyuki Shimizu, Yuji Tachikawa, and Kazuya Yonekura. 6d $\mathcal{N} = (1,0)$ theories on T^2 and class S theories: Part I. *JHEP*, 07:014, 2015.

[170] Kantaro Ohmori, Hiroyuki Shimizu, Yuji Tachikawa, and Kazuya Yonekura. 6d $\mathcal{N} = (1, 0)$ theories on S^1 /T^2 and class S theories: part II. *JHEP*, 12:131, 2015.

[171] Albrecht Klemm, Wolfgang Lerche, Peter Mayr, Cumrun Vafa, and Nicholas P. Warner. Selfdual strings and N=2 supersymmetric field theory. *Nucl. Phys. B*, 477:746–766, 1996.

[172] Masayuki Noguchi, Seiji Terashima, and Sung-Kil Yang. N=2 superconformal field theory with ADE global symmetry on a D3-brane probe. *Nucl. Phys. B*, 556:115–151, 1999.

[173] Davide Gaiotto, Gregory W. Moore, and Andrew Neitzke. Framed BPS States. *Adv. Theor. Math. Phys.*, 17(2):241–397, 2013.

[174] N. Seiberg and Edward Witten. Electric - magnetic duality, monopole condensation, and confinement in N=2 supersymmetric Yang-Mills theory. *Nucl. Phys. B*, 426:19–52, 1994. [Erratum: Nucl.Phys.B 430, 485–486 (1994)].

[175] Edward Witten. Solutions of four-dimensional field theories via M theory. *Nucl. Phys. B*, 500:3–42, 1997.

[176] J. L. F. Barbon. Rotated branes and N=1 duality. *Phys. Lett. B*, 402:59–63, 1997.

[177] Kenichi Konishi and Yutaka Ookouchi. On Confinement Index. *Nucl. Phys. B*, 827:59–81, 2010.

[178] Michael R. Douglas and Stephen H. Shenker. Dynamics of SU(N) supersymmetric gauge theory. *Nucl. Phys. B*, 447:271–296, 1995.

[179] Yuji Tachikawa. On gauging finite subgroups. *SciPost Phys.*, 8(1):015, 2020.

[180] Po-Shen Hsin and Ho Tat Lam. Discrete Theta Angles, Symmetries and Anomalies. *SciPost Phys.*, 10:032, 2021.

[181] Rodrigo Barbosa. Deformations of g2-structures, string dualities and flat higgs bundles. 01 2019.

[182] Bobby Samir Acharya, Lorenzo Foscolo, Marwan Najjar, and Eirik Eik Svanes. New G_2-conifolds in M-theory and their field theory interpretation. *JHEP*, 05:250, 2021.

[183] Lorenzo Foscolo, Mark Haskins, and Johannes Nordström. Complete non-compact G2-manifolds from asymptotically conical Calabi-Yau 3-folds. 9 2017.

[184] Mirjam Cvetič, Jonathan J. Heckman, Ethan Torres, and Gianluca Zoccarato. Reflections on the Matter of 3d $\mathcal{N} = 1$ Vacua and Local $Spin(7)$ Compactifications. 6 2021.

[185] Bobby Samir Acharya, Alex Kinsella, and Eirik Eik Svanes. T^3-invariant heterotic Hull-Strominger solutions. *JHEP*, 01:197, 2021.

[186] Davide Gaiotto and Joerg Teschner. Irregular singularities in Liouville theory and Argyres-Douglas type gauge theories, I. *JHEP*, 12:050, 2012.

[187] Csaba Csáki, Andrew Gomes, Hitoshi Murayama, and Ofri Telem. The Phases of Non-supersymmetric Gauge Theories: the $SO(N_c)$ Case Study. 7 2021.

[188] Diego Delmastro and Jaume Gomis. Domain walls in 4d$\mathcal{N} = 1$ SYM. *JHEP*, 03:259, 2021.